Modulation of Canonical Wnt signalling in Mesenchymal Stem Cells using a GSK3β Inhibitor

David A Cook

Thesis submitted for the degree of Doctor of Philosophy (Ph.D)

University of York

Department of Biology

June 2013

Abstract

Multipotent stromal cells/mesenchymal stem cells (MSCs) can differentiate into multiple lineages including osteogenic and adipogenic cells. Wnt signalling has been implicated in controlling MSC fate, but the mechanism is unclear and apparently conflicting data exists. Here I show that a glycogen synthase kinase 3β inhibitor, AR28, is a potent activator of canonical Wnt signalling using β-catenin translocation studies and TCF-reporter assays. AR28 induced axis duplication and secondary regions of chordin expression in *Xenopus laevis* embryos, when injected into the ventral marginal zone, indicative of canonical Wnt signalling. When human MSCs were grown under adipogenic conditions, AR28 caused a significant dose-dependent reduction in FABP5/BODIPY double-positive cells with a corresponding rescue of proliferation. In assays to determine the effects of AR28 on MSC osteogenesis using standard differentiation inducers (β-glycerophosphate, L-ascorbic acid and dexamethasone), AR28 caused a significant decrease in alkaline phosphatase (ALP) activity compared to vehicle controls, indicative of a reduced osteogenic response. However, when using mild osteogenic stimulation, excluding dexamethasone, increases in both ALP and Alizarin Red mineral staining were identified following AR28 treatment, with corresponding increases in proliferation and cell number. This AR28-induced osteogenic response was blocked by mitomycin C, identifying cell proliferation as an important step in Wnt-induced osteogenesis under these conditions. Pre-treatment of MSCs with AR28 for 7 days before osteogenic induction also increased ALP activity and mineralisation. BMP2 treatment of MSCs was capable of inducing both osteogenic and chondrogenic differentiation, to which AR28 caused a switch towards the osteogenic lineage, with synergistic increases in ALP. AR28 simultaneously caused a decrease in the chondrogenic differentiation of MSCs treated with BMP2 through the down regulation of Sox9 transcription. Together these results highlight the potential of GSK3β inhibitors as therapeutic modulators of canonical Wnt signalling, and there use to treat a multitude of bone related disorders.

Table of Contents

List of Figures

List of Tables

Acknowledgements

I would like to thank my supervisors Paul Genever and Patrick O'Shea for their guidance and support throughout the project. I would also like to thank all the members of the Genever group and the ASTL at Charnwood for all the help both in and out of the lab. Simon Fellgett for all the help with the *Xenopus* culture and relevant information, the staff and patients of Harrogate and York District Hospitals and Clifton Park Medical Centre for providing tissue samples, AstraZeneca for providing the AR28 compound and BBSRC and AstraZeneca for supporting this work.

Declaration

The work presented in this thesis was performed by the author between October 2009 and February 2013 in the Department of Biology, University of York, in the lab of Dr. Paul Genever, or in the ASTL, Charnwood, AstraZeneca. All experiments were performed by the author, with the exception of the preparation and injection of the *Xenopus laevis* embryos and *in situ* hybridisation assay, which were performed by Simon Fellgett. Neither this thesis nor any part of it has previously been submitted for acceptance of a higher degree.

Chapter 1: Introduction

1.1 Stem cells

Stem cells are a subset of cells defined by the ability of a single clonal cell to be capable of self renewal, maintaining the cells in an undifferentiated state, and differentiation into a number of mature cell types (Weissman et al, 2001). The first evidence for the existence of stem cells was published in 1961, where, through the use of random chromosome markers, clonal colonies were identified and later shown to be composed of both differentiated cells and cells that could be used to reconstitute secondary hosts to produce all the blood cell lineages (Becker et al, 1963; Till & McCulloch, 1961; Wu et al, 1968). These cells were later isolated and termed haematopoietic stem cells (HSCs) (Spangrude et al, 1988). Subsequently many types of stem cells from many tissues have been identified including skin (Blanpain et al, 2004), muscle (Wagers & Weissman, 2004), neural (Cattaneo & McKay, 1990), mesenchymal (Pittenger et al, 1999) and inner cell mass (Evans & Kaufman, 1981).

Stem cells are broadly categorised into two main types, embryonic and adult stem cells, by the tissue from which they are isolated. Embryonic stem (ES) cells are isolated from the inner cell mass of the developing embryo and can give rise to all the cell types of the developing organism, while adult stem cells are more germ layer- and tissue-specific giving rise to a smaller range of cell types. Stem cells can be further categorised by the number of cell types they are able to form, a property known as potency. The degree of potency can vary depending on the type of stem cell, and has been categorised into five families (Wagers & Weissman, 2004). Totipotent stem cells, which can differentiate into all the embryonic and extra-embryonic cells types; pluripotent stem cells can produce all the cell types of the three germ layers; multipotent stem cells can form multiple closely related cell types from a single germ layer; oligopotent stem cells can only differentiate into a few very closely related cell types; unipotent stem cells are only capable of forming a single cell type, but maintain their ability to self renew.

1.1.1 Embryonic Stem cells

ES cells are derived from the inner cell mass of a developing embryo before gastrulation, and therefore are capable of forming cells from all three germ layers. ES cells were first isolated from mouse embryos in 1981 (Evans & Kaufman, 1981; Martin, 1981), but it was some time until Thomson *et al.* generated the first human ES cell line in 1998 (Thomson et al, 1998). While both mouse and human ES cells are derived from cells of the inner cell mass, they differ in some of their properties. For example, mouse ES cells require leukaemia inhibitory factor (LIF) to maintain their pluripotency and proliferative state (Niwa et al, 2009), yet LIF does not act to maintain pluripotency in human ES cells (Dahéron et al, 2004). Human ES cells do however require a feeder layer of cells, traditionally derived from mouse embryonic fibroblasts (MEFs) (Thomson et al, 1998) to allow adhesion and provide a range of factors to maintain the pluripotency (Eiselleova et al, 2008). However, recently other sources of feeder layers, particularly of human origin have been investigated (Eiselleova et al, 2008), as well as feeder free systems (Xu et al, 2001). The pluripotency of mouse ES cells can be confirmed by the reconstitution of embryos and the generation of chimeric mice (Suda et al, 1987), while in humans, pluripotency can be demonstrated by the formation of teratomas after injection into severe combined immunodeficient (SCID) mice (Thomson et al, 1998) or other immunocompromised mouse models. Despite these discrepancies in the requirement for LIF and feeder layers for the maintenance of pluripotency, the capacity of ES cells to be maintained in culture and proliferate indefinitely is thought to be due to a range of key transcription factors, including Oct4, Nanog and Sox2, but also epigenetic factors and miRNAs (Chen & Daley, 2008).

The availability of a cell type capable of self renewal followed by the differentiation into any adult tissue offers clear uses in the treatment and repair of any damaged tissue in the adult body (Keller & Snodgrass, 1999), but the very nature of ES cells themselves makes their use in both research and therapeutics controversial. Firstly, ES cells are derived from the inner cell mass of a developing embryo, therefore in order to generate an ES cell line a fertilised embryo must be destroyed. While embryos are often obtained from excess/discarded *in vitro* fertilised embryos (Shand et al, 2012), there are examples of embryos purposefully fertilised for ES cell

extraction (Lanzendorf et al, 2001). The creation of embryos specifically for ES isolation via nuclear transfer to generate patient-specific cells, reducing immune rejection, is also being considered (de Wert & Mummery, 2003). Secondly, as ES cells are pluripotent, and characterised by their ability to form teratomas when implanted into animal models, there is also a clear safety issue in the use of ES cells in human patients. This problem can be avoided by the differentiation of the self renewing ES cells *in vitro* into the chosen mature differentiated cell type, which would not be proliferative or tumourigenic. However, full differentiation of ES cells into many cell types cannot be performed *in vitro*, and any remaining pluripotent cells would have the capacity to form teratomas in the patient.

A recent discovery by the Yamanaka laboratory, which demonstrated the generation of mouse (Takahashi & Yamanaka, 2006) and human (Takahashi et al, 2007) ES-like cells from somatic cells, by the forced expression of the pluripotency genes Oct4, Sox2, Klf4, and c-Myc, termed induced pluripotent stem (iPS) cells, offer many advantages over ES cells in terms of ethics and the potential for autologous cell treatments. However, they possess many difficulties of their own such as viral transformation techniques and epigenetic memories of the parental cells (Kim et al, 2010).

1.1.2 Adult Stem cells

Adult stem cells are present as small populations of cells found in tissues of adults, and for a long time were thought to be restricted to tissues with high turnover/repair such as the gut, skin, testis and blood, but are now thought to be much more extensive, with the identification of populations of adult stem cells in the brain, ovaries, heart and bone marrow (Wagers & Weissman, 2004). Adult stem cells are capable of self renewal and differentiation into multiple cell types, and are thought to reside within a niche in the adult tissues, maintaining the stem cells in a multipotent state, until the surrounding tissue is in need of repair or maintenance of homeostasis. Adult stem cells were originally presumed to have relatively restricted potency, to that of the tissue of origin, however there is emerging, sometimes controversial, evidence for the transdifferentiation into cells of other tissues (Raff, 2003), leading to increased therapeutic potential.

Although adult stem cells have the obvious disadvantage compared to ES cells of reduced potency, they offer several advantages over ES cells in their use in both basic science research and therapeutics. Firstly, as adult stem cells are obtained from adult tissues, the ethical issues that surround the generation of ES cell lines are not relevant, and cells can be obtained for scientific research upon informed consent. Secondly, adult stem cells are much less tumourigenic than ES cells, with reduced potency reducing the risk when implanting into patients. Thirdly, there is the possibility to use autologous cells during transplantation, or manipulate the endogenous stem cell population without the need for extraction and *in vitro* expansion or differentiation. Indeed, these advantages over ES cells have allowed adult stem cell therapeutics to progress to the clinic with much more ease than ES cells. Bone marrow transplants have been used for many years to treat leukaemia patients, and replenish all the cells of the blood via HSCs. Similarly, autologous epidermal stem cells have been expanded *in vitro* and transplanted for the treatment of wounds or burns (Shi et al, 2006). A third source of stem cells, mesenchymal stem cells or multipotent stromal cells (MSCs), are becoming an increasingly popular source of cells, with therapeutic potential for a multitude of reasons and are discussed in detail bellow.

1.1.3 Mesenchymal Stem Cells

The existence of a mesenchymal stem cell was first proposed by Friendenstein *et al* (1966), who reported a population of bone marrow stromal cells capable of generating bone following heterotopic transplantation. These precursors were subsequently shown to be a subset of fibroblast like cells capable of forming colonies, termed colony-forming unit fibroblasts (CFU-Fs), when selected by adherence to plastic surfaces (Friedenstein et al, 1970). Cells derived from a single CFU-F could be cultured *in vitro* and were able to proliferate, whist maintaining their ability to differentiate into osteoblasts, adipocytes and chondrocytes (Pittenger et al, 1999). Together, these data are characteristics of the two hallmarks of stemness described above; the ability to self renew, and to differentiate into multiple lineages. Consequently these cells came to be commonly known as mesenchymal stem cells.

1.1.3.1 MSC markers and isolation

The study of MSCs *in vivo* and the isolation of MSC populations has been hindered by the lack of specific cell surface markers for immuno-phenotype identification. Cultured human MSCs do express a panel of cell surface markers, such as CD105, CD73 and CD90, and lack the haematopoietic markers CD45, CD34 and CD14 (Dominici et al, 2006), however these can be donor-, isolation- and passage-dependent and may not represent the true *in vivo* MSC population. Various cell markers are now being used to isolate populations of MSCs from the heterogeneous plastic adherent cultures, such as Sca-1^+/Thy-1^+ (Locatelli et al, 2003) and CD271 (Quirici et al, 2002), however no single marker has yet been universally adopted causing difficulty in the comparison of results from different labs.

Consequently, the majority of work studying the properties of MSCs has been performed using cultured MSCs selected by adherence to culture plastic. However, this generates problems of its own, with different species, isolation techniques, culture conditions and donor sites generating increased complexity in the system. Furthermore, some studies of MSC differentiation have been performed not with primary cells, but with cell lines such as C3H10T1/2 (Jackson et al, 2005; Kulkarni et al, 2006) and MC3T3-E1 for osteogenesis (Hakki et al, 2012), and MC3T3-L1 for adipogenesis (Bennett et al, 2002), preventing the direct extrapolation of the findings to human MSCs. In addition to the difficulties faced due to the use of a range of cell lines and species, there is the added problem of MSC donor variation combined with heterogeneous MSC populations. As MSCs are a primary cell line they are likely to differ in their properties between donors (Frank et al, 2002; Phinney et al, 1999; Siddappa et al, 2007), both in the proliferation rate and capacity to differentiate toward particular lineages. Furthermore, as MSCs are solely selected by their adherence to plastic, the resulting cell population is often heterogeneous, containing multipotent stem cell, but also a population of less potent, early lineage committed cells (Minguell et al, 2001). Together, these factors cause a difficulty in accurate reproduction between donors, in particular when combining absolute values, and as such comparisons between donors are often limited to trends.

As mentioned above, MSCs are classically derived from the bone marrow (Pittenger et al, 1999), however they have now been isolated from many adult stromal tissues (da Silva Meirelles et al, 2006; Kern et al, 2006; Sakaguchi et al, 2005), with the more common sources for *in vitro* differentiation analysis being bone marrow, skeletal muscle, adipose tissue, periosteum and synovium. While cells isolated from all these tissue sources show similar epitope profiling irrespective of the source tissue, differences are observed in the colony forming capacity and differentiation capabilities of these cells (Sakaguchi et al, 2005). Adipose-derived cells were shown to be less efficient at chondrogenic differentiation, whilst the periosteum extracted MSCs demonstrated poor adipogenic differentiation (Sakaguchi et al, 2005). Furthermore MSCs extracted from umbilical cord blood where not able to differentiate toward the adipogenic lineage at all (Kern et al, 2006). Therefore the choice of MSC source is very important when considering experimental design and therapeutic uses.

1.1.3.2 Therapeutic potential of MSCs

Since their discovery, MSCs have generated a lot of interest in the biomedical field as a source for stem cell therapies, with their relatively simple *ex vivo* expansion, multilineage capacity and potential for autologous transplantation. Indeed, clinical trials have been performed in patients with osteogenesis imperfecta, where allogeneic bone marrow-derived MSCs were given to patients after bone marrow transplantation. MSC engraftment was shown and a marked increase in patient recovery was detected (Horwitz et al, 2002). Another group implanted autologous bone marrow MSCs into articular cartilage defects of osteoarthritic patients (Wakitani et al, 2002). Mouse models have also demonstrated the potential for MSCs in skeletal muscle repair, with engraftment and myogenic differentiation of human synovial membrane-derived MSCs leading to muscle repair in Duchenne muscular dystrophy mouse models (De Bari et al, 2003). These studies, and others, coupled with cell scaffold engineering offer clear uses and delivery options for mesodermal tissue repair. Tissue engineering techniques such as these involve the generation of a biocompatible scaffold on which cells are cultured before implanting into the patient, and in the case of MSCs this requires a thorough understanding of the differentiation process to ensure correct function of the implanted construct.

However, a lack of cell selection markers and the need to expand MSCs in culture creates problems of its own, most notably the rapid telomere shortening, a marker of ageing, and the resulting senescence of the MSCs (Baxter et al, 2004). Any cells which are then used in therapeutic treatments after *in vitro* expansion will therefore have greatly impaired proliferation, differentiation and cell homing capability. Another area in which MSCs offer therapeutic potential is in regard to their immunosuppressive capacity. While MSCs offer the obvious potential of tissue repair and replacement mentioned above, they also offer a broader therapeutic potential, through the regulation of the immune response. Upon activation MSCs secrete soluble mediators, such as nitric oxide, prostaglandin, indoleamine 2,3-dioxygenase, Interleukin-6, and human leukocyte antigen-G. These mediators can then regulate the proliferation and function of a variety of immune cells (Ghannam et al, 2010). MSCs also demonstrate an ability to home to sites of inflammation, through the migration towards chemokines and cytokines (Sordi et al, 2005). Therefore there is a great deal of interest in the study of MSCs to treat inflammation through non-invasive systemic administration of MSCs (Ghannam et al, 2010).

1.1.3.3 In vitro differentiation of MSCs

MSCs have the ability to differentiate into multiple cell types including osteoblasts, adipocytes, chondrocytes, stomal cells and myocytes (Figure 1.1.1), and various methods have been developed to mimic these processes *in vitro*. Osteoblasts develop through a series of phases, initiated by cellular proliferation, followed by extracellular matrix (ECM) maturation and matrix mineralisation. These changes in cellular activity correlate with a pattern of maturation of the cells from committed osteoprogenitors to pre- and finally terminally differentiated osteoblasts. This process of cell maturation can be induced *in vitro* by the addition of bone morphogenetic proteins (BMPs), often BMP-2 (Banerjee et al, 2001), or the addition of a differentiation cocktail of dexamethasone, ascorbate and β-glycerophosphate (Jaiswal et al, 1997). While both these methods are capable of inducing the osteogenic differentiation of MSCs, it is likely that they act through different mechanisms to generate a comparable response. This differentiation process ultimately leads to the formation of osteoblasts expressing osteoblast-specific genes such as a temporal increase in alkaline phosphatase (ALP) during osteogenic

commitment, followed by increases in osteopontin (OP), osteonectin (ON), bone sialoprotein (BSP) and osteocalcin (OC), accompanied by the deposition of a mineralised matrix upon osteoblast maturation.

As with osteoblasts, adipocytes mature though a series of increasingly committed cell types, before becoming terminally differentiated adipocytes, expressing adipocyte-specific markers such as fatty acid binding protein (FABP) 4 and 5 (Samulin et al, 2008), fatty acid synthase (FAS), lipoprotein lipase (LPL), and glucose transporter 4 (GLUT4) and forming lipid vesicles. *In vitro* adipogenesis can be induced in MSCs by the addition of a differentiation cocktail of dexamethasone, isobutylmethylxanthine (IBMX), indomethacin and insulin.

Methods to induce the process of chondrogenesis have also been developed *in vitro*. Chondrogenic differentiation *in vivo* requires an initial condensation of the MSCs, which is mimicked *in vitro* by culturing MSCs as micromass pellets. Chondrogenic differentiation can then be induced by the presence of transforming growth factor-β (TGF-β3) resulting in the appearance of a chondrocyte-like phenotype characterised by an upregulation of cartilage-specific molecules such as collagen type II and X, aggrecan, versican, biglycan, and decorin (Pelttari et al, 2008). Differentiating chondrocytes mature through a sequence of defined steps, initially the MSCs differentiate into a proliferative non-hypertrophic stage termed chondroblasts. This stage is characterised by a change from collagen type-I to type-II, IX and XI expression and a highly ordered columnar organisation. This stage is then followed by a hypertrophic stage, marked by the expression of collagen type-X, which is vital for vascular invasion, osteoblast differentiation, and bone formation during embryonic development.

MSCs can also be induced to form other mesodermal cells, such as myocytes and stromal cells, as well as the more unusual cardiomyocytes (Li et al, 2006; Rangappa et al, 2003). There is also some evidence to suggest that MSC have a greater potency, and can differentiate towards mesoderm, neuroectoderm and endoderm tissues (Jiang et al, 2002; Tropel et al, 2006). However, this thesis will concentrate on the three main differentiation processes, osteogenesis, adipogenesis and chondrogenesis.

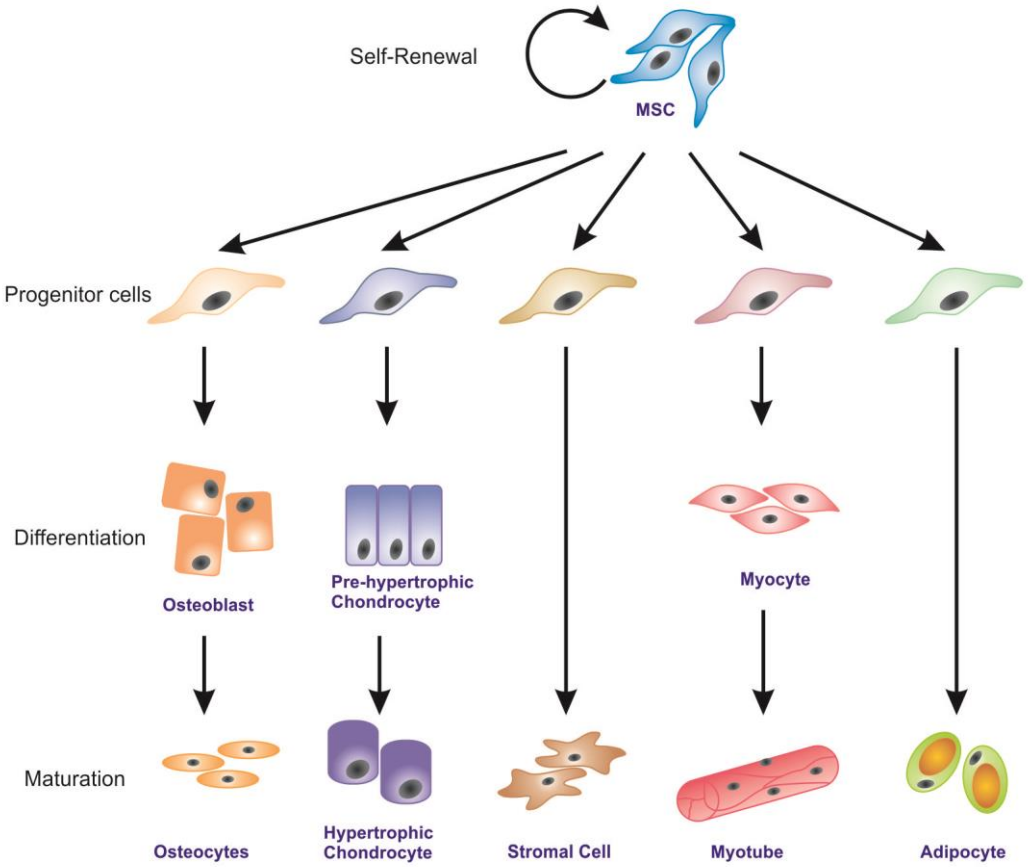

Figure 1.1.1. Schematic showing the potency of MSCs, and the progression of differentiation along the various lineages.
MSCs are a multipotent cell capable of self renewal, and differentiation into multiple mesenchymal lineages, including osteoblasts, osteocytes, chondrocytes and adipocytes. MSCs differentiate through a series of committed progenitor cells, and differentiated stages before final maturation into fully committed terminally differentiated cells. Adapted from Caplan and Bruder (2001)

1.2 Transcriptional Control of MSC differentiation

The differentiation of MSCs into the three predominant lineages of osteoblasts, adipocytes and chondrocytes is governed by a variety of transcription factors. The important and best studied ones are reviewed in detail below.

1.2.1 Osteogenesis

1.2.1.1 Runx2

Runx2 is considered the major transcription factor controlling osteoblast commitment and differentiation, and is a member of the Runt-domain gene family expressed in mesenchymal cells early in skeletal development and throughout osteoblast differentiation, with molecular and genetic studies indicating its necessity in osteoblast differentiation of mesenchymal cells (Ducy et al, 1997; Komori et al, 1997; Xiao et al, 1998). Runx2 was initially identified as an important transcription factor in osteogenesis by its binding to a cis-element on the osteoblast-specific OC gene, and its forced expression in osteoblast precursor cells, MC3T3-E1, caused the transcription of OC and Type I collagen alpha 1 chain (Col1A1). Additionally, it was shown that over expression of Runx2 can induce osteogenesis *in vitro* and *in vivo*, demonstrated by increased osteoblastic markers, OP and OC, increased ALP expression and mineralisation *in vitro*, while *in vivo* studies showed accelerated healing in critical-sized skull defects (Zheng et al, 2004). Runx2 null mice showed the converse to also be true, with a complete absence of ossification, due to the maturational arrest of osteoblasts (Komori et al, 1997). Runx2 exerts is pro-osteogenic effects through its consensus sequence, first named the osteoblast-specific element (OSE), which can be found in the promoter region of many osteoblast genes, such as Col1A1 (Rossert et al, 1996), OP (Hijiya et al, 1994), BSP (Marie, 2008) and OC (Ducy & Karsenty, 1995). Binding to these regions allows for the regulation of gene expression, resulting in the establishment of an osteoblast phenotype (Marie, 2008).

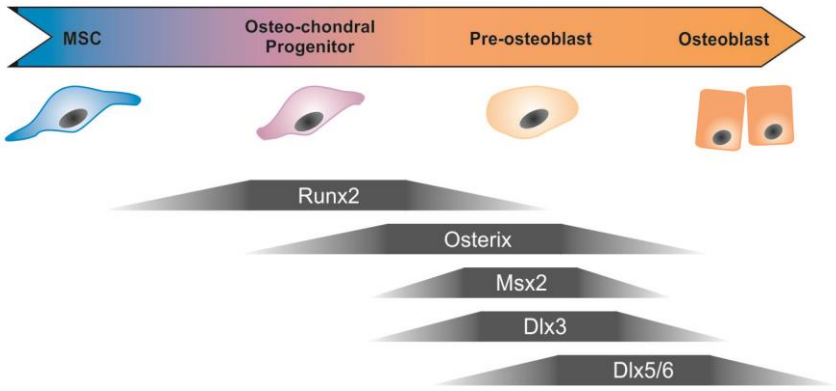

Figure 1.2.1. Schematic showing the expression levels of transcription factors during the osteogenic differentiation of MSCs.
Osteogenic differentiation of MSCs progresses through a series of increasingly committed progenitors before finally becoming mature osteoblasts capable of mineralisation. This process is accompanied by the expression of a range of transcription factors. The onset of differentiation is driven by the expression of Runx2 and osterix prior to the increase in the expression of the homeobox proteins Dlx3/5/6 and Msx2, which together regulate the maturation of the osteoblasts. Adapted from Frith and Genever (2008)

More recent work has also implicated Runx2 in the trans-differentiation of preadipocytes into osteoblasts. Takahashi (2011), demonstrated that over expression of Runx2 in the preadipocyte cell line, 3T3-E1, decreased the adipocyte markers Peroxisome proliferator-activated receptor (PPAR) γ2 and CAAT/enhancer binding protein (C/EBP) α and resulted in increased osteogenic markers such as ALP, OC and BSP (Takahashi, 2011). This trans-differentiation was further enhanced by the addition of dexamethasone or the over expression of the mitogen-activated protein kinase phosphatase-1 (MKP-1). Dexamethasone, a synthetic glucocorticoid, acts to enhance the activity of Runx2 by reducing the amount of Runx2 phosphoserine levels via MKP-1 (Phillips et al, 2006). While others have demonstrated the phosphorylation of Runx2 on tyrosine, theonine and serine residues increases during dexamethasone induced osteogenesis (Shui et al, 2003).

1.2.1.2 Osterix

Osterix (Osx) has also been shown to be an important transcription factor involved in osteoblast commitment. Osx-deficient mice were shown to have an absence of osteoblasts and defective bone formation (Nakashima et al, 2002), however, Osx appears to act downstream of Runx2 (Figure 1.2.1) as Osx is not expressed in Runx2 null mice, but Runx2 expression remains in Osx null mice (Nakashima et al, 2002). The studies into the effects of over expression of Osx are a little less clear, with multiple groups demonstrating that Osx over expression is sufficient to induce osteogenesis (Tu et al, 2006; Wu et al, 2007), whereas Kurata *et al* (2007) recorded that Osx over expression was capable of initiating osteogenesis, shown by early marker expression, but failed to generate terminally differentiated osteoblasts (Kurata et al, 2007). This is further confirmed by experiments where human MSCs were subjected to over expression and knockdown of Osx, generating little effect alone, but in combination with BMP6 resulted in increased and reduced osteogenesis respectively (Zhu et al, 2012). This group were also able to show that Osx over expression lead to an increase in osteoblast-specific ECM proteins, suggesting a role for Osx in the initiation of matrix deposition.

Osx has also been implicated in the commitment decisions of osteo-chondro progenitor cells (Tominaga et al, 2009). Mouse bone marrow MSCs, ST-2 and

C3H10T1/2 cells were induced to differentiate by BMP6 treatment, which resulted in the differentiation to both osteoblasts and chondrocytes in a cell type dependent manner. MSCs, and to a smaller extent ST-2 cells formed osteoblasts when treated with BMP6, whilst C3H10T1/2 cells did not. However, C3H10T1/2 cells differentiated strongly toward chondrogenesis. ST-2 cells again differentiated slightly towards chondrogenesis, while MSCs failed to form chondrocytes. The level of Osx in these different cell types was studied and shown to be highest in MSCs, and lowest in the C3H10T1/2 cells (Tominaga et al, 2009). Furthermore, over expression of Osx in the C3H10T1/2 cells switched the differentiation from chondrogenic to osteogenic in response to BMP6, suggesting Osx acts during the lineage commitment decision of osteo-chondro progenitor cells, pushing the cells towards an osteogenic lineage.

It is thought that Osx may act, at least in part through the formation of a complex with the nuclear factor of activated T cells (NFAT), resulting in activation of Col1A1 promoter activity (Koga et al, 2005). A proposal backed up by the constitutive activation of NFAT leading to increased bone formation and bone mass (Winslow et al, 2006).

1.2.1.3 Homeobox proteins

Dlx and Msx are homeodomain transcription factors homologous to the *Drosophila* Distal-less and muscle specific homeobox genes. The expression patterns of Dlx5 and 6 are very similar, and are present throughout almost all of the skeletal elements (Chen et al, 1996). Over expression and knock out studies of these genes show a partial redundancy, and have implicated them in osteoblast differentiation. Over expression of Dlx5 accelerated osteoblast differentiation *in vitro* (Tadic et al, 2002), while Dlx5 knockout mice had craniofacial and sensory skeletal defects (Depew et al, 1999). Double knockouts of Dlx5 and 6 presented more severe defects (Robledo et al, 2002), implying partial redundancy or compensation between the two transcription factors. A third member of the Dlx family, Dlx3, has also been implicated in osteogenic differentiation. Dlx3 expression in the mouse embryo was associated with new bone formation and regulation of osteoblast differentiation. Furthermore, Dlx3 was expressed in *ex vivo* osteoblasts, which when over expressed

or reduced by RNAi knock down resulted in increased and decreased osteogenesis respectively (Hassan et al, 2004).

In contrast to the expression of Dlx transcription factors in regions of osteoblast differentiation and bone formation, Msx2 is expressed in the proliferating osteogenic precursors (Hassan et al, 2004). Fitting with this expression pattern, over expression of Msx2 prevented osteogenic differentiation and mineralisation of primary cultured chick calvarial osteoblasts, while over expression of the antisense mRNA resulted in decreased proliferation and enhanced osteogenesis (Dodig et al, 1999). Therefore homeobox proteins can act to both enhance osteogenesis, but also maintain the precursors in a proliferative undifferentiated state.

1.2.2 Adipogenesis

1.2.2.1 PPARγ

As with Runx2 in osteogenesis, there is a key transcription factor involved in the adipogenic differentiation of MSCs, peroxisome proliferator activated receptor-γ (PPARγ) (Figure 1.2.2). PPARγ is a nuclear hormone receptor, thought to be the master regulator of adipogenesis. Alternative splicing generates 2 isoforms of PPARγ, PPARγ1 is ubiquitously expressed whilst PPARγ2 is restricted to adipose tissues and is a more potent stimulator of adipogenesis (Mueller et al, 2002). PPARγ was discovered as key player in adipogenesis through its interaction with the 5'-flanking region of the FABP4 gene, a gene capable of inducing adipocyte-specific gene expression. It was subsequently shown to be expressed very early in the differentiation of adipocytes, with forced over expression of PPARγ inducing adipogenesis in cultured fibroblasts (Tontonoz et al, 1994). Interestingly, the capacity of PPARγ to induce adipogenesis is not limited to fibroblastic cells; myoblastic cell lines transdifferentiated to adipocytes upon ectopic expression of PPARγ and C/EBPα, and PPARγ activation (Hu et al, 1995). Complementary experiments have also been performed. PPARγ deletion in fibroblasts resulted in reduced adipogenesis (<2% efficiency) despite the addition of another stimulator of adipogenesis, C/EBPα (Discussed in 1.2.2.2) (Rosen et al, 2002), suggesting C/EBPα acts through PPARγ to stimulate adipogenesis. These results and others suggest

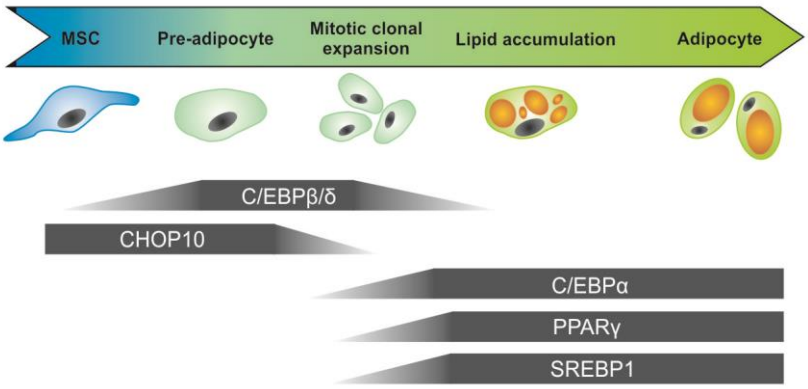

Figure 1.2.2. Schematic showing the expression levels of transcription factors during the adipogenic differentiation of MSCs.
Adipogenic differentiation of MSCs progresses through a series of gradually committed progenitors prior to terminal differentiation. Hormonal signals induce the expression of C/EBPβ/δ in early commitment and mitotic clonal expansion (MCE) before CHOP10 is reduced, allowing C/EBPβ to stimulate C/EBPα and PPARγ, which increase each other's expression through a positive feedback mechanism, causing the upregulation of adipogenic genes, and adipocyte maturation. Adapted from Frith and Genever (2008)

PPARγ is both sufficient and indispensable for adipogenic differentiation. While PPARγ is widely considered the master regulator of adipogenesis, it has also been implicated in the reciprocal regulation of adipogenesis and osteogenesis. Akune *et al* (2004) showed that embryonic stem cells from homozygous PPARγ-deficient mice would spontaneously differentiate into osteoblasts, while PPARγ haploinsufficiency resulted in enhanced bone formation with increased osteogenesis from bone marrow progenitors both in vivo and ex vivo.

1.2.2.2 C/EBPs

CAAT/enhancer binding proteins (C/EBPs) are members of the basic-leucine zipper class of transcription factors, which function as homo- or heterodimers with other C/EBP family members. Three C/EBP family members have been shown to play a role in adipogenesis, C/EBPα, β and δ. C/EBPα has the most prominent role, dramatically demonstrated by the over expression of C/EBPα in fibroblastic cells, which resulted in the induction of adipogenesis in up to 50% of the cells (Freytag et al, 1994); conversely antisense mRNA knockdown resulted in reduced adipose phenotype in differentiated MC3T3-L1 cells (Lin & Lane, 1992). *In vivo* mouse models were able to confirm these *in vitro* findings, with the restriction of C/EBPα expression to the liver in mice, which subsequently presented reduced adipose tissue formation (Linhart et al, 2001). The study of endogenous C/EBP levels during adipogenic differentiation of cultured cells showed that C/EBPα is expressed late in the differentiation process immediately prior to the activation of the many adipocyte specific genes (Figure 1.2.2). The other two isoforms, C/EBPβ and δ are only transiently expressed, accumulating during the early stages of differentiation (Figure 1.2.2), before diminishing prior to terminal differentiation (Yeh et al, 1995). This early transient increase in C/EBPβ and δ allows them to act by relaying the hormonal signals such as dexamethasone and methylisobutylxanthine, leading to the activation of C/EBPα (Yeh et al, 1995). This signal transduction is likely to function through the activation of PPARγ, via C/EBP binding sites in the PPAR promoter. This PPARγ expression is then thought to activate C/EBPα, which then enters a positive feedback loop, increasing the expression of PPARγ. This process is apparent through the generation of PPARγ and C/EBPα null cell lines (Rosen et al, 1999; Wu et al, 1999), where PPARγ null cells fail to express C/EBPα despite normal early

differentiation (Rosen et al, 1999). Additionally, C/EBPα null fibroblasts have reduced levels of PPARγ expression, which can be rescued by retroviral transfection and expression of C/EBPα (Wu et al, 1999). It is thought that this positive feedback loop maintains the expression of these two important transcription factors through to terminal differentiation of the adipocytes.

1.2.2.3 SREBP1

Another transcription factor of note for its pro-adipogenic effects is Sterol regulatory binding element protein-1 (SREBP1)/Adipocyte differentiation and determination factor-1 (Add1). Dominant negative expression of SREBP1 in MC3T3-L1 cells sharply repressed adipogenic differentiation, while over expression of SREBP1 in the fibroblastic line, NIH-3T3, increased adipogenesis in a synergistic manner with PPARγ over expression, suggesting its involvement in this pathway (Kim & Spiegelman, 1996). SREBP1 exerts it pro- adipogenic effects through the interaction with E-box domains in the PPARγ promoter regions, allowing further regulation of PPARγ gene expression (Fajas et al, 1999).

1.2.2.4 Negative regulation of adipogenesis

As with osteogenesis, there are inhibitors of adipogenesis allowing for tight regulation of the differentiation process. C/EBP homologous proteins (CHOPs) negatively regulate adipogenesis through interactions with C/EBPs. An example of this effect is elegantly demonstrated by the Lane laboratory (Tang & Lane, 2000; Tang et al, 2003a; Tang et al, 2003b). During adipogenesis, growth-arrested pre-adipocytes re-enter the cell cycle and undergo mitotic clonal expansion (MCE) prior to the expression of C/EBPα and PPARγ which act as antimitotics. As discussed above, C/EBPβ/δ relay the hormonal signals through the upregulation of C/EBPα and PPARγ, and are expressed early in the differentiation program, prior to MCE. However, in order to allow MCE to occur, C/EBPβ must not activate C/EBPα and PPARγ until cell division has occurred. This was shown to be achieved through the binding of CHOP10 to C/EBPβ prior to MCE, preventing it from binding the C/EBPα and PPARγ promoter regions. When the dividing cells entered S phase,

CHOP10 was down regulated leading to alleviation of C/EBPβ inhibition, and adipogenic progression (Tang & Lane, 2000) (Figure 1.4.2).

The activity of SREBP1 is also negatively regulated during adipogenesis, by the binding of Inhibitor of DNA binding (Id) proteins which prevent SREBP1 from binding to the E-box DNA regulatory sequences (Moldes et al, 1999). Another transcription factor important in the negative regulation of adipogenesis is the GATA binding transcription factor family. GATA2 and 3 have been shown to be expressed in pre-adipocytes, and their down regulation leads to enhanced adipogenesis. Forced expression of GATA2 and 3 prevents the switch from pre-adipocytes to mature adipocytes, in part through binding directly to PPARγ (Tong et al, 2000), but also through the formation of protein complexes with C/EBPα or β (Tong et al, 2005).

1.2.3 Chondrogenesis

1.2.3.1 Sox family of transcription factors

As with both adipogenesis and osteogenesis, there is an apparent master regulator of chondrogenesis, Sox9. Sox9 is a member of a family of transcription factors that contain a High mobility group (HMG) -type DNA binding domain, and is expressed throughout chondrogenic differentiation until the cells become hypertrophic, where it is rapidly shut off (Zhao et al, 1997) (Figure 1.2.3). The requirement for Sox9 is clearly demonstrated in the work by Akiyama *et al* (2002), where deletion of Sox9 expression in the mesenchymal cells of limb buds led to the complete absence of chondrogenic mesenchymal condensations in the developing limbs, while deletion of the Sox9 gene in mesenchymal condensations led to the arrest of chondrogenesis at this stage (Akiyama et al, 2002), demonstrating roles in both mesenchymal condensation and chondrogenic progression.

Furthermore, Sox9 was identified as part of a triad of Sox genes, with L-Sox5 and Sox6, which are sufficient for the induction of chondrogenesis in embryonic stem cells (Ikeda et al, 2004). L-Sox5 and Sox6 differ from Sox9 in that they do not possess a transactivation domain and therefore do not affect gene expression directly, but are thought to alter gene expression through the recruitment of other

transcriptional activators (Frith & Genever, 2008). L-Sox5 and Sox6 are co-expressed with Sox9 during chondrogenesis (Figure 1.2.3) and therefore share expression patterns with the chondrogenic marker type 2 collagen alpha 1 (Col2A1), prompting further studies into the role of these transcription factors in chondrogenesis. L-Sox5- and Sox6-deficient mice present chondrogenic defects, with the dual knockout generating a more severe phenotype, suggesting some redundancy. However, in contrast to Sox9-deficient mice, Sox5/6-deficient mice do develop chondrogenic mesenchymal condensations (Smits et al, 2001), implicating their role later in the differentiation process. It is thought that these three Sox transcription factors work in collaboration to activate chondrocyte-specific markers, with enhanced Col2A1 reporter expression when all three Sox genes are coexpressed in non-chondrogenic cells (Lefebvre et al, 2001). Similarly, the three Sox proteins have been shown to cooperatively activate the chondrocyte marker, type XI collagen alpha 2 (Bridgewater et al, 1998). As discussed above, Sox transcription factors are required for the progression of chondrogenesis, but over expression of the Sox triad also causes chondrogenesis arrest at the pre-hypertrophic cell stage preventing terminal differentiation (Ikeda et al, 2004). It is thought that this terminal differentiation inhibition is at least in part due to the action of two genes, S110A1 and S100B, members of the S100 protein family which carry the Ca^{2+}-binding EF-hand motif. These proteins are expressed during the late proliferative and pre-hypertrophic stages of chondrogenesis, and when over expressed in chondrogenesis inhibited the terminal differentiation step. Furthermore, S100B protein expression is responsive to the Sox triad through enhancer elements in the 5' flanking region (Saito et al, 2007).

1.2.3.2 Runx2

As described above, Runx2 is a master regulator of osteogenesis, but it also has important roles in regulating chondrogenesis. The initial evidence for this was presented in the Runx2 null mice used to identify its function in osteogenesis. It was noted that these mice also had cartilage defects as well as the more obvious bone defects (Kim et al, 1999). Runx2 null mice had a lack of hypertrophic chondrocytes, implying an important role for Runx2 in this step. The expression levels of Runx2 are at their highest in chondrocytes during the hypertrophic stage

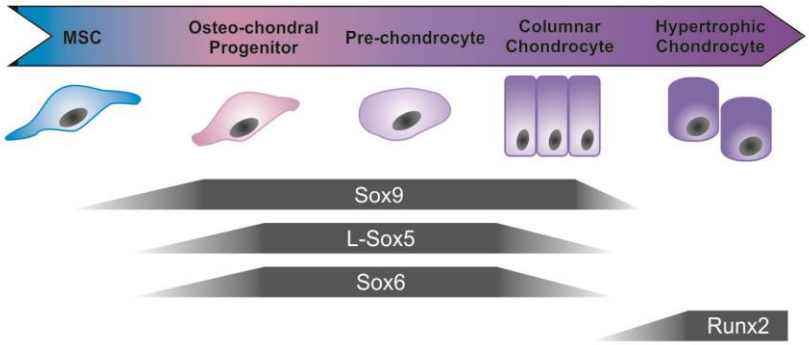

Figure 1.2.3. Schematic showing the expression levels of transcription factors during the chondrogenic differentiation of MSCs.
Chondrogenic differentiation of MSCs progresses through a series of increasingly committed pre-hypertrophic progenitors, before undergoing hypertrophy and becoming terminally differentiated hypertrophic chondrocytes. Sox9 is expressed upon the onset of chondrogenesis, which activates L-Sox5 and Sox6 which act together to promote the pre-hypertrophic stages of chondrogenic differentiation. The Sox triad is then switched off and Runx2 is up regulated and induces hypertrophy and the maturation of the chondrocytes. Adapted from Frith and Genever (2008)

(Kim et al, 1999) (Figure 1.2.3), and over expression of Runx2 during hypertrophy caused enhanced maturation and increased endochondral ossification (Enomoto-Iwamoto et al, 2001).

1.3 Cell signalling

Cell signalling pathways are important in many aspects of embryonic development and adult tissue homeostasis, including that of MSC self renewal and differentiation. Three pathways that have been extensively linked to MSC differentiation are that of Wnt, TGFβ-superfamily and Hedgehog signalling, and are described in more detail below.

1.3.1 Wnt signalling

Wnt molecules are a family of cysteine-rich secreted glyco-lipoproteins, approximately 40kDa in size, that regulate many processes including development, cell proliferation and cell fate (Clevers & Nusse, 2012). Wnt signalling acts through two known pathways, the canonical pathway involving β-catenin, and the β-catenin independent pathways termed the non-canonical pathways. The canonical Wnt pathway is the better studied and will be discussed in more detail here. Canonical Wnt ligands mediate their effects by binding to their receptors frizzled (Fzd) and co-receptors, low-density lipoprotein receptor related protein (LRP) 5 and 6. This leads to the inhibition of a protein destruction complex, resulting in the stabilisation and nuclear translocation of β-catenin, inducing gene transcription via the T Cell Transcription factor/Lymphoid enhancer-binding factor (LEF/TCF) family of transcription factors. In the absence of Wnt signalling, the destruction complex is not inhibited and can therefore perform its function to phosphorylate β-catenin, leading to degradation by the proteosome (Figure 1.3.1).

Human and most other mammalian genomes contain 19 Wnt genes, which fall into 12 conserved subfamilies. Furthermore Wnt genes can be found in all multicellular organisms, including sponges, but not single cellular organisms, highlighting the crucial role of Wnt in evolution and cellular patterning (Clevers & Nusse, 2012). The first successful purification of a functional Wnt ligand was achieved by Willert

et al. (2003), who were able to purify Wnt3a capable of stabilising β-catenin, a downstream target of canonical Wnt signalling. Wnt3a was shown to be palmitoylated on a conserved cysteine, and the removal of the palmitate caused the protein to become water soluble, and lose the ability to stabilise β-catenin. The importance of this palmitoleic acid lipid modification has subsequently been reinforced by structural studies of the Xenopus Wnt8 protein in complex with a Fzd receptor (Janda et al, 2012). The proteins where shown to interact in two places, one of which included the palmitoleic acid lipid.

The Wnt ligands bind a heterodimeric complex, composed of a Fzd receptor component, and a LRP5/6 co-receptor. The ten mammalian frizzled receptors, are seven transmembrane receptors with large cysteine-rich extracellular domains, important for Wnt ligand binding (Janda et al, 2012). The interaction between Wnt ligands and the frizzled receptors is promiscuous, with the ability of a single Wnt ligand to bind multiple Fzd receptors and vice versa (Bhanot et al, 1996; Wodarz & Nusse, 1998). As stated above, a co-receptor of either LRP5 or 6 is required for signal transduction (Wehrli et al, 2000), which act as a complex to transduce the signal. A crucial step in canonical Wnt signalling transduction is the recruitment of Axin to the cytoplasmic tail of the LRP5/6 co-receptor (Mao et al, 2001), which is a process regulated by the phosphorylation of the LRP5/6 cytoplasmic tail by GSK3β and casein kinase 1 (CK1) (Zeng et al, 2005).

While LRP5/6 transduces the signal, through the binding of Axin, Fzd function is required for LRP5/6 phosphorylation, furthermore, the forced association of Fzd and LRP6 is sufficient to trigger the phosphorylation of LRP6 (Zeng et al, 2008). One model for the involvement of the Frizzled receptors draws from the requirement of Dishevelled (Dvl)/Fzd interaction for the recruitment of Axin to LRP5/6 and its subsequent phosphorylation (Bilic et al, 2007; Zeng et al, 2008). This is thought to act through the binding of Dvl to the Axin component of the destruction complex, causing its recruitment to the Fzd/LRP receptor complex by Dvl binding to Fzd. This allows for the phosphorylation of LRP5/6 by GSK3β, inducing Axin/ LRP5/6 interaction (Zeng et al, 2008).

The mechanism by which Axin recruitment to the LRP5/6 co receptor leads to signal transduction can be explained by first understanding the mechanism for maintaining low levels of β-catenin in the cell. In resting cells, β-catenin is efficiently captured by a destruction complex, composed of Axin, Adenomatous polyposis coli (APC), Dvl, CK1 and GSK3β. This destruction complex causes the phosphorylation of β-catenin, first by CK1 at Ser45, priming β-catenin for phosphorylation by GSK3β at Thr41, Ser37, and Ser33 (Liu et al, 2002). This phosphorylation primes β-catenin for recognition by the F-box-containing protein β-TrCP ubiquitin E3 ligase, leading to the ubiquitination of β-catenin and its degradation by the proteosome (Aberle et al, 1997; Kitagawa et al, 1999), removing β-catenin from the complex thereby recycling the destruction complex for further β-catenin phosphorylation (Li et al, 2012). However, upon Wnt ligand binding to the Fzd receptor and co-receptor LRP5/6, Dvl and Axin are recruited to the receptor complex, as described above, leading to the disruption of β-catenin phosphorylation and degradation by the destruction complex allowing for β-catenin accumulation in the cytoplasm of the cell. The precise mechanism underlying this process is not clear, but a recent publication (Li et al, 2012) suggests that the recruitment of the destruction complex to the receptor complex prevents the ubiquitination of β-catenin, and therefore the removal of β-catenin from the destruction complex by the proteosome. This leads to the saturation of the destruction complex, allowing for the accumulation of β-catenin in the cytoplasm, where it can go on to translocate into the nucleus and alter gene expression.

Ultimately, canonical Wnt signalling exerts its effect through transcriptional control by β-catenin and its interaction with the TCF/LEF1 family of transcription factors (Behrens et al, 1996; Molenaar et al, 1996). TCF/LEF1 proteins are HMG (high mobility group) DNA-binding factors, which bind to a DNA sequence termed the Wnt responsive element (WRE), AGATCAAAGG (van de Wetering et al, 1997). In the inactive state, without β-catenin binding, TCF/LEF1 transcription factors interact with Groucho transcriptional repressors preventing gene expression (Cavallo et al, 1998). Upon Wnt activation and β-catenin translocation to the nucleus, Groucho is displaced by β-catenin, which then interacts in a complex with DNA, generating DNA bending and causing alterations in local chromatin structure (Behrens et al, 1996). The complex also recruits various transcriptional coactivators and histone

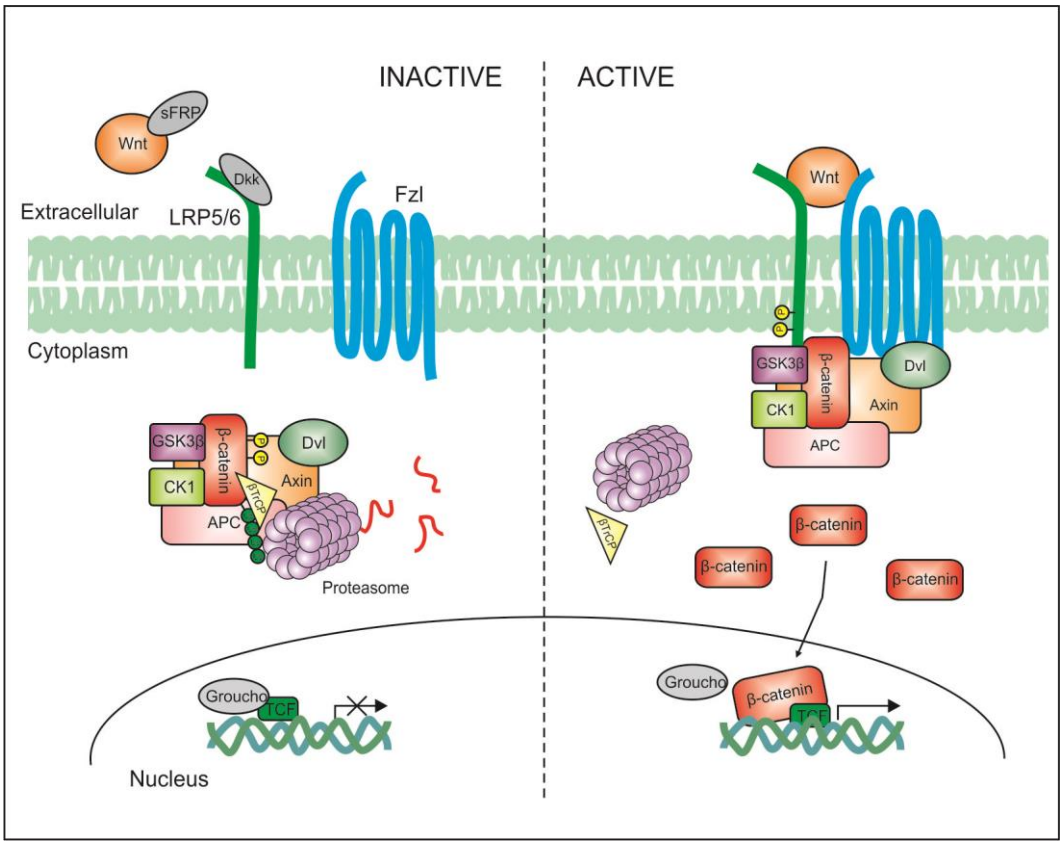

Figure 1.3.1. Schematic of Canonical Wnt signalling
In the absence of Wnt signalling, a destruction complex containing Axin, APC, GSK3β, CK1, βTrCP phophorylates β-catenin, leading to degradation by ubiquitination and the proteosome. Canonical Wnt signalling mediates its effect by binding to the receptors frizzled (Fzd) and co-receptors, LRP 5/6. This causes recruitment of the destruction complex to the membrane through Axin and Dvl interactions with the LRP5/6 co-receptor and Fzd receptor respectively. This leads to the dissociation of βTrCP and the proteosome from the destruction complex, and prevents the degradation of β-catenin, resulting in the stabilisation and nuclear translocation of β-catenin, inducing gene transcription via the LEF/TCF family of transcription factors.

modifiers to induce gene transcription (Clevers & Nusse, 2012). The process by which β-catenin enters the nucleus to interact with TCF/LEF1 transcription factors and instigate transcription is poorly understood, although recent work suggests a role for microtubule rearrangement and active transport of β-catenin upon Wnt activation (Sugioka et al, 2011)

In addition to the complexity of regulation dictated by the large array of Wnt ligands and receptors, there is also a range of negative regulators of the canonical Wnt pathway. Two protein families important in Wnt regulation are secreted Frizzled-related proteins (sFRPs) and Wnt inhibitory proteins (WIFs). Both of these are capable of binding to Wnt ligands, preventing the binding of Wnt proteins to their Fzd receptors. sFRPs can also bind the Fzd receptors themselves, blocking Wnt ligand binding (Bovolenta et al, 2008). A further two families, the Dickkopf (DKK) and WISE/SOST families, act by disrupting the formation of the Fzd/LRP receptor complex by binding to the LRP5/6 co-receptor (Semenov & He, 2006; Semënov et al, 2005). A final example of negative Wnt regulation is that of the Shisa protein family. Shisa acts within the endoplasmic reticulum, by interacting with immature forms of Fzd, preventing the post translational maturation and trafficking of the receptor (Yamamoto et al, 2005).

1.3.2 TGFβ-Superfamily Signalling Pathways

The TGFβ-superfamily is a large family of growth factors, containing at least 30 members in mammals. However, these can be categorised into two main groups; the transforming growth factor (TGF)β-like group that includes TGFβs, Activins, Nodals and some Growth and Differentiation Factors (GDFs), and the Bone Morphogenetic Proteins (BMP)-like group comprised of BMPs, most GDFs and Anti-Müllerian Hormone (AMH).

TGFβ-superfamily ligands are translated as large precursor proteins, consisting of a large amino terminal prodomain, important in protein folding, and a highly conserved carboxy-terminal region, containing the active ligand. These precursors dimerise due to disulphide linkages via conserved cysteine residues before being cleaved by proprotein convertases, to leave the TGF-β ligands non-covalently

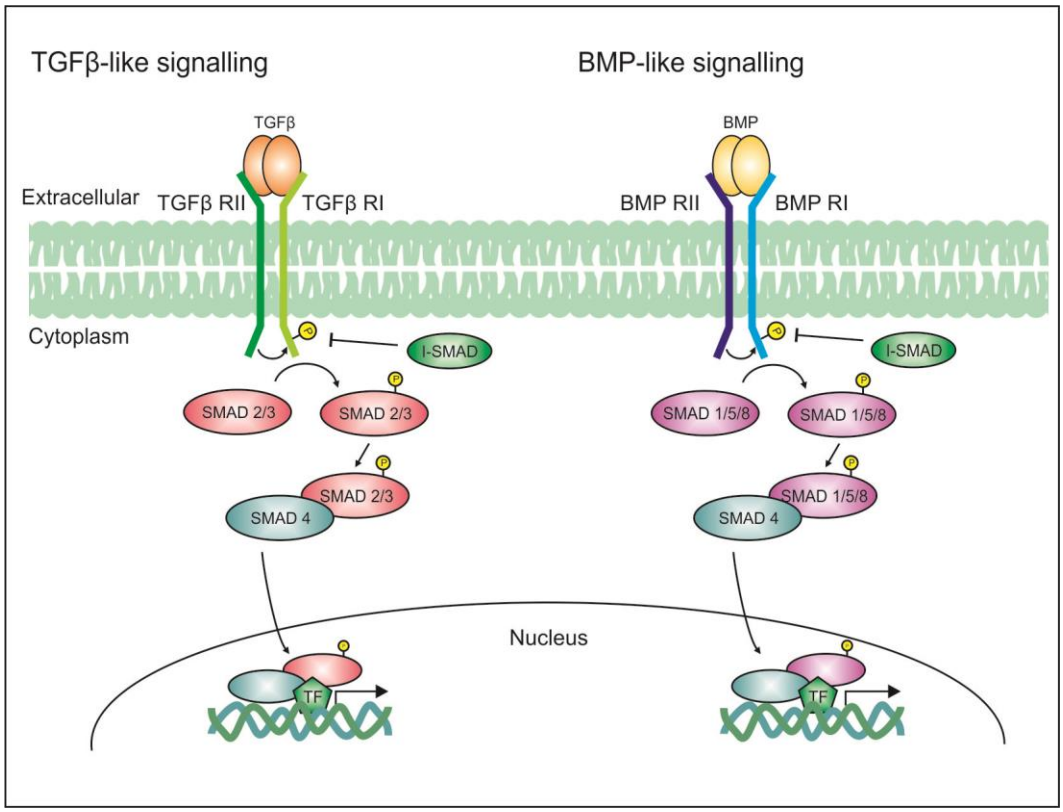

Figure 1.3.2. Schematic of TGFβ superfamily signalling
TGFβ/BMPs signal through a receptor heterodimer complex on the cell surface. The interaction with the ligand brings the type I (RI) and type II (RII) receptors together, allowing for the phosphorylation, and activation of RI, by the constitutively active RII. RI then phosphorylate and activate their respective R-SMADs, which in turn bind to the Co-SMAD (SMAD 4). This R-SMAD/Co-SMAD complex then enters the nucleus where it interacts with transcription factors to induce gene expression

associated with their prodomains, which are then secreted from the cell. The prodomain is thought to localise TGF-β ligands toward their target cells via interactions with extracellular matrix proteins (Harrison et al, 2011). Generally, ligands form homomeric complexes, although the existence of heteromeric complexes has been noted. These dimeric complexes then transmit their signal via a heteromeric receptor complex, comprising of type I and II transmembrane serine/threonine kinase receptors (Figure 1.3.2). In mammals, five Type I and seven Type II receptors exist, characterised by a cytoplasmic kinase domain that has strong serine/threonine kinase activity and weaker tyrosine kinase activity (Moustakas & Heldin, 2009). The effect of ligand binding, creating this heterotetrameric complex, is to bring the constitutively active Type II receptor into contact with the dormant Type I receptor, allowing for the phosphorylation of the Type I receptor, activating the kinase activity, and propagating the signal (Wrana et al, 1994). Despite the seven Type I receptors, they can be categorised into two families, those which propagate TGFβ-like ligand signalling onto TGFβ-like specific SMADS (SMADs 2/3), or those which propagate BMP-like ligand signalling onto BMP-like specific SMADS (SMADs 1/5/8). The phosphorylated Type I receptors phosphorylate the receptor SMADs (R-SMADs), which in turn leads to the interaction of the R-SMADs with SMAD4 (Co-SMAD). This R-SMAD/Co-SMAD complex then translocates to the nucleus of the cell, where they bind to chromatin and interact with other transcription factors and alter gene expression (Moustakas & Heldin, 2009). In the basal state, SMAD proteins continuously shuttle between the nucleus and the cytoplasm by interactions with nucleoporins, however when complexed as R-SMAD/Co-SMAD the transfer into the nucleus requires nuclear import and export factors (Hill, 2009). A third member of the SMAD family, the inhibitory SMADS (I-SMADS), also plays an important role in TGFβ-superfamily signalling. I-SMAD expression is activated by TGFβ-superfamily signalling, and they act as negative regulators of the signalling pathway through the binding to the Type I receptor, preventing binding to Type II receptors. I-SMADs also recruit phosphatases and Smurf ubiquitin ligases to down regulate receptor levels by ubiquitination and degradation (Kavsak et al, 2000).

SMAD complexes bind to the DNA at SMAD binding element (SBE) regions, which consist of direct or inverted repeats of its core sequence 5′-AGAC-3′ (Shi et al,

1998). In basal conditions, these SBE regions are bound by the transcriptional repressors SKI and SNON, which are rapidly degraded upon TGFβ-superfamily signalling (Levy et al, 2007). These short SBE regions only allow weak binding to the DNA and often require the interaction with other DNA-binding factors. The first factor that was shown to interact with SMADs to target DNA binding was Foxh1, which binds to the TGFβ R-SMADs 2/3, leading to the proposal that R-SMADs determine gene specificity through interaction with DNA binding partners, while the Co-SMAD acts to promote translational activity. Upon DNA binding, the SMADs recruit coregulators to promote transcription, including basic chromatin remodelling complexes and histone modifying acetyltransferases.

1.3.3 Hedgehog Signalling Pathway

Another well studied signalling pathway shown to be involved in bone development is the hedgehog (Hh) pathway (Hu et al, 2005; Long et al, 2004; St-Jacques et al, 1999) (Figure 1.3.3). Hedgehog signalling was first identified in *Drosophila* , where a single Hh protein regulates many diverse aspects of embryonic and adult patterning. Subsequent work has identified a highly conserved pathway in mammals, which shows a greater degree of complexity. This is most obvious in that there are three Hh proteins; Sonic hedgehog (Shh), Desert hedgehog (Dhh), and Indian hedgehog (Ihh). Some functional redundancy can be seen between these types, however they possess distinct expression profiles with little overlap (Bitgood & McMahon, 1995).

Hh proteins are transcribed as precursor molecules, which require a series of cleavage and translational modification events before secretion from the cell (Varjosalo & Taipale, 2007). All Hh proteins signal through the same receptors and signalling pathway, which is triggered by the binding of Hh to its receptor, Patched (Ptc). In the absence of any Hh interaction, Ptc acts to inhibit the activity of a 7-transmembrane protein, Smoothened (Smo). One explanation for this inhibition was proposed by Taipale *et al*, (2002), where in the absence of Hh, Ptc translocates a small molecule, which can regulate Smo activity, across the membrane bilayer. The small molecule substrate could then be acting either as a Smo agonist before or as an antagonist after translocation by Ptc. Upon Hh binding to Ptc, Smo repression is

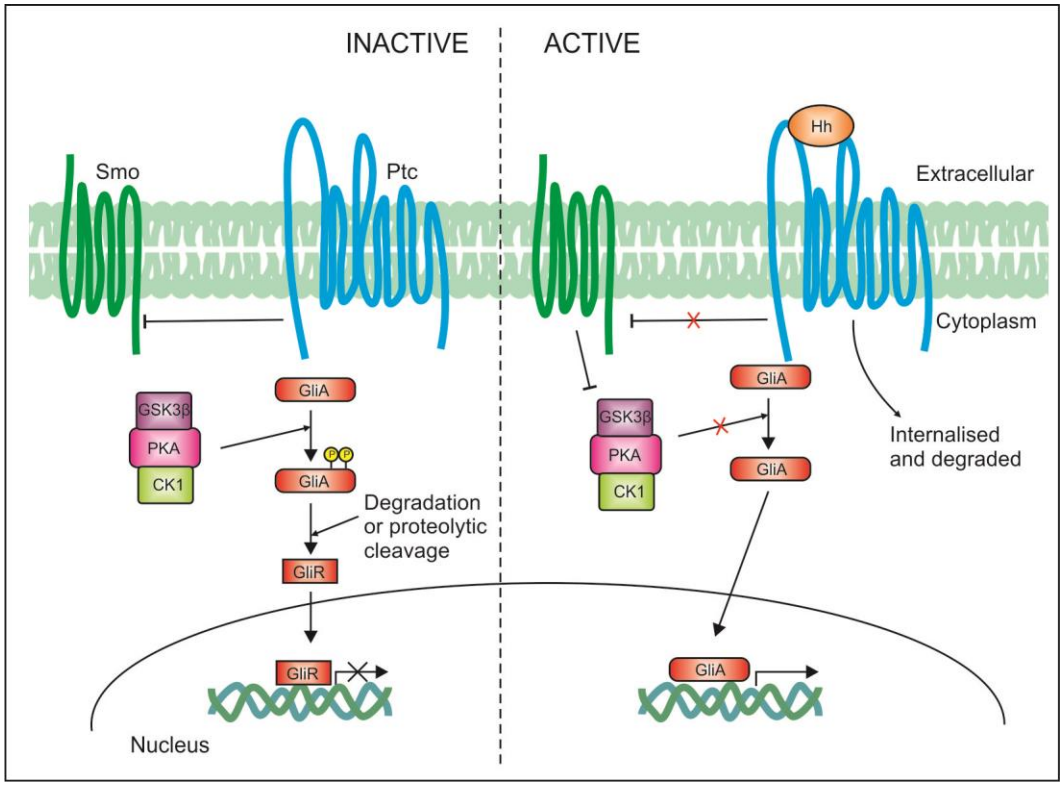

Figure 1.3.3. Schematic of Hedgehog signalling
In the absence of any Hedgehog ligand the Hedgehog signalling complex phosphorylates the Gli family of transcription factors, leading to degradation or proteolytic cleavage to transcriptional repressors (GliR). In the presence of Hedgehog ligand, signalling is mediated through the binding of Hedgehog to their receptor Patched (Ptc). This causes the inhibition of a second transmembrane protein, Smoothened (Smo), to be relieved. Smo is then able to inhibit the Hedgehog signalling complex preventing the phophorylation of the Gli proteins, priming them for transcriptional activation (GliA).

alleviated leading to signal transduction and the conversion of the Ci/Gli family of transcription factors to an activating state. It is at this stage that an additional level of complexity is generated in mammals. *Drosophila* possess a single Ci transcription factor, while there are three Gli transcription factors in mammals; Gli1, 2, which generally act as transcriptional activators, and Gli3, which acts as a repressor (Gupta et al, 2010).

Smo exerts its effect on signal transduction by inhibiting the hedgehog signalling complex, primarily consisting of GSK3β, protein kinase A (PKA) and CK1. Under inactive conditions, when Smo activity is inhibited by Ptc, this complex acts to phosphorylate the Gli transcription factors, priming the Gli proteins for degradation or proteolytic cleavage. This has the overall effect of increasing the transcriptional repressor forms of the Gli proteins, preventing target gene transcription. Conversely, the release of inhibition of Smo, by Hh binding to Ptc, results in inhibition of the Hedgehog signalling complex, and therefore prevents phosphorylation of the Gli proteins. The predominant Gli state is therefore converted to activatory, leading to the transcription of target genes.

1.4 Cell signalling during MSC differentiation

Cell signalling is important for both the embryonic development and maintenance of adult tissues and organs, including that of MSC differentiation and bone homeostasis. The involvement of three important signalling pathways in MSC differentiation are described below, and their role in the commitment towards osteoblasts, adipocytes and chondrocytes is reviewed.

1.4.1 Osteogenesis

1.4.1.1 Canonical Wnt signalling

Wnt signalling was first implicated in bone regulation by studies of osteoporosis pseudoglioma syndrome patients (characterised by low bone mineral density) who possessed loss of function mutations in the co-receptor LRP5, and therefore reduced canonical Wnt signalling (Gong et al, 2001). Subsequent studies in patients with high bone mass showed the converse to also be true. Mutations in the N-terminus of

LRP5 reduce its binding affinity with the Wnt signalling inhibitor Dkk1, thereby preventing Wnt inhibition, leading to this high bone mass phenotype (Boyden et al, 2002). Mouse models have reinforced these discoveries, in which LRP5 over expression (Babij et al, 2003) and reduced inhibition of Wnt signalling by sFRP1 knock down (Bodine et al, 2004) resulted in increased bone mass and density.

In light of these bone anabolic responses to altered Wnt signalling and the clear correlation between osteo-inducers and increased Wnt signalling, many *in vivo* and *in vitro* studies have been carried out using a range of activators and inhibitors of the Wnt signalling pathway, with the aim of identifying the molecular basis behind the increased bone mass phenotype. One process by which Wnt signalling may act to increase bone formation that has received a lot of attention is the stimulation of osteoblast development. Inhibition of GSK3β enzyme activity using LiCl or small molecules, caused increased β-catenin nuclear translocation, and stimulated the mouse mesenchymal precursor cell line, C3H10T1/2, to express osteoblast specific genes (Jackson et al, 2005; Kulkarni et al, 2006). Similar studies were also carried out using Wnt10b to stimulate the canonical Wnt pathway (Bennett et al, 2005) in bipotential ST2 cells, resulting in increased expression of osteoblast-specific genes and mineralisation. Similarly, over expression of Dkk1 reduces osteoblast differentiation (Krishnan et al, 2006). Further to this, *in vivo* work has shown that administration of LiCl, a GSK3β inhibitor, to C57BL/6 mice for 4 weeks dramatically increased bone formation rate (Clement-Lacroix et al, 2005). One route by which Wnt is thought to promote osteogenesis is through the direct stimulation of Runx2 expression (Gaur et al, 2005). Gaur *et al.* (2005) identified a TCF binding site in the promoter of Runx2 and demonstrated an increase in Runx2 expression in response to co-expression of TCF and canonical Wnt proteins.

However, while there is a good deal of evidence in mouse *in vivo* and *in vitro* for the role of Wnt in inducing osteogenic differentiation, the research in human MSCs is much less conclusive and straightforward. This difference is clearly demonstrated by the work carried out by Boland *et al* (2004), which demonstrated that Wnt3a conditioned media, leading to canonical Wnt signalling, caused inhibition of osteogenic differentiation demonstrated by reduced ALP mRNA and activity and decreased mineralisation (Boland et al, 2004). Induced Wnt signalling did however

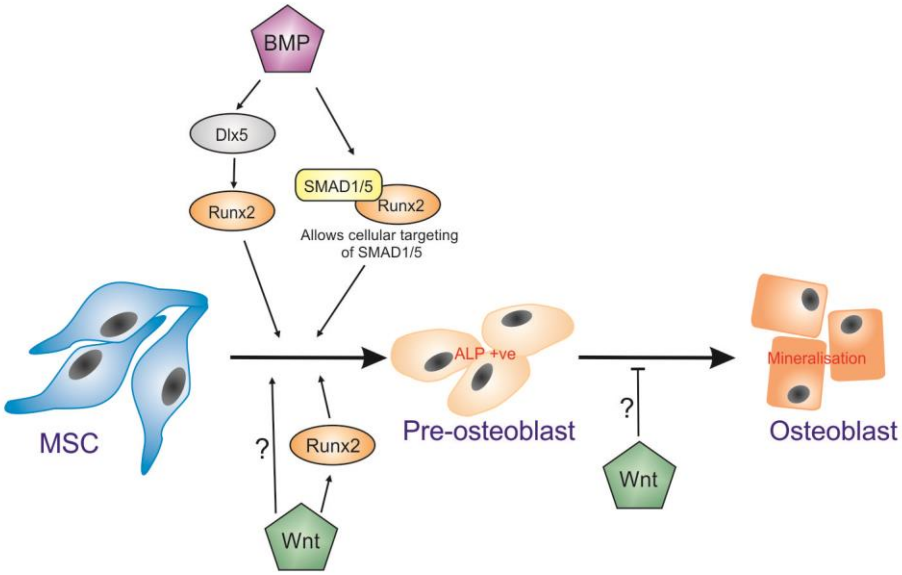

Figure 1.4.1. Schematic showing the interplay between transcription factors and cell signalling during osteogenic differentiation

Both BMP and canonical Wnt signalling play important roles in osteogenic differentiation of MSCs. BMPs induce the expression of Runx2, via Dlx5, leading to the upregulation of osteogenic genes. Runx2, also acts to direct SMAD1/5 transcription factor complexes to specific chromatin loci, where osteogenic genes are grouped. The role of canonical Wnt signalling is less clear. Canonical Wnt signalling appears to increase the initial stages of osteogenesis, generating ALP positive pre-osteoblasts, potentially through the up regulation of Runx2. However, canonical Wnt signalling prevents the final maturation into mineralising osteoblasts.

appear to increase the proliferation rate of human MSCs, whilst at the same time reducing apoptosis. Similar results have been shown in human MSCs by inducing Wnt signalling at different stages of the canonical pathway, including LRP5 and TCF1 (Baksh et al, 2007a), which caused reductions in the osteogenic marker, ALP, and increased cell numbers. Interestingly these studies also identify the non-canonical Wnt signalling pathway, induced by Wnt5a, as an activator of osteogenesis in human MSCs, capable of inhibiting the effect of Wnt3a activity.

One explanation for the discrepancies in the literature is the differentiation state of the cells receiving the Wnt stimulation, and several publications attempt to address this in more detail. Eijken *et al* (2008) used a human foetal osteoblastic cell line, with which they generated a non-differentiating and differentiating population, through the addition of the synthetic glucocorticoid, dexamethasone. By generating these two populations of undifferentiating and differentiating cells, Eijken *et al.* (2008) demonstrated that non-differentiating cells have higher endogenous canonical Wnt signalling, and that increased signalling by LiCl had differential effects on these two populations. Non-differentiating cells generated increased ALP in response to LiCl, indicative of enhanced early osteogenesis, while the differentiating cells had reduced ALP activity upon LiCl treatment, and reduced mineralisation. Using an alternative approach, utilising the range of cell types that can be obtained from mouse models, Quarto *et al*. (2010) used a selection of multipotent, pre-osteoblast and osteoblast cells to study the effect of Wnt manipulation on cells at different stages of osteogenesis. As shown by Eijken *et al.* (2008), the undifferentiated cells had higher basal levels of canonical Wnt signalling, demonstrated by downstream target expression and nuclear β-catenin levels. This approach also allowed for the study of the effect of increased canonical Wnt signalling by Wnt3a on the differentiation of cells at different stages of osteoblast progression. Multipotent cells derived from the adipose tissue or embryonic calvaria failed to differentiate towards osteoblasts in the presence of Wnt3a, however osteoblast cells responded positively to Wnt3a, with increased ALP and mineralisation in combination with differentiation conditions. In addition to these studies, a series of publications studying the effect of LEF1 on osteogenic differentiation demonstrated an inhibitory effect of increased canonical Wnt signalling on osteoblast maturation (Kahler et al, 2006; Kahler & Westendorf, 2003). Conversely, Krause *et al*. (2010) used a mild osteogenic

stimulus to promote the early stages of osteogenesis, and demonstrated an increase in early osteogenic markers such as ALP and Osteoprotegerin in response to GSK3 inhibition with 6-bromoindirubin-3′-oxime (BIO), suggesting an enhancement of the early stages of osteogenesis by canonical Wnt signalling. Collectively it seems that canonical Wnt stimulates differentiation of cells committed to the osteogenic lineage, but can inhibit the differentiation of multipotent cells, and prevent the terminal differentiation of mature osteoblasts (Figure 1.4.1).

Furthermore, increased canonical Wnt signalling has regularly been linked to increased bone mass in response to osteo-inductive substances such as Fibroblast growth factor (FGF) 2 (Fei et al, 2011), estrogen-related receptor α (Auld et al, 2012), strontium (Yang et al, 2011), bisindoylmaleimide I (Zhou et al, 2012), sclerostin (Jawad et al, 2013) and miR-142p (Hu et al, 2013), again suggesting an important role for canonical Wnt signalling in the increased differentiation and maturation of osteoblasts. However, despite the clear involvement of canonical Wnt in these situations, the manner in which they function remains unclear.

1.4.1.2 TGFβ-superfamiliy signalling

In addition to canonical Wnt signalling, BMPs have also been shown to play an important role in the osteogenic differentiation of MSCs. BMPs were first identified as proteins that were capable of inducing endochondral bone formation and increasing osteoblast differentiation *in vitro* (Sampath et al, 1992). However it is now known that BMPs play vital roles in a wide variety of embryonic processes, including gastrulation, neural development and endothelial cell function (Gitelman et al, 1995; Valcourt & Moustakas, 2005). This review of the literature will however concentrate on the roles of BMPs on the differentiation of MSCs. As stated above, the application of recombinant BMPs to *in vitro* pre-osteoblast cultures results in increased osteoblastogenesis, demonstrated by increased ALP, OC expression and matrix mineralisation (Sampath et al, 1992), while the blocking of BMP signalling both arrests osteogenesis and prevents the programmed cell death of mature osteoblasts. BMPs are thought to induce osteoblast differentiation through the activation of Runx2 (Lee et al, 2000). Work in multiple mouse cell lines has demonstrated that this increase in Runx2 activity in response to BMPs is indirect and

acts through Dlx5 (Lee et al, 2003a). Runx2 is also thought to interact with SMAD1 and 5. These SMAD-Runx2 complexes are directed by the Runx2 targeting signals to sub-nuclear foci where gene targets for both transcription factors are present. This suggests that SMAD transcriptional activation is at least in part dependent on the targeting factors of Runx2 (Zaidi et al, 2002) (Figure 1.4.1). It is interesting to note that BMP2 stimulation of Dlx5 increased the expression of Osx independently of Runx2, implicating Dlx2 as an important regulator of early and late BMP-induced osteogenesis (Lee et al, 2003b).

Another member of the TGFβ-superfamily, TGFβ also plays a role in the regulation of osteogenic differentiation. Unlike BMP-specific SMADs, TGFβ SMADs do not induce osteogenesis, but in fact act to repress the pro-osteogenic effects of BMPs. This inhibition is mediated through SMAD3, which interacts with Runx2 repressing its transcriptional activity (Alliston et al, 2001).

1.4.1.3 Hedgehog signalling

Hh signalling, and more specifically Ihh signalling, has been linked to osteogenesis, and is indispensable for osteoblast development during endochondral ossification. This was strikingly shown in $Ihh^{-/-}$ mice, which demonstrated a complete failure of osteoblast development in endochondral bones (St-Jacques et al, 1999). Further to this, genetic manipulation of Smo, resulting in removal of Smo from the perichondral cells using a Cre-LoxP system, resulted in the failure of osteoblast differentiation (Long et al, 2004). In addition to these *in vivo* experiments, the role of Hh signalling in mesenchymal commitment has been studied *in vitro*. The induction of the hedgehog pathway, by addition of recombinant Hh protein, in C3H10T1/2 cells, induced osteogenesis, with ALP activity detectable after just two days of treatment (Hu et al, 2005).

Furthermore there is evidence for interactions between the Hh and Wnt pathways in relation to osteogenesis. $Ihh^{-/-}$ mice showed a disrupted Wnt signalling phenotype at E14.5 and E16.5, with an absence of nuclear β-catenin staining in the perichondral cells, as compared to the positive staining of the wild type mice (Hu et al, 2005). To investigate the functional relationship between Hh and Wnt signalling as inferred by

the $Ihh^{-/-}$ mice, the same group used an *in vitro* C3H10T1/2 differentiation model, in which Ihh over expression led to ALP expression in the Ihh-expressing cells. This osteogenic differentiation was however reduced by ~50% when the cells were co-transfected with either DKK or double negative Tcf4 constructs. In addition to this, Wnt5a, Wnt7b and Wnt 9a mRNA levels were significantly induced over controls in response to 24 and 48 hours of Hh treatment. This body of work suggests that Hh signalling acts upstream of Wnt signalling and that Wnt signalling is required, at least in part, for the osteogenic inducing potential of Hh.

1.4.2 Adipogenesis

1.4.2.1 Canonical Wnt signalling

In addition to the large number of studies looking into the role of canonical Wnt signalling in osteogenesis, it is also well studied with relation to adipogenic differentiation. Many studies have been performed which implicate canonical Wnt signalling as an inhibitor of adipogenesis (Prestwich & Macdougald, 2007), and some of the key findings are discussed here. Upon canonical Wnt stimulation adipogenesis of MC3T3-L1 cells is completely inhibited, but does not affect the expression of the early adipocyte transcription factors, C/EBPβ and δ. It does however block the expression of C/EBPα and PPARγ and the downstream gene, FABP4 (Bennett et al, 2002). The inhibition of PPARγ is thought to be via the activation of chicken ovalbumin upstream promoter transcription factor II (COUP-TFII), leading to the recruitment of the silencing mediator of retinoid and thyroid hormone receptors (SMRT) co-repressor complex (Figure 1.4.2). This binds to the PPARγ gene, maintaining the chromatin in a hypoacetylated state repressing its expression (Okamura et al, 2009). Conversely, the expression of Wnt inhibitors, reducing endogenous Wnt, causes the spontaneous adipogenic differentiation of pre-adipocytes (Bennett et al, 2002).

This work, along with related findings, identifies canonical Wnt as an important switch in the lineage decisions of MSCs, with canonical Wnt maintaining the cells in a multipotent state until its coordinated removal results in adipogenesis. Recently,

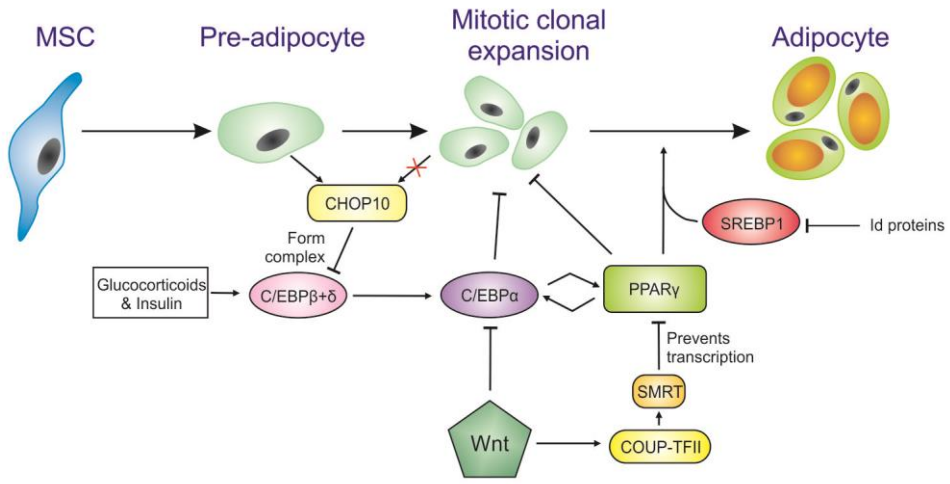

Figure 1.4.2. Schematic showing the interplay between transcription factors and cell signalling during the adipogenic differentiation
Hormonal signals such as glucocorticoids and insulin lead to the upregulation of C/EBPβ+δ, which in turn up regulate C/EBPα expression. C/EBPα and PPARγ enter a positive feedback loop, increasing each other's expression. PPARγ is then able to induce expression of adipocyte genes and induce adipocyte maturation. Canonical Wnt signalling inhibits adipocyte maturation via COUP-TFII and SMRT, inhibiting PPARγ transcription. Both C/EBPα and PPARγ inhibit the mitotic clonal expansion stage, and therefore their expression must be delayed. This is achieved through the expression of CHOP10 in pre-adipocytes, which interacts with C/EBPβ, preventing its up regulation of C/EBPα.

work has been carried out studying the relationship between adipogenesis and osteogenesis in response to canonical Wnt signalling (Liu et al, 2009). Liu *et al* (2009) were able to show that human MSCs under dual osteogenic and adipogenic conditions, preferentially formed osteoblasts in response to Wnt3a administration. This response was shown to be due to differential inhibition of the two differentiation processes, where adipogenesis is totally inhibited at low Wnt stimulation, and osteogenesis is only partially inhibited. This suggests that under dual lineage differentiation conditions, differences in sensitivity to Wnt inhibition may alter the equilibrium and shift the commitment from adipocytes toward osteoblasts.

1.4.3 Chondrogenesis

1.4.3.1 Canonical Wnt signalling

Canonical Wnt signalling is also influential in the differentiation of MSCs into chondrocytes. This was demonstrated by Day *et al* (2005) who generated mice with ectopic induction of canonical Wnt signalling in the developing limb bud. These mice showed enhanced ossification and reduced chondrocyte formation. Furthermore, inactivation of β-catenin, therefore preventing canonical Wnt created the opposite phenotype, with ectopic chondrocyte differentiation, and reduced osteogenesis (Day et al, 2005). These findings correlate with those in human MSC culture, where inhibition of canonical Wnt signalling by sFRPs and DKK over expression causes enhanced chondrogenesis, with up regulation of Col2A1, Sox9 and glycosaminoglycan expression, and a decrease in Col1A1. However, Wnt inhibition does not induce the expression of type X collagen alpha 1 (Col10A1) (Im et al), suggesting Wnt inhibition can induce early chondrocyte differentiation, but not final maturation and hypertrophy. *In vitro* investigations studying the activation of canonical Wnt in chick upper sternal chondrocytes, by the over expression of Wnt8c, 9a or β-catenin, demonstrated that canonical Wnts where in fact required for, and could increase chondrocyte hypertrophy. Canonical Wnt activation led to decreased Sox9 and Col2A1 expression, whilst increasing the hypertrophic markers Col10A1 and Runx2. Canonical Wnt exerts these effects, at least in part, through the LEF/TCF activation of Runx2 and in turn induces the expression of Col10A1 (Dong

et al, 2006). In summary, down regulation of canonical Wnts can increase the early stages of chondrogenesis, increasing Sox9 and Col2A1, but its up regulation is required for the final maturation, and hypertrophy, through Runx2 and Col10A1 upregulation, and reduction of Sox9.

1.4.3.2 TGFβ-superfamiliy signalling

BMPs not only induce osteoblast differentiation, but also have pro-chondrogenic characteristics, and have been shown to increase the expression of type II and X collagen in growth plate cultures (De Luca et al, 2001). BMPs exert their effect on chondrogenesis through the chondrogenic master regulator Sox9. Beads soaked in BMP4 implanted into mouse mandibular explants induced ectopic cartilage formation in the proximal position of the explants. These same areas also had upregulation of the Sox9 transcription factor, implicating its role in BMP induced chondrogenesis. Interestingly, BMP4-soaked beads did not induce chondrogenesis in the rostral position, despite similar up regulation of Sox9. However, upregulation of the homeodomain transcription factor Msx2 was also seen in the areas surrounding the beads, and to a much greater degree in rostral region of the explants. Furthermore, ectopic expression of Msx2 prevented the BMP4-induced chondrogenesis, and reduced endogenous chondrogenesis (Semba et al, 2000). This body of work demonstrates that BMP induction of chondrogenesis via Sox9, is also dependent on the expression of Msx2, generating a threshold for chondrogenesis, thereby providing a means for positional regulation of chondrogenesis *in vivo*.

In contrast to the inhibitory effect of TGFβ signalling on osteogenesis, it is required for the *in vitro* chondrogenic differentiation of multipotent mesenchymal cells, acting through the p38, ERK-1, and JNK MAP Kinases (Lutz & Knaus, 2002).

1.4.3.3 Hedgehog signalling

Chondrogenesis is also reliant on the complex cross-talk between the BMP and Shh signalling pathways. Shh signalling initiates the expression of the homeobox protein, Nkx3.2, while BMP signals act to maintain its expression (Murtaugh et al, 2001), allowing the transcription repressor activity of Nkx3.2 to block the activity of

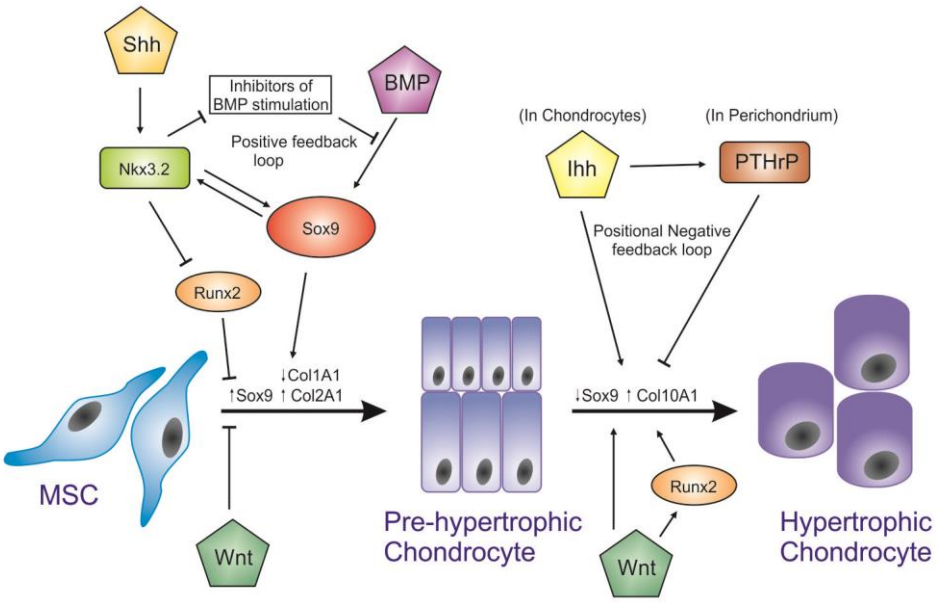

Figure 1.4.3. Schematic showing interactions between transcription factors and signalling pathways during chondrogenic differentiation
Shh and BMPs act together to generate a positive feedback loop with Sox9 and Nkx3.2, stimulating the differentiation of MSCs into prehypertrophic chondrocytes, while Wnt signalling inhibits the initiation of chondrogenic differentiation. Wnt signalling is, however, required for the switch between pre-hypertrophic and hypertrophic chondrocytes, through increased Runx2 activity, leading to reduced Sox9 expression and increased Col10A1. Ihh expression in pre-hypertrophic chondrocytes stimulates the switch to hypertrophic chondrocytes, and also causes PTHrP expression in the surrounding perichondrium, which in turn inhibits hypertrophy in the leading edge of the developing limb, generating a positional negative feedback loop

inhibitors of BMP-induced chondrogenesis. Interestingly, Nkx3.2 also acts to repress Runx2 activity, which otherwise prevents the onset of differentiation (Lengner et al, 2005). Furthermore, Nkx3.2 can induce the expression of Sox9 (Zeng et al, 2002), which in turn can increase expression of Nkx3.2, generating a positive feedback loop maintaining the expression of pro-chondrogenic factors (Figure 1.4.3). In summary, BMP acts to induce Runx2, stimulating osteogenic differentiation, yet acting alongside Shh signalling during chondrogenesis, generates and maintains high levels of Nkx3.2 leading to the down regulation of Runx2 and increased Sox9, allowing the onset of chondrogenesis.

Ihh is also implicated in the switch between pre- and hypertrophic differentiation, where it is thought to act with parathyroid hormone-related protein (PTHrP) to generate a negative feedback loop regulating the onset of hypertrophy. Ihh signalling by the developing chondrocytes targets the surrounding perichondrium, where it leads to PTHrP expression. PTHrP then signals to the pre-hypertrophic chondrocytes preventing the initiation of hypertrophic differentiation (Vortkamp et al, 1996) (Figure 1.4.3). It is postulated that the level of Ihh/PTHrP signalling can regulate the distance between the joint region and the onset of hypertrophy.

1.5 GSK3β inhibitors

GSK3β inhibitors have commonly been used as Wnt mimetics, through the disruption of the destruction complex, leading to β-catenin stabilisation, allowing its nuclear translocation and gene activation. The use of GSK3β inhibitors to stimulate the canonical Wnt pathway offers two clear advantages over the use of Wnt ligands; 1) they act downstream of the ligand-receptor complex formation, alleviating the complexities originating from the large array of both ligands and receptors (discussed in 1.3.1), preventing differences in the response to a particular stimulus by cells expressing subtly different receptors. 2) Small molecule inhibitors are much easier and cheaper to produce than functionally active Wnt proteins, increasing their potential as therapeutic canonical Wnt modulators.

In fact GSK3β inhibition has been extensively studied for its capacity to correct a variety of bone disorders in mouse models. Lithium, a naturally occurring GSK3β

inhibitor has been shown to increase the bone mass of mice after oral administration for 4 weeks, and restore that of LRP5 deficient animals (Clement-Lacroix et al, 2005). In a similar manner, Wnt signalling was shown to be required for fracture repair in mouse models, and lithium treatment after fracture lead to enhanced repair (Chen et al, 2007a). These findings support the observations from human patients, in which lithium treatment reduced the risk of fracture (Vestergaard et al, 2005), and patients treated with lithium carbonate for neurological disorders had significant increases in bone mass (Zamani et al, 2009). Lithium is however a relatively non-specific and weak inhibitor of GSK3β (Davies et al, 2000), leading to the generation of pharmacological inhibitors of GSK3β, with increased specificity and potency, such as 6-bromoindirubin-3′-oxime (BIO), LY603281, and AR28. LY603281 was shown to increase the bone density and strength in mice after 60 days administration (Kulkarni et al, 2006), and restored both the bone volume and marrow adiposity due to oestrogen deficiency in ovariectomised rats (Kulkarni et al, 2007). Similarly, AR28 administration both by subcutaneous injection and orally lead to increased bone mass and trabecular bone thickness in mice, and is discussed in more detail below (Gambardella et al, 2011; Marsell et al, 2012; Sisask et al, 2013).

1.5.1 AR28

AR28 (or AZD2858) is designed around a pyrazine structure, with the addition of multiple functional groups (Figure 1.5.1 A) and has been shown to be a potent inhibitor of GSK3, with an IC_{50} of 5 nM for GSK3β, and relatively high specificity over a panel of other kinases (Gambardella et al, 2011). Using X-ray crystallography, it was shown that AR28 interacts with the ATP binding site of the GSK3β protein (Figure 1.5.1 B), preventing ATP binding and therefore enzyme activity (Berg et al, 2012). Furthermore, inhibition of GSK3β by AR28 has been shown to increase nuclear β-catenin in C3H10T1/2 cells after 24 hours treatment, which is indicative of activation of the canonical Wnt signalling pathway (Gambardella et al, 2011).

Due to the links between canonical Wnt signalling and bone anabolism, AR28 has been studied in several mouse models. Initial work demonstrated that subcutaneous injection into BALB/c mice lead to increased bone density after 14 days of

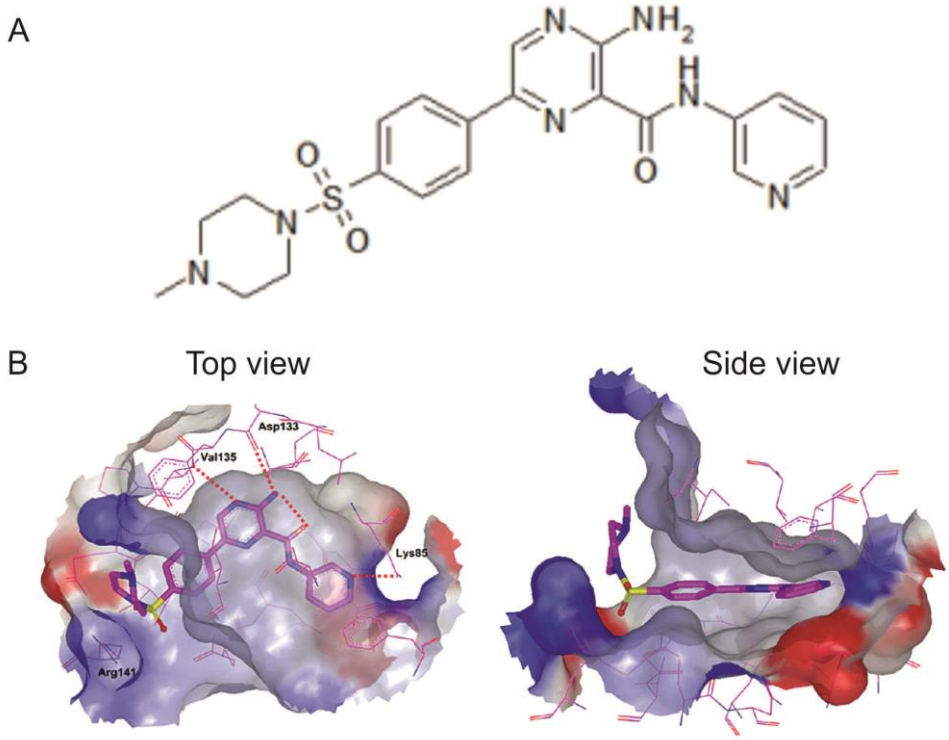

Figure 1.5.1. AR28 chemical structure and protein interaction
A) Chemical structure of AR28. B) X-ray crystal structure of AR28 in the ATP binding site of GSK3β, showing hydrogen bond formation between compound and amino acids of GSK3β (Taken from Berg *et al*, (2012)).

treatment, and that this was likely through the increased proliferation of mesenchymal progenitors which were then driven to the osteogenic lineage (Gambardella et al, 2011). Subsequent studies demonstrated the capacity for oral administration of AR28, with detectable levels of AR28 in the circulating blood of Sprague Dawley rats (Marsell et al, 2012). As with subcutaneous injection, orally-administered AR28 caused increased bone mass, preferentially at sites of trabecular bone. Compression and diaphysea strength were also increased by AR28 administration. This increase in bone mass was accompanied by increases in serum marker levels for bone formation and resorption, suggesting an increase in bone formation and remodelling is responsible for the increases in bone mass, and not a reduction in resorption (Marsell et al, 2012). Finally, oral administration of AR28 one day after the generation of femoral fractures in rat models lead to enhanced fracture repair within 3 weeks of treatment, with increased mineral density and content in the calluses (Sisask et al, 2013). Interestingly, AR28 treated fractures healed without the formation of cartilage islets, suggesting a strong osteogenic induction, but inhibition of cartilage formation by GSK3β inhibition.

1.6 Project Aims

Despite the ever growing number of publication linking the effect of proteins to increased osteogenesis through the upregulation of canonical Wnt (Hu et al, 2013; Jawad et al, 2013; O'Shea et al, 2012; Zhou et al, 2012), the mechanism by which canonical Wnt signalling leads to these increases remains unclear. Therefore the aims of this project are to investigate these discrepancies in the literature, through the activation of canonical Wnt signalling downstream of receptor binding, by GSK3β inhibition, and identify its role in human MSC differentiation. Initial work aims to further characterise the ability of AR28, a GSK3β inhibitor, to activate the canonical Wnt signalling pathway *in vitro*, through study of β-catenin stabilisation and TCF/LEF1 transcription factor activation, but also in *in vivo* conditions using *Xenopus* axis duplication studies. Following AR28 characterisation, it will be used to uncover the unresolved questions regarding the differentiation of MSCs, focussing on osteogenesis in particular. Differentiation will be studied using a range of osteogenic cues, to study the effect of activated canonical Wnt signalling on different stages of differentiation. Finally, the effect of canonical Wnt activation under bi-

potential conditions will be identified, as during *in vivo* differentiation multiple cues are likely to be acting upon mesenchymal precursors simultaneously. A highly regulated signalling pathway such as canonical Wnt signalling is therefore a likely candidate for regulation of the response to these various signals, controlling lineage commitment decisions.

Chapter 2: Materials and Methods

2.1 Materials

All chemicals were purchased from Sigma Aldrich (St. Louis, MO, USA) unless otherwise stated. All cell culture flasks and plates were purchased from Corning Life Sciences (Corning, NY, USA). Cell culture media, foetal bovine serum (FBS), phosphate buffered saline (PBS), TrypLE Express and Trypsin-EDTA were purchased from Invitrogen (Carlsbad, CA, USA). All Dulbecco's Modified Eagle Medium (DMEM) used contained L-glutamine and high glucose (Cat# S41966-052). The TOPFlash plasmid was a kind gift from R Moon (University of Washington, Seatle, WA USA). The 4Col2E plasmid was a kind gift from Shuji Muramatsu (Asahi Kasei Pharma Corp.). The Gli-BS and m3'Gli-BS plasmids were kind gifts from Hiroshi Sasaki (CDB, Riken , Kobe, JP) The pRK5-Sox9 plasmid was made by Aixin Cheng in the Genever Lab (Cheng & Genever, 2010). Recombinant BMP2 was purchased from NIBSC (South Mimms, UK). Recombinant mouse Wnt3a was purchased from R&D systems (Minneapolis, MN, USA).

2.2 General Methods

2.2.1 Cell Culture methods

2.2.1.1 Cell line culture conditions

The mouse multipotent stromal cell line, C3H10T1/2, and Human Embryonic Kidney cell line, HEK293, were cultured in DMEM with 10% FBS and 100U/ml Penicillin/100µg/ml Streptomycin (1% P/S). Cells were passaged upon reaching 90% confluency at 1:4 using trypsin/EDTA. All cells were incubated at 37°C in 5% CO_2 /95% air humidified atmosphere.

2.2.1.2 Extraction of MSCs from Femoral heads

Extraction was performed as described in Etheridge *et al.* (2004) Briefly, trabecular bone was mechanically removed from the femoral head and transferred to a tube

containing 10 ml DMEM containing P/S. The trabecular bone was then minced, and the bone fragments allowed to settle before the media was transferred to another tube. Fresh media was added to the bone fragments and the bone minced again before the media was transferred to another tube. The process was repeated two more times before medium was added to the bone fragments and vortexed for 1 minute before the media was transferred to a separate tube. The collected medium was then centrifuged for 5 minutes at 450g and the supernatant removed. The pellet was resuspended in 16 ml of medium and passed through at 70 µm cell strainer (BD Falcon, Oxford, UK). The cell solution was then layered over 12 ml of Ficoll-Paque Plus (GE Healthcare, Waukesha, WI, USA) and centrifuged at 250g for 30 minutes with low braking. The white mononuclear layer was then collected from the interface and added to 10 ml wash buffer (5 mM EDTA, 0.2% Bovine Serum Albumin (BSA) in PBS). The cells were centrifuged at 450g for 5 minutes and the supernatant removed before resuspension in MSC expansion media (DMEM, 15% FBS, 1% P/S) and seeded onto cell culture plastic T75 flasks. The cells were allowed to settle for 3-4 days before the medium was replaced. The cells were then expanded as below.

2.2.1.3 Extraction of MSCs from knee samples

Bone samples from knee surgery were dissected into small pieces and placed cut face down onto cell culture treated plastic petri dishes, and covered in MSC expansion media. Cells were allowed to migrate out of the bone tissue and attach to the flasks for 1 week before bone fragments were removed and the media replaced. Cells were then expanded as below.

2.2.1.4 MSC and hADSC expansion

Bone marrow MSCs extracted as described above were cultured in MSC expansion media (DMEM, 15% FBS, 1% P/S). Cells were passaged upon reaching 90% confluency at 1:3 using trypsin/EDTA. Human adipose derived stem cells (ADSCs) were cultured in MesenPRO RS (Invitrogen, Carlsbad, CA, USA). Cells were passaged upon reaching 90% confluency using TrypLE Express and counted and

seeded at $4x10^3$ cell/cm^2. All cells were incubated at 37°C in 5% CO_2 /95% air humidified atmosphere.

2.2.1.5 Mycoplasma testing

All cell cultures were regularly tested for mycoplasma contamination. Cells were washed twice in PBS and fixed with 100% methanol for 5 minutes. Samples were washed twice more in PBS before the addition of DAPI at 1µg/ml. Samples were incubated for 5 minutes in the dark before the DAPI was removed and the samples washed in PBS, and finally stored in PBS. Samples were viewed using fluorescence microscopy to identify the presence or absence of mycoplasma, identifiable as small pin pricks of DAPI positive staining in the cell cytoplasm.

2.2.1.6 Cell Assay Culture Conditions

For all cell assays, basal media was composed of DMEM, 10% FBS and 1% P/S. For differentiation assays, MSCs and hADSCs were seeded at $2x10^4$ cells/cm^2 unless otherwise stated and allowed to attach overnight. For osteogenic differentiation, the medium was then replaced with osteogenic medium (Basal medium plus 50µg/ml L-Ascorbic acid-2-phosphate, 5mM β-glycerophosphate and 10nM Dexamethasone, unless stated otherwise). BMP2 treatments were performed at 100ng/ml in Basal medium. For adipogenic differentiation, the medium was replaced with adipogenic medium (Basal medium plus 1µM Dexamethasone, 500µM 3-isobutyl-1-methylxanthine (IBMX), 1µg/ml Insulin and 100µM indomethacin). For micromass chondrogenic differentiation, $2x10^5$ MSCs in basal media were centrifuged at 450g for 5 minutes in a universal tube for each pellet. The pellets were then allowed to contract into a micromass pellet for 48 hours before the media was replaced (Day 0) with chondrogenic media (Basal media plus 50 µg/ml L-ascorbic acid-2-phosphate, 100 nM dexamethasone, 40 µg/ml L-proline, 1% ITS^+1, 10 ng/ml TGFβ3). Medium was changed every 3-4 days.

2.2.2 Microbiology Methods

2.2.2.1 Bacterial Transformation

DNA plasmids were transformed into competent *E. coli* strain Hi-coli-5A (Advantagen Ltd, Dundee, UK). 1 µl of purified plasmid was added to 50 µl of competent *E. coli* and incubators on ice for 30 minutes. Heat shock was performed at 42ºC for 30 seconds, and returned to ice for 2 minutes. 250 µl of SOC medium (Sigma-Aldrich, St. Louis, MO, USA) was added to the *E. coli* and incubated at 37ºC at 200 rpm for 1 hour. 100 µl was then plated onto an LB-agar plate containing an appropriate antibiotic and incubated at 37°C overnight. Colonies were picked and cultured overnight at 37ºC at 200 rpm in LB media (10 g tryptone, 10 g NaCl, 5 g yeast extract per litre). Glycerol stocks were generated by combining 750 µl *E. coli* culture and 250 µl sterile 50% glycerol, and stored at -80ºC.

2.2.2.2 Plasmid Purification

Plasmid DNA was purified from transformed *E. coli* cultures. 5 ml LB media was inoculated with scrapings from glycerol stocks, and cultured at 37ºC at 200 rpm for 8 hours. 200 ml cultures were then inoculated with 1 ml of the small inoculated culture and grown overnight at 37ºC at 200 rpm. Plasmid purification was performed using midi-prep kits (Macherey-Nagel) and NucleoBond Finalizers (Macheret-Nagel, Dueren, DE). Plasmids were eluted in nuclease free H_2O, and the concentration determined using a NanoDrop 1000 Spectrophotometer (Thermo Scientific, Waltham, MA, USA).

2.2.3 Transfection of mammalian cell cultures

2.2.3.1 Lipofectamine transfection of C3H10T1/2 Cells

Cells were seeded (without antibiotics) and allowed to attach overnight. The cells were then transfected, using Lipofectamine and Plus Reagent (Invitrogen, Carlsbad, CA, USA). Optimised DNA and lipofectamine volumes are given in specific chapter methods sections. DNA was combined with Plus reagent and DMEM and incubated

for 15 minutes at room temperature. Lipofectamine diluted in DMEM was added to the DNA solution and incubated a further 15 minutes at room temperature. DNA solutions were diluted in DMEM as described in specific chapter methods sections and added to the cells, followed by incubation at 37ºC for 3 hours. The same volume of DMEM + 20% FBS was then added to each well, and incubated overnight. Media was then changed to assay conditions, and cultured for the desired time the next day.

2.2.3.2 Lipofectamine LTX transfection of HEK293 Cells

Cells were seeded (without antibiotics) in 24 well plates and allowed to attach overnight. The cells were then transfected, using Lipofectamine LTX and Plus Reagent (Invitrogen, Carlsbad, CA, USA). Optimised DNA and lipofectamine LTX volumes are given in specific chapter methods sections. DNA and Plus reagent were combined in 100 µl Optimem before the addition of Lipofectamine LTX solution. The DNA/Lipofectamine LTX mix was then incubated at room temperature for 10 minutes. The DNA/Lipofectamine LTX mix was added to the wells containing 500 µl complete culture medium. Samples were incubated at 37ºC overnight. Media was then changed to assay conditions, and cultured for the desired time.

2.2.4 Dual Glo Luciferase assay

After a determined time period, reporter activity was analysed using the Dual Glo Luciferase assay system (Promega, Fitchburg, WI, USA), first measuring Firefly luciferase, generated by the reporter plasmids, followed by Renilla luciferase using a TopCount NXT luminometer (Packard). Briefly, the culture medium was removed, the cells were washed twice with PBS and the media replaced with 50 µl DMEM (No Phenol Red) per well. 50 µl luciferase reagent was added to each well and incubated in the dark for 10 minutes. The Firefly luciferase was then measured using the 96 well plate luminometer. 50 µl Stop and Glo solution was added to each well, and samples incubated in the dark for 10 minutes. The Renilla luciferase was measured using the 96 well plate luminometer. For analysis, Firefly luciferase was normalised to Renilla to reduce the effect of differences in transfection efficiencies between wells.

2.2.5 Protein Based Methods

2.2.5.1 Protein sample preparation

Total cell lysates were produced by lysis in RIPA buffer (Invitrogen, Calsbad, CA, USA) supplemented with protease inhibitor cocktail 3 (Calbiochem, Nottingham, UK) and 1mM Na_3VO_4. Nuclear and cytoplasmic fractions were prepared using NE-PER Nuclear and Cytoplasmic Extraction Kit (Thermo Scientific, Waltham, MA, USA). Briefly, cells were harvested with trypsin-EDTA, and centrifuged to pellet the cells. The cells were then washed by suspending in PBS before centrifugation, and the supernatant removed producing a pellet volume of ~5 µl. 50 µl of ice cold CER I buffer was added to the cell pellet, before being vortexed for 15 seconds. Samples were incubated on ice for 10 minutes, followed by addition of 2.5 µl of buffer CER II. Samples were mixed and incubated on ice for 1 minute. Samples were then pelletted by centrifugation at 16,000 g for 5 minutes and the supernatant (cytoplasmic fraction) transferred to another tube. The insoluble pellet was then suspended in 25 µl ice cold buffer NER by vortexing, and incubated on ice for 40 minutes with vortexing every 10 minutes. The samples were then centrifuged at 16,000 g for 10 minutes and the supernatant transferred to new a tube (nuclear fraction). Samples were stored at -80ºC.

2.2.5.2 BCA Protein Assay

Protein concentrations were calculated using a BCA protein assay (Thermo Scientific, Waltham, MA, USA). 10µl of each standard (BSA supplied with kit) or unknown sample replicate was pipetted into a microplate well. 200µl of the Working Reagent (50:1, Reagent A:B) was added to each well and incubated at 37°C for 30 minutes. The plate was cooled to room temperature, and the absorbance measured at 570nm on a plate reader. A standard curve was generated from the standard samples, allowing the unknown samples concentrations to be calculated.

2.2.5.3 SDS-PAGE

Protein samples were separated by size using SDS-polyacrylamide gel electrophoresis (SDS-PAGE) using a Bio-Rad mini gel electrophoresis kit. Resolving gel composition of 375 mM Tris pH 8.8, 10% acrylamide, 0.1 % SDS, 0.05% APS, 0.01% TEMED. Stacking gel composition of 125 mM Tris, pH 6.8, 4% acrylamide, 0.1% SDS, 0.05% APS, 0.01% TEMED. Protein samples were diluted in 4x Laemmli buffer, boiled for 5-10 minutes before loading onto the gel. Gels were run at 180V until the dye front reached the bottom of the gel. Running buffer was composed of 25 mM Tris, 192 mM glycine, 0.1% SDS.

2.2.5.4 Transfer to PVDF membrane and immune blotting

SDS-PAGE gels were transferred to PVDF membranes (GE Healthcare, Little Chalfont, UK) using a Bio-Rad wet tank transfer kit. Transfer buffer composition; 25mM Tris, 192mM Glycine, 20% methanol. Transfer was performed at 200mA for 2 hours. After transfer the membrane was blocked in 4% milk Tris buffered Saline Tween20 (TBS-T); 20mM Tris, 137mM NaCl, 0.1% Tween-20. Primary antibodies were used as described in specific chapter methods sections. After primary antibody probing, the membranes were washed in TBS-T before incubation with horseradish peroxidise-conjugated (HRP) secondary antibodies identified in specific chapter methods sections for 2 hours at room temperature. Immunoreactive bands were visualised by enhanced chemiluminescence (ECL) reagent (GE Healthcare, Little Chalfont, UK) and chemi-imager. Bands were quantified using ImageJ Software.

Chapter 3: Characterisation of AR28

3.1 Introduction

There are many ways to study the effects of enhanced canonical Wnt signalling *in vitro*. Three of the most common methods used are; the administration of recombinant Wnt ligands or Wnt-conditioned media to the cell culture, over-expression or knockdown of pathway components, and stabilisation of β-catenin though GSK3β inhibition. However, there are pros and cons for each method. Whilst using recombinant Wnt ligands should in principle supply the most biologically relevant levels of canonical Wnt activation, there are multiple problems associated with their use. Firstly, the availability of bioactive recombinant Wnt ligands is limited. While this is continuously improving with the generation of new ligands, there is the added complexity of ligand-specific effects, an area which is still relatively poorly understood. As mentioned previously, Wnt ligands can signal through multiple pathways, the canonical pathway, of interest here, and the non-canonical pathways. This offers the first level of complexity as several ligands are thought to be active through both pathways, while others are not clear (Mikels & Nusse, 2006). A second level of complexity is due to the current poor understanding of the differing effects of known canonical Wnt ligands in different situations, and the frizzled receptor and LRP co-receptor combinations to which they bind. With 19 Wnt ligands, and 10 Frizzled receptors (Mikels & Nusse, 2006), in combination with one of two co-receptors, one cannot even be certain that the cell of interest in any particular situation will be able to respond to the chosen ligand. This instantly makes it very difficult to draw conclusions about the ability of a particular ligand to generate a canonical Wnt response, and therefore the response of the cells to the Wnt stimulus.

In an attempt to circumvent these problems of ligand availability and specificity, manipulation of the pathway by altering the expression of key signalling molecules has been an attractive alternative. This can be done through the over-expression of positive regulators of the pathway; such as Wnt ligands (Wright et al, 1999), and β-catenin (Gould et al, 2007; Kim et al, 2006), or the down regulation of negative regulators; such as GSK3β (Cho et al, 2009), or DKK1 (Fleming et al, 2008). While

this does offer strong stimulation of the canonical Wnt pathway as a whole, it allows for little regulation of the degree or duration of the activation.

The final method described here is the use of small molecule GSK3 inhibitors, to prevent the phosphorylation of β-catenin and its subsequent degradation. This allows for a more controlled stimulation of the canonical Wnt pathways, and inhibitors can be added at a range of concentrations for different time periods. Furthermore they are much more translatable for therapeutic uses. LiCl (de Boer et al, 2004; Etheridge et al, 2004; Spencer et al, 2006) and 6-bromoindirubin-3′-oxime (BIO) (Krause et al, 2010; Wang et al, 2009) are two commonly used inhibitors of GSK3 and are regularly used to mimic canonical Wnt signalling *in vitro*. However, they are not ideal, with off target effects and toxicity (Davies et al, 2000; Liu et al, 2011; Meijer et al, 2003). In addition to the non-specific effects of the inhibitors on GSK3β, GSK3β itself is not specific to the canonical Wnt signalling pathway, with involvement in hedgehog signalling (Jia et al, 2002) and regulation of the NFAT transcription factor (Kaytor & Orr, 2002).

There are multiple ways to study Wnt activation *in vitro*, most commonly the identification of nuclear β-catenin within the cell (Gambardella et al, 2011; Krause et al, 2010; Spencer et al, 2006), or increased stable dephosphorylated β-catenin levels (Boland et al, 2004; Krause et al, 2010; Kulkarni et al, 2006). More specific analysis of canonical Wnt activation examines the degree of TCF/LEF1 transcription factor activity (Boland et al, 2004; Etheridge et al, 2004; Kulkarni et al, 2006). The family of TCF/LEF1 transcription factors is the ultimate response to increased canonical Wnt signalling, generating the Wnt-dependent changes in gene expression. Therefore, the degree of activity of this transcription factor family gives an indication of the functional canonical Wnt response generation by whichever stimulation.

As mentioned previously, canonical Wnt stimulation is an appealing therapeutic target, and any method of stimulation must therefore also be able to generate a functional canonical Wnt response *in vivo*. One body of research which has provided a valuable method for studying the ability of compounds to stimulate canonical Wnt signalling *in vivo* is the *Xenopus* model of embryonic development.

Spemann *et al* first identified the importance of the Spemann organiser in developmental organisation in 1924 and showed that grafting a second organiser region onto the ventral side of the embryo caused the duplication of the embryonal axis (Spemann H., 1924). The signalling mechanisms that underlie the initial positioning of the organiser region are now known (Figure 3.1.1) and together, they form the principles of the *in vivo* canonical Wnt activation assay (Kuhl & Pandur, 2008). Briefly, during the blastula stage of embryonic development, there is an accumulation of β-catenin in the dorsal side of the embryo that occurs in response to canonical Wnt signalling. This, in combination with VegT and Vg1 signals from the vegetal region, leads to the positioning of the Nieuwkoop centre. The Nieuwkoop centre releases *Xenopus* Nodal related factors which induce the formation of the Spemann organiser (De Robertis & Kuroda, 2004; Takahashi et al, 2000).

The canonical Wnt activation assay is carried out by the injection of the proposed canonical Wnt stimulus into the ventral side of the embryo. If successful in stimulating the canonical Wnt pathway, this leads to the generation a second area of increased β-catenin. Which, in turn, leads to the duplication of the various organiser regions, and results in the duplication of the embryonal axis (Figure 3.1.1), providing a clear readout for canonical Wnt stimulation. The accumulation of nuclear β-catenin also causes the formation of the blastula Chordin and Noggin expression (BCNE) centre, in the dorsal animal cap and marginal zone above the Nieuwkoop centre, resulting in the expression of BMP inhibitors, such as chordin and noggin (Wessely et al, 2001), which can be used as markers for induced β-catenin.

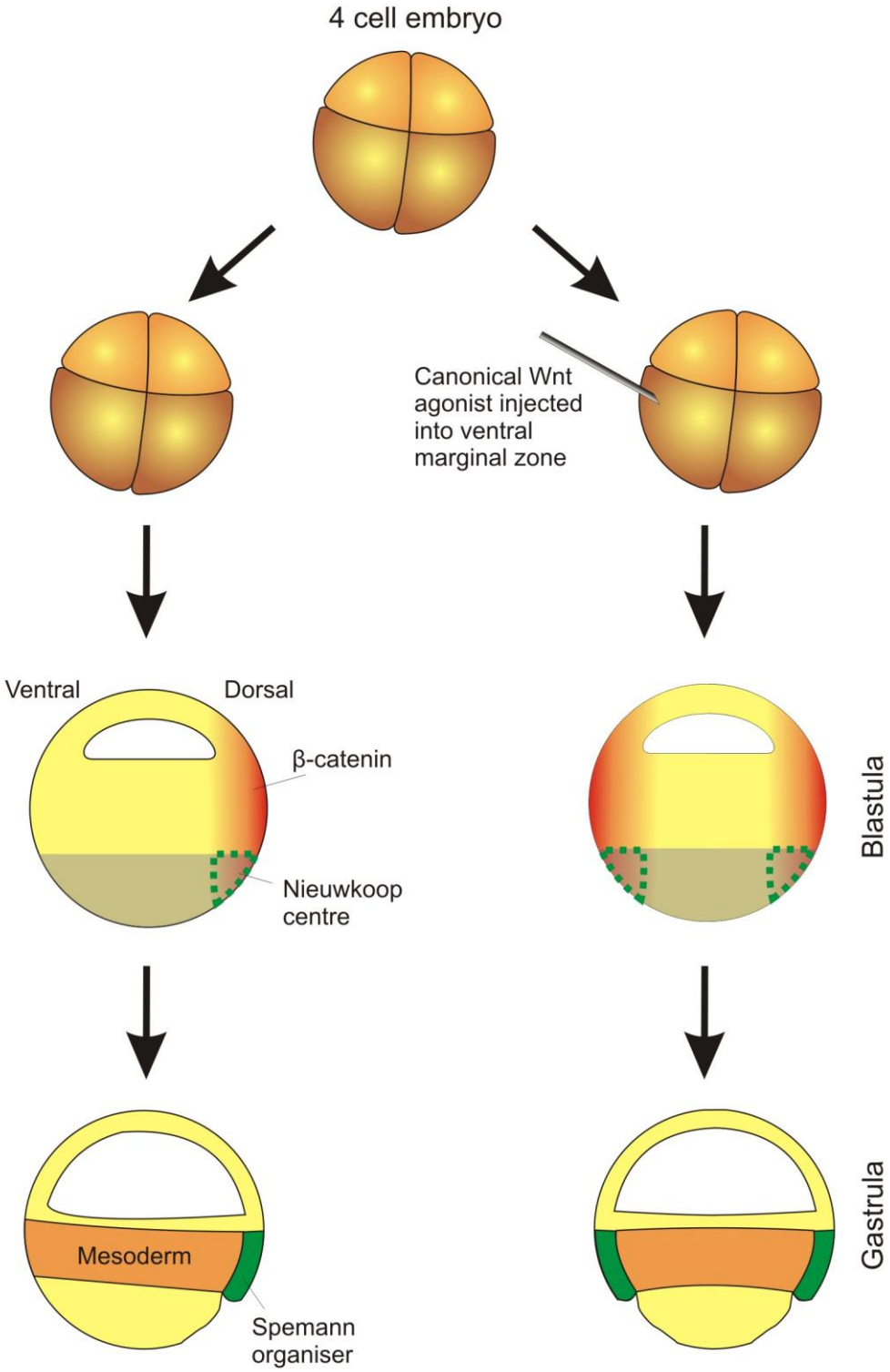

Figure 3.1.1. Schematic of *Xenopus* embryonic patterning and duplication by Canonical Wnt

Injection of canonical Wnt agonists in the ventral side of the embryos leads to the duplication of the β-catenin accumulation, leading to the formation of second Nieuwkoop centre, and therefore Spemann organiser, which ultimately leads to the duplication of the embryonal axis.

3.2 Aims

The general aims of the work presented in this chapter are to characterise the ability of the GSK3β inhibitor, AR28, to stimulate the canonical Wnt signalling pathway in mesenchymal progenitor cell cultures and the *in vivo Xenopus* model, and to determine its potency in relation to other commonly used canonical Wnt activators.

More specifically the aims are to:

- Characterise the MSCs extracted from both femoral heads and knees using a panel of markers by flow cytometry.
- Identify the effect of AR28 on β-catenin stabilisation and nuclear translocation.
- Identify the capacity of AR28 to stimulate TCF/LEF1 transcription factor activity and compare this to other known canonical Wnt stimulators.
- Determine the ability of AR28 to induce canonical Wnt signalling *in vivo* using *Xenopus* embryonal development as an assay for increased canonical Wnt signalling.

3.3 Methods

3.3.1 Analysis of MSC markers

MSC markers were analysed using a panel of antibodies to cell surface proteins by flow cytometry. MSCs were washed twice in PBS and removed from the cell culture flasks using wash buffer (5 mM EDTA, 0.2% BSA in PBS). Cells were centrifuged and resuspended in 1 ml of wash buffer before separating into 10 separate tubes in volumes of 100 µl. Primary antibodies were added to the cells at the concentrations shown in Table 3.3.1. and incubated on ice for 45 minutes. 1 ml of wash buffer was added to each sample before centrifugation at 400g for 5 minutes at 4ºC and the supernatant removed. Samples labelled with fluorescently-conjugated antibodies

Table 3.3.1. MSC marker antibodies

Target	Conjugate	Host	Dilution	Supplier	Catalogue No.
CD45	FITC	Mouse	1:100	Caltag Labs	MRC04501
CD166	PE	Mouse	1:50	BD Pharmingen	559263
CD44	FITC	Mouse	1:10	BD Pharmingen	555478
CD34	FITC	Mouse	1:50	Miltenyi biotech	130-081-001
CD90 (5E10)	Purified IgG	Mouse	1:100	ebioscience	14-0909-81
CD105 (SN7)	Purified IgG	Mouse	1:100	ebioscience	14-1057-81
CD29	Purified IgG	Mouse	1:100	BD Pharmingen	36741A
CD73	Purified IgG	Mouse	1:100	BD Pharmingen	550256
Anti-mouse IgG	Alexafluor 647	Donkey	1:200	Invitrogen	A-31571

were resuspended in 500 µl of wash buffer and stored on ice. Samples for secondary antibody probing were resuspended in 100 µl wash buffer and the AlexaFlour 647 Donkey anti-mouse antibody applied at 1:200 dilution, before incubation on ice for 45 minutes. Samples were then washed again with 1 ml wash buffer and centrifuged to remove the supernatant. Samples were resuspended in 500 µl wash buffer and stored on ice. Marker expression was analysed using CyAn^{TM} ADP Analyzer

(Beckman Coulter, Fullerton, CA, USA) at the appropriate excitation and emission wavelengths and analysed using Summit software.

3.3.2 β-catenin Immunocytochemistry

Cells were fixed with 4% paraformaldehyde for 15 min, before blocking in PBS + 1.1% BSA + 0.1% triton X-100 for 2 hours at RT. Incubation with anti-active β-catenin (BD Transduction laboratories) at 1.25 µg/ml, or IgG control in blocking buffer was performed overnight at 4°C. The cells were washed in PBS before addition of the secondary antibody, Donkey anti-mouse IgG Alexafluor 647 (Invitrogen, Calsbad, CA, USA) at 1:500. Samples were incubated for 2 hours at 4°C in the dark. The secondary antibody was removed and the samples washed 3 times in PBS before mounting. Samples on coverslips were mounted on slides using VECTASHIELD mounting medium with DAPI (Vector laboratories, Burlingame, CA, USA). The cells in chamber slides were treated with DAPI at 1 µg/ml. before storing in PBS.

3.3.3 Western Blot analysis of Sox9 and β-catenin

Nuclear and cytoplasmic fractions or total protein lysate samples were obtained and separated by SDS-PAGE and transferred to PVDF membranes as described in

Table 3.3.2. Optimised antibody concentrations for Western Blot analysis

Target	Conjugate	Host	Conc.	Supplier	Cat. No.
β-catenin	Purified IgG	Mouse	0.25 µg/ml	BD Transduction Laboratories	610154
Active-β-catenin (8E7)	Purified IgG	Mouse	1 µg/ml	Millipore	05-665
Lamin B (M20)	Purified IgG	Goat	0.25 µg/ml	Santa Cruz Biotech	SC-6217
GAPDH	Purified IgG	Mouse	0.5 µg/ml	Genetex	28245
Anti-mouse IgG	HRP	Goat	0.1 µg/ml	Santa Cruz Biotech	SC-2005
Anti-rabbit IgG	HRP	Swine	0.17 µg/ml	DAKO	P0399
Anti-goat IgG	HRP	Rabbit	0.25 µg/ml	DAKO	P0449

2.2.5.3 and 2.2.5.4. Antibody probing was performed using the antibodies concentrations given in Table 3.3.2. Densitometry of the protein bands was performed using Image J.

3.3.4 TOPFlash / Gli-BS Reporter assays

C3H10T1/2 cells were seeded in white opaque 96 well plates at $1x10^4$ cells/well (without antibiotics), and allowed to adhere overnight. Cells were then transfected with the TOPFlash or Gli-BS reporter plasmid in combination with the pCMV-Renilla plasmid using Lipofectamine as described in 2.2.3.1. Optimised conditions are given in Table 3.3.3. After 24 hours, the cells were treated with AR28, BIO, LiCl, recombinant mWnt3a or vehicle controls. After the specified time, the reporter activity was assayed using the Dual Glo Luciferase assay system (2.2.4).

Table 3.3.3. Optimised transfection conditions for C3H10T1/2 in 96 well plates
See 2.2.3.1 for protocol.

DNA/Reagent	Amount/well
TOPFlash/Gli-BS	30 ng
pCMV-Renilla	3 ng
Plus Reagent	0.3 µl
Lipofectamine Reagent	0.3 µl
DMEM	4 µl
DMEM for final dilution	32 µl

3.3.5 *Xenopus laevis* protocols

3.3.5.1 X. laevis culture

Xenopus laevis (*X. laevis*) females were primed by subcutaneous injection with 50 units of human chorionic hormone (HCG) a week before the experiment. *X. laevis* females were induced by injecting 250 units of HCG and incubated overnight (for 15 hours) at 18°C. Eggs were fertilised using a sperm suspension generated from male *X. laevis* testes, homogenised in water. Embryos were cultured in NAM/10 (Normal Amphibian Medium) in 55mm Petri dishes coated with 1% agarose at 21°C and de-jellied after 45 minutes of culture in 2.5% L-cysteine hydrochloride monohydrate, pH 7.8, followed by culture in NAM/10.

3.3.5.2 Bathing of X. laevis embryos in BIO and AR28

Embryos were cultured until the four cell stage, at which point they were transferred to NAM/10 containing either BIO at 10 and 50 µM, AR28 at 10, 50, and 100 µM, or 1% DMSO control. Embryos were incubated at 18ºC until the embryos reached the 8 cell stage, before washing in NAM/10, followed by culture in NAM/10 until the embryos reached Nieuwkoop and Faber stage (NF) stage 40 (Nieuwkoop & Faber, 1994). Embryos were then fixed in 4% formaldehyde in PBS.

3.3.5.3 X. laevis injection

Embryos were cultured until the four cell stage when AR28 or DMSO control was microinjected into the ventral marginal zone of a single blastomere. Embryos were cultured until NF stage 40 and fixed in 4% formaldehyde in PBS.

3.3.5.4 Sectioning and Histological staining of X. laevis Embryos

Fixed Embryos were stained using borax carmine (10% in 35% ethanol) overnight. Embryos were destained in acid ethanol and then cleared using a series of histoclear (National Diagnostics, Charlotte, NC, USA) washes before being embedded in paraffin wax and sectioned. Sections were counterstained with picro-blue-black (97.5% saturated picric acid, 0.25% naphthalene blue black).

3.3.5.5 Chordin In-situ Hybridisation

Digoxigenin (Roche, Welwyn Garden City, Hertfordshire, UK) labelled *chordin* (IMAGE:5161617) probe was generated as previously described (Freeman et al, 2008). Injected embryos were cultured until Nieuwkoop and Faber stage 10.5, fixed in MEMFA (0.1 M MOPS, 2 mM ethylenediaminetetraacetic acid [EDTA], 1 mM $MgSO_4$, 3.7% formaldehyde) for 1 hour at room temperature and stored in methanol at -20˚C. Whole mount *in-situ* hybridisation was carried out using a modified version of the Harland protocol (Tindall et al, 2005).

3.4 Results

3.4.1 MSC Characterisation

In order to demonstrate that the cells extracted from both femoral head bone marrow and bones from knee surgery expressed cell surface proteins typical of MSCs, randomly selected cultures were subject to a panel of markers by flow cytometry. All samples tested were positive for MSC markers (CD44, CD166, CD29, CD73, CD90, CD105) and negative for the haematopoietic markers (CD34, CD45). Example flow cytometry results from a femoral head (Figure 3.4.1) and knee (Figure 3.4.2) extracts are presented here. Both donors gave positive shifts by flow cytometry analysis for MSC markers with the exception of CD166 on the femoral head sample, which showed no change. Both samples showed no expression of either haematopoietic markers.

3.4.2 AR28 causes nuclear translocation of β-catenin *in vitro*

During the canonical Wnt signalling cascade, β-catenin is stabilised within the cytoplasm by the inactivation of the destruction complex. This stabilisation of β-catenin results in an increase in the nuclear translocation of β-catenin. Therefore to analyse the *in vitro* capability of AR28 to induce a canonical Wnt response, the stabilisation of β-catenin was studied by immunocytochemistry. Mouse multipotent mesenchymal cell line, C3H10T1/2, cells were seeded on coverslips and allowed to attach before treatment with AR28 and vehicle controls for 24 hours. Samples were then immunostained against β-catenin and counterstained with DAPI. IgG controls showed small amounts of non-specific staining, with slight increased staining towards the centre of the cell. Despite this non-specific staining in the IgG controls, probing with the antibody for β-catenin in unstimulated and DMSO control cells showed a clear absence of β-catenin in the nucleus of the cells, with strong staining in the cytoplasm of the cells. This cytoplasmic staining is likely identifying β-catenin in its other cellular function as a matrix protein. However, when treated with 2.5μM AR28 for 24 hours, clear nuclear staining for β-catenin was detected (Figure 1.2.1).

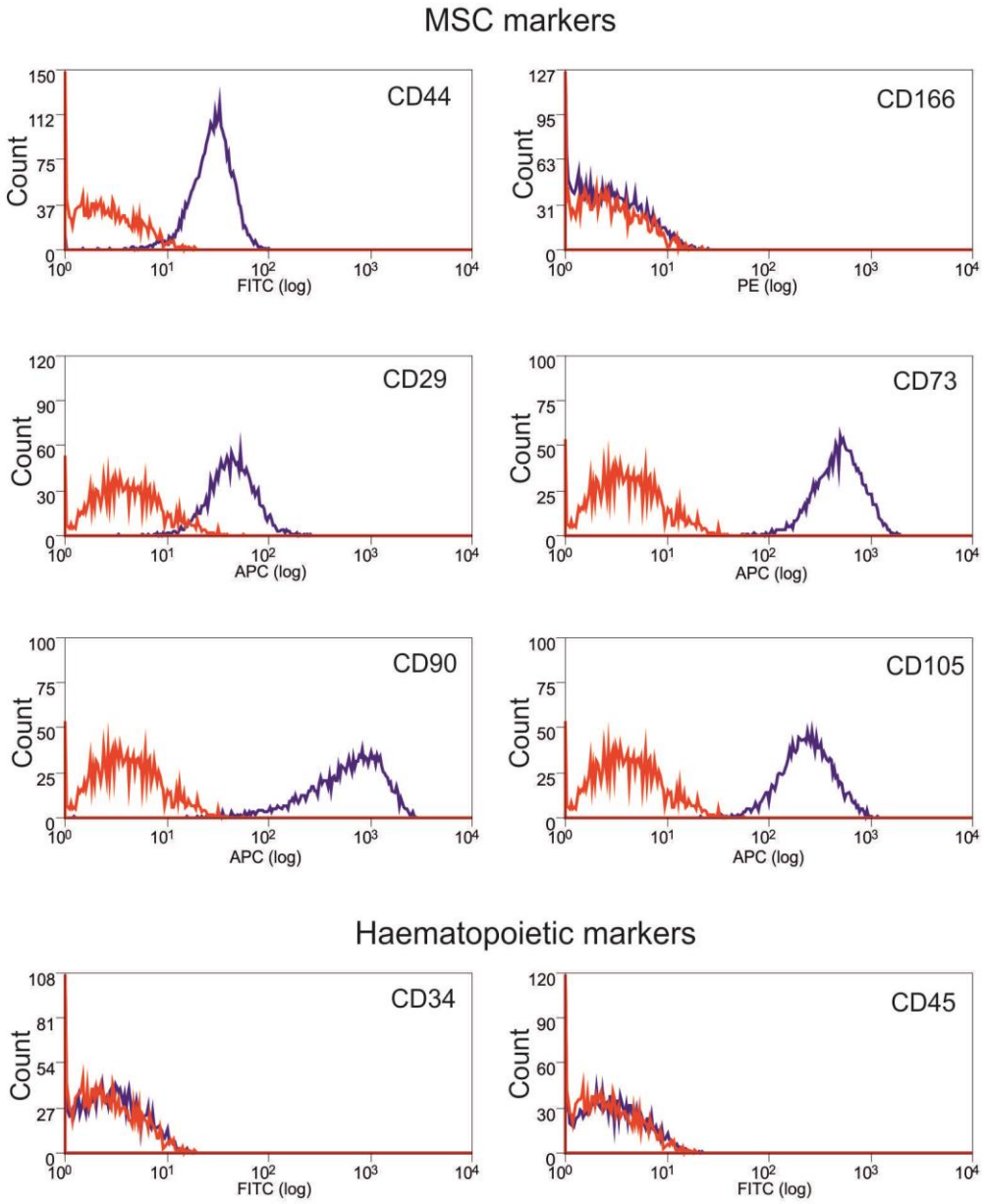

Figure 3.4.1. Flow cytometry analysis of femoral head extract.
MSCs from a femoral head culture (FH388) were antibody probed for MSC (CD44, CD166, CD29, CD73, CD90 and CD105) and haematopoietic (CD34 and CD45) markers in solution and analysed by flow cytometry. The results are presented as histograms of marker expression (Blue) relative to control (Red) fluorescence. Positive shifts in fluorescence, demonstrating antibody staining and protein expression, were observed for the MSC markers, while no change was detected for the haematopoietic markers.

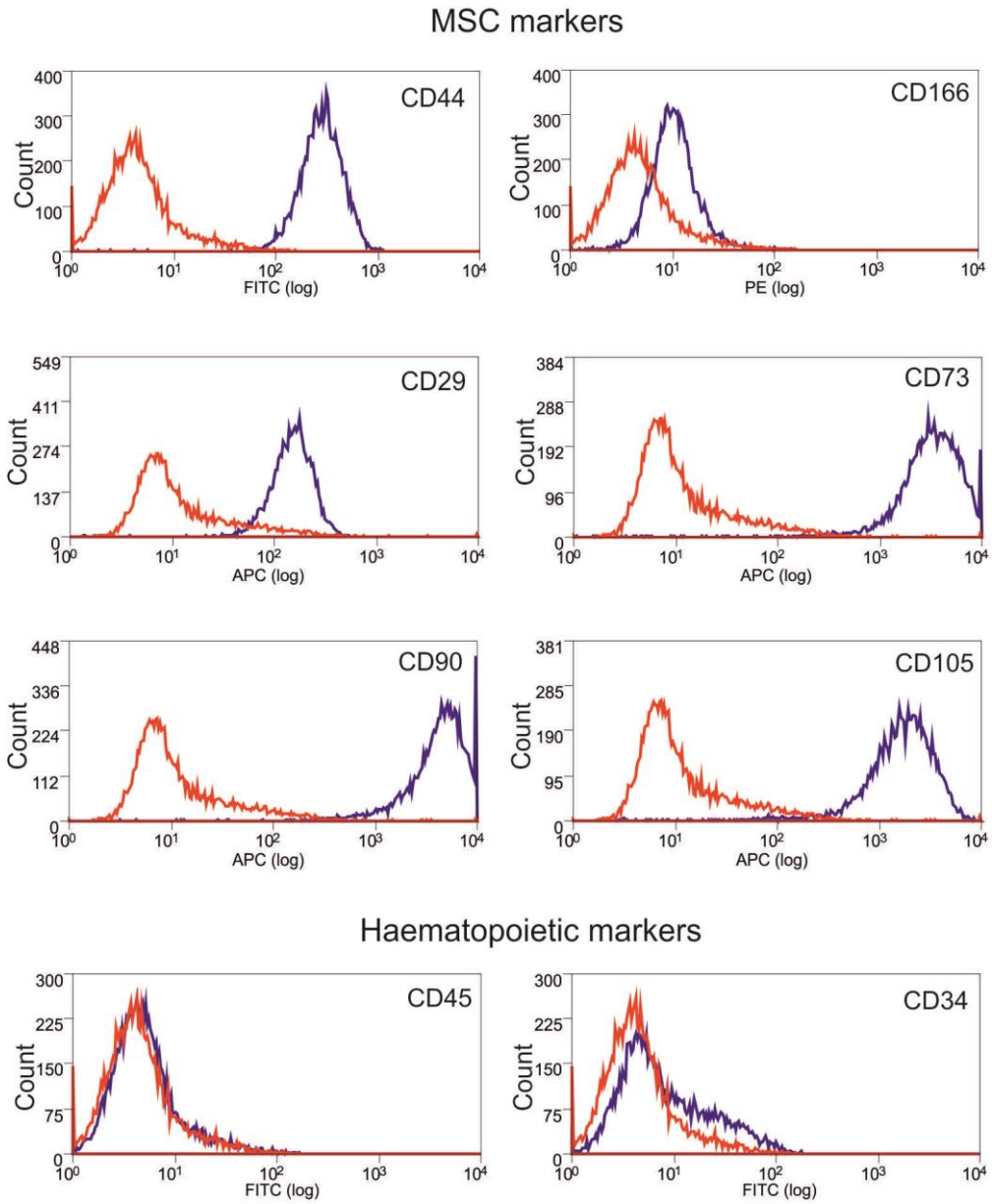

Figure 3.4.2. Flow cytometry analysis of knee extract.
MSCs from a knee culture (K16) were antibody probed for MSC (CD44, CD166, CD29, CD73, CD90 and CD105) and haematopoietic (CD34 and CD45) markers in solution and analysed by flow cytometry. The results are presented as histograms of marker expression (Blue) relative to control (Red) fluorescence. Positive shifts in fluorescence, demonstrating antibody staining and protein expression, were observed for the MSC markers, while no change was detected for the haematopoietic markers.

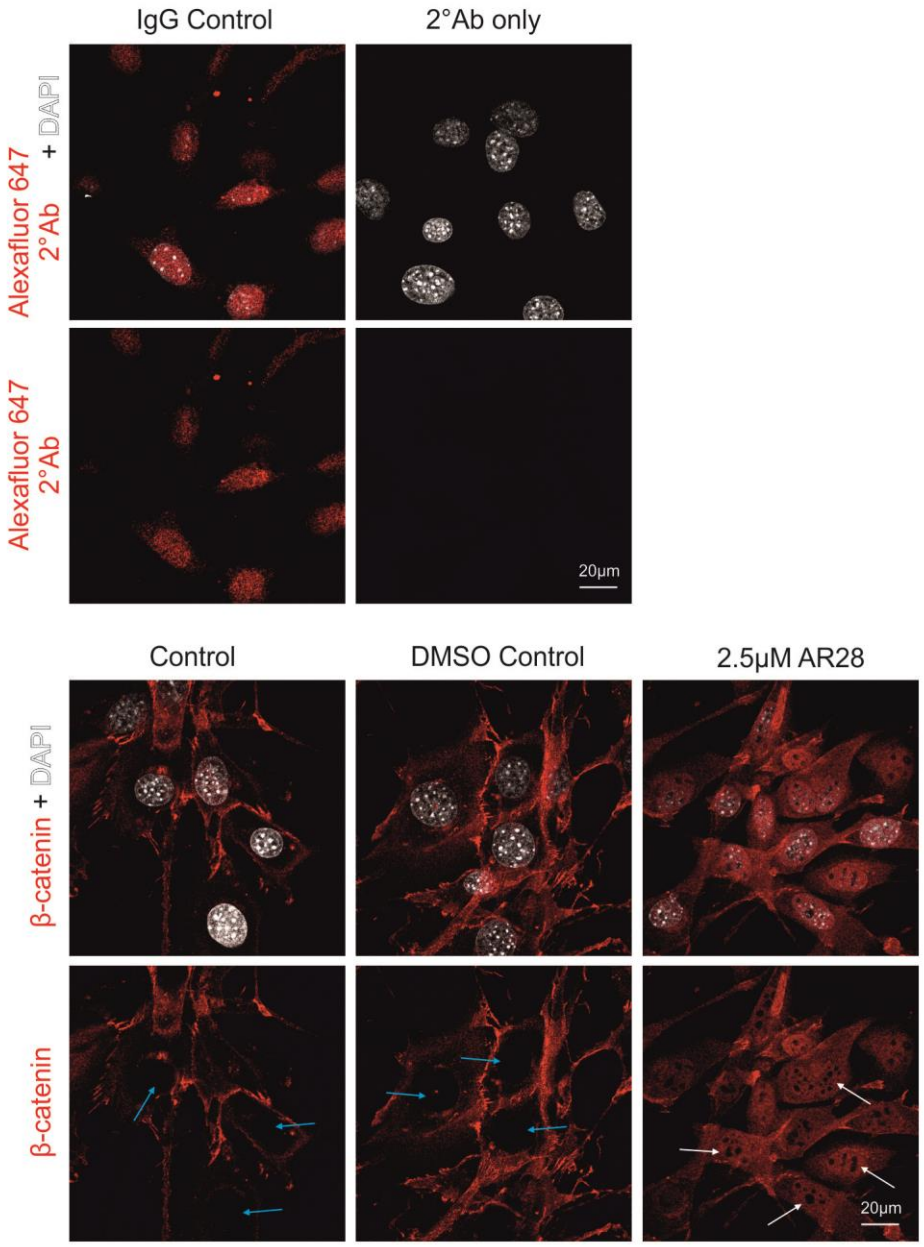

Figure 3.4.3. Nuclear localisation of β-catenin in C3H10T1/2 cells.
C3H10T1/2 cells were cultured for 24 hours in basal media (control images) plus treatment with 2.5 µM AR28 or vehicle control (DMSO). Samples were fixed and immuno-cytochemically stained against β-catenin (red) and DAPI (white) before imaging using confocal microscopy. IgG and secondary antibody (AlexaFluor 647) controls were also performed and showed no clear localisation. Both the no treatment and DMSO vehicle control showed cytoplasmic β-catenin staining, with an absence in the nucleus of the cells (blue arrows), while cells treated with 2.5 µM AR28 had clear, strong β-catenin staining both in the cytoplasm and nucleus of the cells (White arrows). Arrows indicate β-catenin nuclear staining.

IgG Control
Alexafluor 647
2°Ab
Alexafluor 647
2°Ab
+ DAPI
2°Ab only
Alexafluor 647
2°Ab
Alexafluor 647
2°Ab
+ DAPI
DMSO Control
Control
2.5μM AR28
10μM AR28
β-catenin + DAPI
β-catenin
20μm

Figure 3.4.4. Nuclear localisation of β-catenin in human MSCs
MSCs were cultured for 24 hours in basal media (control images) plus treatment with 2.5 μM AR28 or vehicle control (DMSO). Samples were fixed and immuno-cytochemically stained against β-catenin (red) and DAPI (white) before imaging using confocal microscopy. IgG and secondary antibody (AlexaFluor 647) controls were performed and showed no clear localisation. Both the no treatment and DMSO vehicle control showed cytoplasmic β-catenin staining, with an absence in the nucleus of the cells, while cells treated with 2.5 μM AR28 had clear, strong β-catenin staining both in the cytoplasm and nucleus of the cells. Arrows indicate β-catenin nuclear staining.

Similarly, to check the ability of AR28 to cause nuclear translocation of β-catenin in human MSCs, MSCs were plated in chamber slides and allowed to attach before treatment with AR28 and vehicle controls for 24 hours. As with the C3H10T1/2 cells, untreated and vehicle control cells showed no nuclear β-catenin staining. However when treated with 2.5μM AR28, nuclear β-catenin staining was detected (Figure 3.4.4). Furthermore, when 10μM AR28 was used, enhanced nuclear staining was detected, suggesting a dose dependent response to AR28 in the activation of canonical Wnt signalling. Again small amounts of non-specific staining were detected in the IgG and Secondary antibody only controls, but were faint, with no patterning.

3.4.3 AR28 causes dose dependent stabilisation of β-catenin

3.4.3.1 AR28 increases nuclear and cytoplasmic β-catenin

While β-catenin immunostaining allows for the identification of β-catenin stabilisation, it is difficult to quantify the extent of stabilisation, and therefore canonical Wnt activation. In order to gain a more quantifiable readout of β-catenin stabilisation, β-catenin protein levels were analysed by SDS-PAGE and Western blot. MSCs were seeded at $1x10^4$ cells/cm^2 and allowed to attach overnight before treatment with AR28 and vehicle controls for 24 hours. Nuclear and cytoplasmic protein fractions were then extracted using the NE-PER nuclear and cytoplasmic extraction kit. Samples were run on an SDS-PAGE gel and transferred to a nitrocellulose membrane for anti-β-catenin antibody probing. Densitometric analysis identified a dose-dependent increase of both cytoplasmic and nuclear β-catenin when normalised to endogenous loading controls (GAPDH – cytoplasmic, Lamin B –

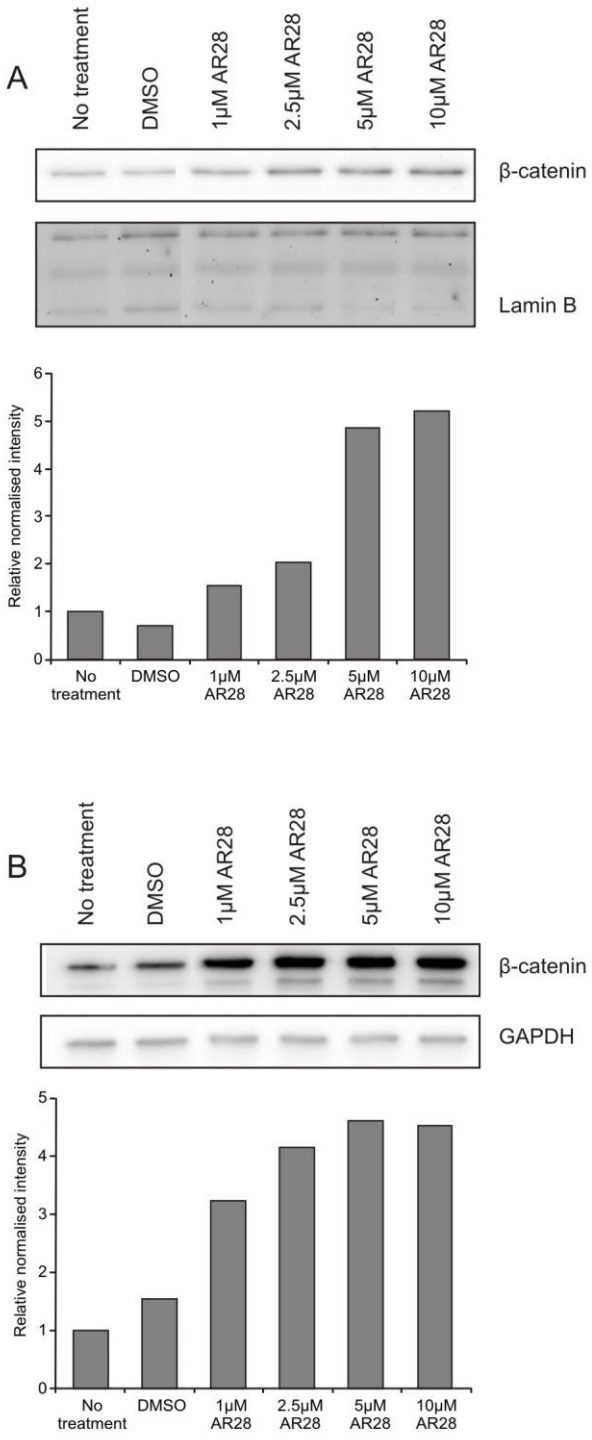

Figure 3.4.5. Western blot analysis of total β-catenin in nuclear and cytoplasmic fractions of AR28 treated MSCs

A) Nuclear and B) cytoplasmic protein fractions were obtained from MSCs cultured for 24hours with AR28 at the concentrations given, vehicle control (DMSO) or a no treatment control, followed by Western blot analysis for β-catenin. Subsequent probing for Lamin B or GAPDH was performed for nuclear and cytoplasmic fraction loading controls respectively. Densitometric analysis of the bands was performed using ImageJ, and plotted relative to the no treatment control.

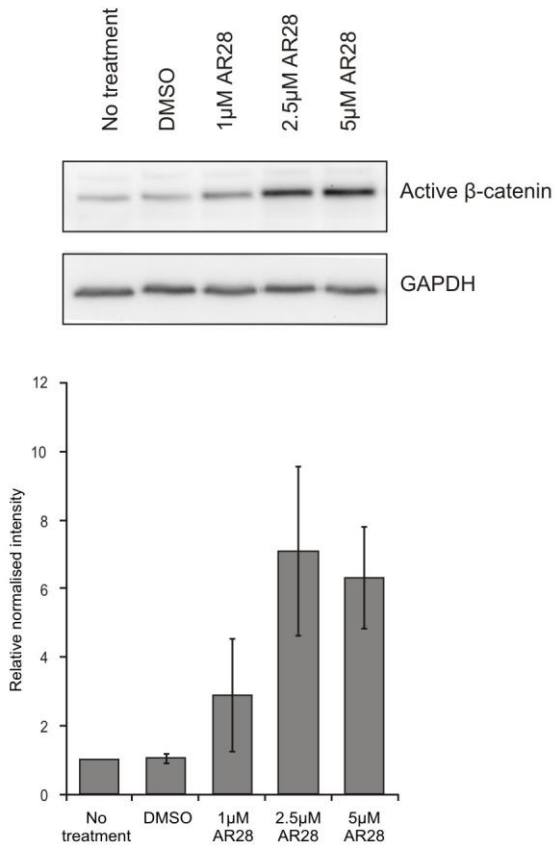

Figure 3.4.6. Western blot analysis of Active-β-catenin in AR28 treated MSCs

Total cell extracts were obtained from 3 MSCs donors cultured with AR28 at the concentration given, vehicle control (DMSO) or a no treatment control for 24hours, and analysed by western blot. Membranes were probed against Active-β-catenin and GAPDH for the loading control. An example blot is shown here. Densitometric analysis of the bands was performed using ImageJ, relative to the no treatment control, and the three donor samples grouped, with the mean (± standard deviation) relative normalised intensity displayed as a bar chart.

nuclear) (Figure 3.4.5). However, while this showed clear increases in stabilised β-catenin, the Lamin B antibody identified multiple different sized proteins (Figure 3.4.5A), making normalisation difficult. Furthermore, the nuclear/cytoplasmic fractionation relies on the complete removal of the soluble cytoplasmic fraction, allowing for cytoplasmic protein contamination within the nuclear fraction.

3.4.3.2 AR28 increases the level of stable β-catenin

In order to counter this problem total protein samples were generated from similar experiments, lysed with RIPA buffer. These samples were generated from 3 separate donors and run on SDS-PAGE gels and transferred to nitrocellulose membranes before probing with an anti-active-β-catenin (anti-ABC) antibody. The anti-ABC antibody detects β-catenin dephosphorylated on Ser37 or Thr41. This form is therefore not targeted for degradation by the proteosome and represents the active form of β-catenin capable of interacting with transcription factors and inducing gene expression. Hence, these samples did not require fractionation or nuclear loading controls. As with the total β-catenin, the active-β-catenin showed a dose-dependent increase, in response to increasing AR28 concentrations, which appeared to have peaked by 2.5 μM, with higher concentrations having little further effect in enhancing the β-catenin stabilisation (Figure 3.4.6).

3.4.4 TCF/LEF1 reporter assay

While the experiments described above show the ability of AR28 to generate an increase in stabilised β-catenin, in order to analyse the transcriptional responses generated by AR28 a TOPFlash luciferase reporter was used, which utilises four copies of the TCF/LEF1 response element to report Wnt signalling activity. TOPFlash analysis was carried out in C3H10T1/2 cells, as MSCs frequently suffer from low transfection efficiencies. C3H10T1/2 cells were seeded at $1x10^4$ cells per well of a 96 well plate, followed by transfection with both the TOPFlash reporter (M50) and a constitutively expressing Renilla (pCMV-Renilla) plasmid. TCF activity was then measured as Firefly luciferase normalised to Renilla luciferase.

3.4.4.1 AR28 can stimulate TCF/LEF1 reporter activity

Initial studies compared AR28 treatment with two other commonly used activators of canonical Wnt signalling, LiCl and recombinant Wnt3a, over a 24 hour treatment period. LiCl is commonly used at 20 mM, while recombinant Wnt3a is shown to cause a range of effects over concentrations of 5-100 ng/ml (Liu et al, 2009). Using the TOPFlash assays, AR28 caused a dose-dependent increase in luciferase activity with increases ranging from 10-fold to 500-fold with 0.1 μM and 2.5 μM AR28 respectively. These increases were comparable to the effects caused by Wnt3A (5-100 ng/ml). LiCl, an alternative GSK3β inhibitor, was less effective at eliciting a Wnt response, only causing a 10-fold increase in reporter activity compared to NaCl controls when used at 20 mM (Figure 3.4.7 A). A similar assay, using a mutated form of the TOPFlash reporter plasmid, containing mutated TCF/LEF1 binding sites, showed no change in response to either AR28 at the same concentrations of LiCl treatments (Figure 3.4.7 B), confirming the validity of the increases in TCF/LEF1 activity.

3.4.4.2 AR28 stimulated TCF/LEF1 reporter activity is time and dose dependent

The TOPFlash reporter was also able to identify changes in transcriptional activation in response to differing concentrations and treatment duration of AR28, and compare this to another commonly used GSK3β inhibitor, BIO (Figure 3.4.8). AR28 administration generated a strong TCF reporter response in a time- and concentration-dependent manner, with increasing luciferase expression with concentration and time. 1 μM AR28 was able to generate clear increases in reporter activity within 4 hours of treatment, which continued to increase overtime. Similarly, higher AR28 concentrations generated large increases from 4 hours onwards, increasing in intensity with time, and not reaching a plateau by 40 hours (Figure 3.4.8 A). However, BIO at similarly high concentrations generated early increases in reporter expression, but peaked by 36 hours at around 100-fold increased expression (Figure 3.4.8 B) compared to over 1000-fold increases by AR28 at 40 hours.

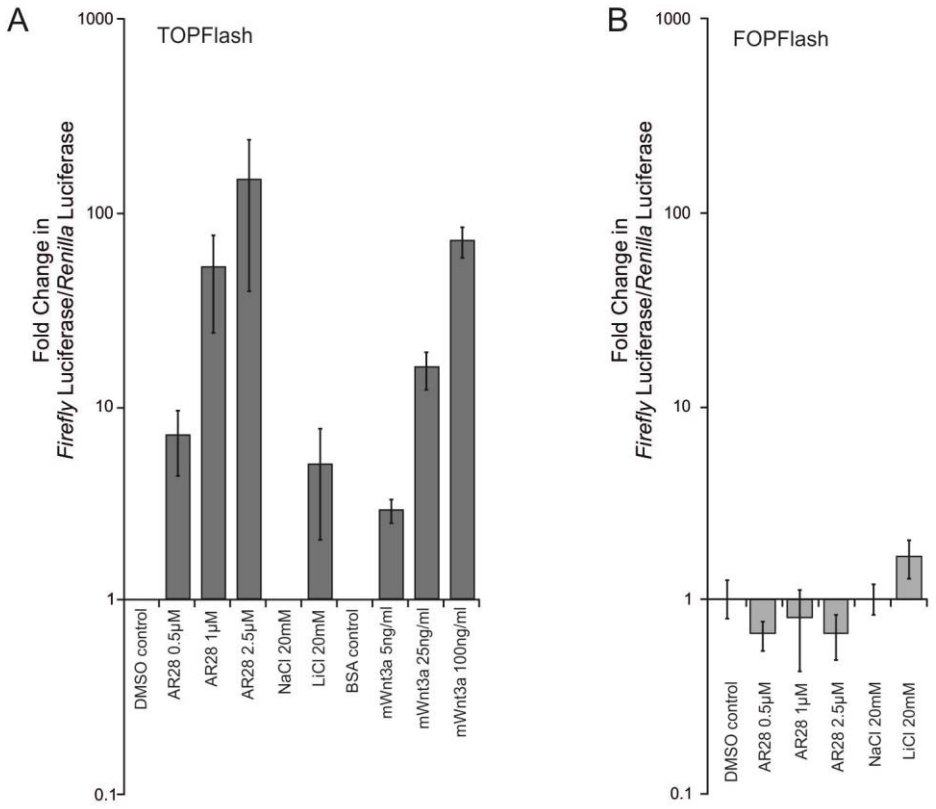

Figure 3.4.7. TOPFlash analysis ofAR28 compared to other Canonical Wnt stimulators

A) C3H10T1/2 cells were co-transfected with the TOPFlash (LEF1/TCF firefly reporter) plasmid and pCMV-Renilla before being treated with a range of canonical Wnt stimuli. *Firefly* and *Renilla* luciferase were assayed after 24 hours. Reporter activity (*Firefly* luciferase) was normalised to *Renilla* luciferase and the mean of 6 independent technical replicates calculated for each treatment. The relative increases, compared to respective vehicle controls, were then calculated. The graph presents mean ± standard deviation of normalised data from three independent biological samples, each consisting of six independently transfected and treated technical replicates. B) C3H10T1/2 cells were co-transfected with the FOPFlash plasmid and pCMV-Renilla before being treated with a range of canonical Wnt stimuli. *Firefly* and *Renilla* luciferase were assayed after 24 hours. *Firefly* luciferase was normalised to *Renilla* luciferase. The relative increases, compared to respective vehicle controls, were calculated. The graph presents mean ± standard deviation of six independently transfected and treated technical replicates.

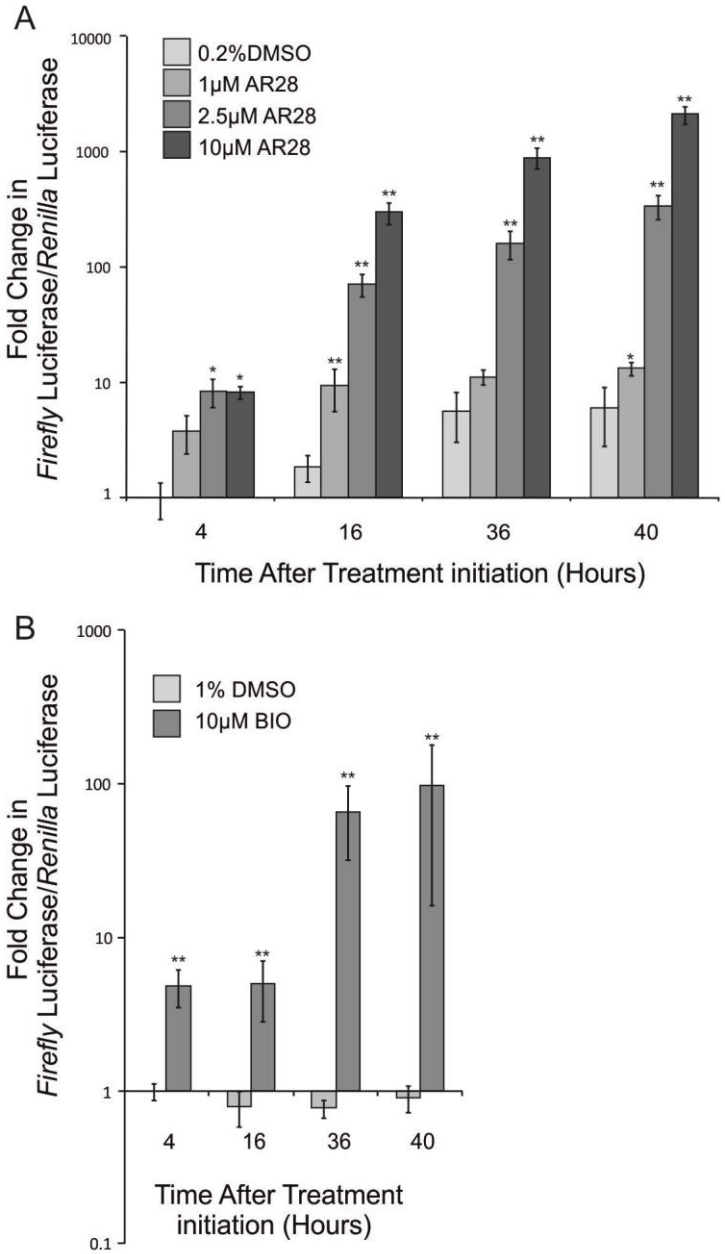

Figure 3.4.8. TOPFlash analysis of GSK3 inhibition over a 40 hour time-course

C3H10T1/2 cells were co-transfected with the TOPFlash (LEF1/TCF firefly reporter) plasmid and pCMV-Renilla before being treated with A) a range of AR28 concentrations or B) 10 μM BIO. Firefly and Renilla luciferase were assayed after 4, 16, 36 and 40 hours of treatment. Reporter activity (Firefly luciferase) was normalised to Renilla luciferase and the mean of 6 independent technical replicates calculated for each treatment. The relative increases, compared to respective vehicle controls, were then calculated. Values given as the mean fold change ± standard deviation of six independently transfected and treated technical replicates. n=6, * $p<0.05$, ** $p<0.005$, *** $p<0.001$. Statistical significance is relative to vehicle control at relevant time point, by Mann-Whitney U and Kruskal-Wallis tests.

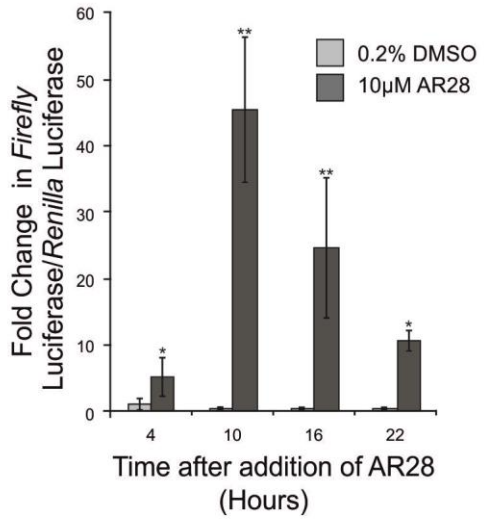

Figure 3.4.9. TOPFlash analysis of AR28 pulse treatment
C3H10T1/2 cells were co-transfected with the TOPFlash (LEF1/TCF firefly reporter) plasmid and pCMV-Renilla before being pulse treated with 10 μM AR28 for 4 hours before its removal. Firefly and Renilla luciferase were assayed at 4, 10, 16 and 22 hours after treatment initiation. Reporter activity (Firefly luciferase) was normalised to Renilla luciferase and the mean of 6 independent technical replicates calculated for each treatment. The relative increases, compared to respective vehicle controls, were then calculated. Values given as the mean fold change ± standard deviation of six independently transfected and treated technical replicates. n=6, * $p<0.05$, ** $p<0.005$, *** $p<0.001$. Statistical significance is relative to vehicle control at relevant time point, by Mann-Whitney U and Kruskal-Wallis tests.

3.4.4.3 AR28 induced TCF/LEF1 reporter stimulation is reversible

This system was also able to study the effect of pulse treating with AR28. TOPFlash transfected C3H10T1/2 cells were pulse treated with 10 μM AR28 for 4 hours before removal of the compound. The reporter expression peaked shortly after removal of AR28, but then began to decline again over time (Figure 3.4.9). However, reporter levels did not reach basal levels within the 22 hour time period of the experiment.

3.4.5 AR28 does not stimulate the Hedgehog pathway

As discussed in section 1.3.3 GSK3β is also involved in transduction of the Hedgehog signalling pathway, therefore to identify any effect of AR28 on this pathway C3H10T1/2 cells were transfected with a hedgehog reporter plasmid (Gli-BS) (Sasaki et al, 1997) and treated with AR28, purmorphamine or a combination of both for 24 hours. The cells were co-transfected with pCMV-Renilla as a transfection control. Purmorphamine is a Hedgehog agonist, which acts by stimulating the Smo transmembrane protein, leading to signal transduction upstream of Gli transcription factor phosphorylation. Purmorphamine at a concentration of 1 μM generated a significant ($p<0.005$) 2.5 fold increase in Gli reporter activity, while AR28 appeared to create small decreases in Gli reporter activity at 2.5 μM ($p<0.05$). However, when added in combination AR28 did not affect the increase in reporter activity generated by purmorphamine (Figure 3.4.10 A). Cells transfected with a mutated version of the Gli reporter plasmid (m3'Gli-BS) did not present any change in reporter expression in response to either AR28 or purmophamine (Figure 3.4.10 B).

3.4.6 AR28 induces embryonal axis duplication in *Xenopus laevis*

In order to analyse the ability of AR28 to selectively activate a functional Wnt response, an *in vivo Xenopus* model system was used. It is known that during *Xenopus* embryonic development there is a β-catenin gradient toward the dorsal side of the embryo, and that this is important for the positioning of the BCNE centre and Nieuwkoop centre, which in turn dictates the location of the Spemann organiser (De Robertis & Kuroda, 2004). It is also well documented that the injection of Canonical Wnt ligand RNA into the ventral side of the embryo before organiser

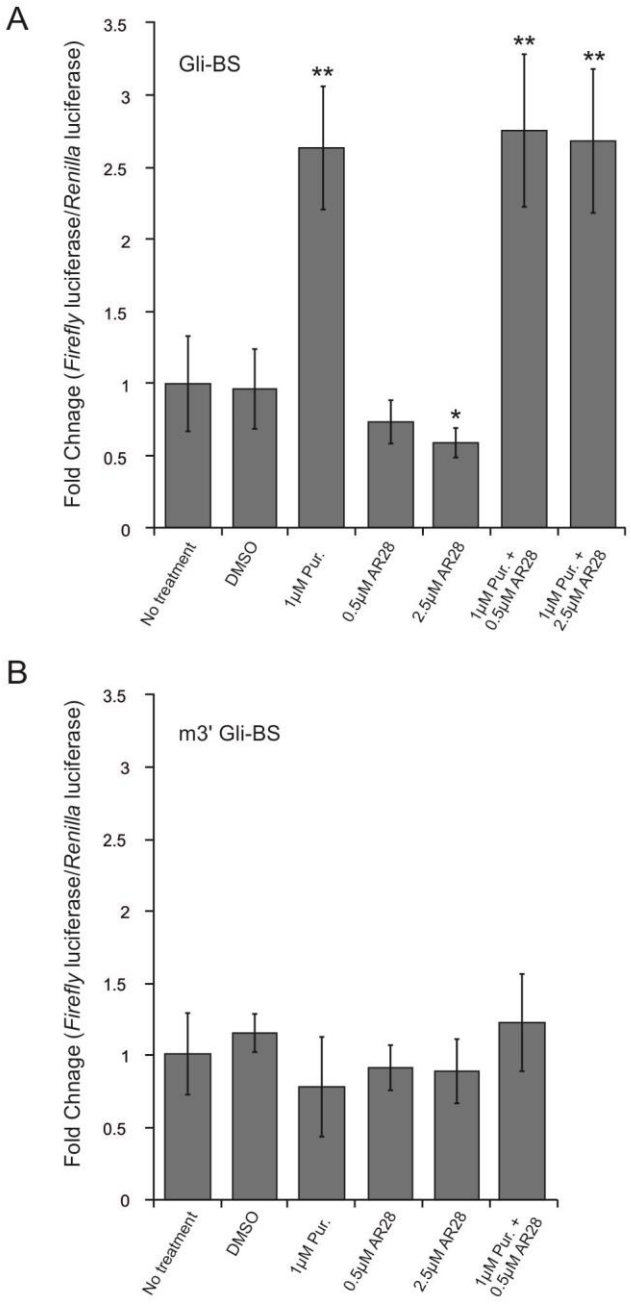

Figure 3.4.10. Hedgehog reporter analysis of AR28 treatment
C3H10T1/2 cells were co-transfected with the A) Gli-BS or B) 3' Gli-BS plasmids and pCMV-Renilla before being treated with purmorphamine (Pur.) and/or AR28 at the concentrations shown. Firefly and Renilla luciferase were assayed after 24 hours. Reporter activity (Firefly luciferase) was normalised to Renilla luciferase and the relative increases, compared to no treatment, were calculated. The graph presents mean ± standard deviation of six independently transfected and treated technical replicates

region formation results in the formation of a second Spemann organiser region (Sokol et al, 1991).

3.4.6.1 BIO, but not AR28 causes dorsalisation when added to bathing medium

A more straightforward assay however is to bathe the embryos in a Wnt stimulus during this early stage of β-catenin patterning, causing an increase in β-catenin throughout the embryo, in turn leading to the dorsalisation of the embryo (Meijer et al, 2003). *X. laevis* embryos at 4 cell stage were bathed in either BIO or AR28 until they reached the 8 cell stage. The embryos were then allowed to progress to NF 40. As in published data (Meijer et al, 2003) 50 μM BIO was able to induce complete dorsalisation in 90% of the embryos (Figure 3.4.11.), while 10 μM BIO was only capable of partially dorsalising 6%. In contrast, AR28 was unable to induce dorsalisation of the embryos at concentrations of 10 and 50 μM. When used at 100 μM, one of 30 embryos was identified as partially dorsalised (Figure 3.4.11.)

3.4.6.2 AR28 causes axis duplication upon injection

It was proposed that AR28 was unable to diffuse across the vitalline membrane; therefore, *X. laevis* embryos were injected with 4.2 nl of AR28 at concentrations of 100-400 μM into the ventral marginal zone at the four cell stage of development, and allowed to progress to NF 40. AR28 generated a dose-dependent axis duplication of the *X. laevis* embryos, which was first visible at NF 20, with embryos showing the characteristic Y-shaped neural tube formation. At the later stage of NF 40, the embryos had developed Y-shaped dorsal axes and second heads (Figure 3.4.12), with 58% of the injected embryos showing some level of axis duplication with 200 and 400 μM AR28, compared to 0% in the DMSO and uninjected controls. Furthermore, the severity of the axis duplication increased with increasing AR28 concentrations, identified by a higher occurrence of duplicated eyes, with 37% of embryos with extra eyes when injected with 400 μM, compared to only 5% in the 200 μM samples (Table 3.4.1).

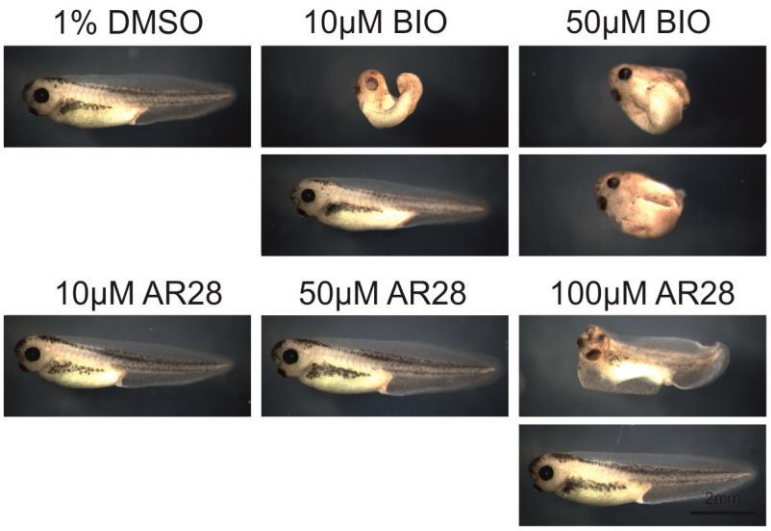

Figure 3.4.11. BIO, but not AR28, induces dorsalisation in *X. laevis* embryos when added to bathing medium
Example images of NF stage 40 embryos, bathed in BIO or AR28 at concentrations given. Embryos were treated between the 4 and 8 cell stage for 40 minutes at 18ºC. BIO was able to completely dorsalise 90% of treated embryos when used at 50 μM, and partially dorsalise 6% at 10 μM. AR28 was unable to dorsalise embryos with 10-100 μM treatments, with the exception of one of 30 treated embryos at 100 μM which appeared partially dorsalised.

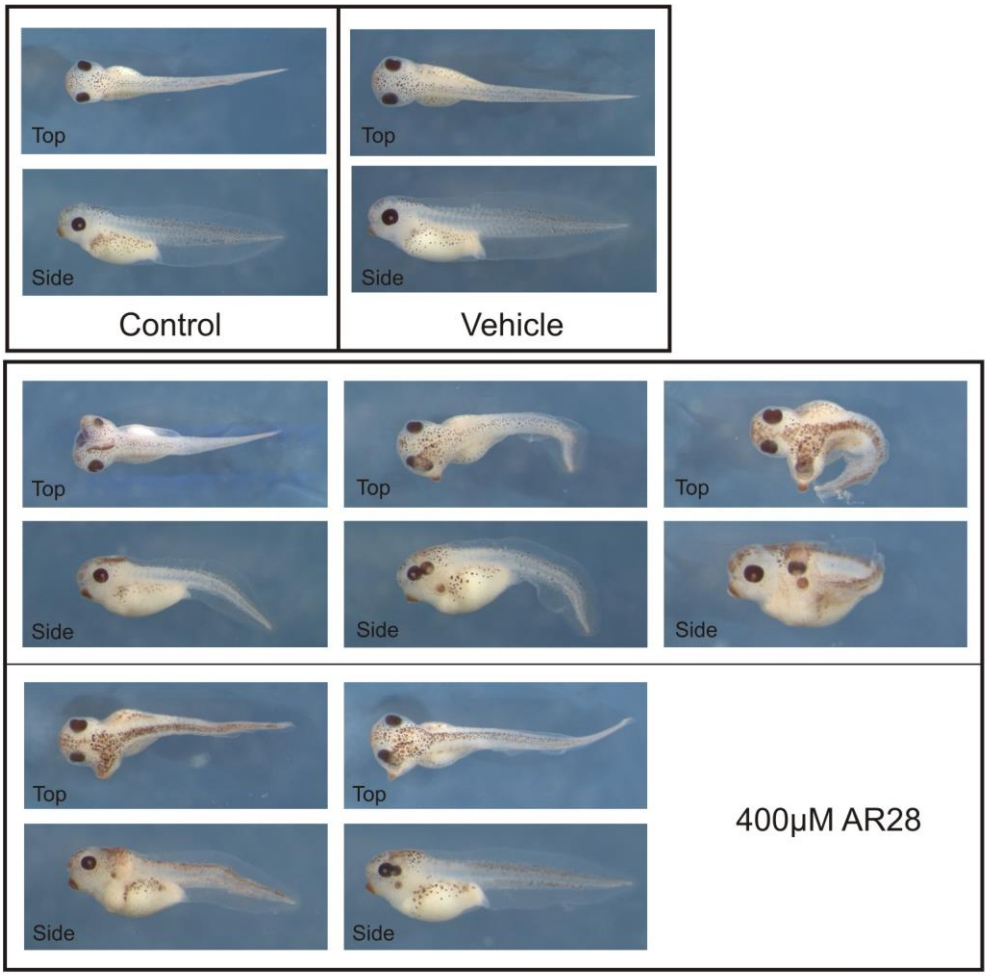

Figure 3.4.12. AR28 induces axis duplication when injected into the ventral marginal zone of four cell *X. laevis* embryos

4.2 nl 400 µM AR28 or 1% DMSO (vehicle control) was injected into the ventral marginal zone of four cell *X. laevis* embryos, which were allowed to progress to NF stage 40. The developed *X. laevis* tadpoles demonstrated clear second axis formation in a proportion of the embryos (example images of embryos with axis duplication), with the percentage of duplicated embryos given in Table 3.4.1. Control embryos (Uninjected, and vehicle injected) showed normal single axis development.

To confirm the formation of second neural tube structures in the duplicated axes, embryos with second axis from the 400 μM treatment and control samples were wax embedded, sectioned and histologically stained. The embryos with second axes clearly showed secondary neural tube formation (Figure 3.4.13, arrows), again with varying degrees of severity. In addition to secondary neural tube formation some samples also had other secondary structures such as eyes (Figure 3.4.13, red arrow) and other internal organs.

3.4.6.3 Injection of AR28 induces secondary regions of Chordin expression

Axis duplication of *Xenopus* embryos is a well documented result of increased canonical Wnt signalling (Sokol et al, 1991), however similar effects can also be generated by manipulating other signalling pathways such as BMPs that act after organiser region formation (Suzuki et al, 1994). Chordin is a marker for the Spemann organiser (Sasai et al, 1994), offering a more specific readout of canonical Wnt activation. Therefore, embryos were prepared and injected with 400 μM AR28 and controls as above and allowed to develop to NF 10.5, followed by fixation and in-situ hybridisation against chordin. Injection of 400 μM AR28 resulted in clear second regions of chordin expression in the ventral side of the embryo in 95% of the injected samples, with no secondary regions detected in control embryos (Figure 3.4.14). The size of the secondary chordin expressing region was not uniform across the embryos, suggesting different degrees of axis duplication.

Table 3.4.1. *X. laevis* axis duplication by AR28

4.2 nl 400 µM AR28 or 1% DMSO (vehicle control) was injected into the ventral marginal zone of four cell *X. laevis* embryos, which were allowed to progress to NF stage 40. Embryos were then counted and assigned a degree of axis duplication.

	Normal Phenotype	Second Axis	Second cement glands	Second eyes	Total No. Embryos	Wnt Phenotype
No injection	16 (100%)	0	0	0	19	0
1% DMSO	27 (100%)	0	0	0	19	0
100 µM AR28	16 (67%)	7 (29%)	0	1 (4%)	24	8 (34%)
200 µM AR28	8 (42%)	6 (32%)	4 (5%)	1 (5%)	27	11 (58%)
400 µM AR28	8 (42%)	2 (10%)	2 (10%)	7 (37%)	16	11 (58%)

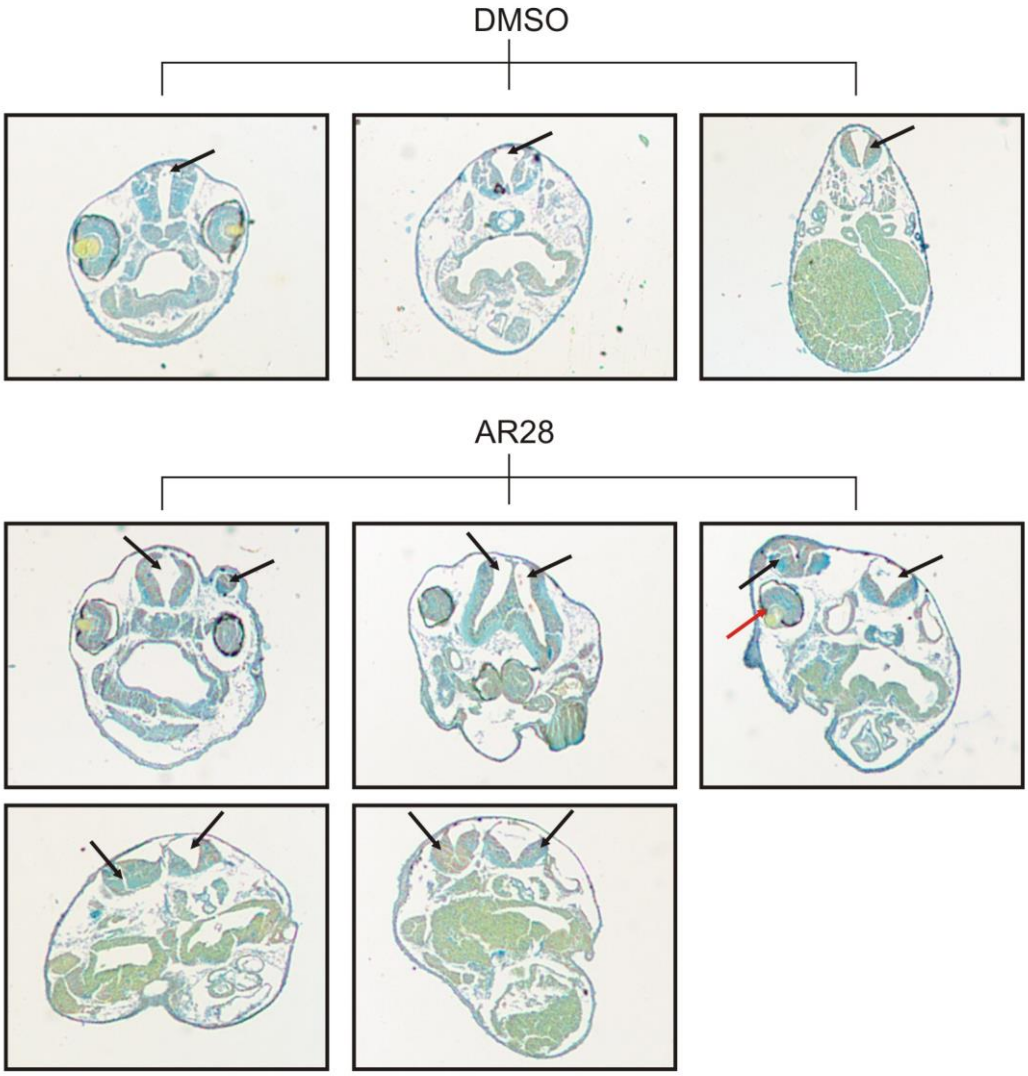

Figure 3.4.13. Histologically stained sections of *X. laevis* embryos injected with AR28.
X. laevis embryos which showed clear axis duplication after 4.6 nl of 400 µM AR28 injection, and DMSO injected control embryos were wax embedded, sectioned and histologically stained. DMSO injected control embryos showed normal development with a single neural tube and body axis. AR28 injected Embryos showed clear second neural tube formation (Black arrows) in all the sectioned embryos, and second body axis and eye (red arrow) structures in some embryos.

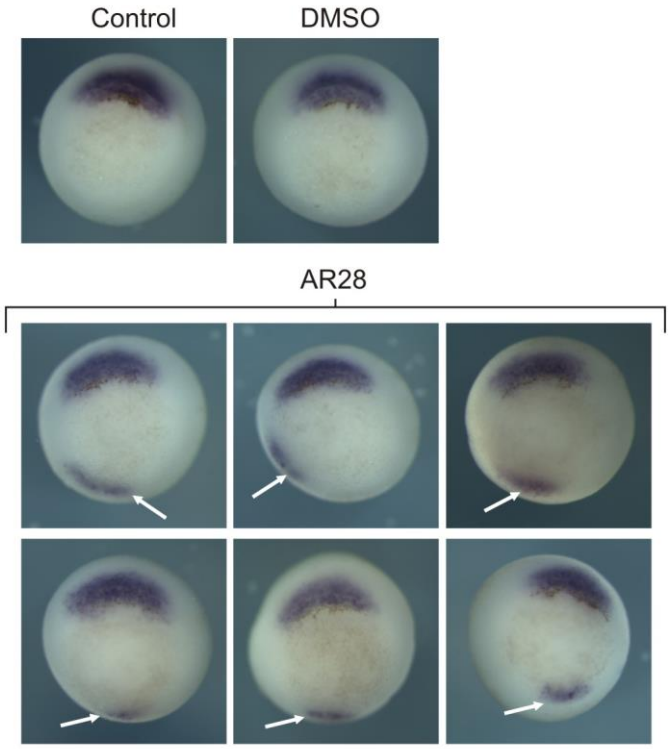

Figure 3.4.14. Chordin in-situ hybridisation of AR28 injected *X. laevis* embryos

4.2 nl 400 μM AR28 or 1% DMSO (vehicle control) was injected into the ventral marginal zone of four cell *X. laevis* embryos, which were allowed to progress to blastula stage. Samples were fixed and probed for chordin by in situ hybridisation. Control and vehicle injected (DMSO) embryos showed single regions of chordin expression in the ventral side of the embryos, while 98% of AR28 injected embryos showed a second region of chordin expression in the dorsal side of the embryo, with varying degrees of intensity. Arrows identify second regions of chordin.

3.5 Discussion

The MSCs extracted and tested from both femoral heads and knees were positive for the MSC markers selected, except for CD166 in the femoral head sample presented here. The panel of markers was selected from the many commonly used MSC markers (Salem & Thiemermann, 2010), however there are often differences between donors, species and culture methods. Furthermore, the International Society for Cellular Therapy defined MSCs as CD105, CD73 and CD90 positive, with other MSC markers less strictly required (Dominici et al, 2006; Horwitz et al, 2005). The International Society for Cellular Therapy also identify the importance of being negative for the Haematopoietic markers CD34 and CD45, with which all samples here complied.

AR28 was first published on by Gambardella *et al*. (2011). In this study, AR28 was shown to be selective to GSK3 over a panel of other kinases, with an IC_{50} of 5 nM. The ability of AR28 to stimulate the canonical Wnt signalling pathway had only been briefly examined in this work. Gambardella *et al*. (2011) studied canonical Wnt activation by calculating nuclear:cytoplasmic β-catenin from immunocytochemical images of AR28-treated C3H10T1/2 cells. The work presented in this chapter also demonstrated increased nuclear staining in C3H10T1/2 cells in response to AR28. In addition to the staining in C3H10T1/2 cells, nuclear staining was also detected in AR28 treated human MSCs, however concentrations of 2.5 μM or higher were needed to generate clear increases in nuclear β-catenin staining within 24 hours. Further quantification of this increase in β-catenin stability was performed by western blot analysis of both cytoplasmic and nuclear β-catenin, which demonstrated a clear increase in both cytoplasmic and nuclear β-catenin levels upon AR28 treatment. However, nuclear loading controls were poor and it was difficult to ensure complete nuclear/cytoplasmic fractionation, making it hard to confirm the presence of active stabilised β-catenin available for cell signalling. The use of an anti-ABC antibody allowed for the study of total cell lysates, alleviating the difficulties with fractionation, whilst at the same time allowing for the identification of the level of the active form of β-catenin involved in canonical Wnt signal transduction. This more sensitive approach also allowed for increases in

active β-catenin, and therefore canonical Wnt signalling, to be detected upon lower AR28 treatments of 1 μM.

In addition to these increases in stable β-catenin induced by AR28, which complimented the work by Gambardella *et al*. (2011), the work presented here also provides more functional information by the use of TCF/LEF1 reporter assays. These reporter assays demonstrated significant increases in the canonical Wnt transcription factor activity in a clear dose dependent manner. Furthermore BIO was not able to generate comparable increases in TCF reporter activity to AR28 over a 40 hour period, with approximately 10 fold lower reporter expression. The increase in reporter expression also appeared to plateau at around a 100-fold increase in reporter activity compared to controls by 40 hours, corresponding with a reduction in *Renilla* expression, indicative of reduced cell numbers. AR28 is therefore more potent than BIO at stimulating a canonical Wnt response *in vitro.* Furthermore BIO caused reductions in *Renilla* luciferase expression levels over the 40 hour incubation period that were not seen in controls or AR28 treated samples, suggesting a detrimental toxic effect on cell number and reporter expression. In support of this, BIO has been shown to inhibit the JAK/STAT pathway, leading to apoptosis (Liu et al, 2011). The comparison of AR28's ability to stimulate the canonical Wnt signalling pathway relative to ligand activated signal transduction was also possible. Recombinant Wnt3a was chosen as a comparator as it has been shown to stimulate osteogenesis in C3H10T1/2 cells (Winkler et al, 2005) and is therefore related to these studies by cell type and differentiation. This direct comparison between AR28 and recombinant Wnt3a demonstrated that AR28 is capable of generating increases in TCF transcriptional activity in a biologically relevant, ligand activated, range and one which allows comparison to other work (Liu et al, 2009).

Reporter assays were also used to demonstrate the specificity of AR28 treatment for the activation of canonical Wnt signalling over Hedgehog signalling. Another function of GSK3β, in addition to canonical Wnt signal transduction, is during the phosphorylation of the Gli family of transcription factors involved in Hh signal transduction. Phosphorylation leads to the cleavage or degradation of the transcription factors, altering them to an inhibitory form (See 1.3.3). Inhibition of this phosphorylation process would therefore increase the activatory forms of the Gli

transcription factors and induce gene expression. Conversely AR28 treatment caused small decreases in Hedgehog reporter activity when added alone. However, these changes where small, and a similar reduction was not detected upon co-stimulation of the Hh pathway by purmorphamine. This would suggest that while GSK3β is involved in Hh signal transduction it is not completely necessary, with Gli phosphorylation and processing/degradation still occurring, possibly through GSK3β activity remaining at sufficient levels after these treatment concentrations or its partial requirement for Gli processing. Therefore any effects caused by AR28 treatment at these concentrations or lower are unlikely to be due to alterations in Hh signalling, but instead due to the large effect upon the canonical Wnt signalling pathway.

As discussed above, canonical Wnt signalling is an attractive therapeutic target for many diseases and of particular interest to this thesis, in osteoporosis treatments as increased Wnt can increase bone mass in mice. Indeed, Gambardella et al. (2011) demonstrated that AR28 is also capable of increasing the bone mass of mice when injected subcutaneously for up to 14 days. Therefore to demonstrate the ability of AR28 to functionally stimulate canonical Wnt signalling *in vivo* an alternative model system was used, in which canonical Wnt signalling affects the embryonic patterning of *Xenopus* embryos. As mentioned above, when *Xenopus* embryos were cultured with AR28 in the growth solution, there was no effect on embryo development, whereas BIO was able to completely dorsalise 90% of the embryos. The ability of BIO to dorsalise *Xenopus* embryos confirms previous work by Meijer et al. (2003) in which both LiCl and BIO were capable of diffusing into the *Xenopus* embryo and inducing an increase in β-catenin throughout the embryo. AR28 was unable to cause the dorsalisation of *X. laevis* embryos by this technique, despite demonstrating greater potency *in vitro*. One explanation for this is that AR28 is less able to diffuse throughout the embryo. This proposition is strengthened by the ability of AR28 to induce embryonal axis duplication by injection into the ventral marginal zone of a four cell *X. laevis* embryo. In order for axis duplication to occur, and not dorsalisation, β-catenin stabilisation must only occur in a small area in the ventral side of the embryo, and not throughout the embryo as achieved by the bathing experiments. Therefore, if AR28 was able to rapidly diffuse throughout the embryo after injection, AR28 would become dilute throughout the embryo, where, if still

potent enough it would cause dorsalisation of the embryos, and not axis duplication. The need for such high AR28 concentrations for the induction of axis duplication may suggest that there is some degree of diffusion, therefore requiring high starting concentrations. Alternatively AR28 may be sequestered or degraded in the *in vivo* environment, whereas it is not during the *in vitro* assays.

Several other GSK3 inhibitors have been developed with similarly high potency and specificity for GSK3, however they have only briefly been shown to induce the canonical Wnt signalling pathway. One small molecule inhibitor of GSK3 is LY603281, which has an IC_{50} of 1.3 nM (Engler et al, 2004). This IC_{50} is lower than that calculated for AR28, and has also been shown to increase total β-catenin in C3H10T1/2 cells with concentrations as low as 0.01 µM (Kulkarni et al, 2006). However, TOPFlash analysis of the ability of LY603281 to increase TCF reporter expression were only able to create up to 7-fold increases in reporter activity over 24 hours, which peaked at concentrations of 0.1 µM. Above this concentration, reporter activity reduced again, to around 3-fold increases with both 1 and 10 µM treatments (Kulkarni et al, 2006). This increase in TOPFlash reporter activity is similar to that calculated for LiCl in this work, and that of the lower AR28 concentrations. However, the increase in reporter activity generated by AR28 did not plateau or peak by 10 µM, the highest concentration tested, and could generate over a 100-fold increase in luciferase expression after 24 hours treatment.

The CHIR-family of GSK3 inhibitors are another interesting comparator, with CHIR-99021 (IC_{50} 6.7 nM) and CHIR-98014 (IC_{50} 0.58 nM) being very potent and specific inhibitors of GSK3 (Ring et al, 2003). Furthermore CHIR-99021 has been studied for its ability to activate the canonical Wnt pathway *in vitro*. CHIR-99021 was able to cause a 2-fold increase in cytoplasmic β-catenin after 4 hours treatment at 3 µM in 3T3-L1 cells (Bennett et al, 2002). This is likely comparable to the ~8 fold increase in active β-catenin seen after 24 hours of treatment, although a direct comparison is not possible due to the difference in experimental design. To my knowledge however, the more potent CHIR-98014 has not been investigated for its ability to stimulate the canonical Wnt pathway. However, the ability of LY603281 or the CHIR family of inhibitors to stimulate the canonical pathway *in vivo* has not been studied.

In conclusion, AR28 is a potent stimulator of canonical Wnt signalling, through the inhibition of GSK3β, allowing for the stabilisation of β-catenin, its translocation into the nucleus of cells, and ultimately increase TCF/LEF1 transcription factor activity and gene expression. AR28 is much more potent than both LiCl and BIO, demonstrated in this work, but also LY603281, when comparing fold changes in TCF reporter expression to published work (Kulkarni et al, 2006). AR28 is therefore a valuable tool for studying the canonical Wnt signalling pathway *in vitro*, capable of generating large increases in signalling with little effect on cell viability. AR28 is less able to diffuse throughout tissues *in vivo* than BIO and LiCl, but once present within the cells is able to generate specific canonical Wnt responses. While this low capacity to diffuse throughout tissues may provide difficulties for administration, it does allow for a more targeted approach to canonical Wnt stimulation *in vivo*.

Chapter 4: AR28 and lineage commitment of MSCs

4.1 Introduction

Enhanced canonical Wnt signalling has been demonstrated to increase bone mass (Gambardella et al, 2011; Kulkarni et al, 2006) and bone remodelling (Krause et al, 2010) in mice in multiple studies, yet the mechanism underlying this bone anabolic effect remains unclear. One explanation is the effect of canonical Wnt signalling on the MSC pool in the bone marrow and how these cells then differentiate into osteoblasts, adipocytes and chondrocytes.

The study of canonical Wnt signalling in *in vitro* mesenchymal differentiation has been performed using a variety of techniques/experimental approaches. Firstly, the canonical Wnt pathway can be stimulated using a range of Wnt ligands and agonists, as discussed in chapter 3. Secondly, a wide array of murine cell lines has been used in preference to primary human MSCs. While several are either bi-potent, ST2 (Bennett et al, 2005), or multipotent, C3H10T1/2 (Date et al, 2004) and C2C12 (Lee et al, 2000), preosteoblast and preadipocyte (MC3T3-E1 (Date et al, 2004) and 3T3-E1 (Bennett et al, 2002) respectively) cells have also been used to gain a better understanding of the differentiation of mesenchymal precursors. While the precursor cell lines allow for a more simplified system, enabling the study of one particular differentiation pathway, they do not account for the potential for differentiation lineage interplay. The use of the bi- and multipotent cell lines begin to address this issue. Immortalised human cell lines, such as SV-HFO (Eijken et al, 2008) are also used, which can alleviate the problems associated with using murine models, yet as with all cell lines they are likely to behave abnormally due to prolonged *in vitro* culture. Human MSCs from a variety of sources are being increasingly utilised (Baksh et al, 2007a; Boland et al, 2004; Krause et al, 2010; Liu et al, 2009) allowing for the study of lineage commitment decisions towards multiple cell types in a human primary cell culture. While MSCs clearly offer many advantages over murine cell lines in their translatability into human medicine, there are disadvantages to their use in experimental procedures. Firstly there is the problem of donor

variation (Frank et al, 2002; Phinney et al, 1999; Siddappa et al, 2007). As MSCs are a primary cell line, they are likely to differ in their properties between donors, both in the proliferation rate and capacity to differentiate toward particular lineages. Furthermore, as MSCs are solely selected by their adherence to plastic, the resulting cell population is often heterogeneous, containing multipotent stem cell, but also a population of less potent, early lineage committed cells (Minguell et al, 2001). Together, these factors cause a difficulty in accurate reproduction between donors, in particular when combining absolute values. Therefore comparisons between donors are often limited to trends. Therefore it is also important to compare results from multiple donors to mitigate for the heterogeneity. MSCs also have poor transfection efficiencies (Baksh et al, 2007b), and cannot be used to generate stable lines without first generating an immortalised cell line (Abdallah et al, 2005), making the use of reporter assays and over-expression studies challenging.

The use of such a range of cell types has created difficulties of its own, with the culture conditions and requirements for differentiation varying with each cell type. This has lead to discrepancies in the findings between different groups using different cell models. While studies in the murine cell lines has repeatedly reported increases in osteoblastic genes in response to canonical Wnt signalling (Bennett et al, 2005; Jackson et al, 2005; Kulkarni et al, 2006) reports using human MSCs have demonstrated reductions in osteogenesis and increases in MSC proliferation in response to increased signalling (Baksh et al, 2007a; Boland et al, 2004; Liu et al, 2009). In this chapter the combination of the potent canonical Wnt activator AR28 (Characterised in chapter 3) is used in combination with human MSCs to gain a more thorough understanding of the effect of canonical Wnt stimulation on the tri-lineage differentiation of MSCs.

4.2 Aims

The general aims of the work presented in this chapter are to identify the effect of induced canonical Wnt signalling, by AR28, on the differentiation of human MSCs to gain a better understanding of the way in which AR28 increases bone mass in mice.

More specifically the aims are to:

- Characterise the effect of AR28 on CFU-F formation.
- Identify the effect of AR28 on the adipogenic differentiation of MSCs, in order to confirm the inhibitory effect of canonical Wnt signalling on this process.
- Determine the effect of AR28 on the osteogenic differentiation of MSCs using both the classical osteogenic media, and a milder stimulus by the exclusion of dexamethasone, to gain a better understanding of the role of Wnt signalling in osteogenic commitment.
- Identify the effect of AR28 on chondrogenic differentiation of MSCs cultured as micromass pellets.

4.3 Methods

4.3.1 CFU-F assay

MSCs were counted and seeded at 10 cells/cm^2 in 96 well plates in DMEM, 20% hyclone FBS (Thermo Scientific, Waltham, MA, USA), and 1% P/S. Cells were allowed to attach overnight prior to AR28 treatments. After 4 days, the media was replaced (containing standard FBS) and every 3-4 days thereafter. The cells were cultured for approximately 2 weeks or until discrete colonies could be identified under the microscope. The colonies were washed 2 times in PBS and fixed in 95% ethanol for 5 minutes. The ethanol was removed and the cells stained for 30 minutes in 0.5% Crystal Violet (in 95% ethanol). The Crystal Violet was removed and the plates washed in tap water to remove excess stain. The plates were then allowed to dry before imaging on a light box.

4.3.2 MTT assay

MSCs were seeded at 1x10^4 or 2x10^4 cells/cm^2 in 96 well plates, and allowed to attach overnight. Treatments were applied in replicates of 6, and replaced every 3-4 days. The cells were cultured for 4 or 7 days before the media was removed and replaced with 100 µl basal media plus 25 µl 5 mg/ml MTT (in PBS). Media and MTT was also added to 6 well with no cells as background controls. The samples were cultured at 37ºC, 5% CO_2 for 2 hours to allow the cells to convert the soluble MTT into insoluble formazan. The media/MTT was then removed and formazan solubilised by 30 minutes incubation in acidic isopropanol (0.04M HCl in 100% isopropanol). Once in solution, the absorbance was measured at 570 nm. The mean blank value was subtracted from the sample absorbance readings, and presented as the mean absorbance ± standard deviation for each treatment.

4.3.3 p-Nitrophenyl Phosphate (pNPP) alkaline phosphatase assay.

At the desired time point cells, cultured in 96 well plates, were washed with 0.2M Carbonate Buffer (0.2M Na_2CO_3, 0.2M $NaHCO_3$, pH 10.2), and lysed in 150µl lysis buffer (0.1% Triton X-100 in carbonate Buffer). Cells were then freeze-thawed (-80°C/37°C) 3 times and stored at -80°C. Upon thawing, the cells were pipetted up

and down to ensure full lysis and 50µl transferred to both a new 96 well plate for the pNPP assay, and a black 96 well plate for the picogreen assay.

4.3.3.1 pNPP assay

For alkaline phosphatase (ALP) activity, standards were generated using p-nitrophenol (pNP) diluted in 0.2M carbonate Buffer, and 100µl added per well of the clear plate. 50µl of working substrate (1 stock substrate: 2 dH_2O. [Stock substrate = 10mg pNPP, 9ml 0.2M carbonate buffer, 1ml 100mM $MgCl_2$]) was then added to each sample well and incubated at 37°C for up to 1 hour before the absorbance at 405nm was measured.

4.3.3.2 Picogreen assay

To measure the DNA content, the wells were treated with Quant-iT picogreen reagent (Invitrogen, Carlsbad, CA, USA). 50 µl of picogreen working reagent (50:1, Tris-EDTA : picogreen) was added to each sample and salmon sperm DNA standards. The fluorescence was then measured using a plate reader (458 nm excitation and 538 nm emission).

Standard curves were created for both pNP and DNA and the sample concentrations calculated. The number of nmoles of pNP produced per minute of incubation could then be calculated for each well before normalising to DNA to give nmoles pNP/min/µg DNA.

4.3.4 Alkaline Phosphatase Enzyme Histochemistry and von Kossa staining

At the desired time point the cells, cultured in 24 well plates, were washed with PBS, followed by treatment with ALP reagent mix (0.2mg/ml naphthol AS-MX in 1% N,N-dimethylformamide diluted in 0.1M Tris (base) pH 9.2, plus 1mg/ml Fast Red TR). Cells were then washed in PBS before fixation with 4% paraformaldehyde for 5 mins, followed by single washes in PBS and dH_2O. Mineralisation was visualised using the von Kossa technique with the addition of 1% silver nitrate solution and left on a light box for 30 mins. Cells were subsequently washed with dH_2O, treated with

2.5% sodium thiosulphate for 5 minutes and washed again with dH_2O, before storage in 20% glycerol in PBS and imaged using bright field microscopy.

4.3.5 Alizarin Red S staining

Cells were cultured in 24 well plates and treated as described. Calcification of osteogenic monolayers was visualised using Alizarin Red Staining. Cells were washed with PBS followed by fixation with 4% PFA for 15 minutes. The cells were then washed 3 times in PBS before staining with 40mM Alizarin Red S solution (pH4.2) for 20min at room temperature. The cells were finally washed three times in PBS, followed by washes in tap water to remove non-specific staining. Plates were allowed to dry prior to imaging.

4.3.6 Oil Red O staining

Cells were cultured in 96 well plates and treated as described. Lipid droplets were visualised using Oil Red O staining. Cells were washed with PBS followed by fixation with 4% paraformaldehyde for 10 mins. The cells were then washed once in dH_2O and incubated in 60% isopropanol for 5 mins. The isopropanol was removed and followed by an incubation in Oil Red O staining solution (0.3% Oil Red O in 60% isopropanol) for 10 mins, washed once in 60% isopropanol and 3 times with dH_2O. The samples were stored in 20% glycerol in PBS and imaged using bright field microscopy. For quantification, Oil Red O was extracted using 100% isopropanol (50µl/well) for 10 minutes and the absorbance measured (490nm).

4.3.7 FABP5/BODIPY staining

Cells, cultured in glass bottom 96 well plates, were fixed at the desired time point in 4% paraformaldehyde for 15 min, followed by washing in PBS. The cells were then blocked in PBS supplemented with 1.1% BSA and 0.2% Triton-X-100 for 30 minutes at room temperature. Anti-FABP5 (Table 4.3.1) was added overnight at 4°C in blocking buffer. The cells were washed in blocking buffer before addition of Alexa Flour 647 donkey anti-goat IgG and Hoechst 33342 (Table 4.3.1) in blocking buffer for 1 hour at room temperature. The cells were washed three times in PBS

followed by BODIPY (Table 4.3.1) staining in PBS for 40 minutes at room temperature. Cells were washed and stored in PBS at 4°C. Images were taken using an automated ImageXpress 5000A (Molecular Devices) and analysed using Definiens analyzer software.

Table 4.3.1. FABP5/BODIPY antibody and stain concentrations

Antibody/stain	Host	Concentration /dilution	Supplier	Catalogue No.
Anti-human FABP5	Goat	5 µg/ml	R&D Systems	AF3077
Alexa Flour 647 anti-goat IgG	Donkey	1:500	Invitrogen	A21447
Hoechst 33342	N/A	1 µM	Invitrogen	H3570
BODIPY	N/A	200 nM	Invitrogen	D3933

4.3.8 Mitomycin C treatment

MSCs were seeded at $2x10^4$ cells/cm^2 in 24 well plates and allowed to adhere overnight. The media was removed and replaced with basal media containing 10 µg/ml mitomycin C (Sigma Aldrich, St. Louis, MO, USA). Cells were incubated for 2 hours before removal of the mitomycin C. The cells were washed twice with PBS before addition of osteogenic (excluding dex) media to the cells.

4.3.9 Cell Trace™ CFSE assay

4.3.9.1 Optimisation

MSCs were trypsinised and split into 4 tubes of $1.5x10^5$ cells. One sample was seeded into a single well of a 6 well plate for a no CFSE control. The remaining three were resuspended at $5x10^5$ cell/ml (300 µl) in PBS + 5% FBS. Cell Trace™ CFSE stock solution (Invitrogen, Carlsbad, CA, USA) (5 mM) was added to the cells at 10, 20 and 30 µM, mixing whilst adding. Samples were incubated for 10 minutes at 37ºC before quenching with 3 ml cold PBS + 5% FBS and incubating at 4ºC for 5 minutes. Samples were then centrifuged and washed in warm PBS + 5% FBS 3

times before resuspension in basal media and seeded into wells of a 6 well plate. After 24 hours of culture, cells were detached from culture using trypsin and analysed by flow cytometry using CyAn^{TM} ADP Analyzer (Beckman Coulter, Fullerton, CA, USA) at the appropriate excitation and emission wavelengths and analysed using Summit software.

4.3.9.2 Proliferation assay

MSCs were trypsinised and counted. A sample of cells was seeded back into a well of a 6 well plate for a no CFSE control. The remaining cells were resuspended at $5x10^5$ cells/ml in PBS + 5% FBS and Cell Trace^{TM} CFSE stock solution (5 mM) added to a final concentration of 20 µM. Cells were incubated at 37ºC for 10 minutes before quenching with 10x the volume PBS + 5% FBS and incubated at 4ºC for 5 minutes. The cells were then centrifuged and washed in warm PBS + 5% FBS 3 times before resuspension in basal media and seeded into wells of a 6 well plate at $2x10^4$ cells/cm^2, and allowed to adhere overnight. Samples were then cultured for 7 days in the presence of a combination of media and AR28 conditions. The cells were then detached using trypsin and analysed by flow cytometry using CyAn^{TM} ADP Analyzer (Beckman Coulter, Fullerton, CA, USA) at the appropriate excitation and emission wavelengths and analysed using Summit software.

4.3.10 Ki67 Immunocytochemistry

Prior to fixation, MSCs to be probed for Ki67 were stained by ALP enzyme histochemistry (Section 4.3.4). Cells cultured on coverslips in 24 well plates were fixed with 4% paraformaldehyde for 15 min, before blocking in PBS + 10% goat serum + 0.1% triton X-100 for 2 hours at RT. Incubation with Anti-Ki67 (Abcam) at 1:200 in blocking buffer was performed overnight at 4°C. The cells were washed in PBS before addition of the Goat anti-rabbit IgG Alexafluor 488 (Invitrogen, Carlsbad, CA, USA) secondary antibody at 1:500. Samples were incubated for 2 hours at 4°C in the dark. The secondary antibody was removed and the samples washed 3 times in PBS. Coverslips were mounted on slides using VECTASHIELD mounting medium with DAPI (Vector laboratories, Burlingame, CA, USA).

4.4 Results

4.4.1 AR28 reduces the CFU-F capability of MSCs

One characteristic of MSCs is their capacity to form colonies from single cells, which is measured as the CFU-F capability of the population. To identify how AR28 affects the CFU-F formation, MSCs were seeded at clonal density (10 cells/cm^2, i.e. 960 cells/well of a 6 well plate), and cultured for 2 weeks before fixation and staining with crystal violet to visualise colonies. A representative donor is presented in Figure 4.4.1. Untreated cells formed an average of ~10 colonies per well, which equates to a CFU-F value of ~1%. The vehicle control had no significant effect on CFU-F values, nor did the lowest concentration of AR28, 0.05 µM. However, the higher concentrations of AR28 generated a dose-dependent decrease in number of colonies formed, implying that AR28 has a negative effect of the CFU-F capacity of MSCs.

4.4.2 AR28 inhibits adipogenic differentiation of MSCs

In order to study the effect of AR28 administration on the adipogenic differentiation of MSCs, bone marrow (BM) MSCs and human adipose derived stem cells (hADSC) were seeded at confluency and induced to form adipocytes. These samples were then also treated with either vehicle control (DMSO) or AR28 at varying concentrations for 15 days before fixing and staining with Oil Red O to identify lipid droplet formation. Both the BM MSCs and hADSCs formed lipid droplets in response to the adipogenic media (Figure 4.4.2 A and Figure 4.4.3 A), which was attenuated in response to AR28 treatment. Both the number of lipid droplets and size of the droplets were reduced in AR28-treated samples at all concentrations, but 0.5 µM AR28 was required to cause total inhibition. The Oil Red O was extracted out of the droplets by incubation in 100% isopropanol, allowing for quantification of the staining by absorbance at 450 nm (Figure 4.4.2 B and Figure 4.4.3 B). The BM MSCs showed significant reductions in Oil Red O with as little as 0.05 µM AR28, with absorbance values being reduced to basal levels by 0.5 µM AR28. The hADSCs however, did not show significant reductions in absorbance with the lower concentrations, but still reduced to basal levels with 0.5 µM AR28.

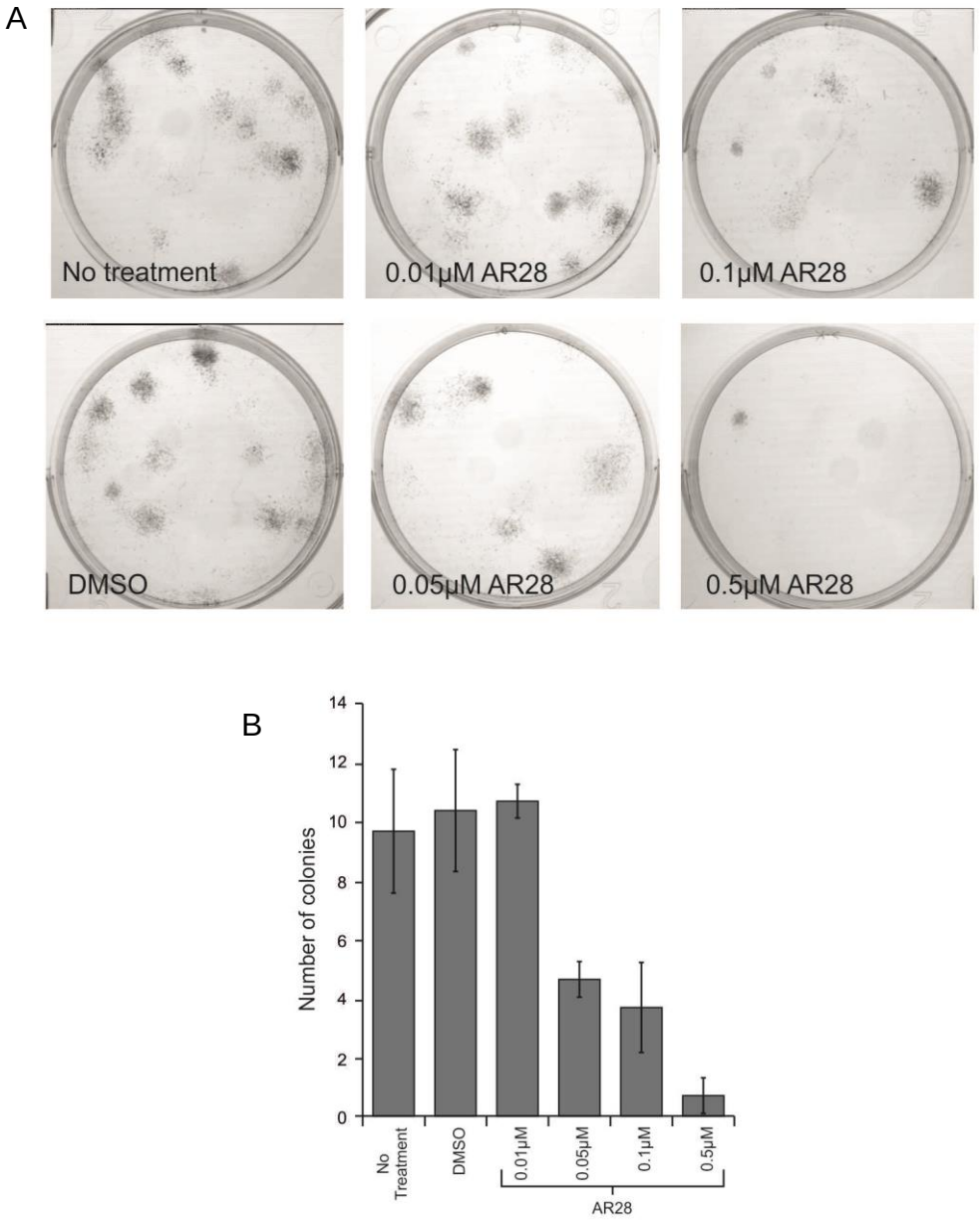

Figure 4.4.1. AR28 inhibits CFU-F capability of BM MSCs
A) Images of a representative donor (K57) showing the effect of AR28 on the CFU-F capability of MSCs. MSCs were seeded at clonal density and allowed to attach before AR28 administration at the concentration given. The MSCs were then cultured for approximately 2 weeks to allow colonies to form and stained with crystal violet before imaging. B) Bar chart showing the number of CFU-F colonies for each treatment. Values given as mean ± stdev, n=3.

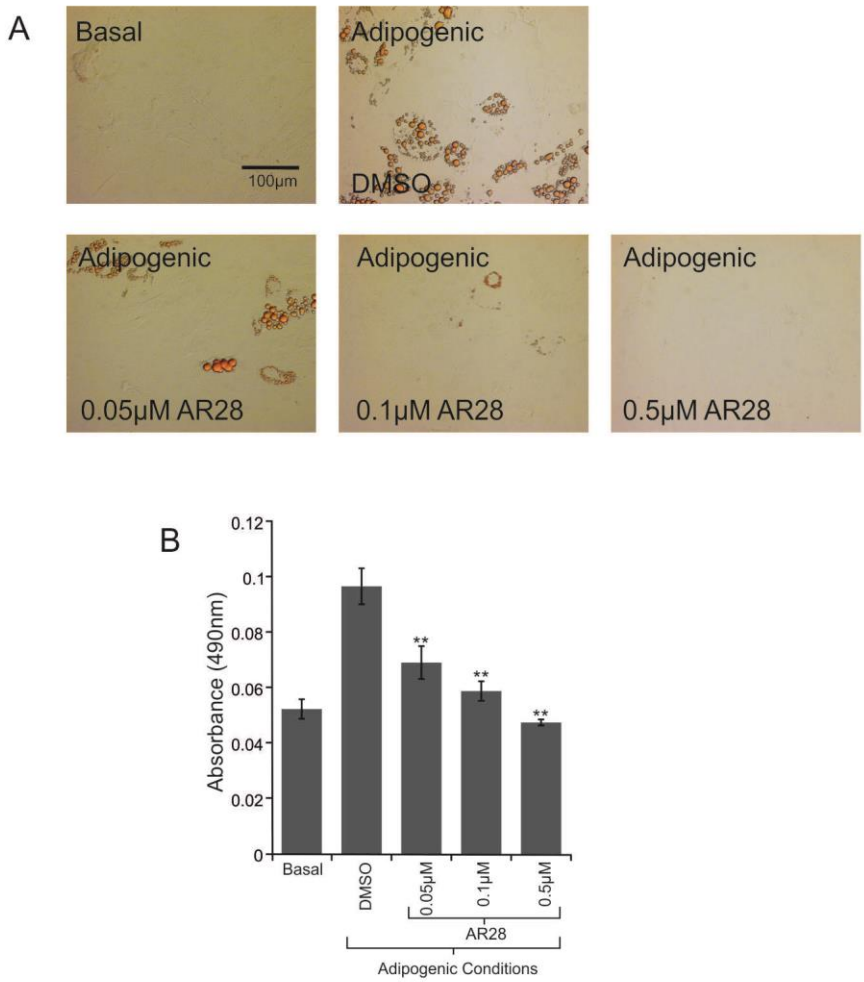

Figure 4.4.2. AR28 inhibits adipogenesis of BM MSCs
Oil Red O staining of a representative MSC donor (FH429) after 15 days adipogenic treatment with AR28 at concentrations shown, or DMSO control. A) Brightfield microscopy images of Oil Red O staining showing lipid droplet accumulation. B) Quantification, by absorbance at 490 nm, of Oil Red O staining after solubilisation in 100% isopropanol. Values given as mean ± stdev. n=6 (independently treated technical replicates), * $p<0.05$, ** $p<0.005$, *** $p<0.001$. Statistical significance is relative to vehicle control, by Mann-Whitney U and Kruskal-Wallis tests.

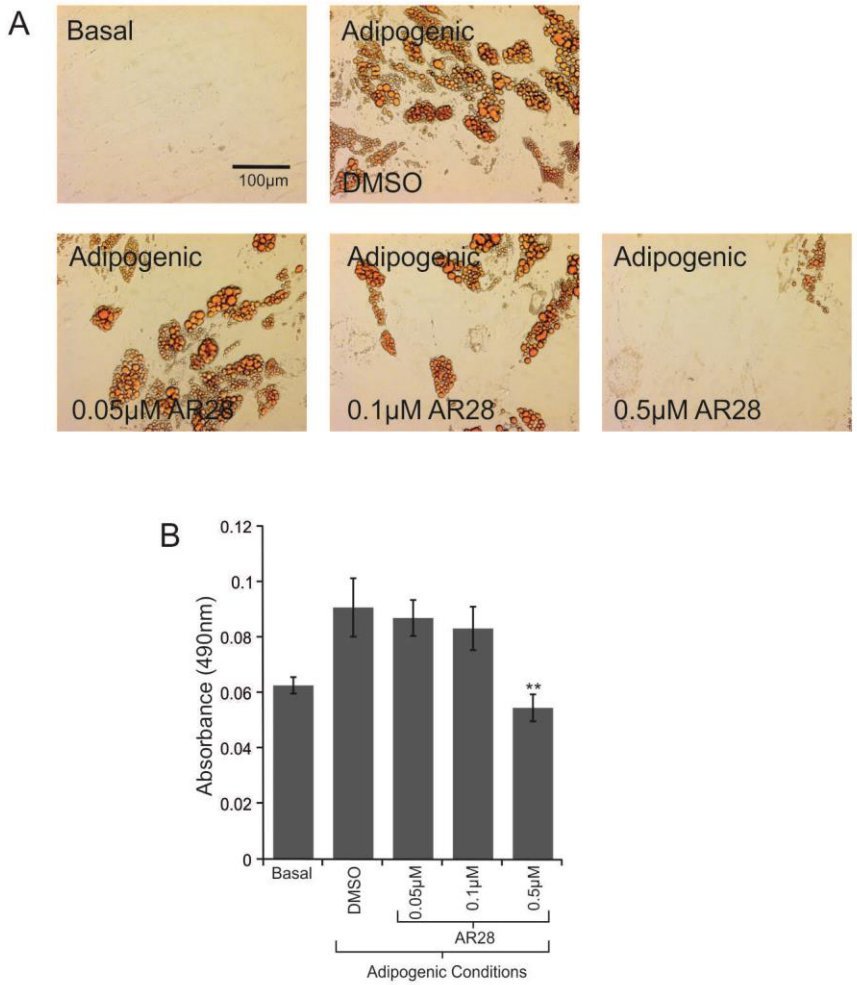

Figure 4.4.3. AR28 inhibits adipogenesis of hADSCs
Oil Red O staining of hADSCs after 15 days adipogenic treatment with AR28 at concentrations shown, or DMSO control. A) Brightfield microscopy images of Oil Red O staining showing lipid droplet accumulation. B) Quantification, by absorbance at 490 nm, of Oil Red O staining after solubilisation in 100% isopropanol. Values given as mean ± stdev. n=6 (independently treated technical replicates), * $p<0.05$, ** $p<0.005$, *** $p<0.001$. Statistical significance is relative to vehicle control, by Mann-Whitney U and Kruskal-Wallis tests.

While these results demonstrate changes in Oil Red O staining within the population they give no information into cell number, and the percentage of cells that have become adipogenic. In order to gain some understanding of this an alternative high content approach was taken. hADSCs were treated with adipogenic supplements as previously described for up to 7 and 14 days, and were then immuno-stained for FABP5 (adipocyte marker), and co-stained with BODIPY (lipid droplets) and Hoecsht 33342 (nuclei). Three colour images were acquired automatically, allowing for 4 images to be taken from each of the 6 independently treated replicates. Using Definiens automated image analysis software (Figure 4.4.4) and defined thresholds the number of nuclei within FABP5/BODIPY double positive areas could be calculated, allowing for the evaluation of the percentage of double positive cells in response to AR28 treatments. The use of a half log serial dilution allowed for a broad range of AR28 concentrations to be analysed, identifying the key range in concentrations for inhibition of adipogenesis as being ~50-500 nM, similar to that identified by Oil Red O staining. Under adipogenic conditions, approximately 50-60% of the cells expressed both FABP5 and contained lipid droplets by 14 days, which was reduced to ~20% with 200 nM AR28, and completely abolished with 632 nM AR28 (Figure 4.4.5 A). Interestingly, the lower concentrations (2-20 nM AR28) at 7 days gave a small but significant increase in adipogenesis, but this was no longer seen by the later time point. This same pattern was detected in a separate independent experiment (results not shown). The second piece of information available from this work is the cell number in response to AR28 treatment. At day 7 there was no effect of AR28 on cell number, yet by day 14, the adipogenic conditions had reduced cell numbers compared to the basal media controls (Figure 4.4.5 B). Furthermore, treatment with 63 and 200 nM AR28 was able to partially rescue this decrease in proliferation, resulting in significant increases in cell number compared to vehicle control. However, above these concentrations AR28 has a detrimental effect on cell number causing greatly reduced numbers of cells at 14 days, suggesting a toxic effect of prolonged exposure to high concentrations of AR28.

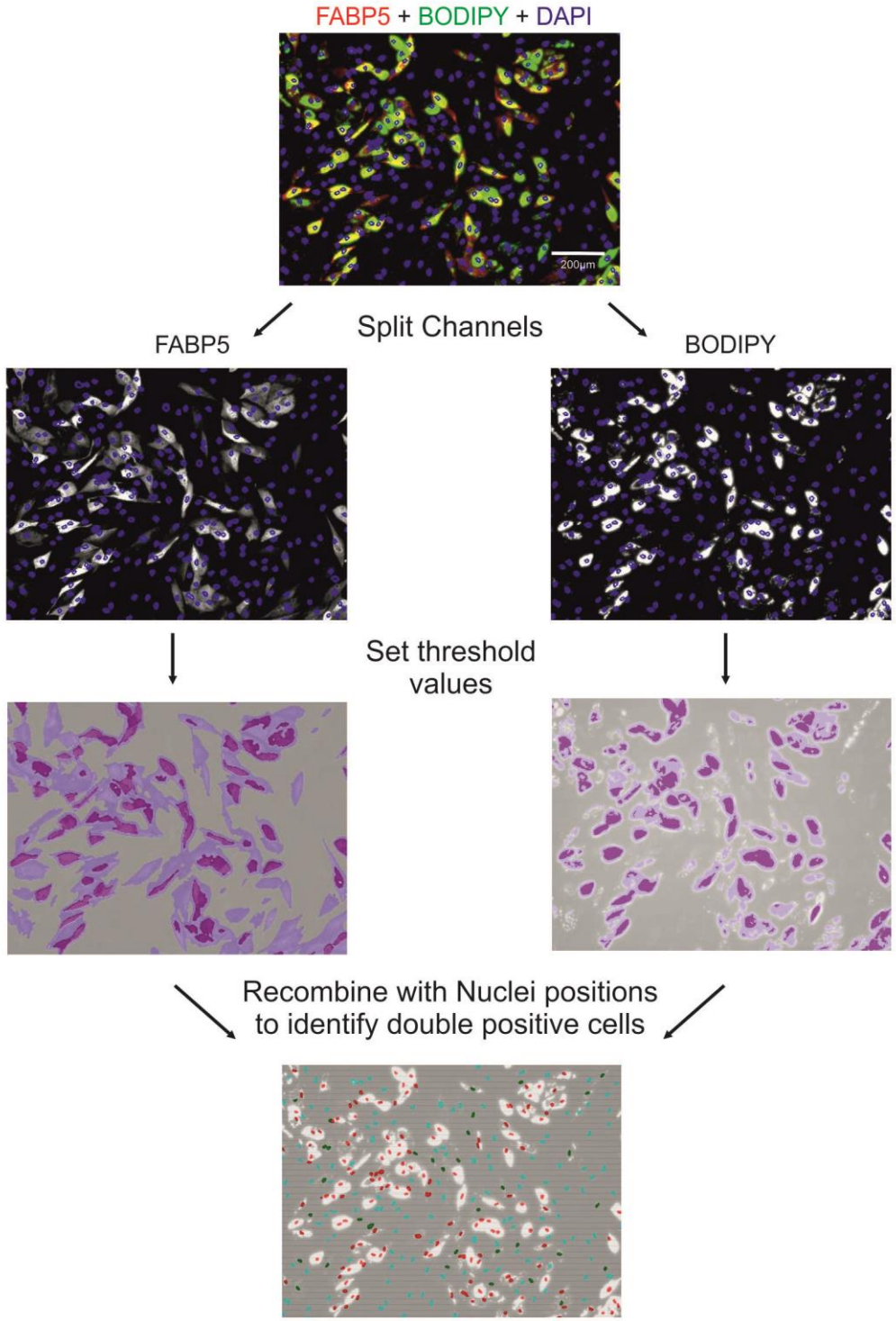

Figure 4.4.4. Schematic showing image analysis process performed by Definiens software.
Definiens analysis software separates the flourescence channels, separating the different antibody staining, allowing threshold levels to be applied to each marker independently, marking positive and negative regions. These threshold maps are then recombined with nuclei positional information from Hoecsht 33342 staining to identify the percentage of FABP5/BODIPY double positive cells within the image.

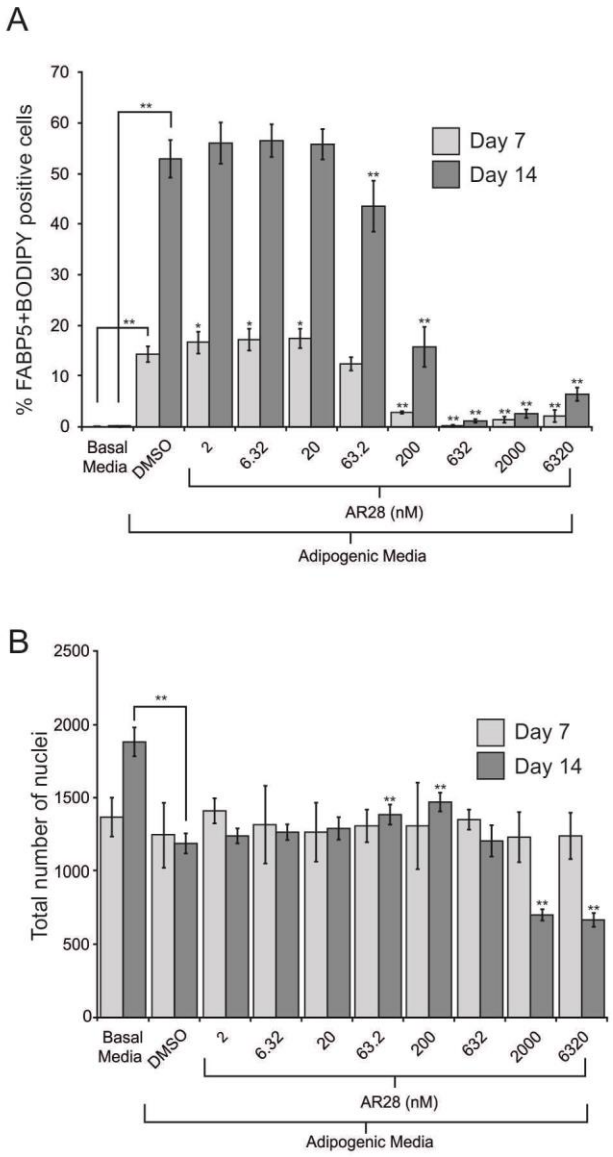

Figure 4.4.5. High content analysis of adipogenesis and the effect of AR28. FABP5 and BODIPY analysis of 7 and 14 day adipogenic hADSC cultures in the presence of AR28 at the concentration given or DMSO control using Definiens analyses of fluorescence microscopy imaging. A) Bar chart showing the number of FAPB5/BODIPY double positive cells in response to different AR28 concentrations. B) Bar chart showing the total number of nuclei in response to different AR28 concentrations. Values given as mean ± stdev., n=6 (independently treated technical replicates), * $p<0.05$, ** $p<0.005$, *** $p<0.001$. Statistical significance is relative to vehicle control at appropriate time point unless stated otherwise, by Mann-Whitney U and Kruskal-Wallis tests.

4.4.3 AR28 inhibits classical dexamethasone induced osteogenesis

In a similar manner, to identify the effect of AR28 on osteogenic differentiation of MSCs, cells were cultured in the presence of classical osteogenic media containing β-glycerophosphate, L-ascorbic acid and dexamethasone (dex). Initial analysis of osteogenesis was carried by measurement of alkaline phosphatase (ALP) activity per well, normalised to DNA content. Multiple seeding densities of $5x10^3$, $7.5x10^3$ and $1x10^4$ cells per well of a 96 well plate were tested in combination with the addition of AR28 to the culture (Figure 4.4.6). All three seeding densities allowed for the osteogenic differentiation of MSCs in response to osteogenic media. Similarly they all responded to AR28 in the same manner, with a dose-dependent inhibition of ALP activity relative to the osteogenic vehicle control, implying reduced osteogenesis. AR28 at 0.5 µM was capable of completely inhibiting any increase in ALP activity, with lower concentrations causing intermediate levels of inhibition. As the starting cell number had little effect on the osteogenic differentiation of MSCs, an intermediate number of $2x10^4$ cells/cm^2 was selected for use in all further experiments. At these cell seeding numbers, other MSC donors and hADSCs were analysed for AR28 effect on osteogenesis. Again, AR28 prevented the increases in ALP activity caused by the osteogenic media in a dose-dependent manner (Figure 4.4.7). The degree of inhibition by the lower AR28 (0.05-0.1 µM) concentrations varied between donors, but as with adipogenesis, complete inhibition of osteogenesis was detected when 0.5 µM AR28 was administered.

To study the patterning of ALP and mineralisation in AR28 treated cultures, an imaging approach was taken. MSCs were cultured in osteogenic media for up to three weeks, before ALP enzyme histochemistry and von Kossa (vK) staining were performed. As seen with the ALP activity assay above, ALP was clearly reduced in cultures containing AR28 in a dose-dependent manner in all donors tested (Figure 4.4.8). Furthermore, while the degree of vK staining (marking the phosphate of the mineralised matrix) varied between donors, it was also reduced by AR28 treatment in all donors.

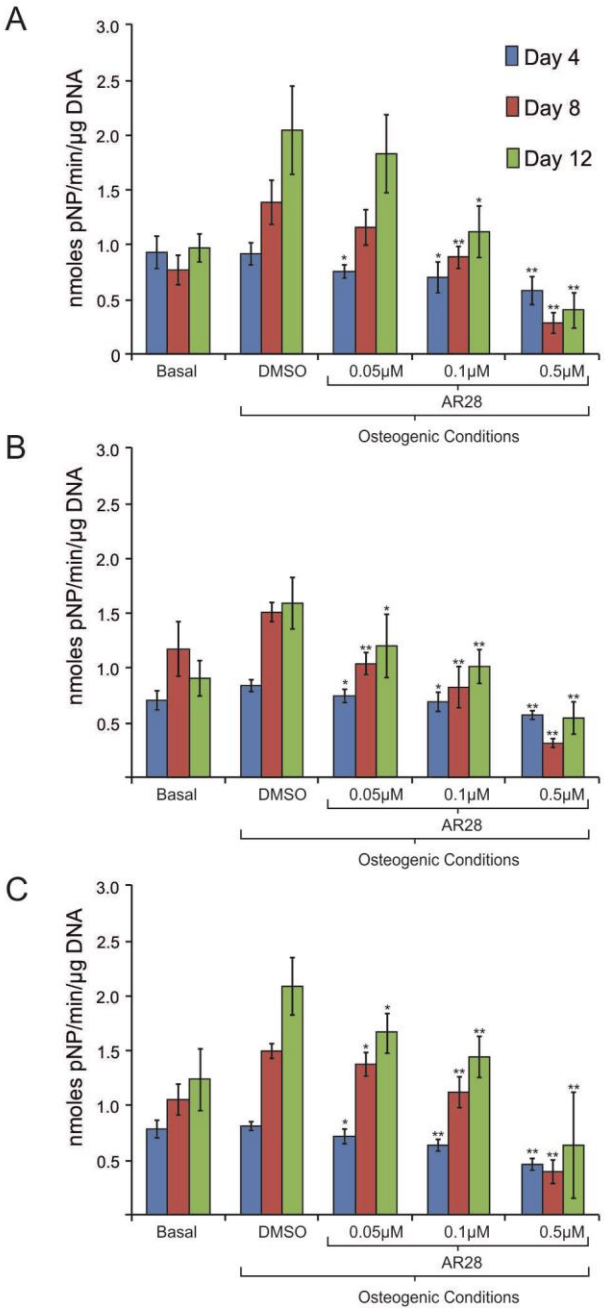

Figure 4.4.6. AR28 inhibits osteogenic induced ALP activity irrespective of cell density.

MSC (FH405) seeded in 96 well plates at A) $5x10^3$, B) $7.5x10^3$ or C) $1x10^4$ cell/well, were cultured in osteogenic (incl. dex) conditions for up to 12 days in the presence of AR28 at the concentrations shown or DMSO control. ALP activity normalised to cell number (given as nmoles pNP/min/µg DNA) was calculated at 4, 8 and 12 days. Values given as mean ± stdev., n=6 (independently treated technical replicates), * $p<0.05$, ** $p<0.005$, *** $p<0.001$. Statistical significance is relative to vehicle control at appropriate time point, by Mann-Whitney U and Kruskal-Wallis tests.

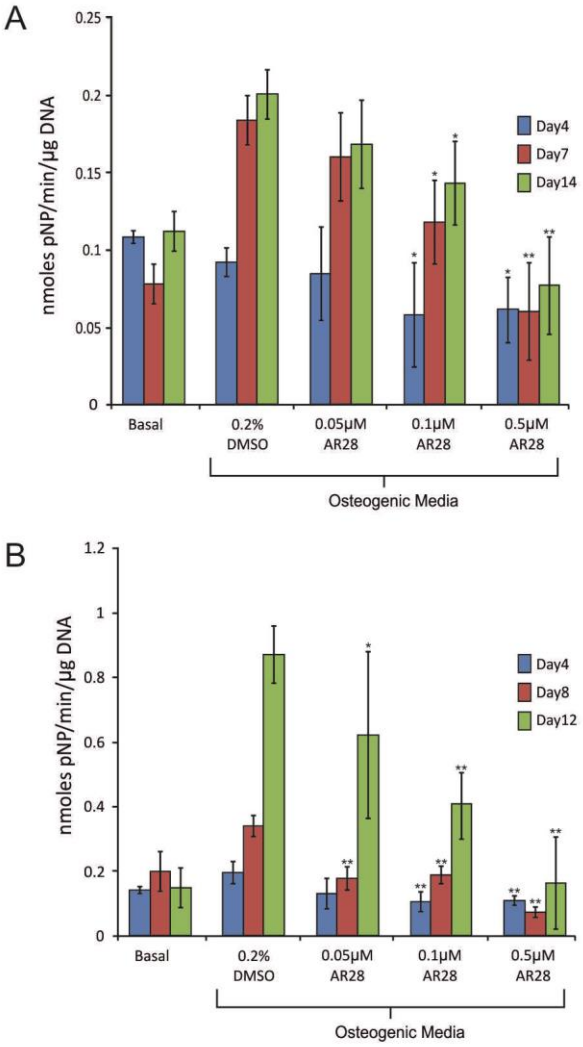

Figure 4.4.7. AR28 inhibits osteogenic induced ALP activity in both BM MSCs and hADScs.
A) MSC (FH429) or B) hADScs seeded in 96 well plates at $2x10^4$ cells/cm^2, were cultured in osteogenic (incl. dex) conditions for up to 12 days in the presence of AR28 at the concentrations shown or DMSO control. ALP activity normalised to cell number (given as nmoles pNP/min/µg DNA) was calculated at 4, 8 and 12 days. Values given as mean ± stdev., n=6 (independently treated technical replicates), * $p<0.05$, ** $p<0.005$, *** $p<0.001$. Statistical significance is relative to vehicle control at appropriate time point, by Mann-Whitney U and Kruskal-Wallis tests.

The calcium deposition in the mineralised matrix was also studied using Alizarin Red S (ARS) staining (Figure 4.4.9). In this case final mineralisation at 21 days appeared unaffected by AR28 treatment. However, early time points showed increases in small amounts of calcium deposition in the matrix upon AR28 treatment, giving a very different picture of mineralisation to the vK staining which was abolished by AR28.

It was proposed that the time at which MSCs are subjected to canonical Wnt signalling may be important in generating positive or negative effects on osteogenesis, therefore MSCs were treated with four day pulses of 0.5 μM AR28 at different time points during osteogenic differentiation (Figure 4.4.10). Osteogenesis was then measured by ALP activity. As previously shown, AR28 addition to the culture for the entire period prevented the increases in ALP activity in response to osteogenic differentiation. However, this process was reversible, as when AR28 was added for the first 4 days of culture, the increase in ALP activity was delayed, but osteogenesis resumed at the normal rate upon AR28 removal, almost reaching control levels by 16 days. When AR28 was added at later points throughout the differentiation process, increases in ALP activity were halted, but resumed to some degree after AR28 removal. The ALP activity results have been plotted relative to DNA content, therefore while increases in ALP activity were halted upon AR28 addition, the cells continued to proliferate, causing the reduced relative ALP activity per cell. It is unlikely that the levels of ALP expression within the cells already expressing ALP is reduced by AR28, but that the percentage of cells within the proliferating population that express ALP is reduced. However, one cannot say for certain from this experiment.

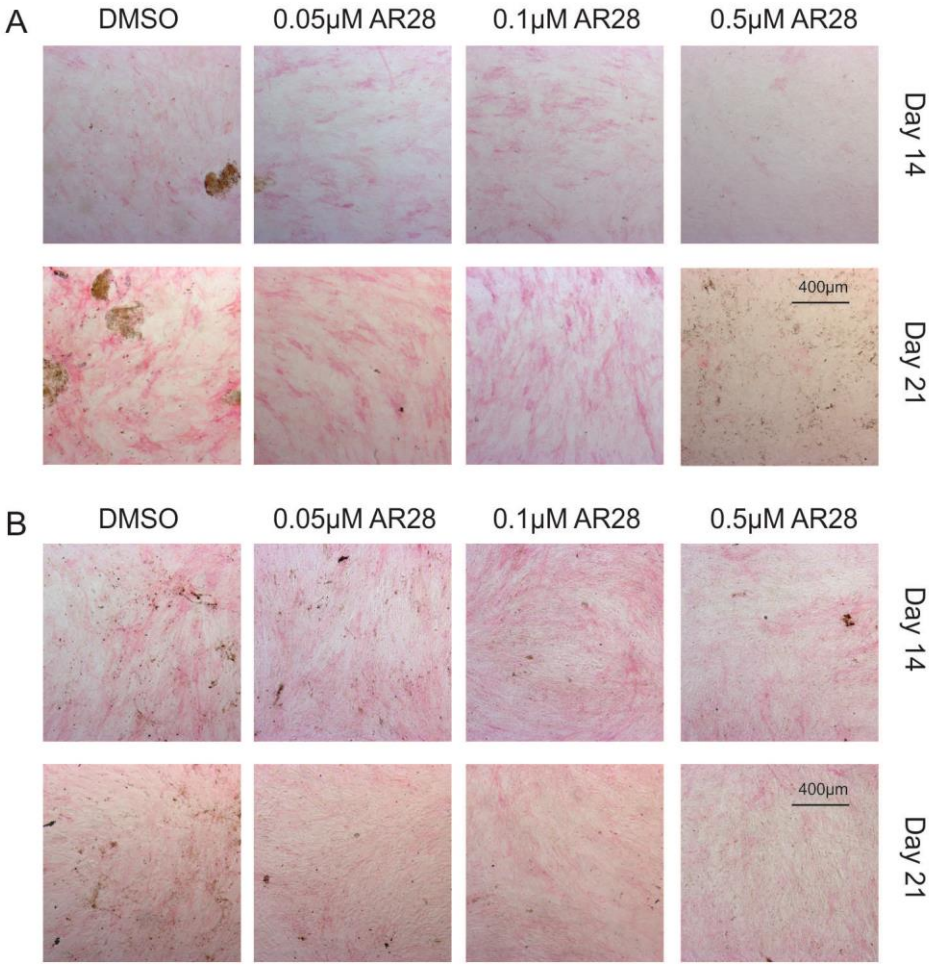

Figure 4.4.8. ALP enzyme histology and von Kossa staining of osteogenic induced MSCs in the absence and presence of AR28.
MSCs (A) FH408, B) FH429) were cultured for 14 or 21 days in osteogenic (Incl. dex) conditions, with AR28 at concentrations given, or DMSO control. Samples were stained for ALP (pink) and von Kossa (brown/black) and imaged by brightfield microscopy. Representative images shown.

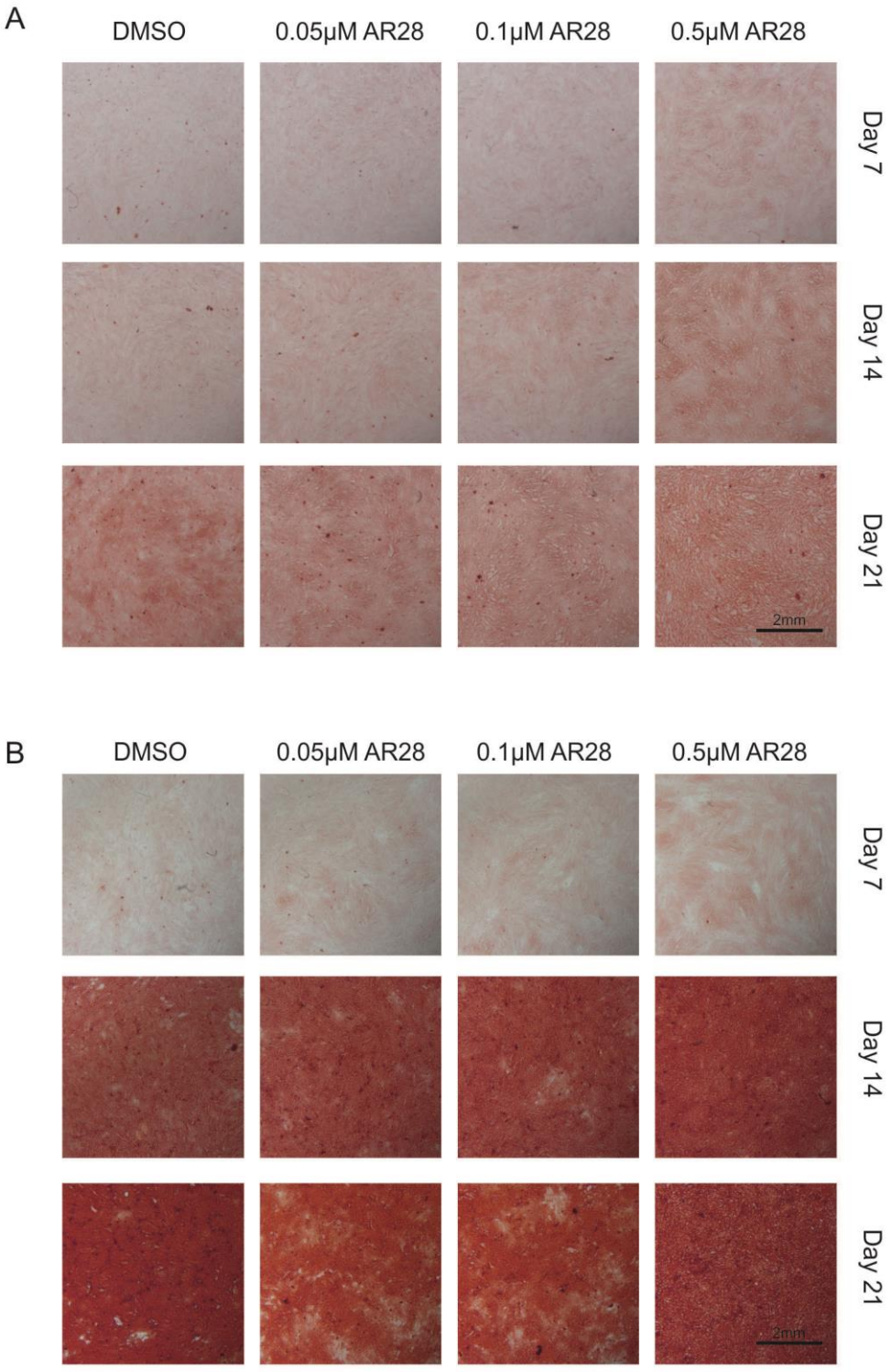

Figure 4.4.9. Alizarin Red S staining of osteogenic induced MSCs in the absence and presence of AR28.
MSCs (A) K16, B) FH408) were cultured for 7, 14 or 21 days in osteogenic (Incl. dex) conditions, with AR28 at concentrations given, or DMSO control. Samples were stained Alizarin Red S and imaged by brightfield microscopy. Representative images shown.

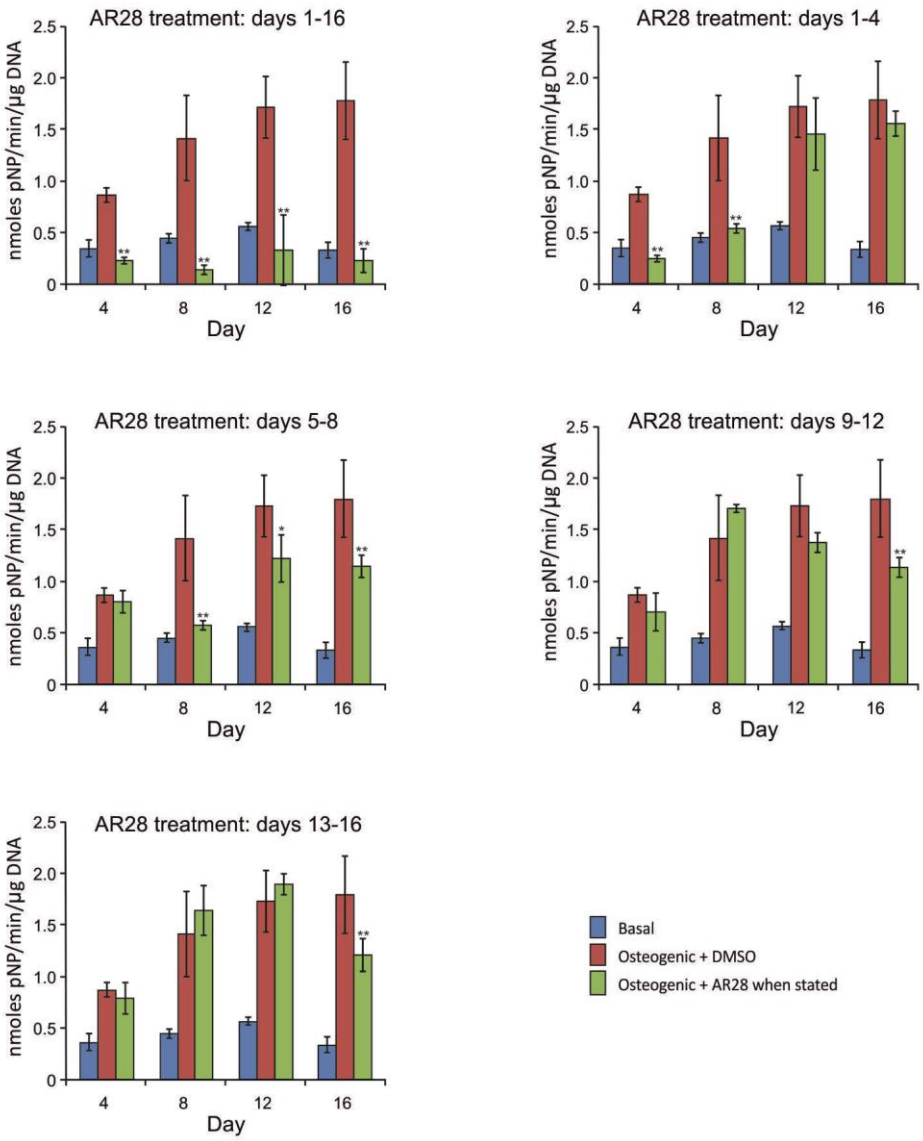

Figure 4.4.10. ALP activity in osteogenic induced MSCs with pulse treatments with AR28.
MSCs (FH367) were cultured in basal (blue bars) or osteogenic (Incl. dex) conditions for up to 16 days, with the addition of 0.5 µM AR28 for the period indicated (green bars) or DMSO control (red bars). ALP activity normalised to cell number (given as nmoles pNP/min/µg DNA) was calculated at 4, 8, 12 and 16 days. Values given as mean ± stdev., n=6 (independently treated technical replicates), * $p<0.05$, ** $p<0.005$, *** $p<0.001$. Statistical significance is relative to vehicle control at appropriate time point unless, by Mann-Whitney U and Kruskal-Wallis tests.
(Similar results from donor FH388 not shown)

4.4.4 AR28 enhances dexamethasone-independent osteogenesis

It has been noted in the literature that activation of the canonical Wnt signalling pathway using BIO or a PPARγ inhibitor can have a positive osteogenic effect when added to a mild osteogenic stimulus, which excludes dex from the osteogenic culture medium (Krause et al, 2010). However, BIO has been shown to have off-target effects, and poor specificity (Liu et al, 2011; Meijer et al, 2003), and PPARγ inhibition indirectly stimulates canonical Wnt signalling and will have many unknown effects. Therefore, to test whether the more potent and specific canonical Wnt stimulator, AR28, could have a positive effect on early osteogenesis, MSCs were treated as previously, but with the exclusion of dex from the osteogenic culture medium. Under these conditions, staining of the cultures revealed very little ALP, vK or ARS staining in the control differentiation samples, which varied depending on donor. However, when treated with AR28, small increases in ALP and ARS staining could be detected. More specifically, MSCs cultured in mild osteogenic media showed very little ALP staining, present in varying amounts depending on donor, in some cases just in a few cells throughout the culture (Figure 4.4.11 A), or evenly throughout the culture at low levels (Figure 4.4.11 B+C). However, irrespective of the osteogenic control ALP levels, increases in ALP could be seen upon AR28 treatment at 14 and 21 days. Again the extent of staining varied between donors, and different AR28 concentrations had optimal effects. For example FH408 had increased ALP with 0.05 and 0.1 µM AR28, but reduced by 0.5 µM, while FH429 and K16 showed highest ALP with 0.5 µM AR28. No vK staining could be detected in any of these cultures suggesting that dex is required for osteogenic maturation and phosphate deposition.

ARS staining of parallel cultures showed a similar pattern, with small amounts of calcium deposition in the control mild osteogenic stimulus. Interestingly donor FH429, which generated the strongest ALP staining in these conditions, also displayed the greatest calcium deposition. Upon AR28 addition to this culture system, clear increases in calcium deposition could be detected by ARS staining, in a dose-dependent manner, with the greatest increases detected with 0.5 µM AR28 for all three donors (Figure 4.4.12).

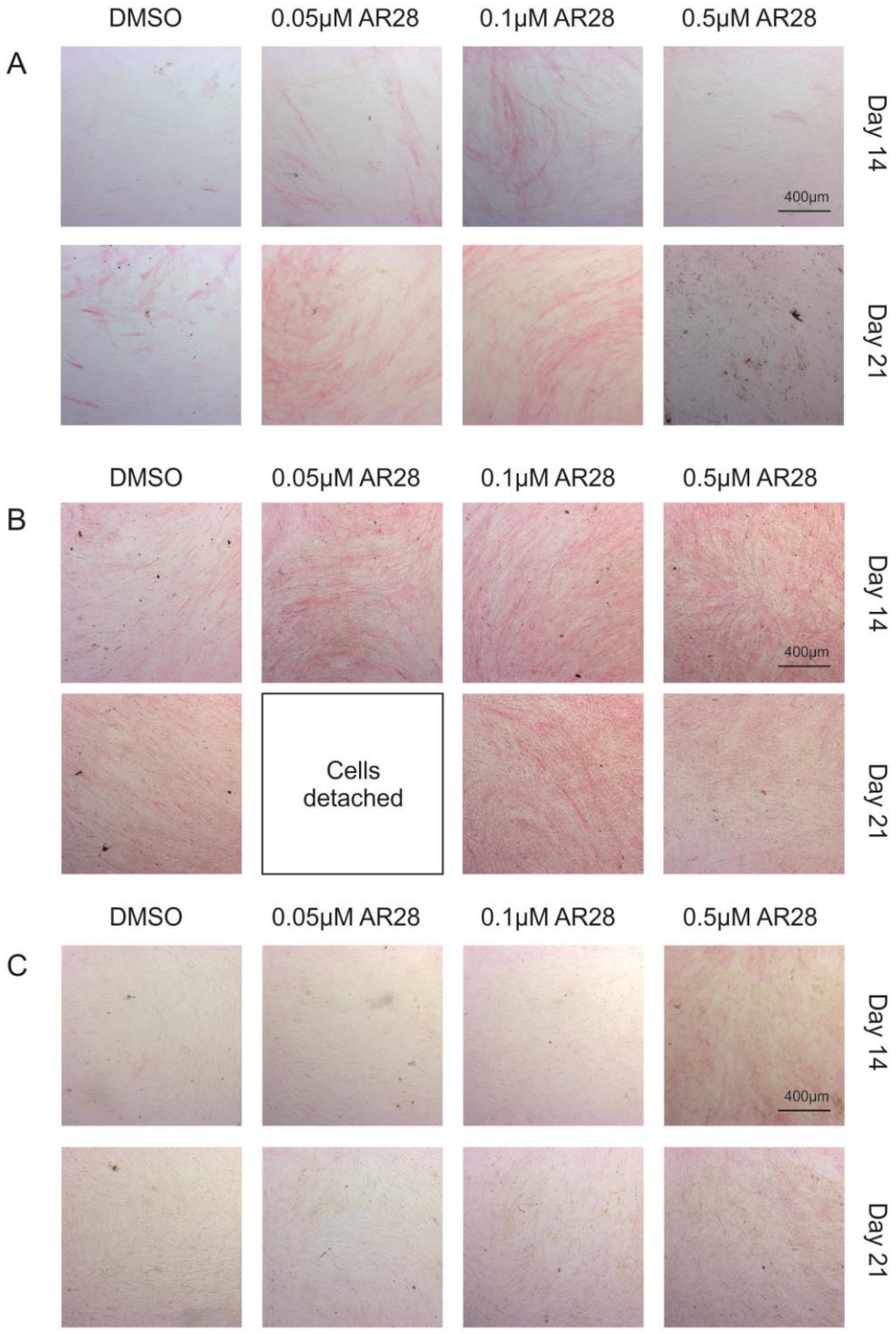

Figure 4.4.11. ALP enzyme histology and von Kossa staining of MSCs cultured in mild osteogenic stimuli (excluding dex) with and without AR28 addition.

MSCs (A) FH408, B) FH429, C) K16) were cultured in mild osteogenic (excluding dex) conditions with AR28 at concentrations given, or DMSO control. After 14 or 21 days cultures were stained for ALP (pink) and von Kossa (brown/black) and imaged by brightfield microscopy. "cells detached" indicates samples that had contracted into pellets.

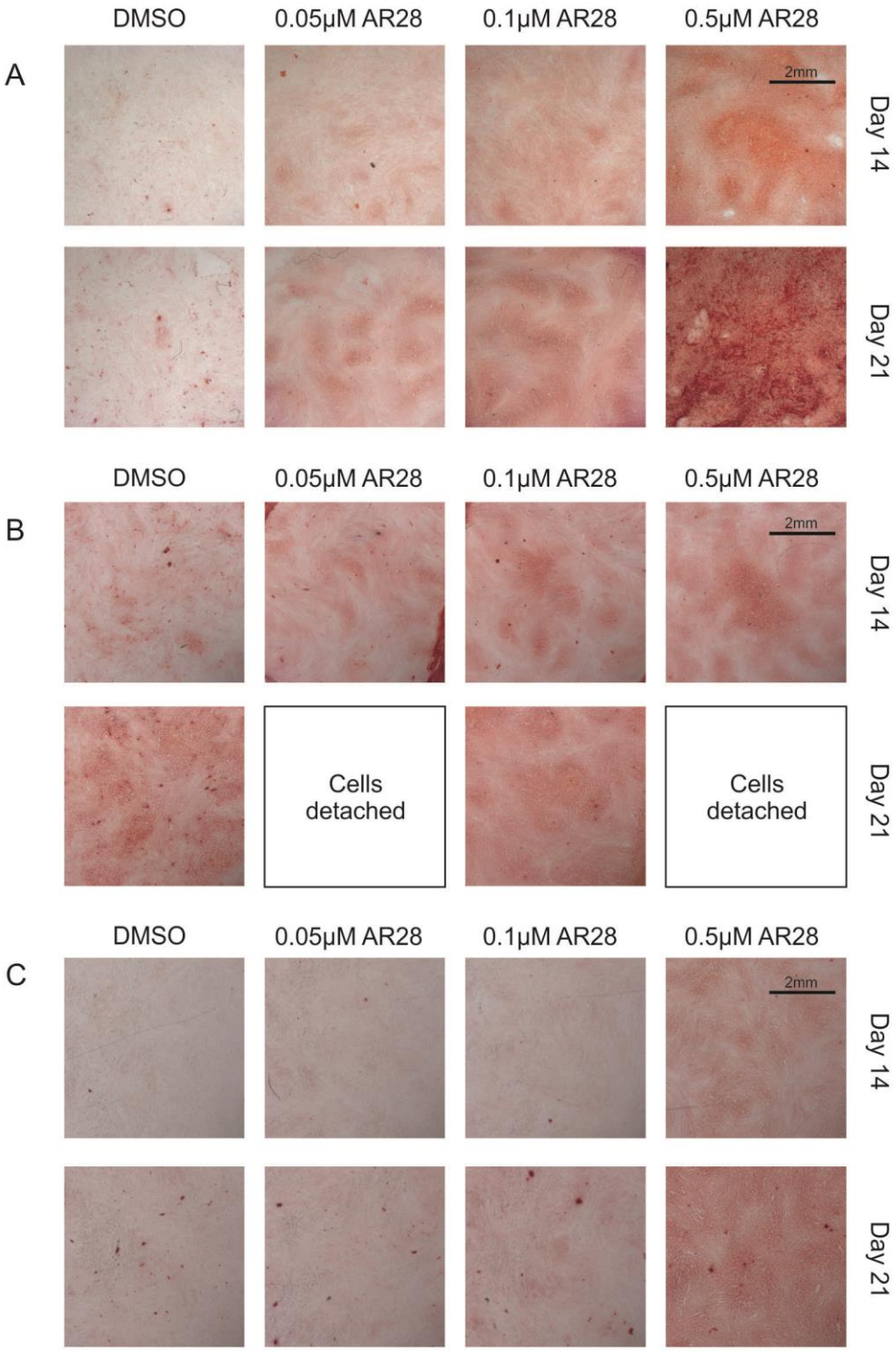

Figure 4.4.12. Alizarin Red S staining of MSCs cultured in mild osteogenic stimuli (excluding dex) with and without AR28 addition.
MSCs (A) FH408, B) FH429, C) K16) were cultured in mild osteogenic (excluding dex) conditions with AR28 at concentrations given, or DMSO control. After 14 or 21 days cultures were stained with Alizarin Red S and imaged by brightfield microscopy. "cells detached" indicates samples that had contracted into pellets.

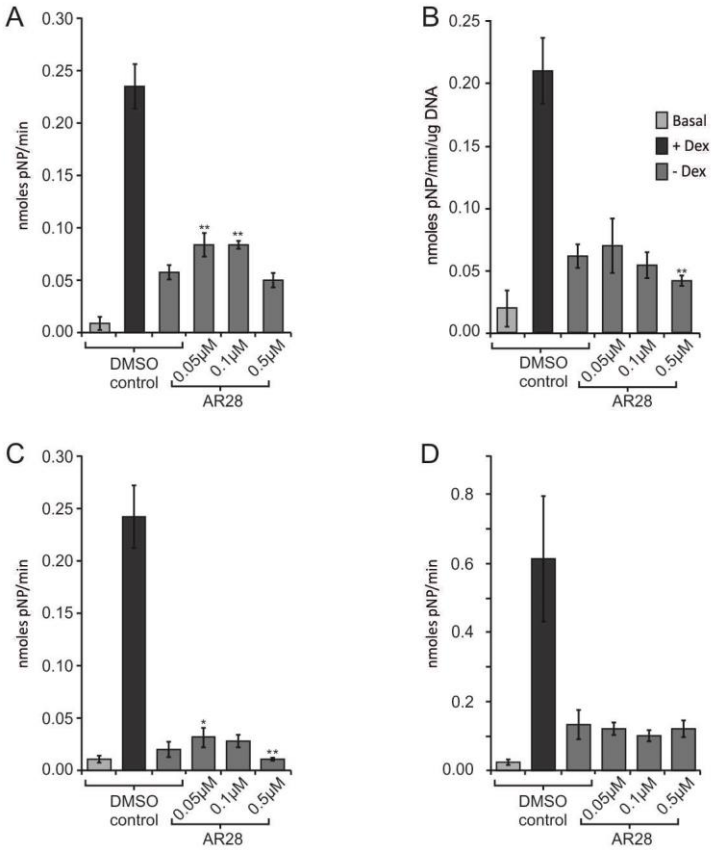

Figure 4.4.13. ALP activity assays of MSCs cultured in mild osteogenic stimuli (excluding dex) with and without AR28 addition.
A-B) MSCs (FH408) were cultured in mild osteogenic (excluding dex) conditions (grey bars) with AR28 at concentrations given, or DMSO control. Basal (light grey bars) or osteogenic (including dex) (black bars) conditions were also performed as controls. After 14 days A) ALP activity (given as nmoles pNP/min) and B) ALP normalised to cell number (given as nmoles pNP/min/µg DNA) were calculated. C) (FH388) and D) (K16) show ALP activity (nmoles pNP/min) of two other donors from similar experiments. Values given as mean ± stdev., n=6 (independently treated technical replicates), * $p<0.05$, ** $p<0.005$, *** $p<0.001$. Statistical significance is relative to mild osteogenic vehicle control, by Mann-Whitney U and Kruskal-Wallis tests.

It is also worth noting that in these mild osteogenic conditions, AR28 caused very confluent layers to form, likely through increased proliferation. In the later time points, this can cause the sheets to contract around the circumference of the well, and eventually round up into a pellet (identified in Figure 4.4.11 and Figure 4.4.12 as "cells detached").

ALP activity assays were also performed using these mild osteogenic stimuli, however the absorbance readings were very low, making detection of the small changes in activity very difficult. Small but significant increases in ALP activity within treated wells could be detected at AR28 concentrations of 0.05 and 0.1μM in one donor (FH408) (Figure 4.4.13 A), but these increases were not apparent when normalised to DNA due to increased cell number in AR28 treated samples (Figure 4.4.13 B). Small changes in ALP activity could be seen in another donor (FH388) (Figure 4.4.13 C), while in another (K16) no changes in ALP were detected (Figure 4.4.13 D).

4.4.5 Increased cell number caused by AR28 is important in the increased differentiation in response to mild osteogenic stimulation

As alluded to previously, AR28 appeared to cause increased cell numbers when added to the mild osteogenic culture medium. To study the proliferation rate further, MTT assays were performed. The MTT assay uses the conversion of the water soluble MTT (3-(4,5-dimethylthiazol-2-yl)-2,5-diphenyltetrazolium bromide) to an insoluble formazan by mitochondrial proteins, which can then be solubilised and the concentration determined by measuring the absorbance at 570nm. The rate of MTT conversion can then be used as an indirect measure of cell number. The effect of AR28 on cell number was analysed by this method in basal, mild osteogenic (excluding dex) and osteogenic (including dex) medium at both $1x10^4$ and $2x10^4$ cells/cm^2 after 4 and 7 days. Significant increases in MTT conversion were detected in all media and cell densities at both time points with AR28 treatment in a dose-dependent manner (Figure 4.4.14 and Figure 4.4.15). The difference between the DMSO control and AR28 treatment was greatest in the mild osteogenic media, yet even in basal media, where little increase in MTT conversion was detected over time in control samples, 0.5 μM AR28 was able to generate significant ($p<0.05$) increases

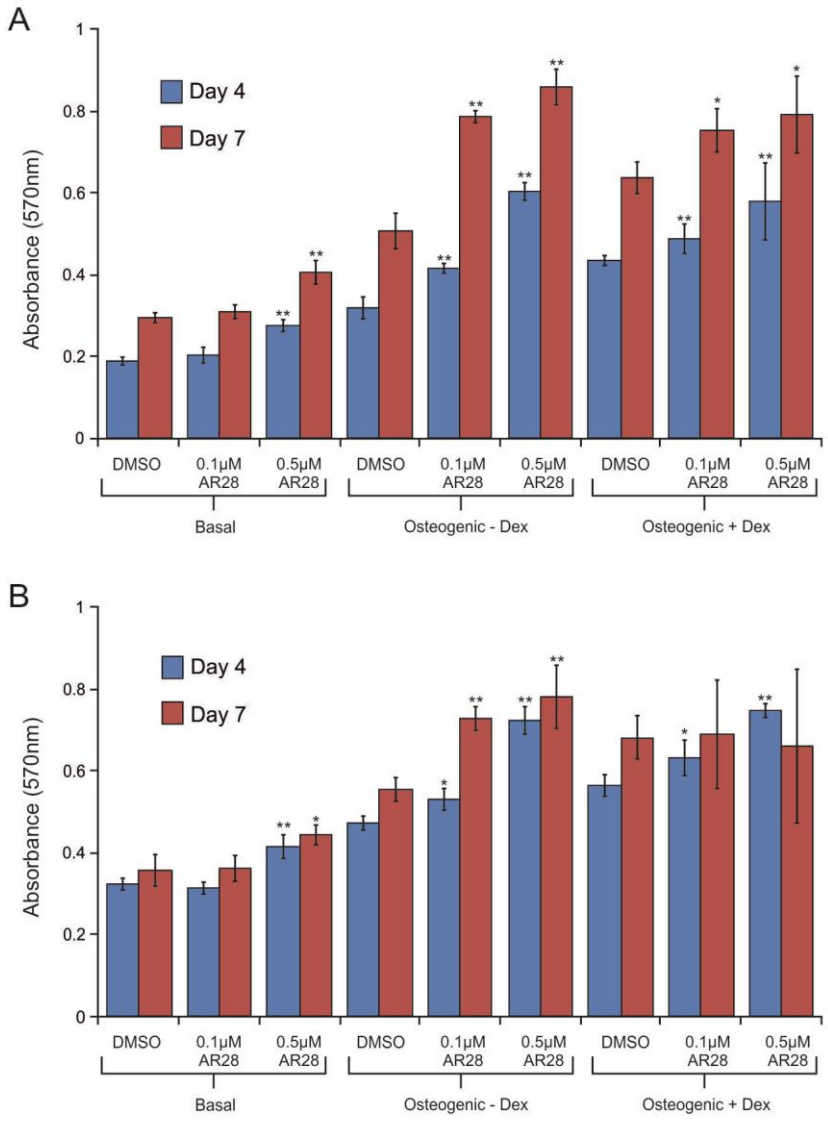

Figure 4.4.14. MTT assay of donor FH429 in response to AR28 in basal and osteogenic media.

MSCs (FH429) were seeded at A) $1x10^4$ or B) $2x10^4$ cells/cm^2 and cultured in Basal, mild osteogenic (Excl. dex) or osteogenic (Incl. dex) conditions with AR28 at the concentration given, or DMSO control. After 4 or 7 days the cultures were assayed for mitochondrial activity by MTT conversion to formazan. This was then solubilised and quantified by measuring the absorbance at 570 nm, and subtracting the blank value. Values given as mean ± stdev., n=6 (independently treated technical replicates), * $p<0.05$, ** $p<0.005$, *** $p<0.001$. Statistical significance is relative to vehicle control at appropriate conditions and time point, by Mann-Whitney U and Kruskal-Wallis tests.

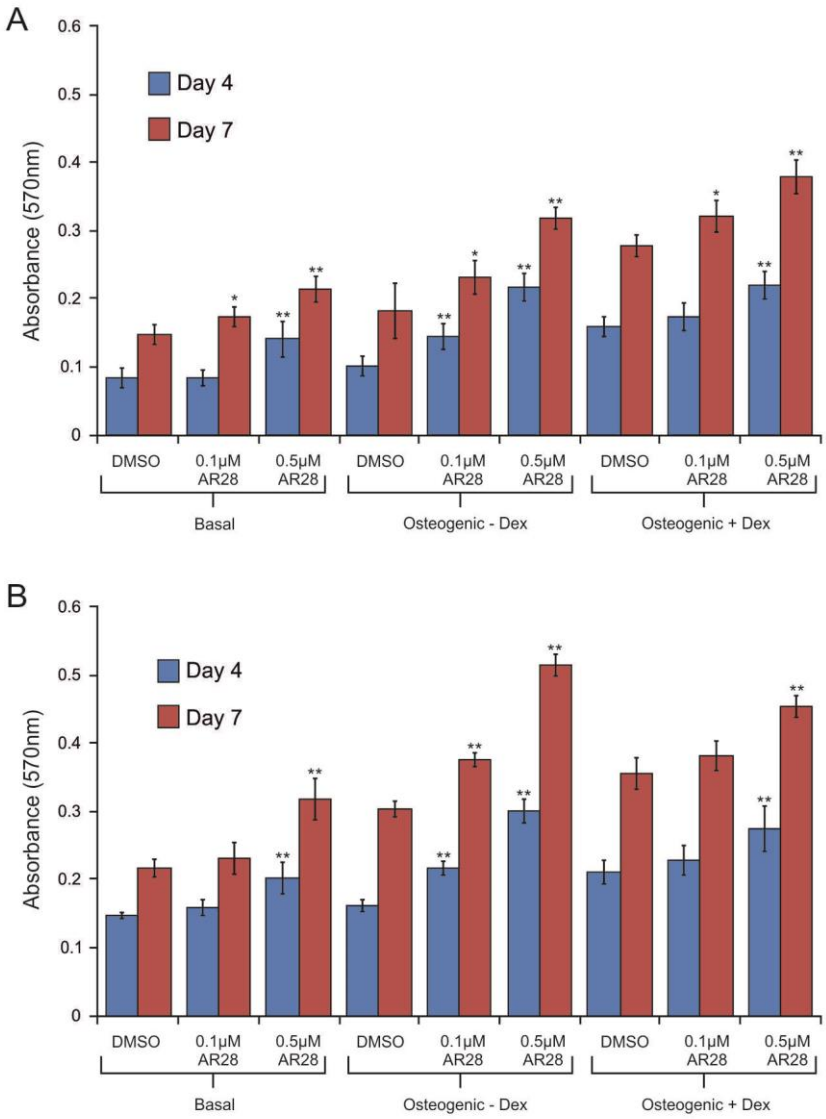

Figure 4.4.15. MTT assay of donor K57 in response to AR28 in basal and osteogenic media.

MSCs (K57) were seeded at A) $1x10^4$ or B) $2x10^4$ cells/cm^2 and cultured in Basal, mild osteogenic (Excl. dex) or osteogenic (Incl. dex) conditions with AR28 at the concentration given, or DMSO control. After 4 or 7 days the cultures were assayed for mitochondrial activity by MTT conversion to formazan. This was then solubilised and quantified by measuring the absorbance at 570 nm, and subtracting the blank value. Values given as mean ± stdev., n=6 (independently treated technical replicates), * $p<0.05$, ** $p<0.005$, *** $p<0.001$. Statistical significance is relative to vehicle control at appropriate conditions and time point, by Mann-Whitney U and Kruskal-Wallis tests.

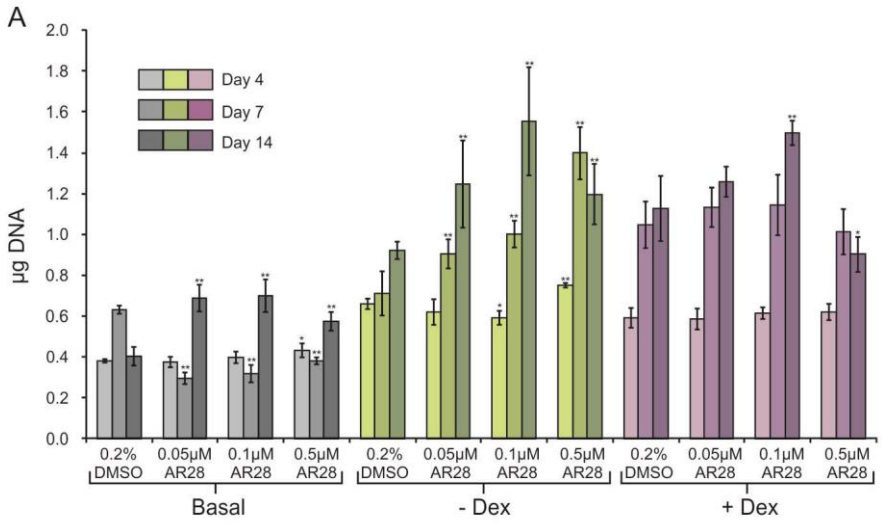

Figure 4.4.16. DNA content of MSC cultures in response to AR28 in basal and osteogenic conditions.
MSCs (FH408) were seeded at $2x10^4$ cells/cm^2 and cultured in Basal, mild osteogenic (Excl. dex) or osteogenic (Incl. dex) conditions with AR28 at the concentration given, or DMSO control. After 4, 7 and 14 days the cultures were assayed for DNA content by picogreen analysis. Fluorescence was measured and the NDA concentration calculated from a standard curve. Values given as mean ± stdev., n=6 (independently treated technical replicates), * $p<0.05$, ** $p<0.005$, *** $p<0.001$. Statistical significance is relative to vehicle control at appropriate conditions and time point, by Mann-Whitney U and Kruskal-Wallis tests.

with 4 days of treatment. These increases in cell number were confirmed by DNA content experiments over longer time periods of 2 weeks, which demonstrated clear increases in DNA content per well of cells treated with AR28. As in the MTT assays, increases in cell number could be detected in basal media and standard osteogenic media, however the largest increases were present in mild osteogenic conditions (Figure 4.4.16). After 7 days, the increases in DNA are dose dependent with the greatest increases with 0.5 µM AR28, but by 14 days 0.5 µM AR28 appears to be having a detrimental effect on cell number. This is similar to the cell death caused by the higher concentrations of AR28 during the adipogenic differentiation described above in which prolonged periods of treatment can begin to reduce cell number.

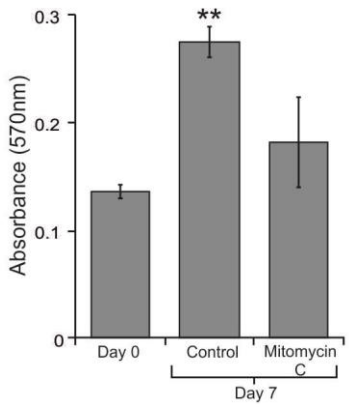

Figure 4.4.17. Mitomycin C treatment inhibits the proliferation of MSCs
MSCs (FH429) were treated for 2 hours with 10 µg/ml mitomycin C followed by culture in mild osteogenic (Excl. dex) conditions for 7 days. Cultures were then assayed for MTT conversion into formazan, which was solubilised and quantified by measuring the absorbance at 570 nm. Without mitomycin C treatment MSCs were able to proliferate over the 7 day period. Mitomycin C treatment prevented this increase in MTT conversion. Values given as mean ± stdev., n=6 (independently treated technical replicates), * $p<0.05$, ** $p<0.005$, *** $p<0.001$. Statistical significance is relative to vehicle control at appropriate conditions and time point, by Mann-Whitney U and Kruskal-Wallis tests.

4.4.5.1 Mitomycin C treatment prevents AR28 induced osteogenesis

It was therefore proposed that the increases in mineralisation were dependent on elevated cell numbers. To test this hypothesis, MSCs were treated with mitomycin C to inhibit their proliferation (Figure 4.4.17), and subjected to the mild differentiation stimulus with and without AR28 addition. As in previous studies, AR28 caused increases in Alizarin Red S staining by 7 and 14 days, however when proliferation was inhibited this increase in mineralisation was blocked (Figure 4.4.18). Furthermore, the increased mineralisation detected was not solely due to an increase in total cell number, as simply doubling the initial seeding density had no effect on Alizarin Red S staining (Figure 4.4.18). It is worth noting that after mitomycin C treatment, the cells appeared more sensitive to the toxic effects of AR28, and by 14 days mitomycin C had a clear effect on cell death with 0.5 µM AR28.

Similar experiments were performed in which MSCs were pre-treated with mitomycin C to prevent proliferation, and subjected to mild osteogenic induction with and without AR28, and analysed by ALP enzyme histochemistry and vK staining. Images from two donors are shown in Figure 4.4.19. A third donor (K9) showed very little staining after 14 days and a particularly high sensitivity to the toxic effects of AR28 after mitomycin C treatment. Both FH402 and K16 showed increases in ALP in response to AR28 treatment in combination with the mild osteogenic stimulus after 14 days, however the effect of mitomycin C treatment is less clear. A higher AR28 concentration, at 0.5 µM, caused fairly severe cell death in the mitomycin C treated cultures as mentioned above. A concentration of 0.1 µM AR28 was less toxic to the cells and allowed for the analysis of the effects of mitomycin C and AR28 treatment on ALP activity. Mitomycin C had no clear effect on AR28 induced ALP activity in FH402 cells (Figure 4.4.19 A), but appeared to increase the intensity, but not the area of the staining in donor K58 samples (Figure 4.4.19 B).

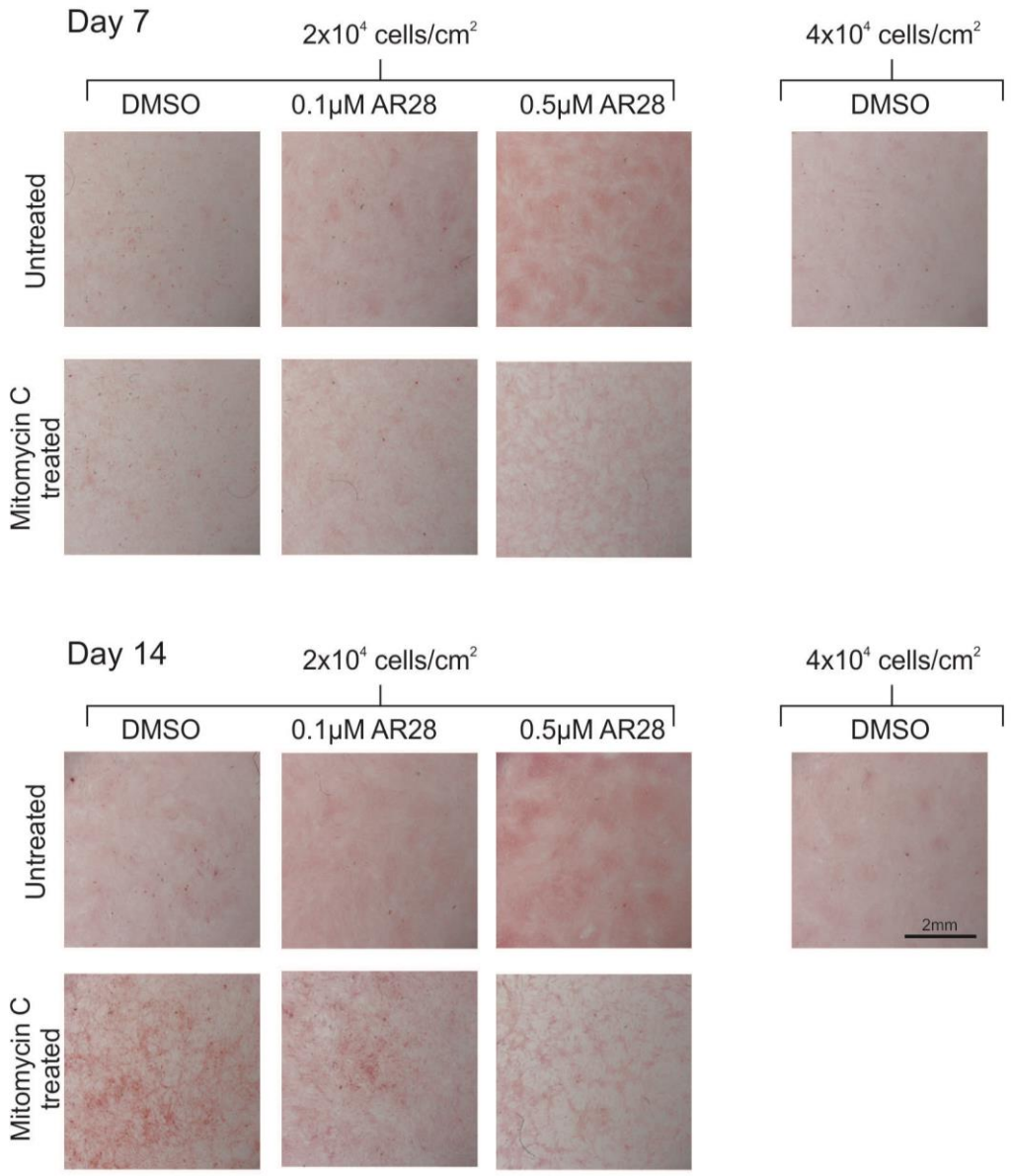

Figure 4.4.18. Mitomycin C treatment inhibits AR28 induced increase in Alizarin Red S staining of MSCs cultured in mild osteogenic conditions.
Representative donor (FH429) of MSCs seeded at $2x10^4$ cell/cm^2 treated with 10 μg/ml mitomycin C for 2 hours followed by mild osteogenic (Excl. dex) differentiation for 7 and 14 days, with AR28 at concentrations given, or DMSO control. DMSO controls were also performed with MSCs seeded at $4x10^4$ cells/cm^2 followed by mild osteogenic (Excl. dex) differentiation. Samples were stained with Alizarin Red S and imaged using brightfield microscopy.

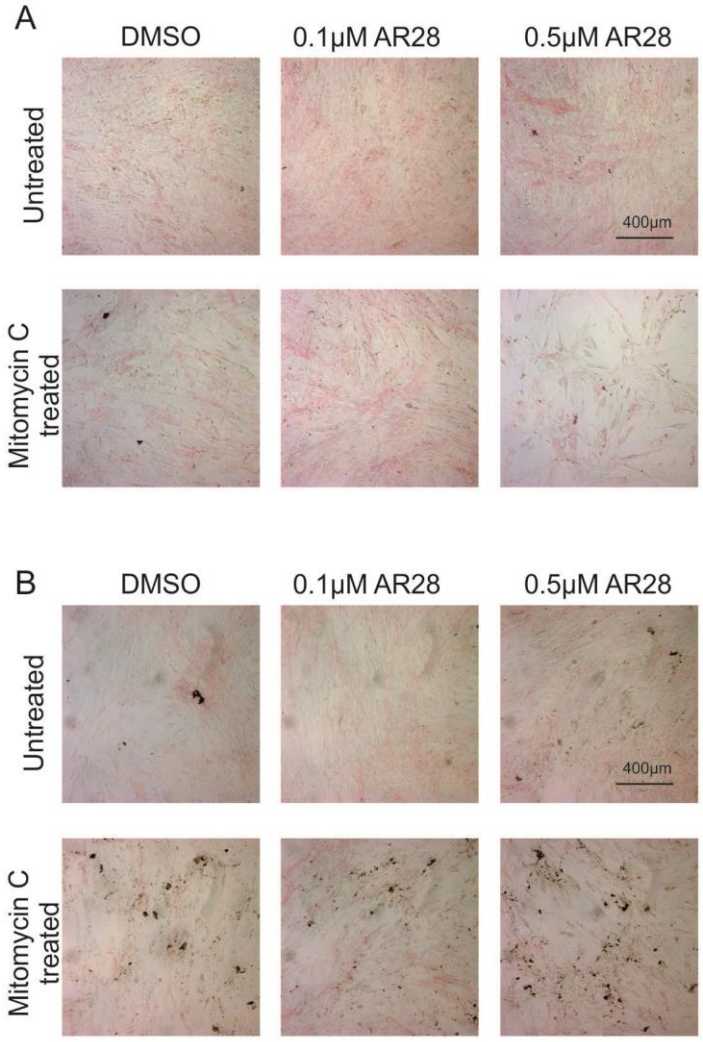

Figure 4.4.19. The effect of mitomycin C treatment on AR28 induced increase in ALP staining of MSCs cultured in mild osteogenic conditions.
Two MSC donors (A) FH402 and B) K58) were seeded at $2x10^4$ cell/cm^2 treated with 10 μg/ml mitomycin C for 2 hours followed by mild osteogenic (excluding. dex) differentiation for 7 and 14 days, with AR28 at concentrations given, or DMSO control. Samples were stained for ALP and imaged using brightfield microscopy.

4.4.5.2 CFSE analysis of AR28 induced proliferation

The above results demonstrate that treatment with AR28 results in increased cell numbers when cultured in the mild osteogenic stimulus, and that this was important for the initial increase in ARS staining. In order to demonstrate an increase in proliferation rate is responsible for this increase in cell number a carboxyfluorescein diacetate, succinimidyl ester (CFSE) incorporation assay was devised, to allow the measurement of cell divisions within the cell population over time by flow cytometry.

CFSE assays identify the number of cell divisions a cell undergoes through the incorporation of the fluorescent CFSE dye, which halves in intensity at each cell division. Therefore by measuring the fluorescence intensity over time it is possible to identify the rate of proliferation within a population of cells. Initially, three CFSE concentrations were tested for the incorporation and fluorescence signal generated. Concentrations of 10, 20 and 30 µM CFSE all generated a positive shift in fluorescence in a dose-dependent manner (Figure 4.4.20 A). A concentration of 20 µM CFSE was chosen to take forward for the remainder of the experiments, as overly high concentrations of CFSE can reduce the proliferation of cells. In addition to this, DMSO is known to cause permeation of cell membranes (Da Violante et al, 2002), therefore DMSO was tested at 0.2% (final concentration used in AR28 treatments) for its effect of CFSE reduction. No differences were detected between control cultures and DMSO-treated cultures (Figure 4.4.20 B). Therefore to study the effect of the mild osteogenic stimulus and AR28 on the rate of proliferation, MSCs were treated with CFSE, allowed to adhere to plastic and then treated with a combination of mild osteogenic and AR28 concentrations. The cultures were then grown for 7 days prior to fluorescence analysis by flow cytometry.

A control sample, treated with 0.5% FBS basal culture medium was used as a non-proliferating control, allowing the treated samples to be compared to this fluorescence intensity. Cells cultured in basal media showed very little change in fluorescence compared to the non-proliferating controls. This is likely due to the cells being seeded at confluency for all osteogenic experiments, causing contact inhibition. Cells in the mild osteogenic stimulus, however, showed a reduction in

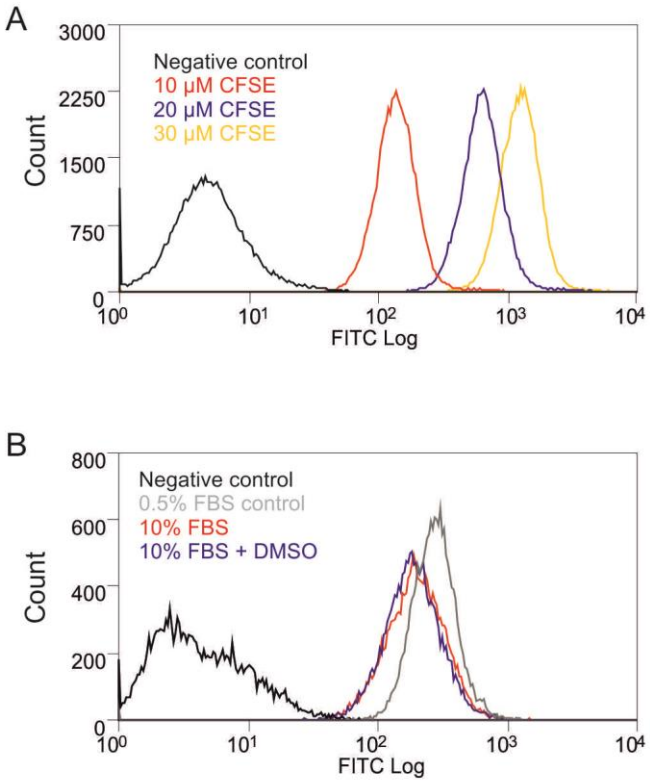

Figure 4.4.20. CFSE proliferation assay optimisation
A) MSCs (K9) were treated with 10, 20 or 30 µM Cell Trace™ CFSE, and allowed to adhere for 24 hours. The cells were then detached and analysed by flow cytometry for fluorescence. B) MSCs (K16) were treated with 20 µM Cell Trace™ CFSE and allowed to attach overnight. A portion of the cells were arrested at parent generation by FBS reduction, and the remainder were treated as stated and cultured for a further 5 days. The cells were then detached and analysed by flow cytometry for fluorescence.

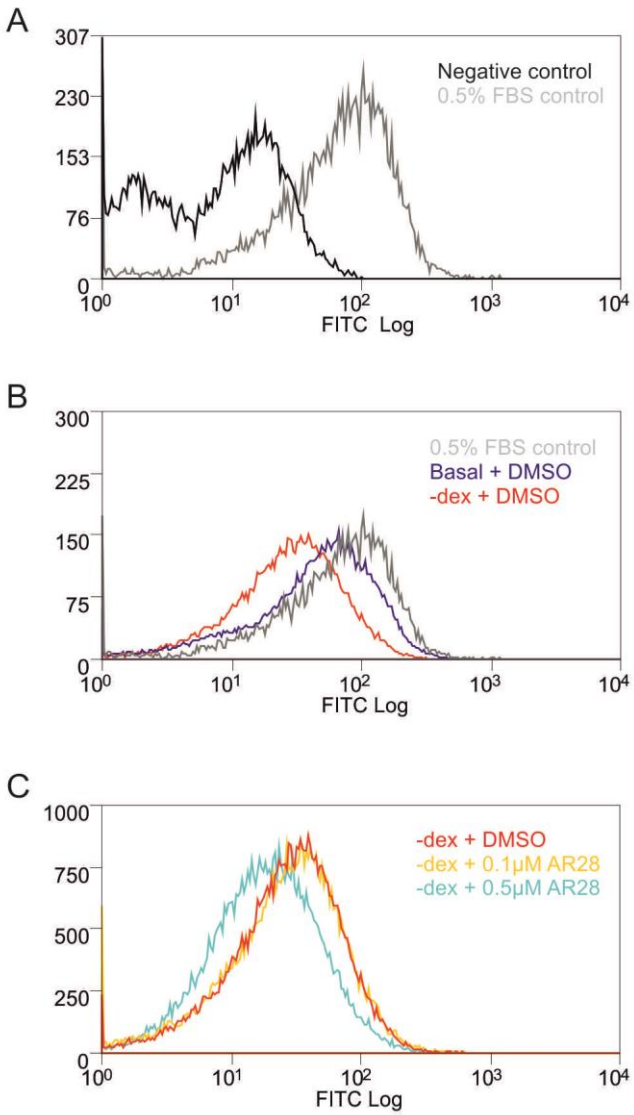

Figure 4.4.21. AR28 increases the rate of cell division of MSCs in mild osteogenic conditions

MSCs (K16) were treated with Cell Trace™ CFSE and allowed to adhere overnight. A portion of the cells were arrested at parent generation by FBS reduction, and the remainder were treated as stated and cultured for a further 7 days. The cells were then detached and analysed by flow cytometry for fluorescence. A) Histogram showing autofluorescence levels in none-CFSE treated MSCs (black) relative to CFSE fluorescence in growth arrested CFSE treated MSCs (grey). B) Histogram showing the reduction in fluorescence due to proliferation in basal (blue) and mild osteogenic (excluding dex) (red) conditions. C) Histogram showing the effect of AR28 treatment (0.1 µM: yellow, 0.5 µM: light blue) on fluorescence intensity in mild osteogenic (excluding dex) conditions.

fluorescence intensity, with a negative shift of the peak. This was further enhanced by the addition of AR28 at 0.5 µM (Figure 4.4.21). Unfortunately, the resolution of the peaks is relatively poor due to the fairly broad non-proliferating peak which is indicative of non-uniform incorporation of CFSE into the cells, likely due to the heterogeneous population of cells. It is possible to sort the cells after CFSE incorporation to select cells with a narrower range of fluorescence, which should allow for greater resolution. However, this may inadvertently select for a particular population of cells, potentially excluding the osteogenic precursors. Despite the poor resolution obtained, this assay was able to identify an increase in proliferation with AR28 exposure within the cell population, compared to controls, indicated by the negative shift in fluorescence, thus demonstrating that the increase in cell number in AR28 treated cultures is due, at least in part, to an increase in cell division and proliferation.

4.4.5.3 Ki67 analysis of AR28 induced proliferation

An alternative approach to study the proliferation of cells is by the use of Ki67 immunocytochemistry. Ki67 is a cellular protein associated with cells within the cell cycle, but is absent in cells in G_0 (Gerdes et al, 1984), and can therefore be used to identify proliferating cells within the population. The advantage of this method is that it can be performed after any length of time and be co-stained with ALP enzyme histochemistry and DAPI. MSCs were cultured in the mild osteogenic stimulus, with and without AR28 for two weeks, before staining for ALP, Ki67 and DAPI. As shown previously, the mild osteogenic media generated some small increases in ALP staining, but this was increased with AR28 treatment (Figure 4.4.22 A). Again this increase in ALP occurred alongside an increase in cell number clearly visible from the images. The nuclei in the images could also be quantified through the measurement of the total area of DAPI staining (Figure 4.4.22 B) using Image J software as a readout of cell number. The area of DAPI staining increased dramatically with AR28 treatment compared to controls, in a dose-dependent manner, with the greatest DAPI area observed with 0.5 µM AR28. The number of nuclei could not be calculated using the software as the cells become too confluent, preventing the software from identifying individual nuclei.

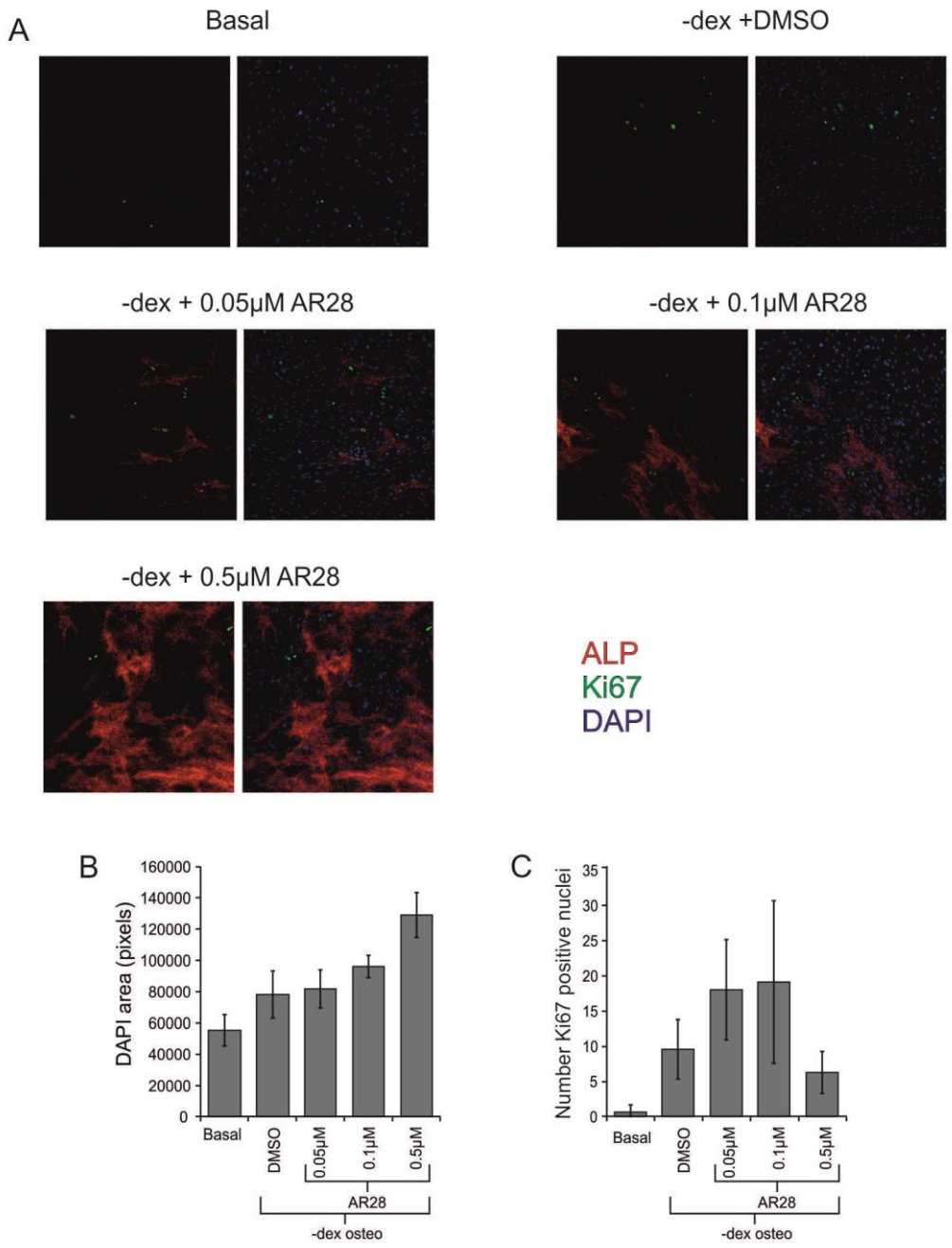

Figure 4.4.22. Ki67 staining of AR28 treated MSCs in mild osteogenic conditions

MSCs cultured in mild osteogenic (Excl. dex) conditions from 14 days with AR28 concentrations as stated or DMSO control. A) Samples were stained for ALP (red), Ki67 (green) and DAPI (blue), and imaged by fluorescence microscopy. B) Total area of DAPI staining/image was calculated using Image J and the mean ± stdev plotted. C) The number of Ki67 positive nuclei per image were manually counted and the mean ± stdev plotted. n=6 (total of 6 images from 2 independently treated technical replicates).

The number of cells expressing the Ki67 protein were manually counted in each image, and the mean plotted (Figure 4.4.22 C). On average, less than one cell per image expressed Ki67 when cultured in basal media, however this increased to approximately 10 cells per image in the mild osteogenic media. Furthermore, AR28 at 0.05 and 0.1 μM increased the number of cells expressing Ki67 further to around 17 cells per image. The number of Ki67-expressing cells varied greatly between images with these AR28 treatments, demonstrated by the large error bars, making it difficult to determine whether this increase in staining was significant from this single experiment. In addition to this, 0.5 μM AR28, which resulted in the greatest number of cells, only had an average of six Ki67 positive cells per image. This highlights the limitation of this fixed end point assay, where only the cells that are in the cell cycle at the end of the two week period are detected, and not any of the cells that have undergone mitosis previously.

Another aim of this assay was to identify which cells were proliferating and in particular, if the ALP-expressing osteogenic precursor cells were induced to proliferate to a greater extent than other cell populations. However, the Ki67 positive cells do not appear to fall primarily in either ALP-positive or negative areas, but are split between both populations. Therefore, while these results backed up those performed previously, showing that AR28 can cause increased ALP staining in mild osteogenic conditions, and that this increase in accompanied by an increase in cell number, it did not provide any additional information due to the nature of the fixed end point, and was therefore not repeated in other donors.

4.4.6 Pre-treatment with AR28 can increase osteogenesis, but not adipogenesis

To study whether the treatment of the MSC population with AR28 prior to differentiation had any effect on the propensity for the cells to form osteoblasts or adipocytes MSCs were treated for 7 days in basal media with or without AR28, before the switch to differentiation conditions and removal of AR28.

AR28 pre-treatment of MSCs in this manner caused clear increases in osteogenesis compared to non-pre-treated controls when differentiated with both the classical and mild osteogenic media. ALP and vK staining of the cultures showed increases in

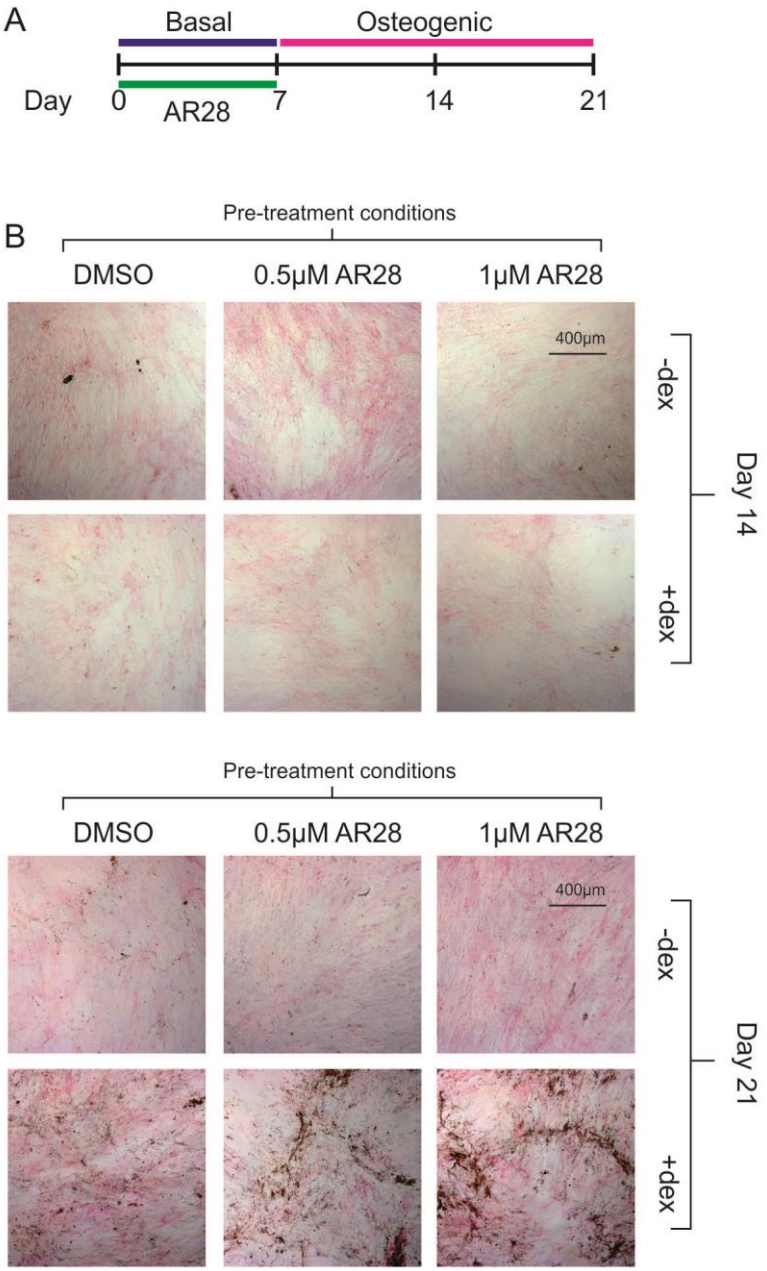

Figure 4.4.23. Pre-treatment of MSCs with AR28 increases ALP and von Kossa staining upon osteogenic induction

A) Schematic of AR28 pre-treatment experiment, showing 7 days of AR28 treatment in basal media before removal of AR28 and addition of osteogenic conditions for a further 14 days. B) Representative donor (FH429) of MSCs pre-treated for 7 days with AR28 or DMSO as stated, followed by a further 7 or 14 days treatment in either mild (-dex) or standard (+ dex) osteogenic conditions. Samples were then stained for ALP and von Kossa and imaged by brightfield microscopy.

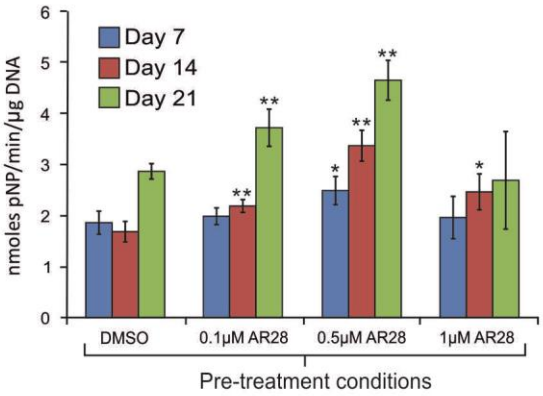

Figure 4.4.24. Pre-treatment of MSCs with AR28 increases ALP activity upon mild osteogenic induction
Representative donor (FH452) of MSCs pre-treated for 7 days with AR28 or DMSO as stated, followed by a further 7 or 14 days treatment in mild osteogenic (excluding dex) conditions. Samples were then assayed for ALP activity normalised to cell number (given as nmoles pNP/min/µg DNA). Values given as mean ± stdev., n=6 (independently treated technical replicates), * $p<0.05$, ** $p<0.005$, *** $p<0.001$. Statistical significance is relative to vehicle control at appropriate conditions and time point, by Mann-Whitney U and Kruskal-Wallis tests.

ALP and vK staining in classical differentiation media in response to 0.5 and 1 µM AR28 pre-treatment, while the mild osteogenic media was only able to increase ALP staining with no visible vK staining (Figure 4.4.23). To gain a quantifiable measure of osteogenic differentiation, pNPP ALP activity assays were performed in samples after AR28 pre-treatment followed by culture in the mild osteogenic stimulus for up to 14 days. Significant increases in ALP activity could be detected at both 7 and 14 days after osteogenic media exchange when pre-treated with 0.5 µM AR28, compared to non-pre-treated controls (Figure 4.4.24). Unlike in the ALP enzyme histochemistry analysis of pre-treatment in 24 well plates above, 1 µM AR28 did not cause any measurable increase in ALP activity compared to vehicle controls. Similarly, MSCs pre-treated with AR28 followed by mild osteogenic stimulus were stained with ARS to identify calcium deposition. As seen with the ALP enzyme histochemistry and vK staining, AR28 pre-treatment caused an increase in ARS staining of the cultures compared to the DMSO pre-treated controls (Figure 4.4.25). The optimal concentration varied between donors, 1 µM pre-treatment causing strong mineralisation in one donor, while 0.5 µM AR28 caused the greatest increase in another.

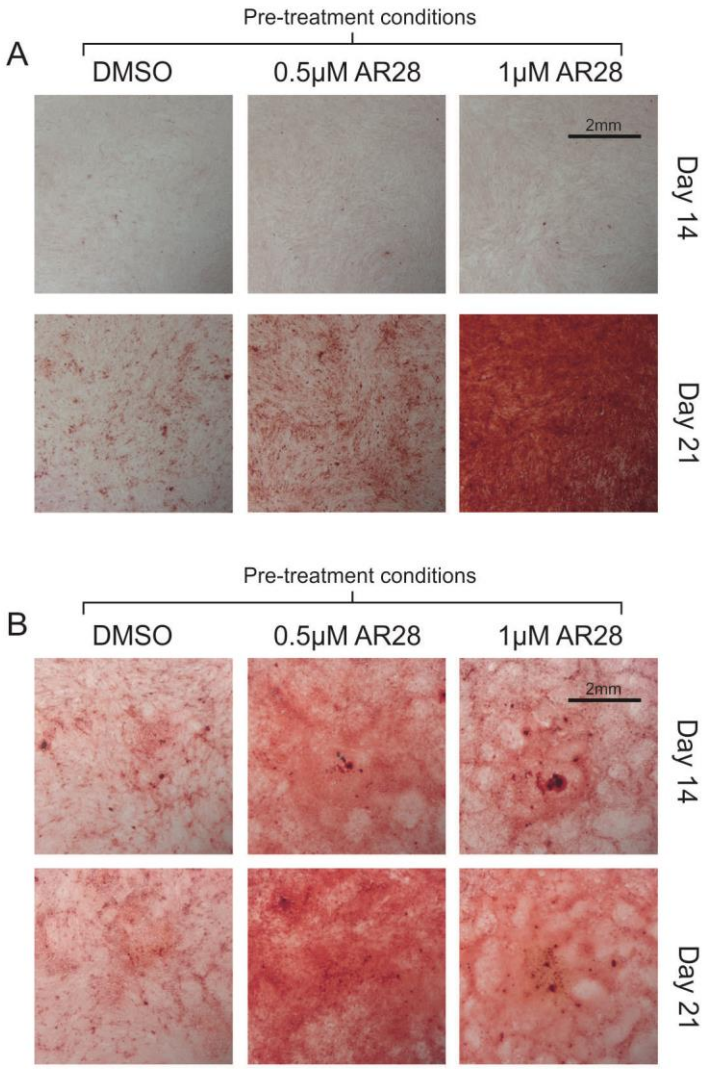

Figure 4.4.25. Pre-treatment of MSCs with AR28 increases Alizarin Red S staining upon osteogenic induction
Representative donors (A) FH408 and B) FH429) of MSCs pre-treated for 7 days with AR28 or DMSO as stated, followed by a further 7 or 14 days treatment in mild osteogenic (Excluding. dex) conditions. Samples were then stained with Alizarin Red S and imaged by brightfield microscopy.

In contrast to the positive effect of pre-treating MSCs with AR28 on osteogenesis, adipogenesis was not increased. Cultures were treated as above, except the differentiation media was exchanged for adipogenic media. Adipogenesis was identified by Oil Red O staining followed by bright field microscopy. MSCs pre-treated with the vehicle control, DMSO, were able to differentiate into adipocytes, showing clear Oil Red O positive lipid droplets forming over 14 days after media exchange. Unlike with osteogenesis pre-treatment with AR28 reduced the capacity of the MSCs and hADSCs to differentiate into adipocytes, with reduced lipid droplet formation (Figure 4.4.26).

4.4.7 AR28 and chondrogenesis

Finally, the effect of AR28 on chondrogenesis was studied. MSCs were cultured as micromass pellets and subjected to chondrogenic media with or without AR28 for 21 days. The pellets were then sectioned before staining for the chondrogenic markers, glycosaminoglycans (GAGs) and type II collagen. Chondrogenic conditions cause an increase in alcian blue staining for GAGs compared to non-chondrogenic cultures. AR28 appeared to have little effect on this increase in GAG staining (Figure 4.4.27). In addition, no increases in Collagen II could be detected in chondrogenic media by immunocytochemistry.

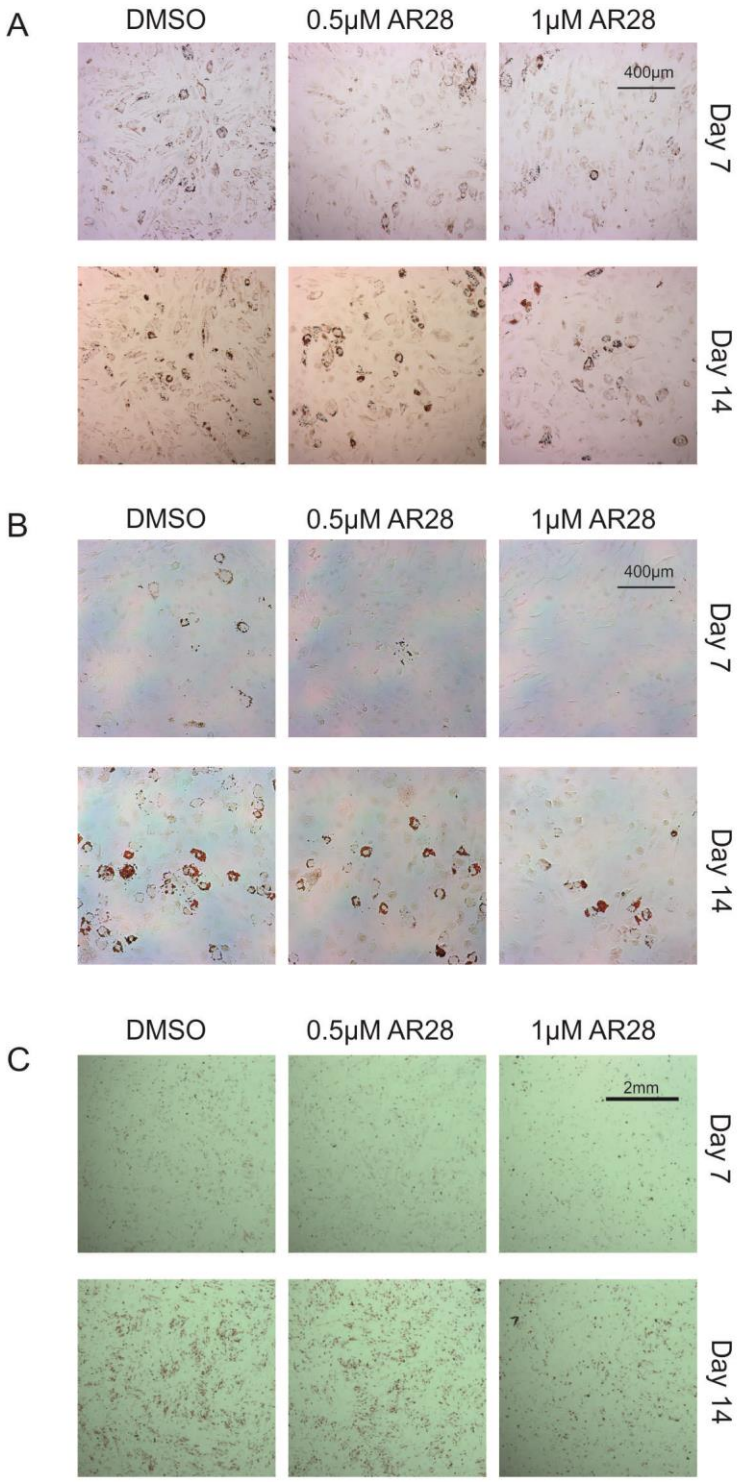

Figure 4.4.26. Pre-treatment of MSCs with AR28 reduces lipid droplet formation upon adipogenic induction

Bone marrow MSCs (A) FH399 B) K9) and C) hADSCs pre-treated for 7 days with AR28 or DMSO as stated, followed by a further 7 or 14 days treatment in adipogenic conditions. Samples were then stained by Oil Red O to identify lipid droplet formation and imaged by brightfield microscopy.

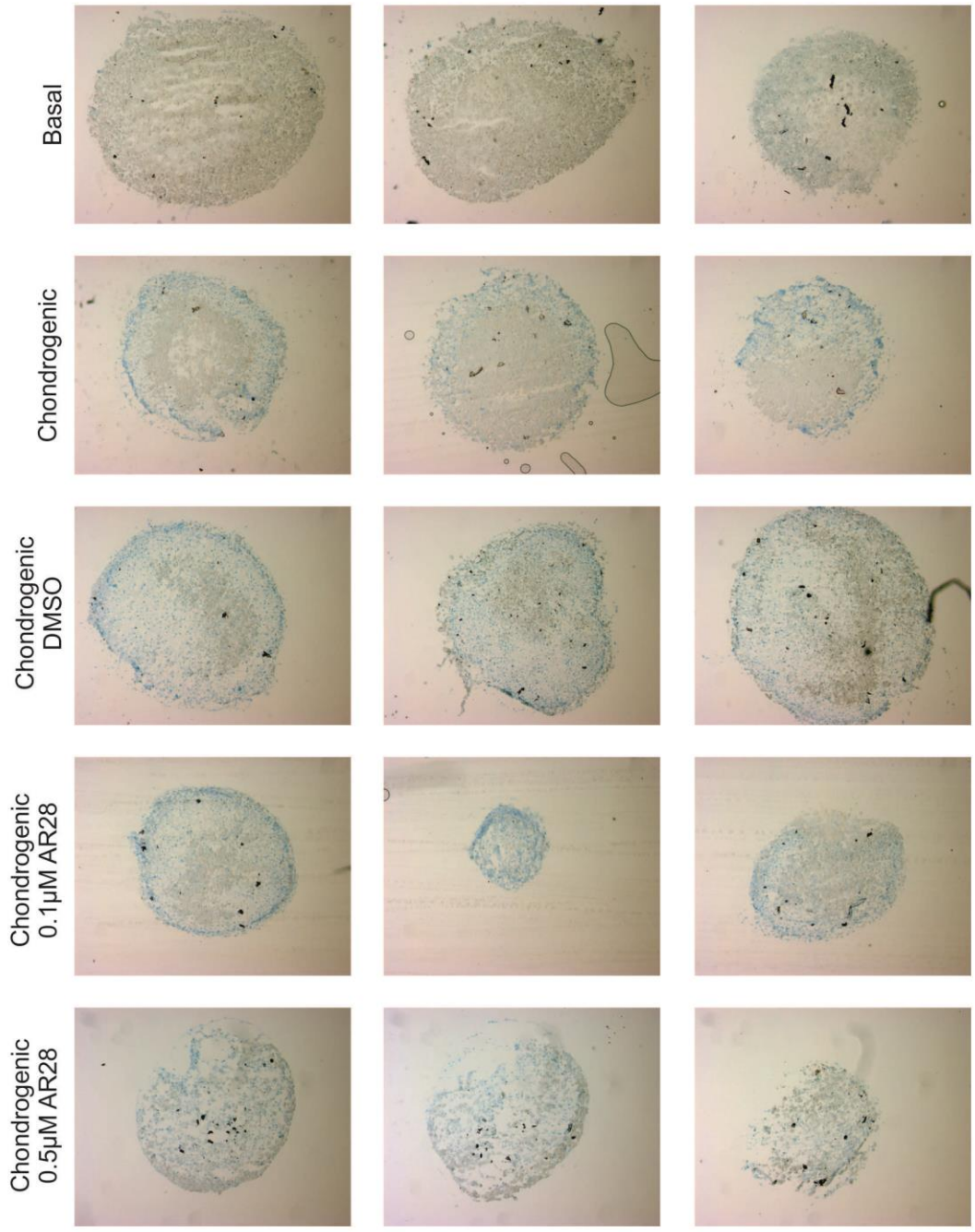

Figure 4.4.27. AR28 treatment has no effect on GAG production in chondrogenic micromass pellets.
MSCs (FH452) were cultured in micromass pellets in chondrogenic conditions for 21 days in the presence of AR28 at concentrations stated, or DMSO control. Control pellets in basal and chondrogenic conditions alone were also generated. Pellets were cryosectioned at 10 µm and stained with Alcian blue to identify GAG levels. Samples were imaged using brightfield microscopy.

4.5 Discussion

AR28 has been demonstrated to enhance bone mineral density (BMD) in mice (Gambardella et al, 2011), and therefore the overall aim of this part of the project was to use *in vitro* studies in human MSCs to gain a better understanding of the processes underlying this increase in BMD. Results presented in chapter 3 demonstrated the suitability of AR28 as a pharmacological Wnt manipulator in *in vitro* cell culture, and MSCs in particular. To further demonstrate the capacity of AR28 to functionally stimulate canonical Wnt signalling and affect cell fate, AR28 was used to study the activation of canonical Wnt signalling during MSC adipogenic differentiation. Canonical Wnt signalling is widely considered a strong inhibitor of adipogenesis (Bennett et al, 2002; Liu et al, 2009), with the inhibition of canonical Wnt signalling required for adipogenesis to occur (Li et al, 2007). Activation of the canonical Wnt pathway by AR28 complemented these *in vitro* results, with clear dose-dependent inhibition of differentiation identified over a two week period, compared to controls and a corresponding increase in proliferation, when assayed by lipid droplet formation or FABP5/BODIPY co-staining. Interestingly, when compared to the effect of recombinant Wnt3a ligand in published studies (Liu et al, 2009), AR28 concentrations of 0.05-0.5 μM generated similar levels of inhibition to 5-100 ng/ml Wnt3a, again suggesting potent activation of the canonical Wnt signalling pathways, allowing the use of low AR28 concentrations. The actions of AR28 can be compared to those of another GSK3β inhibitor, CHIR99021. Work carried out in the preadipocyte cell line 3T3-L1 showed inhibition of adipogenesis with CHIR99021 concentrations of 0.3-1 μM (Bennett et al, 2002), slightly higher than that of AR28 in our studies.

These results confirm the inhibitory effect of canonical Wnt stimulation on adipogenic differentiation, demonstrating the versatility of AR28 as a variable canonical Wnt stimulator. However, the combination of AR28 as a specific variable Wnt stimulator, and the novel FABP5/BODIPY high content approach allowed for the identification of small changes in adipogenesis in response to low level Wnt activation. While Oil Red O staining of cultures is a clear readout for adipogenesis and can be quantified to some degree by measurement of the absorbance of the solubilised staining, it is not very sensitive. Other approaches commonly used are

the analysis of mRNA expression levels by RT-PCR and RT-qPCR (Fu et al, 2005) or protein levels by SDS-PAGE and western blot (Bennett et al, 2002; Li et al, 2007). While these are powerful tools, allowing a quantifiable analysis of up-regulated gene or protein expression of the cell population, they do not allow for the analysis of changes in protein levels on a cell by cell basis. The development of the high content immunocytochemistry and imaging technique allows for changes in protein expression to be analysed on a cell by cell basis in a quantifiable manner. This offers multiple advantages over whole population analysis techniques such as qPCR and western blot, making it possible to identify different populations within the culture, and therefore percentages for positive and negative populations, similar to that of flow cytometry. Clearly, the high content method does not allow for such large numbers of cells to be analysed as during flow cytometry, but it does generate information about cell patterning within the population and total cell numbers. Therefore, this high content screening method provides an invaluable tool in the study of cell differentiation, and with some optimisation and identification of good protein markers for other lineages, could be used not only to study single lineage differentiation, but dual differentiation studies in which multiple populations of cells are developing within the population.

As mentioned above, the increased sensitivity of the high content technique generated new intriguing results regarding the effects of very low level Wnt signalling on the adipogenic differentiation of MSCs. Unlike previous studies, very mild stimulation of the canonical Wnt signalling pathway by AR28 was advantageous for adipogenesis, generating small but significant increases in adipogenesis compared to untreated controls. While these increases were detected on two independent assays, in order to fully confirm and understand the mechanisms behind this increase, multiple donors and other techniques must be used. One potential mechanism to consider is the effect of canonical Wnt signalling on MSC proliferation. Observations from the work presented in this chapter (4.4.5) and that performed by Boland *et al*. (Boland et al, 2004) implicate a role of canonical Wnt signalling in enhancing the proliferation of MSCs. Therefore the low level AR28 treatment may cause small increases in MSC and early adipogenic precursor cell numbers, whilst not generate a strong enough canonical Wnt response to prevent the progression of adipogenic differentiation.

The work focusing on adipogenic differentiation demonstrated the ability of AR28 to manipulate the degree of canonical Wnt signalling within cells, allowing for the use of AR28 as a powerful tool for unlocking the poorly understood effects of canonical Wnt signalling on the chondrogenic and osteogenic differentiation of MSCs. MSCs were cultured under chondrogenic conditions as micromass pellets and submitted to AR28 treatment to induce canonical Wnt signalling. However, the effect of AR28 on classical chondrogenic micromass cultures is inconclusive from these results. Published work suggests the inhibition of the onset of chondrogenesis by canonical Wnt signalling (See section 1.4.3.1), but under the conditions described here no reduction in GAG content after AR28 treatment could be detected. However, the results here are from a single donor, and rely on the upregulation of GAGs in chondrocytes as a marker for chondrogenesis. Analysis of the effects of AR28 on chondrogenesis must be performed on more donors, and analysed by other means looking into chondrocyte specific markers. For example, RT-PCR could be utilised to identify the upregulation of specific genes, such as Sox9, Aggrecan, collagen II, IV and X, allowing not only the degree of chondrogenesis to be analysed, but also the stage at which AR28 may have an effect.

In relation to osteogenesis, it was shown that activation of the canonical Wnt signalling pathway inhibits ALP and vK staining of MSCs when differentiated using the standard differentiation cocktail of β-glycerophosphate, L-ascorbic acid and dexamethasone. This is in agreement with other work (Boland et al, 2004; de Boer et al, 2004; Liu et al, 2009) demonstrating a reduction in ALP and mineralisation in response to canonical Wnt signalling in standard osteogenic conditions. The results from ARS staining were not as clear, with no reduction in calcium deposition in response to AR28 in these strong osteo-inductive conditions. In fact there was an increase in the ARS staining at the earlier time points in particular, which then became masked at the later time points. The reason for this difference in staining to that of the ALP and vK is not known. One explanation for the discrepancies in ARS and vK staining involves the inhibition of ALP activity by AR28 treatment. One role for ALP in is the hydrolysis of phosphomonoesters, including β-glycerophosphate *in vitro,* into inorganic phosphate, a component of the mineralised matrix, whilst at the same time reducing mineralisation inhibitors such as pyrophosphate (Hessle et al, 2002). Therefore, the strong inhibition of

dexamethasone induced ALP detected upon AR28 treatment, could reduce the levels of inorganic phosphate, preventing its incorporation into the matrix, whilst the strong mineralisation inducer dexamethasone is still able to cause calcium acquisition into the matrix by another route. Indeed it would be interesting to study the effect of ALP inhibition, such as that by levamisole, on dexamethasone induced osteogenesis to see if these discrepancies in staining can be replicated. Despite these discrepancies in vK and ARS staining, ARS staining did detect small early increases in calcium content, which may be explained by increased proliferation of the culture as discussed later in this section.

Both the small early increase in ARS staining in response to AR28 and published literature proposing the enhancement of the early differentiation process, accelerating the cells though this osteoblast precursor stage in response to Wnt signalling (Eijken et al, 2008; Krause et al, 2010) led to the study of canonical Wnt stimulation under milder osteogenic inductive conditions. This was achieved through the removal of dexamethasone, leaving both ascorbic acid and β-glycerophophate to provide small osteo-inductive cues. As expected, the removal of dex prevented the strong induction of osteogenesis, generating only low levels of ALP and ARS staining similar to that seen by Eijken *et al* (2008) and Krause *et al* (2010). The addition of AR28 to this culture however increased both ALP and ARS staining over 21 days. These increases in ALP are in agreement with those shown by Krause *et al* (2010), however our studies also identified an increase in mineralisation measured by ARS staining which previous publications did not. However, no increases in vK staining were detected in these cultures, suggesting an increased sensitivity in ARS staining over that of vK. ARS identified uniform increases in calcium content across the culture at early stages, however vK was only able to detect phosphate in the highly mineralised nodules formed in the presence of dex.

These increases in both ALP and ARS were variable between donors, with some donors presenting strong mineralisation in response to AR28 while others only showed small increases. This is likely due to the heterogeneity of the cell population, where some donor populations contain greater contributions of osteogenic precursors, generating different levels of response to osteogenic conditions. This may also explain the difference between this work and previous

publications that used a different donor site, iliac crest aspirates, which are likely to result in similar but different MSC cell populations. The difference could equally be due to the Wnt stimulant used. Krause *et al* (2010) stimulated canonical Wnt using BIO or a PPARγ inhibitor, which are likely to generate smaller increases in canonical Wnt signalling than AR28. Indeed in work presented here, the concentrations of BIO used in this publication were unable to generate increases in TCF reporter expression as great as AR28 (Chapter 3). Krause *et al*. (2010) also indentified negative effects of BIO on cell viability and proliferation at the concentrations used in their assays, which is also likely to have affected cell behaviour. Furthermore, PPARγ is a key regulator of adipogenesis, and therefore will regulate many other factors in addition to canonical Wnt signalling, and its inhibition would prevent the expression of adipogenic genes, potentially enhancing osteogenic precursor numbers and allowing increased osteogenesis in this manner.

In addition to these results, drawing comparisons to previous publications, we have also shown that upregulation of canonical Wnt signalling by AR28 caused an increase in cell number, most notably in the mild osteogenic conditions. This increase in cell number was necessary for the increase in ARS staining in response to AR28, and was, at least in part, due to an increased rate of proliferation, demonstrated by the mitomycin C and CFSE incorporation assays respectively. The effects of Wnt signalling on proliferation complements work of Boland *et al* (2004), who demonstrated increases MSC numbers upon Wnt3a treatment in basal or osteogenic conditions, where both increased proliferation and decreased apoptosis were detected. The method by which AR28 increases proliferation in this situation is unknown, but two likely candidates are the cell cycle protein Cyclin D1 and the transcription factor c-myc. Cyclin D1, a known effecter of Wnt signalling, is transcribed in response to TCF/LEF1 transcription factor activity (Shtutman et al, 1999) and can stimulate cell proliferation *in vitro* (Biliran et al, 2005). C-myc is another gene that is directly up regulated by canonical Wnt signalling and TCF/LEF1 activity (He et al, 1998), and is also linked to increased proliferation and cell cycle progression (Bennett et al, 1994). The involvement of these proteins could be tested by the study of mRNA levels by RT-PCR and western blot, identifying any increases in gene expression in response to increased canonical Wnt signalling.

The cell number and proliferation assays used provided valuable data, showing increased cell number due to increased proliferation in the entire culture, however they were unable to identify if any particular cell type was being affected preferentially. The combination of the staining pattern of ALP in mild osteogenic conditions treated with AR28, showing activity in discrete groups of cells, and increased cell number are suggestive of an increase in the proliferation of the osteogenic precursor cells. This would lead to an increased osteogenic precursor pool, ultimately leading to increased osteogenesis. The importance of proliferation in AR28 enhanced osteogenesis was supported by mitomycin C treatment experiments which demonstrated the requirement of proliferation for increased ARS staining in mild osteogenic media. However, there was no clear reduction in ALP activity upon mitomycin C treatment. The reason for this is unknown, however one area of research which may provide some reasoning is that of the interplay between cell cycle arrest and differentiation (Myster & Duronio, 2000). It is possible that the inhibition of proliferation by mitomycin C caused the spontaneous differentiation and maturation of osteoblast precursors, masking any effects of proliferation rate on increased differentiation.

The proposition that AR28 can increase the proliferation of osteogenic precursors is supported by the AR28 pre-treatment experiments, in which one week treatment of the heterogeneous MSC population prior to differentiation induction, caused enhancement of osteogenesis, but a reduction in adipogenesis. These findings indicate that AR28 does not simply cause an increase in multipotent MSC number, but that the effect is specific for osteogenesis. These findings share similarities to those by Gambardella *et al* (2011) who identified *in vivo* amplification of mesenchymal progenitors upon AR28 administration (Gambardella et al, 2011). However, *in vivo* studies showed that these increases in progenitor numbers ultimately led to increased osteoblast cell number, with no increase in adipocytes, implying a preference of these amplified precursors for osteogenesis. However, more detailed work studying the proliferation of cells within the MSC population is required to confirm this hypothesis and fully understand the role of canonical Wnt signalling in MSC lineage commitment.

While increased proliferation of osteoprogenitors could explain the increases in osteogenesis in response to AR28 pre-treatment, it is likely not the only factor at play as only small increases in cell number were detected after 7 days in basal media, and this would not cause a reduction in adipogenesis. Furthermore, this inhibitory affect on adipogenesis provides a clue to an alternative mechanism for increased osteo-induction. Canonical Wnt signalling is known to reduce adipogenesis, as has been shown here, and does this primarily through the inhibition of PPARγ (Okamura et al, 2009). There is also evidence in the literature for the importance of PPARγ as a key transcription factor in the determination of osteogenic differentiation, where knockouts in ES cells resulted in spontaneous osteogenesis (Akune et al, 2004), and inhibition by canonical Wnt signalling in ST2 cells caused increased osteogenic gene expression (Kang et al, 2007). It is possible therefore, that AR28 pre-treatment can increase the number of precursor cells through increased proliferation, whilst at the same time priming them for osteogenesis through the inhibition of PPARγ. Additionally this reduction in PPARγ would lead to a reduction in the number of adipogenic precursor cells within the MSC population causing the reduction/delay of adipogenic differentiation.

The results in this chapter also feed into the important medical field of glucocorticoid (GC)-induced osteoporosis. Long-term exposure to glucocoriticoids is reported to reduce the BMD of patients and increase the fracture risk (de Vries et al, 2007). This process is thought to be in part due to increased adipogenesis, but also the inhibition of osteoblast precursor proliferation, alongside increased terminal differentiation and apoptosis of osteoblasts, leading to reduced osteoblast numbers and mineral deposition (Walsh et al, 2001; Weinstein et al, 1998). Canonical Wnt signalling has been identified as a key player in GC-induced osteoporosis, through the identification of reduced Wnt upon GC administration (Wang et al, 2008) and the rescue of GC-induced osteoporosis by GSK3β inhibition by BIO (Wang et al, 2009). The results presented here indicate the importance of proliferation in the early stages of osteogenic differentiation, and the ability of canonical Wnt signalling to enhance this. Yet, canonical Wnt signalling inhibits the dexamethasone-induced osteogenic and adipogenic differentiation and maturation of MSCs. Therefore, induced canonical Wnt signalling has the potential to reduce GC-induced osteoporosis through the prevention of final maturation and apoptosis of osteoblasts, increasing

the number of osteoblast precursors, likely through increased proliferation, and prevention of adipogenic differentiation. This would prevent the depletion of the osteogenic progenitor pool, allowing for the maintenance of bone density.

Chapter 5: Role of Wnt in dual lineage commitment

5.1 Introduction

Several groups have proposed a hierarchical model for the differentiation of MSCs, progressing through a range of cell types capable of self renewal, but with a gradual reduction in potency. Muraglia *et al*. (2000) proposed a model in which tripotential MSCs spontaneously progressed toward the osteogenic lineage. The adipogenic lineage was the first to diverge, causing the loss of adipogenic capacity, creating osteo-chondro progenitors, which progress together before branching into osteogenic and chondrogenic-specific lineages prior to terminal differentiation. More recently a similar, but more complex model has been derived, which incorporated myoblastic and fibroblastic potential into the hierarchical model (Sarugaser et al, 2009). This model expanded on that of Muraglia *et al*. (2000), and proposed the final, default cell type to be that of the fibroblast, with myocytes suggested to be very first cell type to diverge (Figure 5.1.1). This model also highlights the existence of osteo-adipo progenitors, a proposition supported by various lines of work, which demonstrated clonal lines with lineages restricted to osteogenic and adipogenic differentiation (Pittenger et al, 1999; Sarugaser et al, 2009). The very nature of this progressive hierarchical model dictates the need for signalling inputs to regulate the progression down a particular pathway, and manipulation of cell signalling pathways such as BMPs and Wnts, either endogenously or through extrinsic administration, is likely to alter commitment decisions. Indeed, Liu *et al.* (2009) demonstrated a role for canonical Wnt signalling in the progression toward osteoblasts in preference to adipocytes. Similarly, BMPs have been shown to stimulate MSCs to form both osteoblasts (Cheng et al, 2003; Lee et al, 2000; Sampath et al, 1992) and chondrocytes, suggestive of the directing of commitment towards an osteo-chondral progenitor phenotype. Furthermore, canonical Wnt signalling has been shown to increase BMP-induced osteogenesis in mouse models (Chen et al, 2007b) and cell lines (Tang et al, 2009), yet reduce chondrogenesis (Fischer et al, 2002). Canonical Wnt signalling has also been shown to be important in the regulation of the switch from chondrogenic to osteogenic differentiation during development by conditional

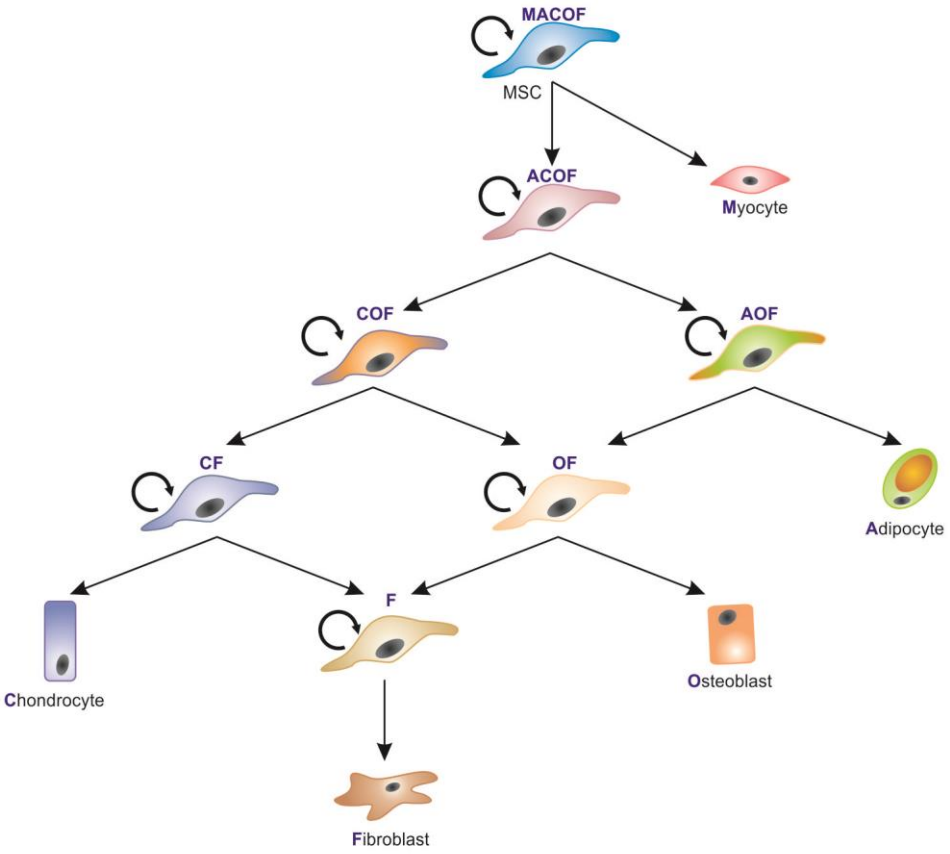

Figure 5.1.1. Schematic of the hierarchical differentiation of MSCs
MSCs spontaneously progress toward the fibroblastic lineage, maintaining their capacity to renew but gradually lose potential as they progress. The myocyte lineage is the first to diverge, causing the loss of myogenic capacity, followed by the divergence of adipocytes. Osteo-Chondro progenitors, progress together before branching prior to terminal differentiation or continuing to the default fibroblastic lineage. The potency of the progenitors is denoted by the initials in blue. (E.g. **COF**: Chondrogenic, Osteoblastic and Fibroblastic potential.) **M**: Myogenic, **A**: Adipogenic, **C:** Chondrogenic, **O**: Osteoblastic, **F**: Fibroblastic
Adapted from Sarugaser *et al.* (2009)

β-catenin knock out and Wnt14 over-expression studies in mouse models (Day et al, 2005; Hill et al, 2005). Increased canonical Wnt signalling within the progenitor cells promoted osteogenesis and chondrocyte hypertrophy whilst blocking chondrocyte differentiation. Conversely, canonical Wnt inhibition resulted in increased cartilage formation at the expense of osteogenesis. However, the *in vitro* studies of BMP-induced osteogenesis and chondrogenesis have only been performed in mouse cell lines with independent analysis of the two differentiation pathways in response to canonical Wnt signalling, however to study the role of these signalling pathways in this bi-lineage environment both differentiation processes should ideally be studied simultaneously.

One method suited to the simultaneous analysis of different differentiation pathways is quantitative reverse transcriptase PCR (qPCR). This quantitative approach allows for the study of a whole array of gene expression profiles in a single sample, permitting the identification of expression levels of osteogenic genes, such as Runx2 and ALP, and chondrogenic genes, such as Sox9, Aggrecan and Col2a1, within a single differentiating sample. The use of such a technique also allows for the identification of the point at which the differentiation process is affected, through the identification of differentiation stage-specific genes.

5.2 Aims

The general aims of the work presented in this chapter are to identify the effect of stimulated canonical Wnt signalling, by AR28 administration, on the differentiation of MSCs cultured in conditions capable of stimulating multiple lineages simultaneously.

More specifically the aims are to:

- Characterise the effect of AR28 on the osteogenic and adipogenic differentiation of MSCs cultured in an osteo/adipogenic induction medium.
- Characterise the effect of AR28 on the osteogenic differentiation of MSCs cultured with BMP2.
- Use cell lines to model the effect of BMP2 and AR28 on Sox9 activity and stability.
- Characterise the effect of AR28 on the simultaneous osteogenic and chondrogenic differentiation of MSCs cultured in BMP2, using reverse transcription real time PCR.

5.3 Methods

5.3.1 Dual differentiation studies

MSCs or hADSCs were seeded at $2x10^4$ cells/cm^2 and allowed to adhere overnight. Cells were then cultured in adipogenic/osteogenic dual differentiation conditions (Liu et al, 2009) comprised of 50:50 adipogenic:osteogenic medium (2.2.1.6) with AR28 at concentrations stated. Cells were cultured for the desired length of time with media change every three or four days.

5.3.2 BMP2-induced osteogenesis

MSCs were seeded at $2x10^4$ cells/cm^2 and allowed to attach overnight. Cells were then cultured in Basal media (2.2.1.6) with the addition of 100 ng/ml recombinant BMP2 and AR28 at concentrations stated. Media was changed every three or four days.

5.3.3 Differentiation marker assays

For the osteogenic assays, ALP enzyme histochemistry, von Kossa staining and ALP activity assays were performed as previously described in sections 4.3.3 and 4.3.4. For the adipogenic assays, Oil Red O staining and absorbance and FABP5/BODIPY staining, were performed as described previously in sections 4.3.6 and 4.3.7.

5.3.3.1 ELF97 staining

hADSCs were cultured in glass bottom 96 well plates and treated as described. Cells were fixed in 4% paraformaldehyde for 15 min, followed by washing in PBS. Samples were permeabalised in PBS-0.2%Tween 20 for 10 minutes, and washed in PBS for 10 minutes. The PBS was removed completely from the wells, and 50 µl of 100 µM ELF97 substrate (Invitrogen, Carlsbad, CA, USA) diluted in enhancing/AP buffer (100 mM Tris-HCl, 50 mM $MgCl_2$, 100mM NaCl) was added. The cells were then incubated for 30secs-5minutes for optimisation, or 1 minute for subsequent assays. Samples were then washed in stop/wash buffer (25 mM EDTA, 5 mM Levamisol in PBS) for 10 minutes followed by 2 washes for 5 minutes. Samples

were washed and stored in PBS at 4°C. Images were taken using an automated ImageXpress 5000A (Molecular Devices). Post-acquisition image analysis was performed using the granularity application module of MetaXpress analysis software (Molecular Devices) to identify granules between 2 and 30µm in diameter. Samples were subsequently stained with Hoechst33342 at 1 µM for 10 minutes at room temperature. The same areas of the sample wells were imaged to identify the nuclei, and analysed using the count nuclei application module (MetaExpress).

5.3.4 Sox9 Reporter assays

C3H10T1/2 cells were seeded in white opaque 96 well plates at $1x10^4$ cells/well (without antibiotics), and allowed to adhere overnight. Cells were then transfected with the 4Col2E-Luc reporter and Sox9 over-expression plasmids in combination with the pCMV-Renilla plasmids using Lipofectamine as described in section 2.2.3.1. Optimised conditions are given in Table 3.3.3. After 24 hours the cells were treated with AR28 or DMSO vehicle control and 300 ng/ml BMP2 as stated. After 48 hours the reporter activity was assayed using the Dual Glo Luciferase assay system (2.2.4)

Table 5.3.1. Optimised transfection conditions for C3H10T1/2 in 96 well plates

DNA/Reagent	Amount/well
4Col2E-Luc	30 ng
pCMV-Renilla	3 ng
pRK5-Sox9	25 ng
Plus Reagent	0.3 µl
Lipofectamine Reagent	0.3 µl
DMEM	4 µl
DMEM for final dilution	32 µl

5.3.5 Western Blot analysis of Sox9 and β-catenin

C3H10T1/2 and HEK293 cells were seeded at $1.25x10^5$ cells/well (12 well plate) and $2x10^5$ cells/well (24 well plate) respectively and allowed to adhere overnight. Cells were then transfected using Lipofectamine or Lipofectamine LTX reagents as described in section 2.2.3. Optimised conditions are given in Table 5.3.2.

.

Table 5.3.2. Optimised transfection conditions for C3H10T1/2 and HEK293 cells

DNA/Reagent	Amount/well
C3H10T1/2 cells (12 well plate)	
pRK5-Sox9	600 ng
Plus Reagent	4 µl
Lipofectamine Reagent	4 µl
DMEM	50 µl
DMEM for final dilution	700 µl
HEK293 cells (24 well plate)	
pRK5-Sox9 or empty pRK5 plasmid DMA	Combined to give 300 ng
Plus Reagent	0.3 µl
Lipofectamine LTX Reagent	1 µl
Optimem	100 µl

Total protein lysate samples were obtained and separated by SDS-PAGE and transferred to PVDF membranes as described in section 2.2.5. Antibody probing was performed using the primary antibody concentrations and appropriate HRP-conjugated secondary antibodies given in Table 5.3.3.

Table 5.3.3. Optimised Antibody concentrations for Western Blot analysis

Target	Conjugate	Host	Conc.	Supplier	Cat. No.
β-catenin	Purified IgG	Mouse	0.25 µg/ml	BD Transduction Laboratories	610154
Sox9	Purified IgG	Rabbit	0.4 µg/ml	Abcam	ab36748
GAPDH	Purified IgG	Mouse	0.5 µg/ml	Genetex	28245
Anti-mouse IgG	HRP	Goat	0.1 µg/ml	Santa Cruz Biotech	SC-2005
Anti-rabbit IgG	HRP	Swine	0.17 µg/ml	DAKO	P0399

5.3.6 RNA extraction, reverse transcription and real-time PCR analysis

5.3.6.1 Trizol extraction of RNA

Cells were cultured in 6 well plates and treated according to the assay. At appropriate time-points for RNA analysis, cultures were washed twice in PBS before direct lysis in the well with 0.5 ml Trizol® (Invitrogen, Carlsbad, CA, USA) for 5

minutes at room temperature. The cell lysate was passed through a pipette several times before being transferred to a clean eppendorf and stored at -80ºC. Thawed samples were incubated for 5 minutes at room temperature before the addition of 100 µl chloroform, and thorough mixing by vortexing for 15 seconds. The samples were incubated at room temperature for a further 5 minutes before centrifugation at 12,000g for 15 minutes at 4ºC. The upper aqueous phase was transferred to a clean tube and mixed with 250 µl isopropanol before incubation at 4ºC for 30 minutes. The samples were centrifuged at 12,000g for 15 minutes at room temperature and the supernatant removed. The RNA sample was then washed in 0.5 ml of 75% ethanol and centrifuged at 12,000g for 5 minutes. The supernatant was fully removed and the pellet allowed to air dry. The RNA was then resuspended in 12 µl Nuclease free H_2O. RNA was stored at -80ºC.

5.3.6.2 DNase treatment of RNA

DNase treatment was performed using the DNA-free™ kit, (Invitrogen, Carlsbad, CA, USA). 1.2 µl of DNase I buffer and 1 µl of rDNase I was added to the RNA and mixed gently before incubation at 37ºC for 30 minutes. 1.2 µl of DNase inactivation reagent was then added to the sample and mixed well, followed by incubation at room temperature for 2 minutes, flicking occasionally to mix. The samples were then centrifuged at 13,000g for 1 minute to pellet the inactivation reagent. The supernatant was transferred to a clean tube and the RNA concentration measured using a NanoDrop 1000 Spectrophotometer (Thermo Scientific, Waltham, MA, USA). RNA was stored at -80ºC.

5.3.6.3 cDNA synthesis

Reverse transcription was performed using Superscript II reverse transcriptase (Invitrogen, Carlsbad, CA, USA). 1 µg of RNA was combined with 1 µl Oligo dt primers (Invitrogen, Carlsbad, CA, USA) and 1 µl of 10 mM 2'-deoxynucleoside 5'triphosphates (dNTPs) (Invitrogen, Carlsbad, CA, USA), and made up to 12 µl with nuclease free H_2O. Selected samples were prepared in replicate for no Reverse transcriptase controls. Samples were incubated at 65ºC for 5 minutes, followed by chilling on ice for 2 minutes. A prepared mix of 4 µl 1st strand buffer, 2 µl 0.1 M

Dithiothreitol (DTT) and 1 µl nuclease free H_2O was then added to each sample, and incubated at 42ºC for 2 minutes. 1 µl of SuperScript II reverse transcriptase was then added to each sample, except the no enzyme controls, where H_2O was added instead, followed by incubation at 42ºC for 1 hour and 70ºC for 1 minute. cDNA samples were then diluted with 30 µl nuclease free H_2O and stored at -20ºC.

5.3.6.4 Quantitative reverse transcription PCR

Quantitative reverse transcription PCR (qPCR) was used to analyse changes in gene expression in response to various combinations of BMP2 and AR28. qPCR reactions were set up as in Table 5.3.4 and run on a ABI Prism 7000.

Table 5.3.4. qPCR reaction composition

Volume	Reagent
5 µl	cDNA Sample
1 µl	Forward Primer (20µM)
1 µl	Reverse Primer (20µM)
12.5 µl	SYBR Green Power (Invitrogen)
5.5 µl	dH_2O

Primer optimisation

Primer optimisation was performed using either combined cDNA from osteogenic differentiation of MSCs for the osteogenic genes, or cDNA from homogenised cartilage for chondrogenic genes. A 10-fold serial dilution of the sample was generated, producing a range of concentrations as follows; 1:0, 1:10, 1:100 and 1:1000. These cDNA concentrations were then analysed with the primer pairs in Table 5.3.5. Reaction mixes set up in triplicate as Table 5.3.4 in a 96 well plate format and run on an ABI Prism 7000. Thermocycler settings were; 60ºC for 2 minutes, 95ºC, followed by 40 cycles of 95ºC for 15 seconds and 50ºC for 1 minute. Each cycle was followed up by a dissociation stage of 95ºC for 15 seconds, 60ºC for 20 seconds and 95ºC for 15 seconds. Standard curves were generated from the C_T values for each concentration and the gradient of the regression line determined. The regression line gradients from each primer pair, including the house keeping gene, 40S ribosomal protein S27a (RPS27A), to show the primer pairs were amplifying at

high efficiency that was conserved between primer pairs. Dissociation curves were also generated to ensure the product amplification specificity.

Reverse transcriptase real time PCR

cDNA samples were diluted 1:5 for the genes of interest, and 1:100 for RPS27A, before combining into the reaction mix (Table 5.3.4) in triplicate in a 96 well plate format, and assayed using the ABI Prism 7000. Thermocycler settings were; 60ºC for 2 minutes, 95ºC, followed by 40 cycles of 95ºC for 15 seconds and 60ºC for 1 minute. Results were analysed using 7000 system software and the $2^{-\Delta\Delta Ct}$ method (Livak & Schmittgen, 2001). Threshold levels were set in the exponential phase of the amplification for each primer pair, and the C_T values exported. C_T values for genes of interest were normalised to the RPS27A values, by subtraction of the mean RPS27A C_T value for the particular cDNA sample, to give ΔC_T. The mean ΔC_T of the day 4 control cDNA sample was then subtracted from the ΔC_T making all samples relative to Day 4: No treatment, giving $\Delta\Delta C_T$. $2^{-\Delta\Delta Ct}$ was then calculated to give fold changes in gene expression. Means were then calculated from the technical replicates. Technical errors were given as $C_T \pm$ standard deviation.

Table 5.3.5. qPCR primer sequences

Gene		Nucleotide sequence (3'-5')
RPS27A	Forward	TGGATGAGAATGGCAAAATTAGTC
	Reverse	CACCCCAGCACCACATTCA
Runx2	Forward	AGTGATTTAGGGCGCATTCCT
	Reverse	GGAGGGCCGTGGGTTCT
ALP	Forward	GGGAACGAGGTCACCTCCAT
	Reverse	TGGTCACAATGCCCACAGAT
Sox9	Forward	TTCCGCGACGTGGACAT
	Reverse	TCAAACTCGTTGACATCGAAGGT
Aggrecan	Forward	AGTATCATCAGTCCCAGAATCTAGCA
	Reverse	AATGCAGAGGTGGTTTCACTCA
Coll2A1	Forward	TTGCCTATCTGGACGAAGCA
	Reverse	CGTCATTGGAGCCCTGGAT

5.4 Results

5.4.1 Adipogenic and osteogenic dual lineage commitment

5.4.1.1 ALP/vK and Oil Red O staining

To study the effect of AR28 on the differentiation of MSCs towards osteoblasts and adipocytes simultaneously, MSCs were cultured in a 50:50 mix of osteogenic and adipogenic media for up to 14 days. These cultures were also treated with AR28 between 0.05-0.5 µM or a DMSO vehicle control. Initial analysis of differentiation was performed by ALP/vK staining or Oil Red O for osteogenesis and adipogenesis respectively, and imaged by brightfield microscopy. As controls, to ensure the MSC donor was capable of differentiating toward osteoblasts and adipocytes, standard single lineage differentiation was also preformed, showing strong osteogenic and adipogenic staining for the respective cultures (Figure 4.4.1 A). The dual differentiation conditions, in the absence of AR28 were able to induce both osteogenic and adipogenic differentiation, shown by ALP/vK and Oil Red O staining (Figure 4.4.1 B). Staining was performed in separate wells for osteogenic and adipogenic markers to allow for the two stains to be easily distinguished, however lipid droplet formation can be visualised in the ALP/vK stained cultures without Oil Red O staining. This shows the two differentiated cell types in close proximity, with no separation of the two cell types to different areas of the culture. AR28 addition at 0.5 µM resulted in the complete inhibition of adipogenesis and osteogenesis in the dual lineage cultures, similar to the single lineage experiments (Chapter 4), however the lower concentration of 0.05 µM showed clear inhibition of adipogenesis, with no clear change in osteogenesis (Figure 4.4.1 B).

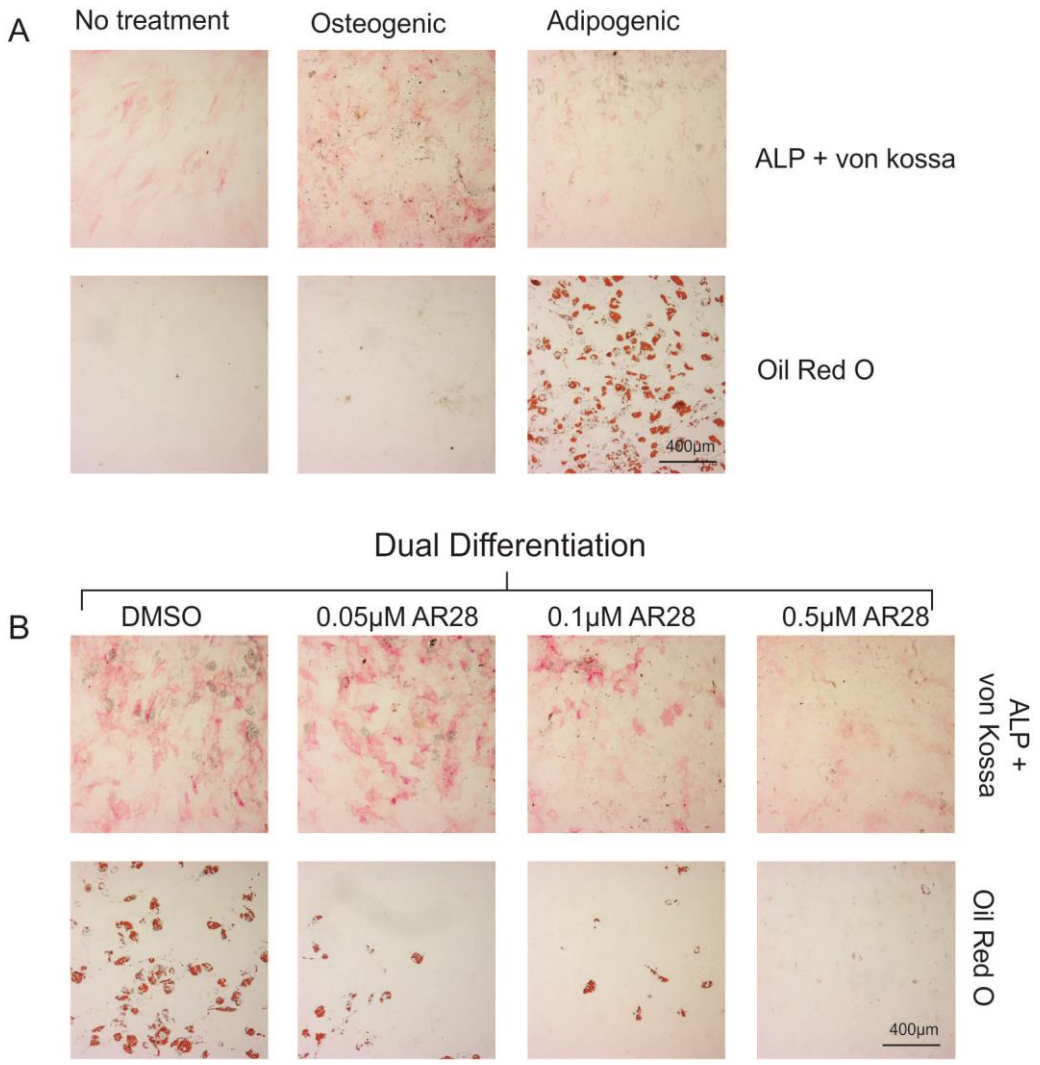

Figure 5.4.1. ALP/vK and Oil Red O staining of adipogenic and osteogenic dual lineage differentiation

A) MSCs (FH390) were cultured in osteogenic or adipognic conditions for 12 days and stained with ALP/vK or Oil Red O.

B) MSCs (FH390) were cultured in Dual differentiation media (50:50 mix of osteogenic and adipogenic media) in the presence of AR28 or DMSO control as stated for 12 days. Samples were then stained with ALP/vK or Oil Red O.

Samples were imaged by brightfield microscopy.

5.4.1.2 Quantitative analysis of ALP activity and Oil Red O

The staining and imaging technique used in the experiment described above is purely qualitative, making it difficult to identify small changes in osteogenesis throughout the well. Therefore, quantitative assays were used to study both osteogenesis and adipogenesis in the dual lineage differentiation conditions. Adipogenesis was studied using Oil Red O staining, and extraction followed by absorbance measurements at 490 nm. As seen with Oil Red O staining and imaging, AR28 clearly inhibited adipogenesis in both single and dual differentiation conditions at all concentrations used, although complete inhibition was not generated until concentrations of 0.5 µM were reached (Figure 5.4.2 A). Interestingly, the donor used here generated an increase in Oil Red O in the presence of the osteogenic media, suggesting a propensity of this donor for adipogenesis.

To study the degree of osteogenesis, the pNPP ALP activity assay was performed (Figure 5.4.2 B). Adipogenic conditions reduced the ALP activity to below the basal levels for the MSCs within 7 days. Single osteogenic differentiation induced a clear increase in ALP activity, which was reduced upon AR28 addition between 0.05-0.5 µM in a dose-dependent manner, as discussed in Chapter 4. Dual lineage conditions were also able to generate an increase in ALP activity, although to a lesser extent than by single osteogenic conditions. Furthermore, AR28 has similar inhibitory effects on ALP activity in the dual lineage conditions, with inhibition at all concentrations used.

5.4.1.3 High content analysis of FABP5/BODIPY double positive cells

As only a small range of concentrations were used to study the effect of AR28 using the techniques described above, the high content FABP5/BODIPY staining technique was used to identify adipogenesis, while a method using Enzyme-Labelled-Fluorescence (ELF) 97 was developed to study ALP activity. These assays were performed using hADSCs, however previous findings (Chapter 4) showed very little difference between hADSCs and bone marrow derived MSCs in relation to the effect of canonical Wnt signalling on osteogenic and adipogenic differentiation. Consistent with the results described in MSCs, AR28 reduced the percentage of

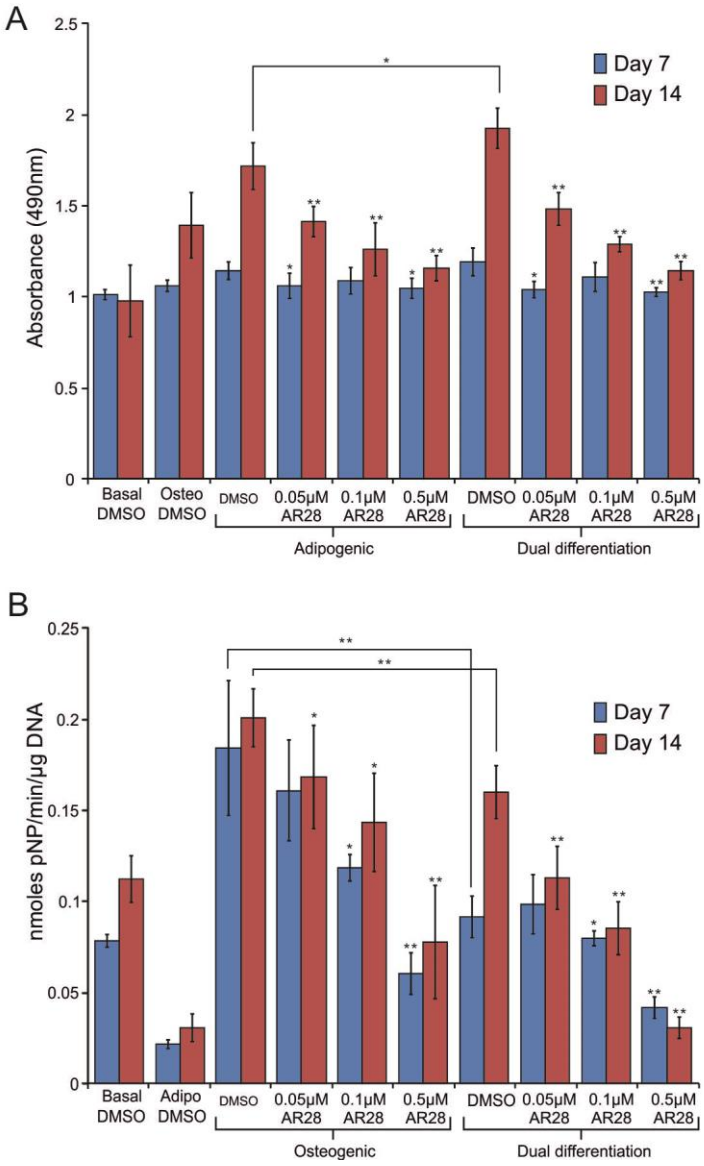

Figure 5.4.2. pNPP assay and Oil Red O absorbance of adipogenic and osteogenic dual lineage differentiation

A) MSC (FH429) seeded in 96 well plates, were cultured in adipogenic, osteogenic and dual lineage condition (50:50 mix) conditions for up to 14 days in the presence of AR28 at the concentrations shown or DMSO control. Samples were stained with Oil Red O before solubilisation in 100% isopropanol and quantification by absorbance at 490 nm.

B) MSC (FH429) seeded in 96 well plates, were cultured in osteogenic, adipogenic, and dual lineage condition (50:50 mix) conditions for up to 14 days in the presence of AR28 at the concentrations shown or DMSO control. ALP activity normalised to cell number (given as nmoles pNP/min/μg DNA) was calculated at 7 and 14 days.

Values given as mean ± stdev., n=6 (independently treated technical replicates), * $p<0.05$, ** $p<0.005$, *** $p<0.001$. Statistical significance is relative to vehicle control at appropriate time point, by Mann-Whitney U and Kruskal-Wallis tests.

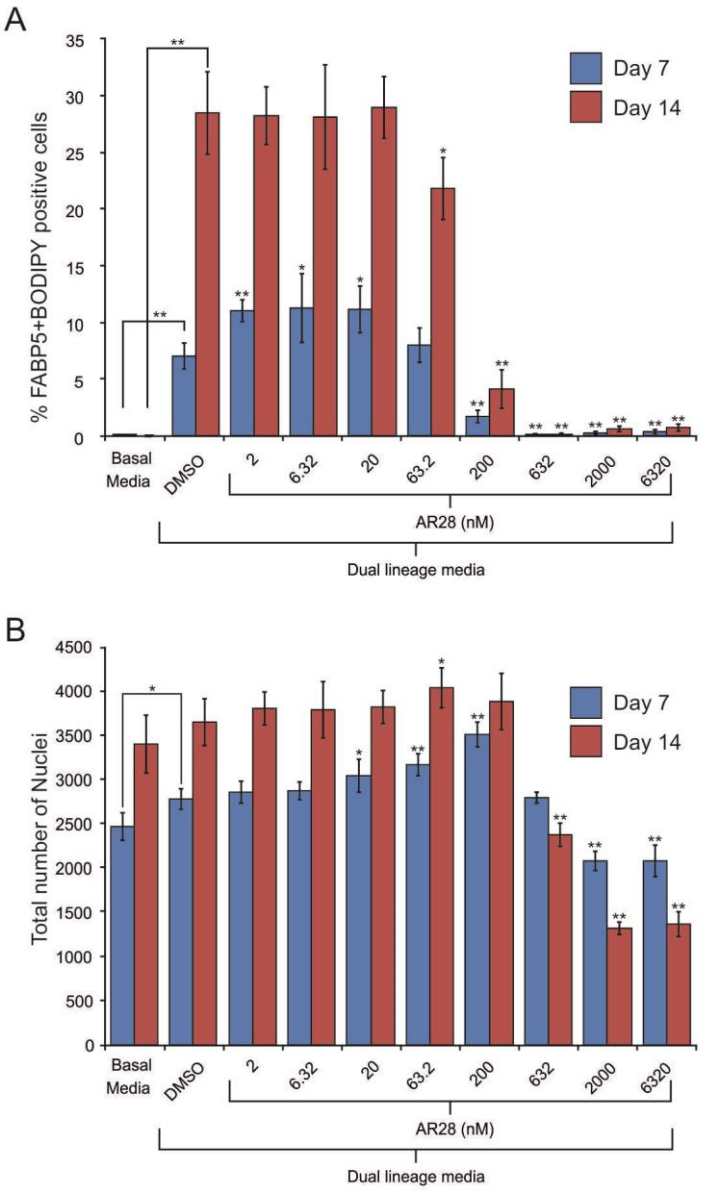

Figure 5.4.3. Definiens analysis of FABP5/BODIPY staining of Dual differentiation cultures

FABP5 and BODIPY analysis of 7 and 14 day dual differentiation (50:50 mix of adipogenic and osteogenic media) hADSC cultures in the presence of AR28 at the concentration given or DMSO control using Definiens analyses of fluorescence microscopy imaging. A) Bar chart showing the number of FAPB5/BODIPY double positive cells in response to different AR28 concentrations. B) Bar chart showing the total number of nuclei in response to different AR28 concentrations. Values given as mean ± standard deviation, n=6 (independently treated technical replicates), * $p<0.05$, ** $p<0.005$. Statistical significance is relative to vehicle control at appropriate time point unless stated otherwise, by Mann-Whitney U and Kruskal-Wallis tests.

FABP5/BODIPY double positive nuclei with concentrations as low as 63 nM, with complete inhibition of adipogenesis by 632 nM in dual lineage differentiation media, at all time point measured (Figure 5.4.3 A). However, unlike single lineage conditions (Chapter 4) the dual lineage differentiation media did not generate a reduction in cell number relative to the basal media control (Figure 5.4.3 B). This is likely due to the presence of proliferative osteogenic precursors in the culture, which as discussed in Chapter 4 appear to proliferate more rapidly upon AR28 treatment, presenting itself as increased cell number over time. As discussed in chapter 4, higher AR28 concentrations of 632 nM and above resulted in a reduction in cell number.

5.4.1.4 High content analysis of osteogenesis using the ELF-97phosphate

The ELF-97 phosphate is hydrolysed by ALP, liberating the ELF97 alcohol, which forms a fluorescent precipitate. This can then by visualised by fluorescence microscopy. ELF97 is considered better than Fast Red TR, with lower diffusion after enzymatic conversion, allowing for greater resolution to be attained (Cox & Singer, 1999). To optimise the time the ELF97 phophatase substrate was incubated with the cells, a range of incubation times (30 secs – 5 minutes) were performed on MSCs cultured in both basal and osteogenic conditions. Images were then acquired by automated fluorescence microscopy (Figure 5.4.4). Image analysis identified an incubation period of 1 minute was sufficient to create increases in fluorescence intensity, while not causing large non-specific ELF97 precipitates to form, and allowing differences between basal and osteogenic cultures to be detected.

The optimised protocol was then used to identify the effect of a large range of AR28 concentrations on osteogenesis induced by dual lineage conditions (Figure 5.4.5). The ELF97 staining presented itself in a highly localised punctate manner, owing to the low diffusion of the insoluble precipitate. The punctate staining pattern allowed for the image analysis of ELF97 staining using a granularity assay, calculating the number of ELF97 foci and the total area of positive staining. Additionally, the mean intensity of the ELF97 foci could be calculated. Samples were also co-stained with Hoechst, allowing for the number of cells per image to be calculated, and therefore the relative ELF97 staining per cell.

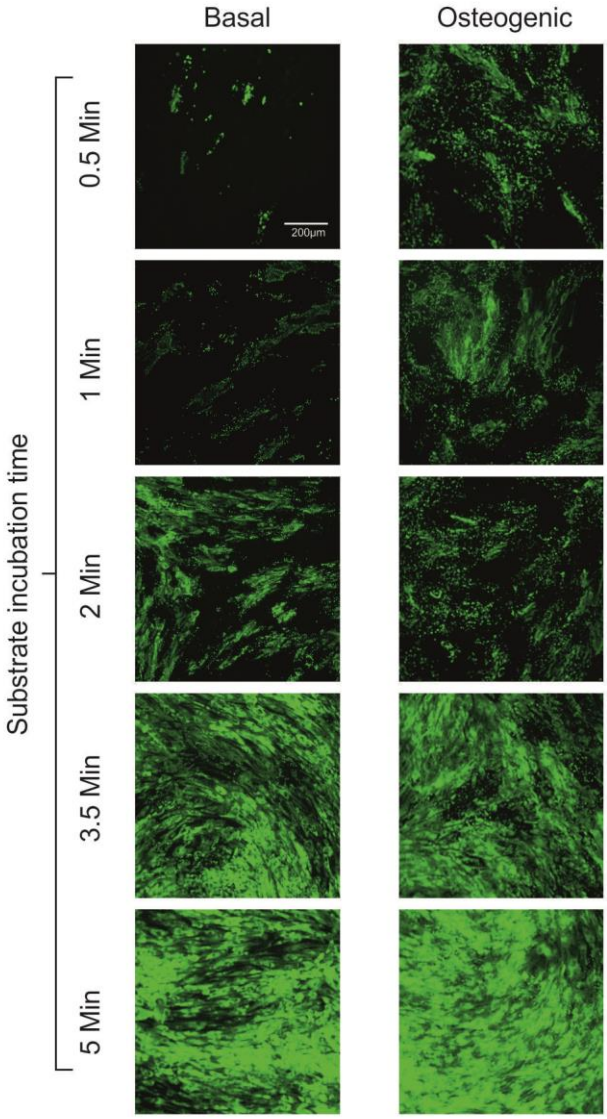

Figure 5.4.4. ELF97 optimisation
hADSCs were cultured in basal or osteogenic media for 21 days before optimisation of the ELF97 assay. Substrate incubation time was optimised by performing a range of incubation periods stated. Samples were imaged using fluorescence microscopy. One minute incubation period was chosen as an optimal time, generating clear increases in ELF97 fluorescence, without large amounts of non-specific precipitation.

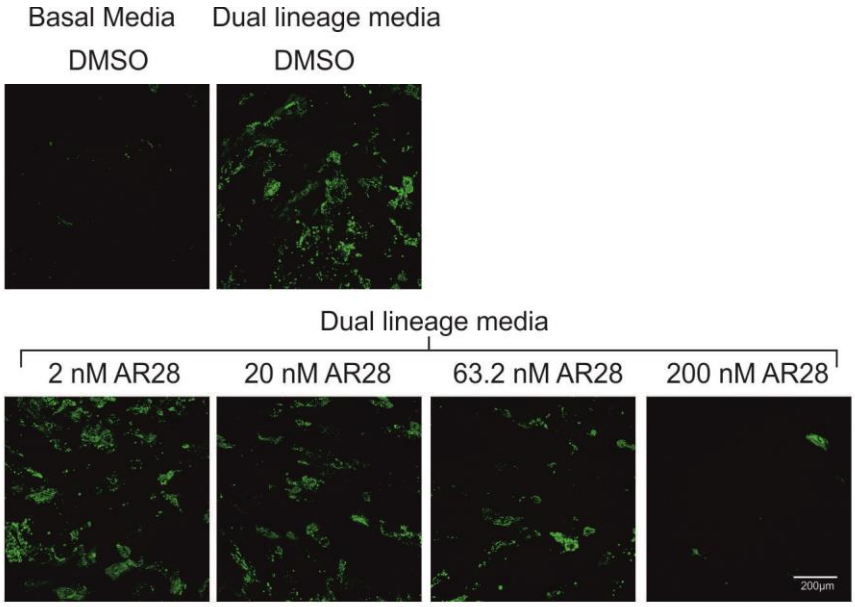

Figure 5.4.5. ELF97 Dual differentiation assay
Example images of hADSCs culture in basal or dual differentiation (50:50 mix of osteogenic and adipogenic media) for 21 days, with the addition of AR28 at concentrations stated or DMSO control. The samples were assayed using ELF97 substrate, and imaged by fluorescence microscopy.

Figure 5.4.6. ELF97 Dual differentiation assay image analysis
(Overleaf)
Image analysis of hADSCs cultured for up to 21 days in dual differentiation media (50:50 mix of osteogenic and adipogenic media), with the addition of AR28 at concentrations stated or DMSO control, and assayed by ELF97, followed by fluorescence microscopy. Samples were co-stained with Hoechst, allowing for cell number to be calculated. Image analysis was performed using a granularity application module (MetaExpress) due to the punctate staining, allowing A) the number of ELF97 positive foci per cell (No. granules/cell number), B) the area of ELF97 staining per cell (Granule area/cell number) and C) the mean intensity of the ELF97 staining (Mean granule intensity) to be calculated. Values given as mean ± standard deviation, n=6 (independently treated technical replicates), * $p<0.05$, ** $p<0.005$. Statistical significance is relative to vehicle control at appropriate time point unless stated otherwise, by Mann-Whitney U and Kruskal-Wallis tests.

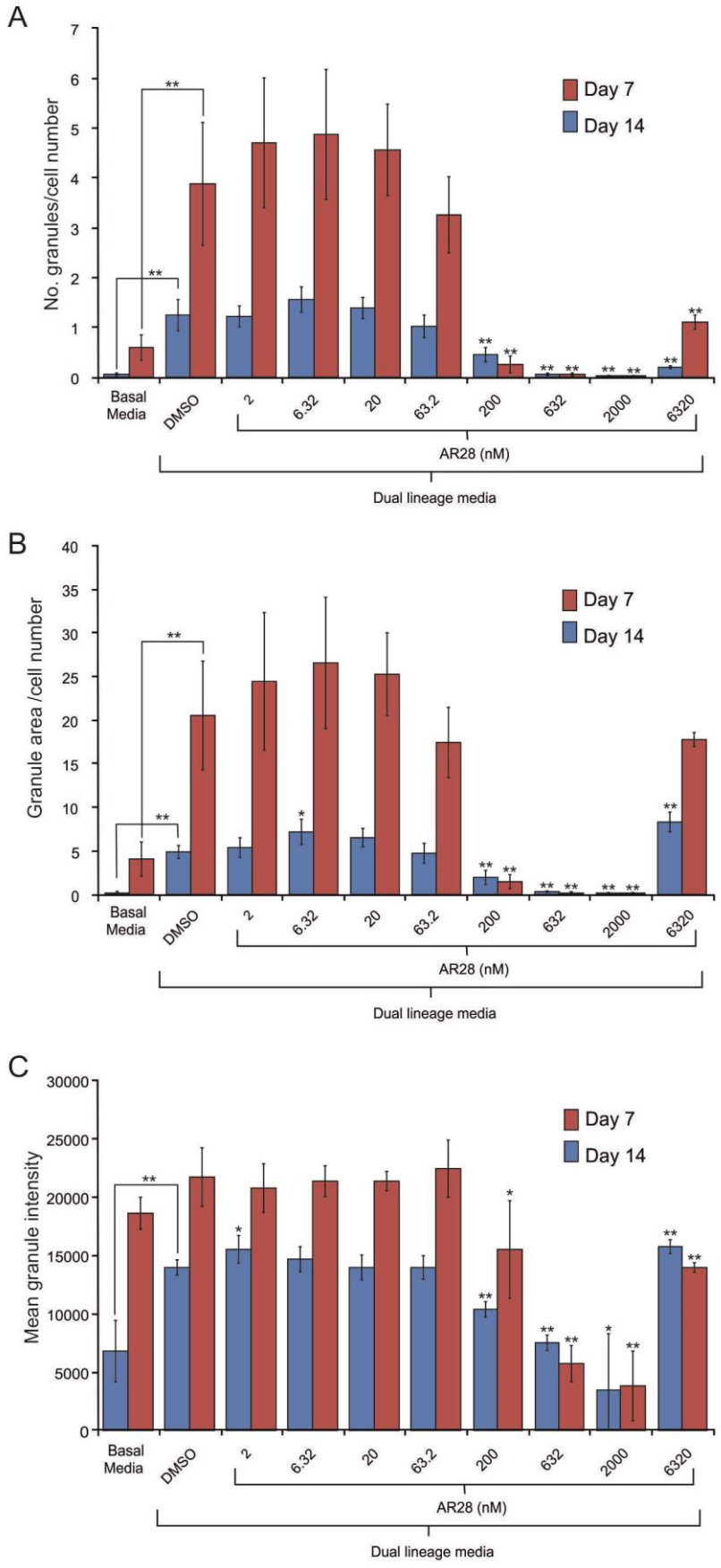
A
No. granules/cell number
Day 7
Day 14
Basal Media
DMSO
2
6.32
20
63.2
200
632
2000
6320
AR28 (nM)
Dual lineage media
B
Granule area /cell number
Day 7
Day 14
Basal Media
DMSO
2
6.32
20
63.2
200
632
2000
6320
AR28 (nM)
Dual lineage media
C
Mean granule intensity
Day 7
Day 14
Basal Media
DMSO
2
6.32
20
63.2
200
632
2000
6320
AR28 (nM)
Dual lineage media

AR28 at 6320 nM lead to large amounts of cell death within 7 days of treatment, resulting in abnormal ELF97 staining, which caused increases in all output measurements that were not the result of differentiation. However, increases in the number of ELF-97 positive foci, and total area of staining were detected in response to the dual lineage conditions relative to the basal media control, with inhibition of this increase in response to AR28 at concentrations of 200 nM and above (Figure 5.4.6 A+B). Similarly, the increase in the average staining intensity was enhanced in differentiation conditions compared to the basal media at day 7, and the intensity was reduced by AR28 at concentrations of 200 nM or above at both time points (Figure 5.4.6 C). In contrast, the lower concentrations of AR28, between 2 and 20 nM, generated slight increases in both the number and total area of ELF97-positive foci (Figure 5.4.6 A+B). However, due to the relatively high variation between the images from the replicate wells they failed to be statistically significant. The intensity of the staining in response to these lower concentrations remained unchanged (Figure 5.4.6 C).

5.4.2 BMP2 and canonical Wnt interactions

5.4.2.1 BMP2 and AR28 act synergistically to stimulate osteogenesis

As an alternative to osteogenic cocktails, BMPs can be used to induce osteogenesis, and have been shown to be dependent on canonical Wnt signalling (Chen et al, 2007b; Cheng et al, 2003; Tang et al, 2009). Therefore to see how AR28-mediated increased canonical Wnt signalling impacted on BMP2 induced osteogenesis, MSCs were treated with 100 ng/ml BMP2, with the addition of AR28 or DMSO vehicle control, and cultured for 7 days before ALP enzyme histochemistry staining (Figure 5.4.7). BMP2 alone caused very little effect on ALP staining of the MSCs, and similarly, AR28 alone did not alter ALP staining. However, together BMP2 and AR28 induced a large increase in ALP staining of the MSC cultures, suggesting a synergistic effect between BMP and canonical Wnt signalling on the induction of osteogenesis. The increase in staining manifested itself as an increase in the number of cells expressing ALP, but also as increased staining intensity for each cell compared to positive cells in control cultures. The combination of BMP2 and AR28

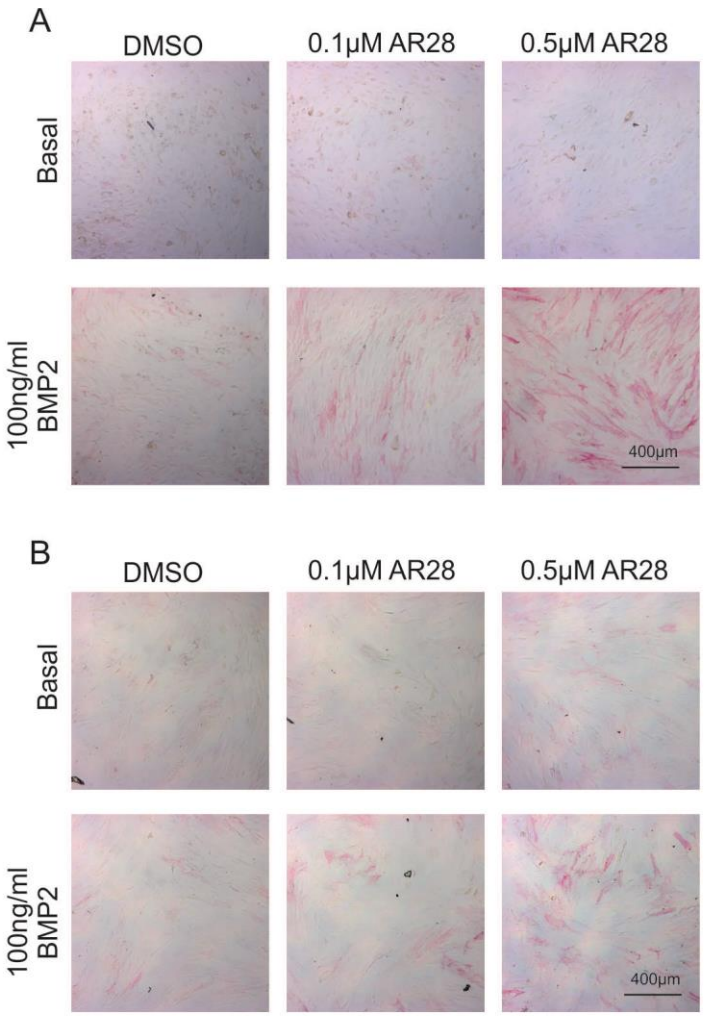

Figure 5.4.7. ALP Enzyme histochemistry showing BMP2 and AR28 act synergistically to enhance osteogenisis

MSCs (A) K9, B) FH429) were cultured for 7 days in basal conditions ± 100 ng/ml BMP2, with AR28 at concentrations given, or DMSO control. Samples were stained for ALP imaged by brightfield microscopy. Representative images shown. BMP2 or AR28 alone caused very little effect on ALP staining, however in combination generated large clear increases in ALP staining.

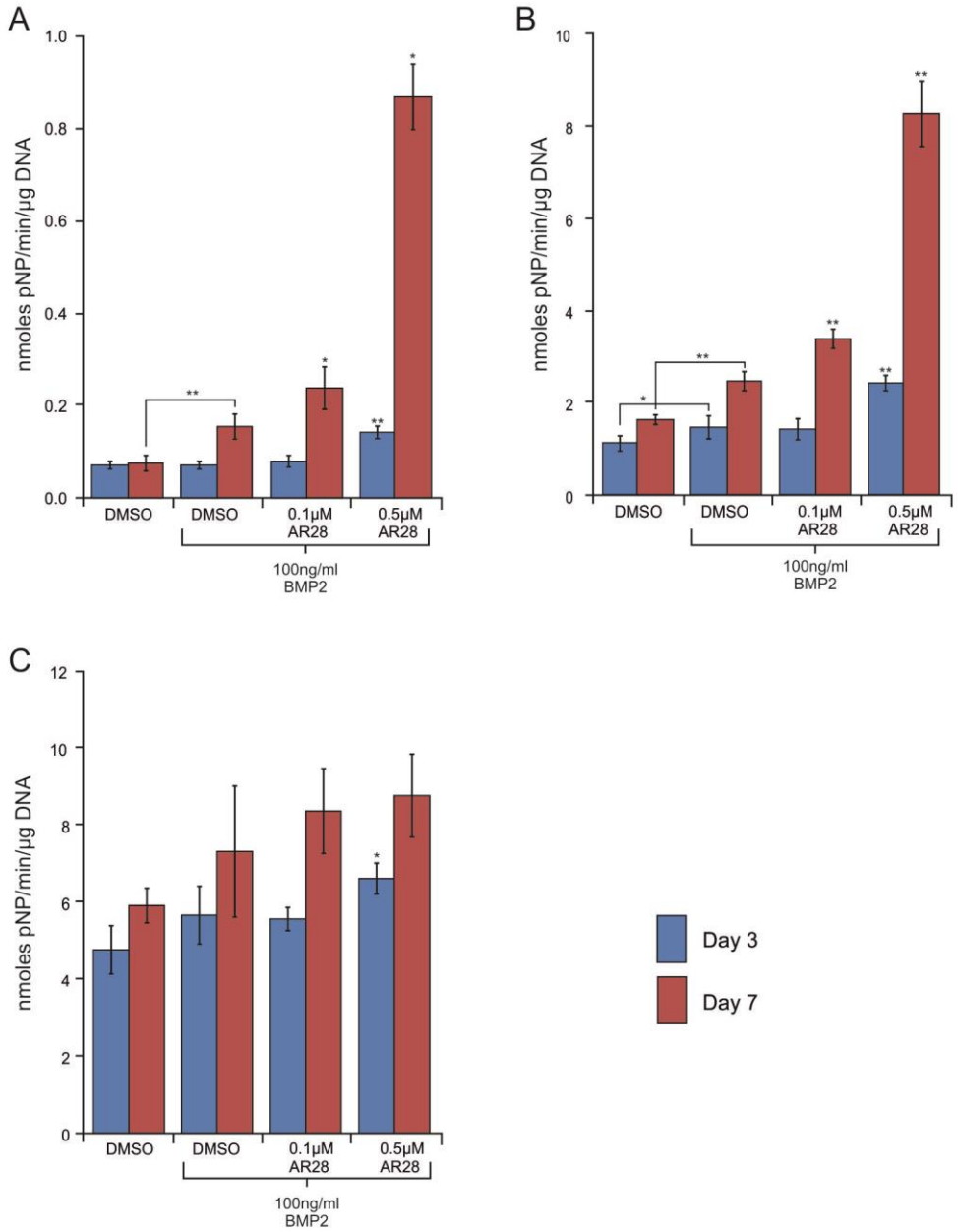

Figure 5.4.8. pNPP assay showing BMP2 and AR28 act synergistically to enhance osteogenisis

MSCs (A) K9, B) FH452 C) FH390) were cultured for up to 7 days in basal conditions ± 100 ng/ml BMP2, with AR28 at concentrations given, or DMSO control. ALP activity normalised to cell number (given as nmoles pNP/min/µg DNA) was calculated at 3 and 7 days. Values given as mean ± stdev., n=6 (independently treated technical replicates), * $p<0.05$, ** $p<0.005$. Statistical significance is relative to BMP2, DMSO control at appropriate time point unless otherwise stated, by Mann-Whitney U and Kruskal-Wallis tests.

can therefore increase the number of cells that progress towards an osteogenic lineage, but also increase the rate of progression.

The degree of ALP activity was also quantified using the pNPP ALP activity assay, normalising to DNA, which showed a very similar trend to the ALP staining (Figure 5.4.8). However, using this more sensitive method, small increases in ALP activity could be detected with BMP2 alone after 7 days treatment. The increase in ALP activity varied greatly between the 3 donors tested, with basal levels of ALP activity being equally variable; however the trend was the same irrespective of the level of ALP activity. As the ALP activity is normalised to DNA, a relative change in cell number could also be calculated. Unlike during the classical osteogenic differentiation, and the more mild form discussed in chapter 4, the increase in ALP activity caused by the combination of BMP2 and AR28 is not accompanied by large increases in cell number, suggesting an alternative mechanism.

5.4.2.2 AR28 inhibits BMP2 induced Sox9 activity

BMPs are also known to stimulate chondrogenesis through the up-regulation and activation of Sox9 (Majumdar et al, 2001). Therefore the ability of BMP2 to stimulate Sox9, and the effect of AR28 was investigated. This was first assayed by the use of a luminescent Sox9 activity reporter generated from 4 tandem repeats of the Sox9 responsive sequence from the collagen II promoter (Muramatsu et al, 2007). The reporter was transfected into C3H10T1/2 cells, alongside pCMV-renilla, as a transfection control, treated with a combination of 300 ng/ml BMP2 and varying AR28 concentrations for 48 hours. BMP2 generated large increases in Sox9 activity, of between ~20 and ~40 fold over basal levels depending on the passage of C3H10T1/2 cells used. The addition of AR28 dramatically reduced this increase in Sox9 activity by approximately 50% at 0.05 µM and down to basal levels by 0.5 µM (Figure 5.4.9 A). In a similar assay, Sox9 activity was stimulated by the over-expression of Sox9 in C3H10T1/2 cells (Figure 5.4.9 B). However, this increase was not affected by AR28, suggesting that AR28 did not cause inhibition of Sox9 transactivity at the level of protein stability or activity, but either during BMP2 signal transduction or DNA transcription/translation.

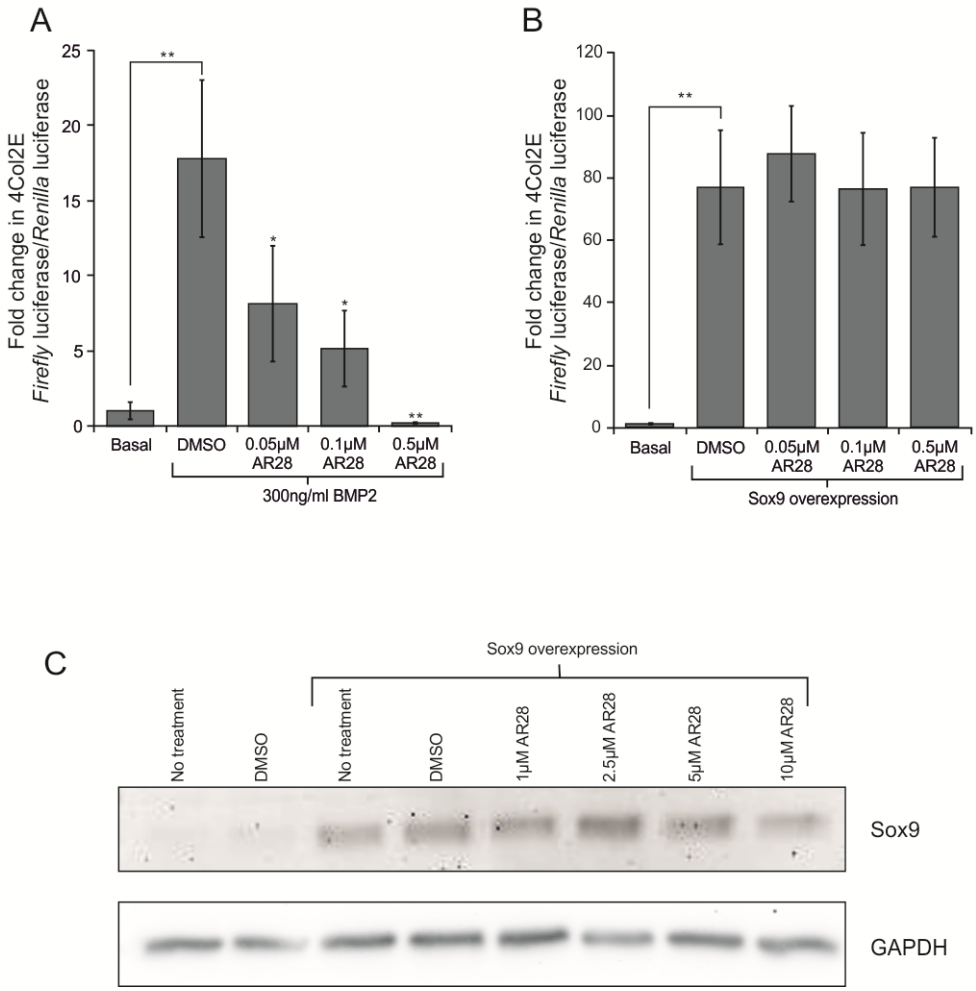

Figure 5.4.9. AR28 inhibits Sox9 activity induced by BMP2, but not Sox9 over-expression.
A) C3H10T1/2 cells were co-transfected with the 4Col2E *firefly* reporter plasmid and pCMV-Renilla before being treated with a combination of BMP2 and AR28 as stated. *Firefly* and *Renilla* luciferase were assayed after 48 hours of treatment. B) C3H10T1/2 cells were co-transfected with the 4Col2E *firefly* reporter plasmid, pCMV-Renilla and pRK5-Sox9 before being treated with AR28 or DMSO control as stated. *Firefly* luciferase was normalised to *Renilla* luciferase. The relative increases, compared to respective vehicle controls, were calculated. The graph presents mean ± standard deviation of six independently transfected and treated technical replicates. n=6, * $p<0.05$, **. Statistical significance is relative to vehicle control at relevant time point, by Mann-Whitney U and Kruskal-Wallis tests. C) Total cell extracts were obtained from C3H10T1/2 cells transfected with pRK5-Sox9 and cultured with AR28 at the concentration given, vehicle control (DMSO) or a no treatment control for 48 hours, and analysed by western blot. Membranes were probed against Sox9 and GAPDH for the loading control.

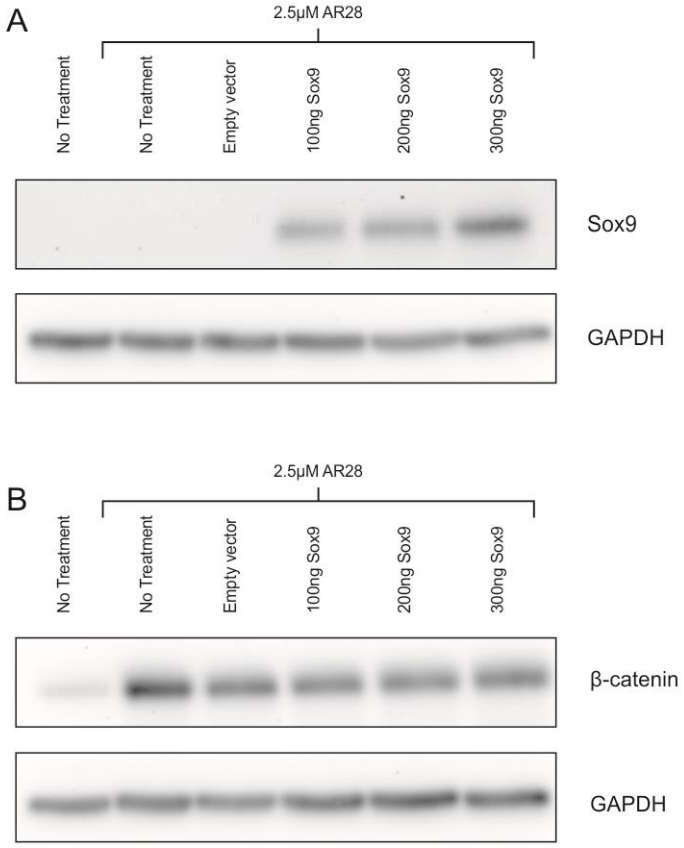

Figure 5.4.10. Sox9 over-expression does not inhibit β-catenin accumulation in response to AR28

Total cell extracts were obtained from HEK293 cells transfected with pRK5-Sox9 and empty pRK5 vector (total 300 ng/well) at the concentrations given (ng plamid/well) and cultured with 2.5 μM AR28, for 48 hours, and analysed by western blot. Membranes were probed against A) Sox9, B) β-catenin, and GAPDH for the loading control.

This was supported by protein analysis of Sox9 over-expression studies in C3H10T1/2 cells. Western blot analysis of Sox9 protein levels demonstrated transfection of the over-expression vector resulted in large increases in Sox9 protein levels after 48 hours. Sox9 protein levels fluctuated slightly between treatments but no clear dose-dependent effect of AR28 on protein levels was detected at concentrations of 1-5 µM. 10 µM AR28 did reduce Sox9 levels slightly (Figure 5.4.9 C), however this is a very high concentration, and could result in off target effects and toxicity. Conversely, Sox9 has been shown to alter the degradation of proteins (Cheng & Genever, 2010), therefore the effect of Sox9 over-expression was assayed for its effect on AR28 induced β-catenin stability. AR28 caused clear increases in the levels of β-catenin in HEK293 cell, but was not affected by the over-expression of Sox9 (Figure 5.4.10).

5.4.2.3 AR28 causes a switch from chondrogenesis to osteogenesis in the response to BMP2

As this work in the mouse multipotent mesenchymal cell line, C3H10T1/2 suggested that BMP2 could stimulate chondrogenic differentiation, and AR28 could inhibit this process at or prior to Sox9 translation, study of gene expression in human MSCs was performed in response to BMP2/AR28 combinations. As the above results had implicated the involvement of BMP2 and AR28 in both osteogenesis and chondrogenesis, qPCR primers for genes in both differentiation pathways were optimised. The primers for the osteogenic genes Runx2 and ALP along with the housekeeping gene RPS27A were optimised using cDNA generated by combining several samples from MSCs cultured in osteogenic conditions, while primers for the chondrogenic genes Sox9, Aggrecan 1 and Collagen IIa1(Col2a1) were optimised using cDNA generated from homogenised human cartilage. qPCR was performed using these primers against a 10-fold serial dilution of the cDNA, amplification plots and dissociation curves were generated and the threshold set to allow for C_T calculation (Figure 5.4.11 A+B). Using the C_T values standard curves were generated for each gene (Figure 5.4.11 C+D). All primers pairs amplified efficiently, demonstrated by standard curves with gradients of approximately -3.

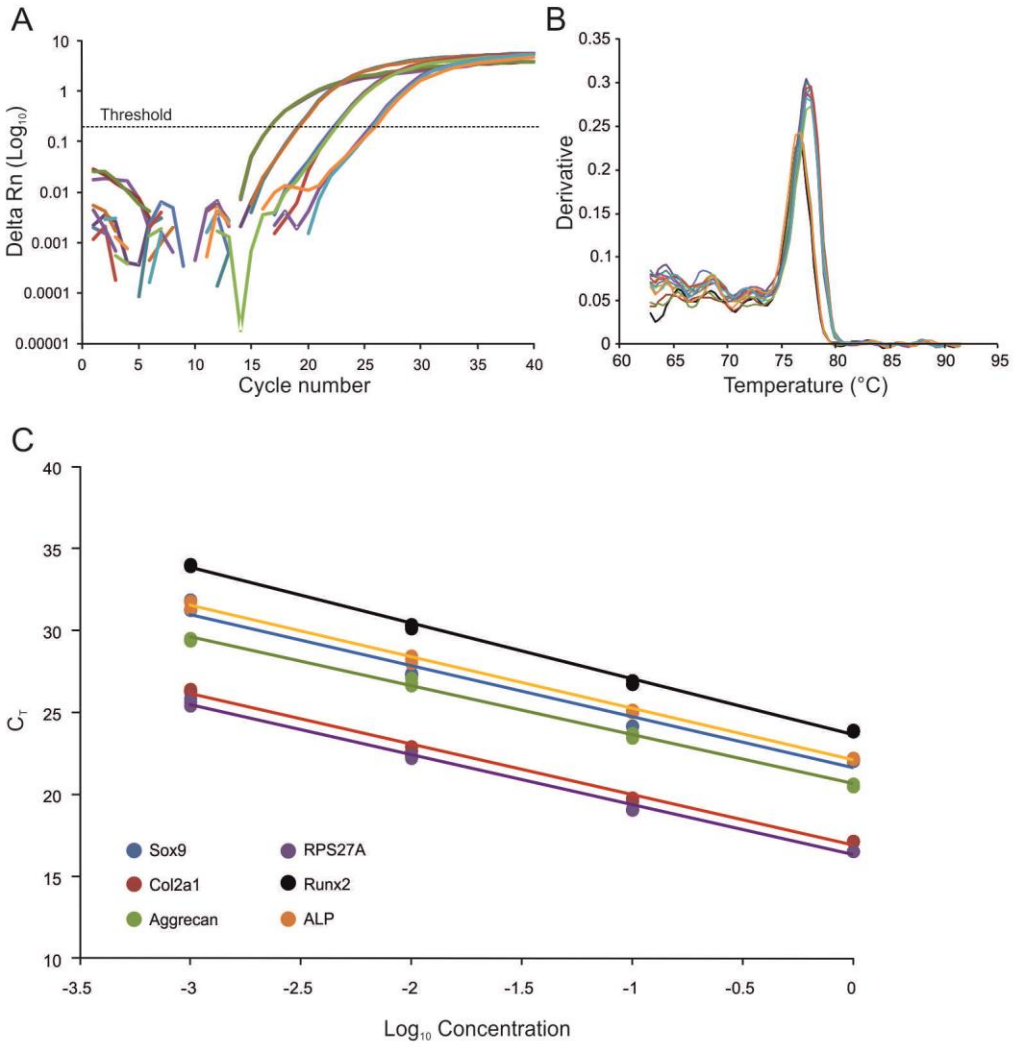

D

	RPS27A	Runx2	ALP	Sox9	Col2a1	Aggrecan
Gradient	-3.1	-3.4	-3.1	-3.1	-3.1	-3.0

Figure 5.4.11. Primer optimisation
Primer optimisation was performed using either combined cDNA from osteogenic differentiation of MSCs for the osteogenic genes, or cDNA from homogenised cartilage for chondrogenic genes. A 10 fold serial dilution of the sample was generated. These cDNA concentrations were analysed with the primer pairs in Table 5.3.5 and run on an ABI Prism 7000. A) Example amplification plot and B) dissociation curves of RPS27A primer pairs. C) Standard curves were generated from the C_T values for each primer pair. D) The gradient of the regression line for each primer pair.

To analyse the effect of BMP2 and AR28 on the expression levels of these genes, three MSC donors were cultured in basal media with the addition of 100 ng/ml BMP2 and 0.5 µM AR28 or DMSO for 24 hours or 5 days. Control samples in basal media alone were also produced. RNA was extracted and cDNA generated for analysis by qPCR. Fold changes in gene expression were produced using the $2^{-\Delta\Delta Ct}$ method, normalising to the housekeeping gene RPS27A, and relative to the 24 hour basal media sample (Figure 5.4.12, Figure 5.4.13 and Figure 5.4.14). Results for Sox9 expression matched the reporter assays in C3H10T1/2 cells, with increased expression in response to BMP2 treatment. The fold-change increase varied between the three donors tested, from approximately 1.5-fold to 3-fold, yet in all donors the increase was repressed by the addition of AR28, back to basal levels. The effect of BMP2 and AR28 on Runx2 expression was less clear. BMP2 generated small increases in gene expression, similar to that for Sox9, however AR28 failed to generate a regular trend between the donors. Irrespective, the effect on the later osteogenic and chondrogenic gene markers was much more striking. As predicted from ALP activity assays, BMP2 caused small increases in ALP expression levels in two of three donors. The third donor, K37, showed a reduction in ALP levels upon BMP2 treatment, but in the same manner as the two other donors, ALP transcript levels increased further upon AR28 addition. The fold-changes in ALP expression varied greatly between donors, which was also the case for the chondrogenic markers Aggrecan and Coll2a1. BMP2 increased both Aggrecan and Coll2a1 after 5 days of treatment in all donors except Coll2a1 in donor FH390, which did not show any changes in expression levels. As with the key transcription factor Sox9, AR28 prevented this increase in chondrogenic markers reducing the expression back to basal levels. In summary BMP2 caused an increase in the chondrogenic markers, Sox9, Aggrecan and Col2a1 after 5 days treatment. This increase in chondrogenic gene expression was inhibited by AR28 addition, with a switch to increases in the osteogenic marker, ALP.

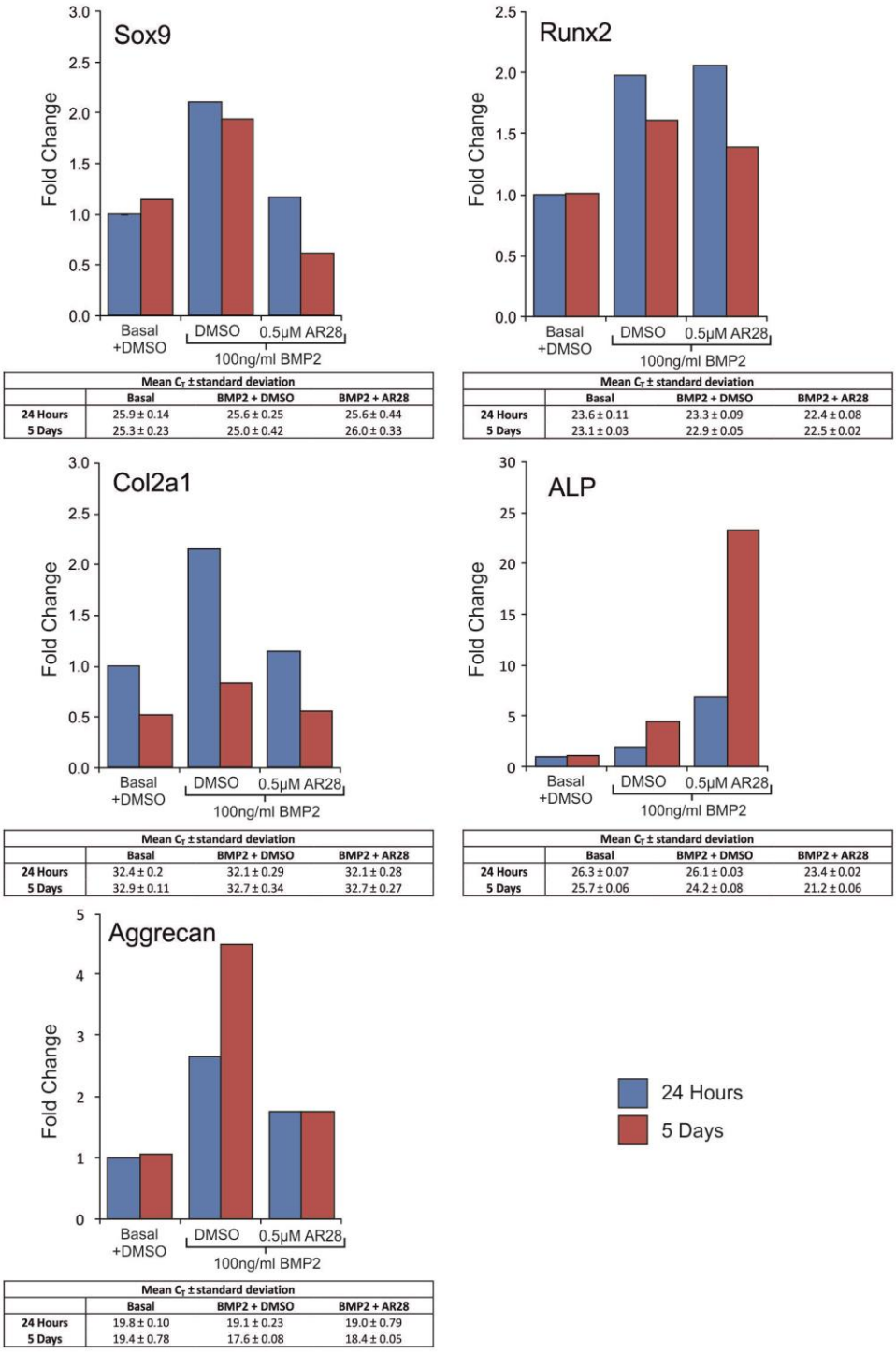

Sox9	Mean C_T ± standard deviation		
	Basal	BMP2 + DMSO	BMP2 + AR28
24 Hours	25.9 ± 0.14	25.6 ± 0.25	25.6 ± 0.44
5 Days	25.3 ± 0.23	25.0 ± 0.42	26.0 ± 0.33

Runx2	Mean C_T ± standard deviation		
	Basal	BMP2 + DMSO	BMP2 + AR28
24 Hours	23.6 ± 0.11	23.3 ± 0.09	22.4 ± 0.08
5 Days	23.1 ± 0.03	22.9 ± 0.05	22.5 ± 0.02

Col2a1	Mean C_T ± standard deviation		
	Basal	BMP2 + DMSO	BMP2 + AR28
24 Hours	32.4 ± 0.2	32.1 ± 0.29	32.1 ± 0.28
5 Days	32.9 ± 0.11	32.7 ± 0.34	32.7 ± 0.27

ALP	Mean C_T ± standard deviation		
	Basal	BMP2 + DMSO	BMP2 + AR28
24 Hours	26.3 ± 0.07	26.1 ± 0.03	23.4 ± 0.02
5 Days	25.7 ± 0.06	24.2 ± 0.08	21.2 ± 0.06

Aggrecan	Mean C_T ± standard deviation		
	Basal	BMP2 + DMSO	BMP2 + AR28
24 Hours	19.8 ± 0.10	19.1 ± 0.23	19.0 ± 0.79
5 Days	19.4 ± 0.78	17.6 ± 0.08	18.4 ± 0.05

Figure 5.4.12. qPCR analysis of chondrogenic and osteogenic markers in response to BMP2 and AR28. (K16)

cDNA samples were generated from MSCs (K16) treated for 24 hours and 5 days with 100 ng/ml BMP2 and 0.5 μM AR28 or DMSO control. Basal media plus DMSO samples were also generated as an untreated control. cDNA samples were analysed by qPCR using primer pairs against Sox9, Aggrecan, Col2a1, Runx2 and ALP, and plotted as relative increases in gene expression relative to day 3 basal media controls. C^T values ± standard deviation of the technical replicates are presented in the corresponding tables.

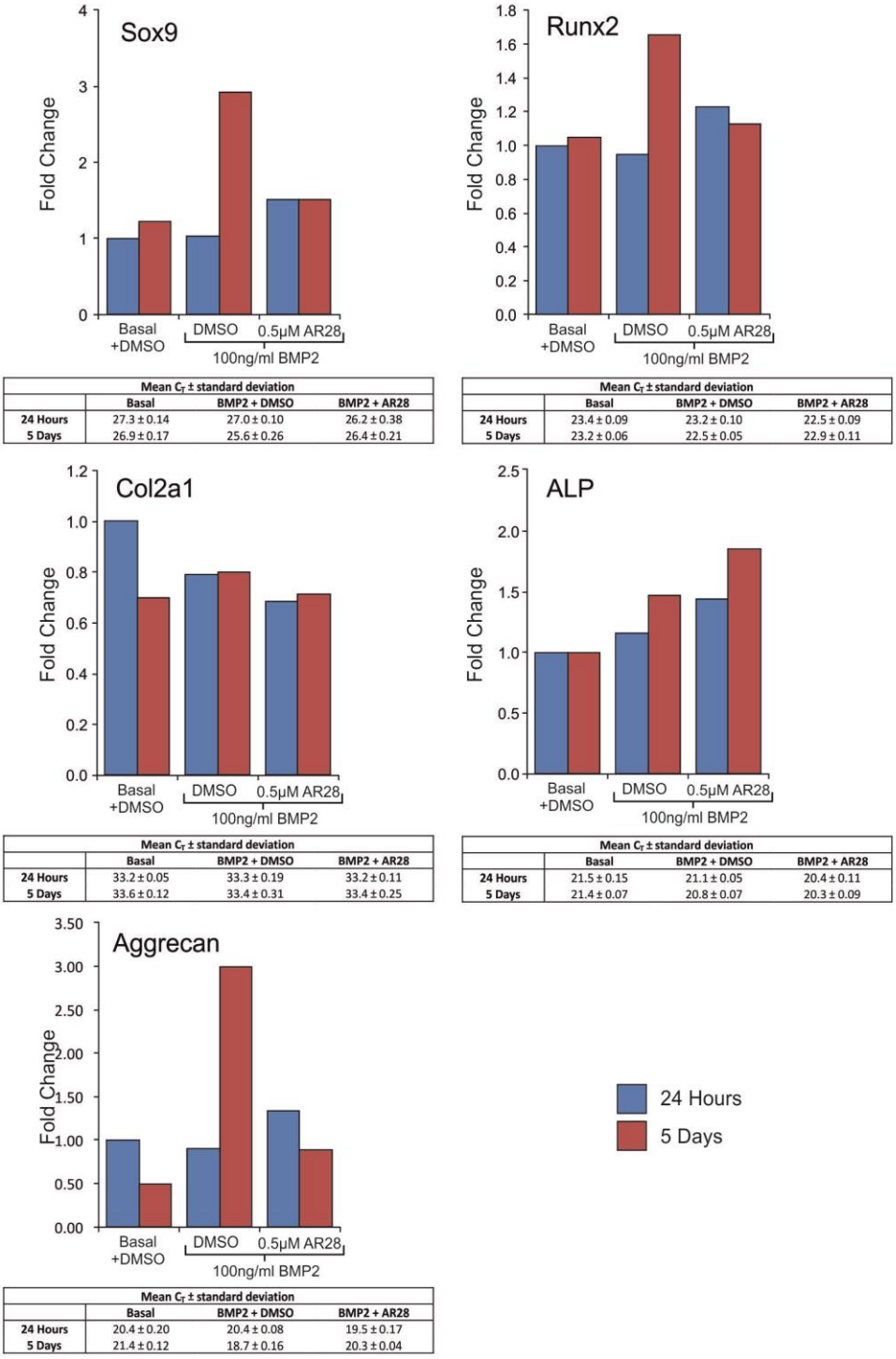

Mean C_T ± standard deviation			
	Basal	BMP2 + DMSO	BMP2 + AR28
24 Hours	27.3 ± 0.14	27.0 ± 0.10	26.2 ± 0.38
5 Days	26.9 ± 0.17	25.6 ± 0.26	26.4 ± 0.21

Mean C_T ± standard deviation			
	Basal	BMP2 + DMSO	BMP2 + AR28
24 Hours	23.4 ± 0.09	23.2 ± 0.10	22.5 ± 0.09
5 Days	23.2 ± 0.06	22.5 ± 0.05	22.9 ± 0.11

Mean C_T ± standard deviation			
	Basal	BMP2 + DMSO	BMP2 + AR28
24 Hours	33.2 ± 0.05	33.3 ± 0.19	33.2 ± 0.11
5 Days	33.6 ± 0.12	33.4 ± 0.31	33.4 ± 0.25

Mean C_T ± standard deviation			
	Basal	BMP2 + DMSO	BMP2 + AR28
24 Hours	21.5 ± 0.15	21.1 ± 0.05	20.4 ± 0.11
5 Days	21.4 ± 0.07	20.8 ± 0.07	20.3 ± 0.09

Mean C_T ± standard deviation			
	Basal	BMP2 + DMSO	BMP2 + AR28
24 Hours	20.4 ± 0.20	20.4 ± 0.08	19.5 ± 0.17
5 Days	21.4 ± 0.12	18.7 ± 0.16	20.3 ± 0.04

Figure 5.4.13. qPCR analysis of chondrogenic and osteogenic markers in response to BMP2 and AR28 (FH390)

cDNA samples were generated from MSCs (FH390) treated for 24 hours and 5 days with 100 ng/ml BMP2 and 0.5 μM AR28 or DMSO control. Basal media plus DMSO samples were also generated as an untreated control. cDNA samples were analysed by qPCR using primer pairs against Sox9, Aggrecan, Col2a1, Runx2 and ALP, and plotted as relative increases in gene expression relative to day 3 basal media controls. C^T values ± standard deviation of the technical replicates are presented in the corresponding tables.

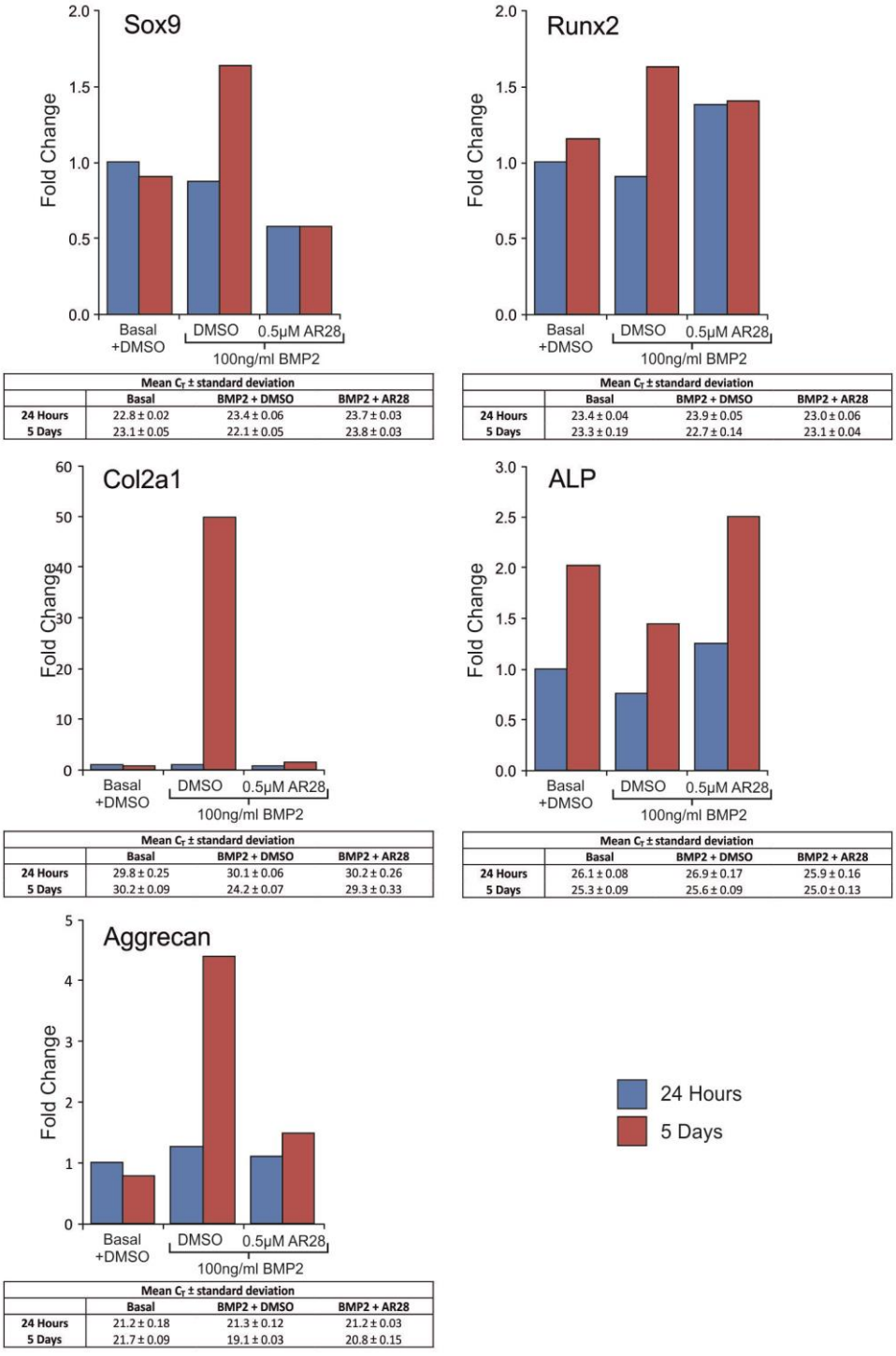

Mean C_T ± standard deviation

	Basal	BMP2 + DMSO	BMP2 + AR28
24 Hours	22.8 ± 0.02	23.4 ± 0.06	23.7 ± 0.03
5 Days	23.1 ± 0.05	22.1 ± 0.05	23.8 ± 0.03

Mean C_T ± standard deviation

	Basal	BMP2 + DMSO	BMP2 + AR28
24 Hours	23.4 ± 0.04	23.9 ± 0.05	23.0 ± 0.06
5 Days	23.3 ± 0.19	22.7 ± 0.14	23.1 ± 0.04

Mean C_T ± standard deviation

	Basal	BMP2 + DMSO	BMP2 + AR28
24 Hours	29.8 ± 0.25	30.1 ± 0.06	30.2 ± 0.26
5 Days	30.2 ± 0.09	24.2 ± 0.07	29.3 ± 0.33

Mean C_T ± standard deviation

	Basal	BMP2 + DMSO	BMP2 + AR28
24 Hours	26.1 ± 0.08	26.9 ± 0.17	25.9 ± 0.16
5 Days	25.3 ± 0.09	25.6 ± 0.09	25.0 ± 0.13

Mean C_T ± standard deviation

	Basal	BMP2 + DMSO	BMP2 + AR28
24 Hours	21.2 ± 0.18	21.3 ± 0.12	21.2 ± 0.03
5 Days	21.7 ± 0.09	19.1 ± 0.03	20.8 ± 0.15

Figure 5.4.14. qPCR analysis of chondrogenic and osteogenic markers in response to BMP2 and AR28 (K37)

cDNA samples were generated from MSCs (K37) treated for 24 hours and 5 days with 100 ng/ml BMP2 and 0.5 μM AR28 or DMSO control. Basal media plus DMSO samples were also generated as an untreated control. cDNA samples were analysed by qPCR using primer pairs against Sox9, Aggrecan, Col2a1, Runx2 and ALP, and plotted as relative increases in gene expression relative to day 3 basal media controls. C^T values ± standard deviation of the technical replicates are presented in the corresponding tables.

5.5 Discussion

Many studies have demonstrated the involvement of canonical Wnt signalling in bone homeostasis and osteoblast differentiation, however Liu *et al* (2009) went further to propose a differential inhibition of adipogenesis and osteogenesis by Wnt3a signalling. When grown in a binary differentiation medium, low level Wnt signalling lead to the inhibition of adipogenesis, without reducing osteogenesis. This reduction in adipogenesis induced an increase in precursor cells available for osteogenic differentiation, and therefore increased osteogenic differentiation.

To investigate whether AR28 could also generate this shift towards osteogenesis in dual differentiation conditions, MSCs were treated with a 50:50 mix of adipogenic and osteogenic medium and subjected to AR28 treatment. Multiple analysis techniques were used to study adipogenesis and osteogenesis, culminating in high content imaging based assays with a wide range of AR28 concentrations to ensure all degrees of canonical Wnt activation were studied. However, these studies did not replicate the differential effects on adipogenesis and osteogenesis described by Liu *et al* (2009), where canonical Wnt activation by Wnt3a lead to an increase in osteogenesis as the expense of adipogenesis when subjected to dual lineage conditions. Under the conditions described here, using either the osteogenic (including dex), adipogenic or dual differentiation conditions, AR28 treatment inhibited both adipogenesis and osteogenesis at similar concentrations, between 0.05 and 0.5 μM, therefore not allowing for the increase in osteogenesis at the expense of adipogenesis. Small, but non-significant increases in osteogenesis were observed using the high content ELF97 assay at low AR28 concentrations, 2 – 20 nM. However, these concentrations did not correspond with decreases in adipogenesis, as would be expected for a change in preference towards the osteogenic lineage. Adipogenesis was also slightly increased at these lower AR28 concentrations at day 7. Therefore these small differences are not due to differential responses to canonical Wnt signalling, but are likely due to an unknown effect on the MSC precursor population, increasing the potential for both lineages.

The discrepancy between these findings and those published by Liu *et al.* (2009) may be due to multiple reasons. Firstly, the medium used to induce the dual

differentiation differs, as the previously published work uses Lonza differentiation supplements, and optimised mesenchymal growth supplements. This may result in different effects of canonical Wnt signalling on the differentiation process creating the differences in differentiation inhibition. Secondly, AR28 is non-selective in its stimulation of the canonical Wnt signalling pathway due to its action downstream of receptor binding, while Wnt3a as used by Liu *et al* (2009) is dependent on the receptor expression on the target cell. It is possible that differentiating adipocytes and osteoblasts have different capacities to respond to Wnt3a, causing varying degrees of differentiation inhibition. Therefore by bypassing the ligand/receptor binding process, AR28 would override any target cell-specific effects, generating the same level of β-catenin stabilisation irrespective of receptor expression. The latter could easily be tested by the analysis of the effect of recombinant Wnt3a or Wnt3a conditioned media alongside AR28 to detect any differences in differentiation.

The results described in this chapter highlight the interactions between BMP2 and canonical Wnt signalling in the differentiation of MSCs towards both osteogenesis and chondrogenesis. In relation to osteogenesis, BMP2 was capable of generating small increases in the early osteogenic marker ALP, implying increased onset of osteogenesis. This is a process well documented in the literature both *in vivo* (Cheng et al, 2001) and *in vitro* (Cheng et al, 2003), and has instigated a range of clinical application studies looking into the use of BMPs to aid in fracture repair (Lissenberg-Thunnissen et al, 2011; Pecina et al, 2001; Southwood et al, 2004). Indeed a product called InFuse has been approved for therapeutic use. However, the response of mouse and human MSCs to BMPs varies, with much lower levels of osteogenesis *in vitro* by human MSCs, and higher concentration requirement for *in vivo* fracture repair (Diefenderfer et al, 2003). Similarly the results presented here showed relatively small increases in ALP by BMP2 alone, with the exception of donor FH390. However, the addition of AR28 to these cultures markedly increased the levels of ALP activity, suggesting the need for activated canonical Wnt signalling in the onset of BMP2-induced osteogenesis. This requirement has been noted before, both in *in vivo* models (Chen et al, 2007b) and C3H10T1/2 *in vitro* studies (Tang et al, 2009). Tang *et al.* (2009) demonstrated that BMP9 and Wnt3a could enhance the others ability to induce ALP activity of C3H10T1/2 cells, and that BMP9-induced osteogenesis was dependent on functional canonical Wnt signalling

by β-catenin knockdown experiments. Therefore despite the inability of canonical Wnt alone to induce osteogenesis of human MSCs, the requirement for functional canonical Wnt signalling in BMP2-induced osteogenesis, as in mice, appears to remain. Additionally Deifenderfer *et al*. (2003) noted a range of degrees of osteogenesis in response to BMPs by human MSCs, which was also identified in the work presented in this chapter. I propose this could be due to varying levels of endogenous canonical Wnt signalling between the donors. To test this hypothesis, western blot analysis of active β-catenin in the different donors could be analysed and compared to the responsiveness of the donors to BMP2 signalling. If the hypothesis is correct, one would expect the donors with the highest endogenous canonical Wnt signalling to respond more positively to BMP2.

The synergistic effect of BMP2 and AR28 on stimulating osteogenesis also suggests a therapeutic role for AR28. As stated above BMPs are being used to heal bone fractures in both animal models and humans, however the concentrations required in humans are relatively high. Various side effects associated with high BMP concentrations are being suggested and studied, and the combination of expensive manufacturing costs of BMPs, and the supra-physiological concentrations make treatment relatively cost-ineffective. Therefore, the addition of a canonical Wnt activator, such as AR28, to the site in combination with BMP signalling could increase the osteogenic differentiation of the endogenous MSCs at lower BMP concentrations, reducing both potential side effects and cost.

BMPs are also known to stimulate chondrogenesis of MSCs, to which the results presented in this chapter conform. BMP2 was capable of stimulating Sox9 reporter expression in C3H10T1/2 cells and up regulating the chondrogenic specific genes, Sox9, Aggrecan and Col2a1, in human MSCs. Furthermore, this increase in both reporter activity and gene expression was inhibited by the addition of AR28 to the culture, simultaneously inducing an increase in the osteogenic specific gene ALP. Canonical Wnt signalling has been shown to be important in the commitment of progenitor cells to form either chondrocytes or osteoblasts during development by a selection of conditional β-catenin knock outs and Wnt14 over-expression studies in mouse models (Day et al, 2005; Hill et al, 2005). These studies demonstrated that increased canonical Wnt signalling within the progenitor cells promoted

osteogenesis and chondrocyte hypertrophy and blocked chondrocyte differentiation, while canonical Wnt inhibition resulted in increased cartilage formation at the expense of osteogenesis. The results described in this chapter also suggest that the interplay between these two key signalling pathways is important in this bi-lineage commitment decision, in which canonical Wnt signalling can act as a switch to alter the differentiation fate from a chondrocyte to an osteoblast, a process that is necessary for endochondral bone formation.

These findings also illustrate the large differences that can be attained between donors, and their preference for a particular pathway. FH390 showed a strong preference for osteogenesis with high basal levels of ALP (ALP activity assay and C_T values) but generated low increases in chondrogenic genes in response to BMP2. While K37 showed relatively poor osteogenic differentiation when assayed for ALP transcription in response to the combination of BMP2 and AR28, but expressed very high levels of Col2a1 (50-fold increase) and Aggrecan (4-fold increase) in response to BMP2 alone. Donor K16 appeared to fall in between these two extremes with similar capacity for both chondrogenesis and osteogenesis. These results demonstrate that MSC cultures from different donors can vary dramatically in their preference to differentiate towards a particular lineage, yet they respond in the same manner in response to BMPs and Wnt, all be it by different degrees.

One mechanism for the up-regulation of Sox9 by BMP2 has been proposed by Jin *et al*. (2006), where BMP2 leads to the down-regulation of canonical Wnt signalling via p38 mitogen-activated protein kinase activation, which reduced the canonical Wnt-induced proteosomal degradation of Sox9. However, I showed that AR28 did not affect either the activity or the stability of over-expressed Sox9 in C3H10T1/2 cells. This lack of response may be due to the unnaturally high levels of CMV-driven Sox9 expression, rendering the Wnt induced degradation obsolete. BMP2 did however increase the mRNA levels of Sox9 in human MSCs which was prevented by AR28 treatment. This provides an alternative explanation for BMP2-induced chondrogenesis where BMP2 can cause increased transcription of the Sox9 gene, which is regulated by canonical Wnt signalling through the reduction in gene expression.

A transcription factor which has been suggested as a key player in the switch between chondrogenesis and osteogenesis of osteochondo progenitor cells is osterix (Tominaga et al, 2009). MSCs, ST-2 and C3H10T1/2 cells were shown to respond differently to BMP6, with C3H10T1/2 cells preferentially differentiating towards chondrocytes, while MSCs and ST-2 cells preferentially formed osteoblasts. This difference was shown to be due to varying expression levels of osterix, where higher expression levels caused osteogenesis. Furthermore, over-expression of osterix in C3H10T1/2 cells caused a reduction in chondrogenesis and an increase in osteogenesis, similar to the switch described in this work when MSCs were treated with a combination of BMP2 and AR28. Due to these similarities, future work may look into the levels of osterix expression and activity in the MSC cultures treated with BMP2 and AR28, in order to identify any changes in Osterix in response to AR28. The requirement of osterix in the switch from chondrogenesis to osteogenesis could also be studied by RNAi knockdown of osterix expression during the combination treatments.

Further information may also be gained by the studying the expression levels of additional genes during the BMP and AR28 combination treatments, either through qPCR or on a more global level by mRNA microarrays. This would allow for the identification of other differentiation genes to be studied, potentially identifying the point at which the switch toward osteogenesis occurs, and any point at which further external signals are required to continue the progression of the differentiation process. The use of a microarray could also lead to the identification of novel or unexpected genes involved in the chondro- osteogenic switch.

Chapter 6: Discussion

The work presented in this thesis provides a comprehensive assessment of the effect of canonical Wnt on the *in vitro* differentiation of human MSCs using a potent and selective GSK3β inhibitor, AR28, with a particular focus on osteogenic differentiation. Briefly, potency and selectivity of AR28 to activate the canonical Wnt signalling pathway was demonstrated (Chapter 3), generating increases in stabilised β-catenin and TCF/LEF1 transcription factor activity *in vitro*, and the duplication of the *Xenopus* embryonic axis upon injection into the ventral marginal zone. AR28 was subsequently used to identify the effect of activated canonical Wnt signalling on human MSC differentiation (Chapter 4). These investigations identified potential reasons for the discrepancies in the literature regarding the effect of canonical Wnt signalling on osteogenic differentiation, whilst identifying novel and valuable insights into the mechanisms behind these effects. Finally the effect of increased canonical Wnt signalling during bi-potential conditions was investigated (Chapter 5), which identified canonical Wnt signalling as an important regulator of the osteo/chondrogenic commitment decision in response to BMP signalling, acting through the down regulation of Sox9 expression and activity, and upregulation of ALP.

6.1 Role of canonical Wnt signalling in MSC differentiation

A large number of studies have looked into the effect of over-expression of canonical Wnt signalling on the differentiation of MSCs towards adipogenic, osteogenic and chondrogenic lineages. However, many contradicting effects are identified by different groups, most strikingly the strong osteo-induction of canonical Wnt signalling on mouse mesenchymal/osteogenic precursor cells, yet apparent inhibition of osteogenic differentiation of human MSCs. More recent work proposes the importance of the stage of differentiation to which canonical Wnt activation is applied (Eijken et al, 2008; Quarto et al, 2010). The work presented in this thesis used a range of osteogenic stimuli and osteogenic outputs to comprehensively study the effect of activated canonical Wnt signalling, by GSK3β inhibition, on the osteogenic differentiation of MSCs, whilst confirming the inhibitory effect of canonical Wnt signalling on adipogenesis. In combination with published work,

these findings have allowed for the generation of a working hypothesis for the role of canonical Wnt signalling in the differentiation of MSCs (Figure 6.1.1).

Results presented in section 4.4.3 and those published by other groups identifies the inhibition of dexamethasone induced osteogenic differentiation of human MSCs by canonical Wnt signalling, yet work by Krause *et al*. (2010) and that presented in section 4.4.4 showed increases in the early marker, ALP in response to canonical Wnt signalling in combination with a mild osteogenic stimulus, excluding dexamethasone. It is therefore proposed that canonical Wnt signalling can act to stimulate the early stage of osteogenic differentiation in the absence of dexamethasone, but is detrimental to the dexamethasone-induced maturation of osteoblasts (Figure 6.1.1). In addition to these findings supporting that of others, the results presented in section 4.4.5 also suggest a mechanism behind this increase in osteogenic precursors. Increases in cell number could be detected in response to canonical Wnt activation, most noticeably when in combination with the mild osteogenic stimuli. It is therefore proposed that canonical Wnt signalling acts to increase the proliferation of the osteogenic precursor cells, increasing the pool of osteogenic precursors, allowing for increased osteoblasts upon maturation (Figure 6.1.1). The pre-treatment experiments presented in section 4.4.6 also support this hypothesis, in which small increases in cell number can be detected after one week treatment with AR28 in basal conditions. These cells showed an increased potential for osteogenesis, possibly through the increased number of osteo-progenitor cells. As adipogenesis was not enhanced, this stimulatory effect cannot simply be due to increased multipotent MSC proliferation, as one would expect all lineages to be enhanced in this case. This work also complies with the proposal for transdifferentiation from adipocytes to osteoblasts by the inhibition of PPARγ. Canonical Wnt signalling is a known inhibitor of PPARγ (Okamura et al, 2009), causing the well documented decrease in adipogenesis. Further work, discussed in section 4.5, also implicates the involvement of PPARγ in regulating osteogenesis, therefore it is highly possible that canonical Wnt signalling could act upon adipogenic precursors, preventing PPARγ expression, causing a switch in gene expression to that of an osteoblast precursor cell (Figure 6.1.1). This would result in the increase in osteogenesis detected after AR28 pre-treatment, and the reduction in adipogenesis. Unlike the work by Liu *et al*. (2009), the study described in section

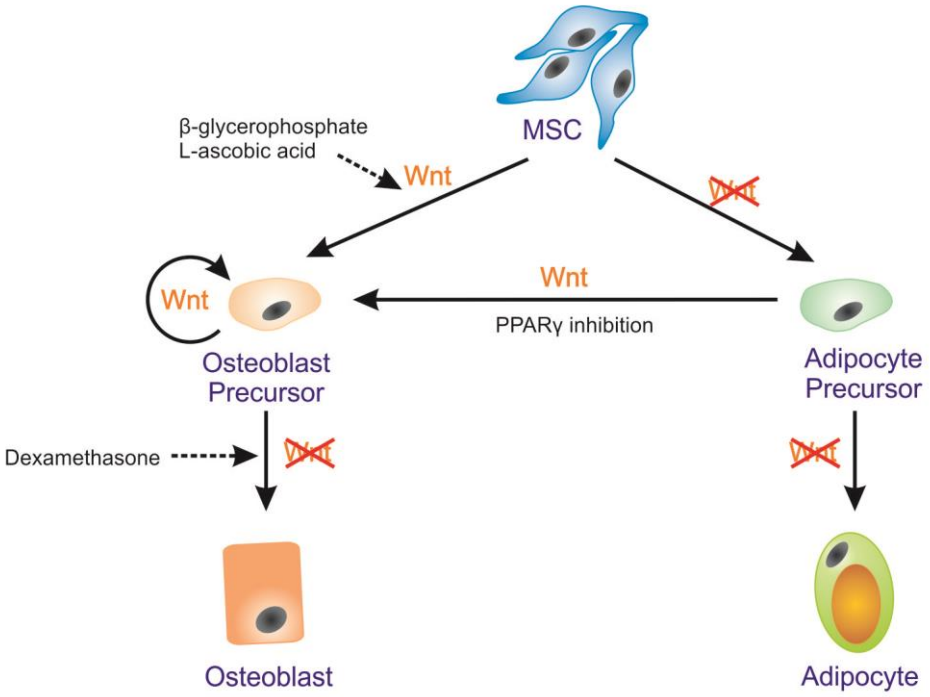

Figure 6.1.1. Schematic showing involvement of canonical Wnt in osteo/adipogenesis of MSCs

Canonical Wnt signalling inhibits adipogenic differentiation of MSCs, and can push pre-adipocytes towards osteoblasts by the inhibition of PPARγ. Canonical Wnt signalling enhances early osteogenic differentiation and increases osteoblast precursor proliferation, but inhibits dexamethasone-induced maturation.

5.4.1 did not show a differential inhibition of adipogenesis and osteogenesis in response to canonical Wnt signalling in the presence of a bi-potential induction media. However, upon pre-treatment with AR28, MSCs differentiate more readily towards osteoblasts, and less towards adipocytes, as mentioned above. Therefore if these cells were subsequently subjected to the bi-potential induction media, one would expect a selective preference towards osteogenic differentiation, suppressing further the inhibition of adipogenesis seen under single lineage conditions.

In addition to the work discussed above regarding the classical differentiation of MSCs using β-glycerophosphate, L-ascorbic acid and dexamethasone, findings presented in section 5.4.2 describe the effect of induced canonical Wnt signalling on BMP2-induced osteogenesis and chondrogenesis. BMPs can induce both osteogenic and chondrogenic differentiation (Cheng et al, 2003; Sampath et al, 1992), and canonical Wnt signalling can increase the progression of osteogenesis, but decrease chondrogenesis (Day et al, 2005; Hill et al, 2005; Tang et al, 2009). However, to my knowledge the work presented here is the first to demonstrate the simultaneous increase in osteogenic markers and decrease in chondrogenic markers in response to canonical Wnt activation in human MSCs. Furthermore, the findings offer novel reasoning for this switch from chondrogenesis to osteogenesis (Figure 6.1.2). Sox9 activity and chondrogenic-specific gene mRNA levels increased in response to BMP2 treatment but were reduced upon canonical Wnt activation by AR28. Furthermore, AR28 had no effect on over-expressed Sox9 protein levels or activity, suggesting a role for canonical Wnt signalling during transcriptional control of the Sox9 gene. These findings suggest a model for BMP2-induced differentiation of MSCs, where BMP2 exposure leads to the generation of an osteo-chondro progenitor cell, which in the absence to canonical Wnt signalling progresses towards a chondrogenic lineage, supported by the low level of osteogenesis in the absence of AR28. Following canonical Wnt activation, the level of Sox9 is reduced through decreased transcription, preventing the upregulation of the chondrogenic genes, and a switch to the osteogenic markers through Runx2 expression.

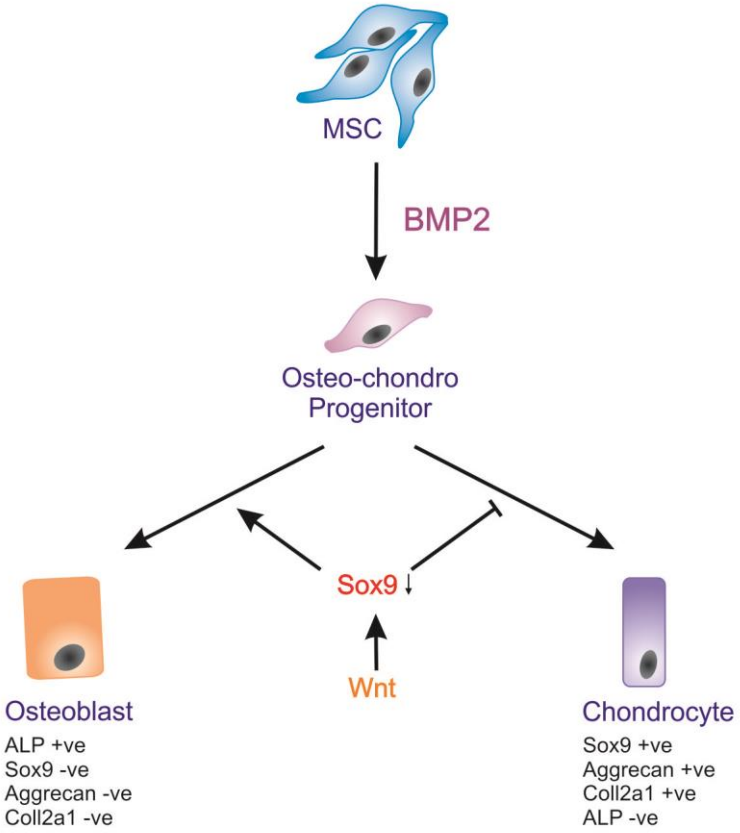

Figure 6.1.2. Schematic showing BMP2 and Canonical Wnt interactions during osteo/chondrogenic differentiation
BMP2 induces MSCs to differentiate towards an osteo-chondro progenitor, which in the absence of canonical Wnt signalling progress towards the chondrocyte lineage due to increased Sox9 expression. In the presence of canonical Wnt, Sox9 expression is reduced, preventing chondrogenesis and allowing osteogenesis via Runx2 expression.

The results discussed above regarding canonical Wnt signalling and the switch to osteogenesis in combination with BMPs, bears resemblance to that of Hh signalling discussed in 1.4.3.3, in which Shh leads to the increased expression and activity of Sox9 through the upregulation of Nkx3.2. It is therefore likely that all three signalling pathways, BMP, Wnt and Hh, are acting in combination in response to environmental and hormonal cues to regulate the chondrogenic and osteogenic differentiation of MSCs.

6.1.1.1 Therapeutic potential of canonical Wnt signalling and MSC differentiation

The use of canonical Wnt activation in the treatment of bone disorders is a reoccurring theme, and the results presented in this thesis support its potential. Canonical Wnt upregulation is known to generate increased bone mass and density in mice and humans. The findings described here suggest that this is likely through the increased proliferation of osteogenic precursor cells, and when in combination with intrinsic BMP signalling, increased differentiation. Activation of the canonical Wnt pathway could therefore be used in the treatment of genetic or age-related bone disorders where increased bone formation is required.

In addition to this straightforward approach, canonical Wnt activation could be used in combination with other treatments to improve their efficiency. For example during glucocorticoid (GC) treatment which can often lead to chronic osteoporosis. Canonical Wnt activation has the potential to tackle many of the effects of prolonged GC treatment as discussed in section 4.5. Conversely, Wnt activation may be used to enhance the effect of BMP treatment during fracture repair, allowing a greater osteogenic response to lower BMP concentrations as discussed in section 5.5. Alternatively, the manipulation of the canonical Wnt pathway by inhibition and activation may allow for the controlled sequential formation of chondrogenic followed by osteogenic cells, mimicking the endochondral ossification process, potentially generating more natural bone.

However, as with all therapeutic applications, safety must be considered. Firstly, off target effects both through the activation of the canonical Wnt pathway in other tissues or by other roles of GSK3β, if using an inhibitor such as AR28, could

generate unknown side effects. These are most relevant for treatments involving systemic administration, such as those for osteoporosis, but much less important when selectively treating an area such as during fracture repair. A second major consideration is that of the oncogenic potential of canonical Wnt signalling (Polakis, 2012). Wnt signalling is often up regulated in tumours, suggesting a link between abnormal Wnt signalling and the onset of cancer, however there remains an absence of data showing the activation of canonical Wnt in normal tissues causes the formation of tumours.

Given these potential drawbacks in canonical Wnt activation within a patient, it is likely that its manipulation may first be used in the generation of biological cell scaffolds prior to implantation, or in cases where the potential benefit : risk ratio would be more acceptable such as treatment of osteolytic leasons in multiple myeloma patients (Heath et al, 2009). The identification of the mechanisms underlying *in vitro* osteogenic differentiation, such as those identified in this thesis, will allow for greater control in the design and formation scaffolds including those containing multiple cell types, through the controlled addition of various inductive cues such as BMPs and canonical Wnt signalling.

6.2 Differentiation stimulus and species-specific effects

The results presented in this thesis may also provide some insights into the discrepancies in the field regarding the effect of canonical Wnt signalling on osteogenic differentiation *in vitro*. There have been a large number of studies in mouse cell lines showing that canonical Wnt signalling can increase the expression of osteogenic markers, while work in human MSCs has generated conflicting data, with reduced osteogenesis in response to canonical Wnt signalling. These differences could easily be thought to be due to differences in the cell types used and differences between mouse and human cells, however I propose an alternative explanation. Osteogenesis of mouse cells rarely uses dexamethasone to induce differentiation, and demonstrate increased expression of bone markers upon canonical Wnt stimulation (Table 6.2.1), while the majority of human MSC osteogenic differentiation requires the use of dexamethasone to stimulate

differentiation and mineralisation, which is inhibited by canonical Wnt signalling (Table 6.2.1). Yet, if human MSCs are differentiated without

Table 6.2.1. Publications relating the effect of Canonical Wnt stimulation on osteogenesis.
Table showing the cell type, differentiation conditions and canonical Wnt stimulus, related to the effect on the osteogenic differentiation. β-glycerophosphate (β-GP), L-Ascorbic Acid (L-Asc), Dexamethasone (Dex).

Author	**Cell type**	**Differentiation media**	**Canonical Wnt stimulus**	**Effect**
Kulkarni *et al.* (2006)	C3H10T1/2	None	LY603281	Increased bone markers mRNA
Jackson *et al*. (2005)	C3H10T1/2	None	Wnt3a	Increased bone markers mRNA
Bennett *et al*. (2005)	ST2	β-GP	Chir-99021 Wnt10b	Increased bone markers and vK
Li *et al.* (2005)	mouse BM osteoblasts	β-GP, L-Asc, **10pM Dex**	Wnt3a conditioned media	Increased mineralisation
Cawthorn *et al*. (2012)	ST2	β-GP, L-Asc	Wnt10a/b over-expression	Increased ALP and ARS
Kang *et al.* (2007)	ST2	β-GP, L-Asc	Wnt10b over-expression	Increased vK and calcium deposition
Heo et al. (2010)	PDL fibroblasts (human)	β-GP, L-Asc	LiCl	Increased ALP and mineralisation
Gregory *et al.* (2005)	hMSCs	β-GP, L-Asc, **100pM Dex**	LiCl	Increased ARS
Liu *et al.* (2009)	hMSCs	Lonza	Wnt3a	Reduced ALP and ARS
Baksh *et al*. (2007a)	hMSCs	β-GP, L-Asc, **10nM Dex**	Wnt3a	Reduced ALP
Boland *et al.* (2004)	hMSCs	β-GP, L-Asc, **10nM Dex**	Wnt3a	Reduced differentiation
De Boer *et al.* (2004)	hMSCs	β-GP, L-Asc, **10nM Dex**	LiCl, Wnt3a	Reduced ALP and mineralisation
Tang *et al*. (2009)	C3H10T1/2	BMP9	Wnt3a, stabilised β-catenin	Increased ALP activity

dexamethasone we and others (Krause et al, 2010) have shown small increases in early stage differentiation can be detected in response to canonical Wnt signalling. Therefore, I propose that it is the requirement for dexamethasone to induce strong osteogenesis, leading to its use in human, but not mouse osteogenic studies that has created these discrepancies between findings. The lack of requirement for dexamethasone in the mouse cell lines has allowed for the study of canonical Wnt signalling in a dexamethasone independent role, similar to that described in this thesis. The use of BMPs as stimulators of osteogenesis may have added further confusion, as both mouse (Tang et al, 2009) and human cells (Chapter 5) respond with increased osteogenesis upon canonical Wnt stimulation in the presence of BMPs. Therefore the choice of osteogenic stimulus is extremely important when studying the role of other factors in the differentiation process, and must be carefully considered to accurately replicate the *in vivo* scenario one is trying to replicate.

6.3 Future directions

The work presented in this thesis generates two main areas of further research to consider. Firstly, the role of canonical Wnt-induced proliferation is shown to be necessary for the osteogenic differentiation of MSCs, and it is proposed to act to increase osteogenic precursor numbers. With this in mind, future work would aim to gain a better understanding of the proliferation of the different populations within the MSC culture. To study the effect of proliferation on the very early precursors, cells would need to be identified by their transcription factor expression and activity. The adipogenic transcription factors C/EBPβ and PPARγ, and the osteogenic transcription factors Runx2 and Osterix are considered the key regulators of the differentiation commitment decisions and are therefore very early markers of the two lineages (Frith & Genever, 2008). The nature of transcription factors dictates that they are expressed in relatively low levels, making immunocytochemistry challenging; however there are antibodies available for the analysis of these transcription factors (Luciani et al, 2010; Nakahara et al, 2010; Plutzky, 1999). If successful, these immunocytochemical techniques would allow for the identification of pre-adipocytes or pre-osteoblasts within the population, which could then be analysed for proliferation by BrdU incorporation or similar imaging based assays. An alternative approach that would allow for the study of cell populations over time

would involve the use of cell lines expressing fluorescent transcription factor reporters. Reporter constructs have been published for several of these key transcription factors (Ducy et al, 1997; Fukui et al, 2000; Gijsbers et al, 2011; Sinha et al, 2010; Strecker et al, 2012), and could be adapted for fluorescent reporter expression. The osteogenic or adipogenic precursors could then be imaged over time in various conditions to see how they respond, both in proliferation and migration, or incorporated into a CFSE assay. However, again there are difficulties associated with this approach, most notably the difficulties in generating stable reporter lines of MSCs. MSCs are a primary cell line, and as such do not proliferate indefinitely in culture, therefore either a multipotent cell line such as C3H10T1/2, ST2 or immortalised MSCs must be used, however these may not behave in the same manner.

The study of osteogenic precursor proliferation *in vivo* may also offer valuable insights into the manner in which canonical Wnt can increase bone mineral density in mouse models. Strecker *et al.* (2012) published the generation of an osterix-cherry reporter mouse, which contained osterix-positive cells within the bone marrow that did not express BSP, and proposed they marked early osteoprogenitor cells. The combination of this reporter mouse and AR28 administration would allow for the analysis of changes in osteogenic progenitor cell numbers and location. There is then also the potential to incorporate BrdU analysis into this system (Thiagarajah et al, 2007) to study the proliferation of the Osx positive cells, providing additional information with regard to the importance of osteogenic precursor proliferation in the AR28 induced increase in bone mineral density.

The second area of work which could be followed up involves the role of canonical Wnt in the commitment decision of BMP2-induced osteochondral progenitor cells. The results presented show a clear switch to osteogenesis in response to canonical Wnt signalling, but the mechanisms underlying this switch are unknown. One potential mechanism involves the transcription factor Osx (See 5.5), and would provide an interesting starting point to continue this investigation.

6.4 Conclusion

The work presented in this thesis has provided confirmation of the ability of AR28 to stimulate the canonical Wnt pathway both *in vitro* and *in vivo*, and shown AR28 to have little effect on other signalling pathways under the conditions studied. This supports the notion that AR28-induced increases in bone mass are dependent on the up-regulation of the canonical Wnt signalling pathway. This work has also lead to an increased understanding of the role of canonical Wnt signalling during MSC differentiation, and provided reasoning for many of the discrepancies in the literature, whilst at the same time identified novel avenues of research to be studied. Furthermore it has confirmed the potential for AR28 as a pharmacological stimulator of the canonical Wnt pathway and supports its use in the therapeutic manipulation of the pathway.

List of Abbreviations

Add1	Adipocyte differentiation and determination factor-1
ALP	Alkaline phosphatise
AMH	Anti-Müllerian Hormone
APC	Adenomatous polyposis coli
ARS	Alizarin Red S
BCNE	Blastula Chordin and Noggin expression
BIO	6-bromoindirubin-3′-oxime
BMP	Bone morphogenetic protein
BSP	Bone sialoprotein
C/EBP	Ccaat-enhancer-binding protein
CFU	Colony forming unit
CHOPs	C/EBP homologoues proteins
CK1	Casein kinase 1
Col10A1	Type X collagen alpha 1
Col11A2	Type XI collagen alpha 2
Col1A1	Type I collagen alpha 1
Col2A1	Type II collagen alpha 1
Dhh	Desert Hedgehog
DKK	Dickkopf
Dvl	Dishevelled
EDTA	Ethylenediaminetetraacetic acid
ES cell	Embryonic stem cell
FABP	Fatty acid binding protein
FAS	Fatty acid synthase
FGF	Fibroblast growth factor
Fzd	Frizzled
GDF	Growth and Differentiation Factor
GLUT4	Glucose transporter 4
GSK	Glycogen synthase kinase
Hh	Hedgehog
HMG	High mobility group
HSC	Hematopoietic stem cells

IBMX	Isobutylmthylxanthine
Ihh	Indian Hedgehog
iPS	Induced pleuripotent stem
LEF/TCF	T Cell Transcription factor/Lymphoid enhancer-binding factor
LIF	Leukaemia inhibitory factor
LPL	Lipoprotein lipase
LRP	Low density lipoprotein receptor protein
MEF	Mouse embryonic fibroblast
MKP-1	Mitogen-activated protein kinase phosphatase-1
MSC	Mesenchymal stem cell
NF	Nieuwkoop and Faber stage
NFAT	Nuclear factor of activated T cells
OC	Osteocalcin
ON	Osteonectin
OP	Osteopontin
Osx	Osterix
PKA	Protein kinase A
PPAR	Peroxisome proliferator-activated receptor
Ptc	Patched
PTHrP	Parathyroid hormone-related protein
RI	Type I receptor
RII	Type II receptor
SBE	SMAD binding element
SCID	Severe combined immunodeficient
sFRPs	Frizzled-related proteins
Shh	Sonic Hedgehog
Smo	Smoothened
SREBP1	Sterol regulatory binding element protein-1
TGF	Transforming growth factor
vK	von Kossa
WIFs	Wnt inhibitory proteins

References

Abdallah BM, Haack-Sørensen M, Burns JS, Elsnab B, Jakob F, Hokland P, Kassem M (2005) Maintenance of differentiation potential of human bone marrow mesenchymal stem cells immortalized by human telomerase reverse transcriptase gene despite [corrected] extensive proliferation. *Biochem Biophys Res Commun* **326:** 527-538

Aberle H, Bauer A, Stappert J, Kispert A, Kemler R (1997) beta-catenin is a target for the ubiquitin-proteasome pathway. *EMBO J* **16:** 3797-3804

Akiyama H, Chaboissier MC, Martin JF, Schedl A, de Crombrugghe B (2002) The transcription factor Sox9 has essential roles in successive steps of the chondrocyte differentiation pathway and is required for expression of Sox5 and Sox6. *Genes Dev* **16:** 2813-2828

Akune T, Ohba S, Kamekura S, Yamaguchi M, Chung UI, Kubota N, Terauchi Y, Harada Y, Azuma Y, Nakamura K, Kadowaki T, Kawaguchi H (2004) PPARgamma insufficiency enhances osteogenesis through osteoblast formation from bone marrow progenitors. *J Clin Invest* **113:** 846-855

Alliston T, Choy L, Ducy P, Karsenty G, Derynck R (2001) TGF-beta-induced repression of CBFA1 by Smad3 decreases cbfa1 and osteocalcin expression and inhibits osteoblast differentiation. *EMBO J* **20:** 2254-2272

Auld KL, Berasi SP, Liu Y, Cain M, Zhang Y, Huard C, Fukayama S, Zhang J, Choe S, Zhong W, Bhat BM, Bhat RA, Brown EL, Martinez RV (2012) Estrogen-related receptor α regulates osteoblast differentiation via Wnt/β-catenin signaling. *J Mol Endocrinol* **48:** 177-191

Babij P, Zhao W, Small C, Kharode Y, Yaworsky PJ, Bouxsein ML, Reddy PS, Bodine PV, Robinson JA, Bhat B, Marzolf J, Moran RA, Bex F (2003) High bone mass in mice expressing a mutant LRP5 gene. *J Bone Miner Res* **18:** 960-974

Baksh D, Boland GM, Tuan RS (2007a) Cross-talk between Wnt signaling pathways in human mesenchymal stem cells leads to functional antagonism during osteogenic differentiation. *J Cell Biochem* **101:** 1109-1124

Baksh D, Yao R, Tuan RS (2007b) Comparison of proliferative and multilineage differentiation potential of human mesenchymal stem cells derived from umbilical cord and bone marrow. *Stem Cells* **25:** 1384-1392

Banerjee C, Javed A, Choi JY, Green J, Rosen V, van Wijnen AJ, Stein JL, Lian JB, Stein GS (2001) Differential regulation of the two principal Runx2/Cbfa1 n-terminal isoforms in response to bone morphogenetic protein-2 during development of the osteoblast phenotype. *Endocrinology* **142:** 4026-4039

Baxter MA, Wynn RF, Jowitt SN, Wraith JE, Fairbairn LJ, Bellantuono I (2004) Study of telomere length reveals rapid aging of human marrow stromal cells following in vitro expansion. *Stem Cells* **22:** 675-682

Becker AJ, McCulloch EA, Till JE (1963) Cytological demonstration of the clonal nature of spleen colonies derived from transplanted mouse marrow cells. *Nature* **197:** 452-454

Behrens J, von Kries JP, Kühl M, Bruhn L, Wedlich D, Grosschedl R, Birchmeier W (1996) Functional interaction of beta-catenin with the transcription factor LEF-1. *Nature* **382:** 638-642

Bennett CN, Longo KA, Wright WS, Suva LJ, Lane TF, Hankenson KD, MacDougald OA (2005) Regulation of osteoblastogenesis and bone mass by Wnt10b. *Proc Natl Acad Sci U S A* **102:** 3324-3329

Bennett CN, Ross SE, Longo KA, Bajnok L, Hemati N, Johnson KW, Harrison SD, MacDougald OA (2002) Regulation of Wnt signaling during adipogenesis. *J Biol Chem* **277:** 30998-31004

Bennett MR, Evan GI, Newby AC (1994) Deregulated expression of the c-myc oncogene abolishes inhibition of proliferation of rat vascular smooth muscle cells by serum reduction, interferon-gamma, heparin, and cyclic nucleotide analogues and induces apoptosis. *Circ Res* **74:** 525-536

Berg S, Bergh M, Hellberg S, Högdin K, Lo-Alfredsson Y, Söderman P, von Berg S, Weigelt T, Ormö M, Xue Y, Tucker J, Neelissen J, Jerning E, Nilsson Y, Bhat R (2012) Discovery of novel potent and highly selective glycogen synthase kinase-3β (GSK3β) inhibitors for Alzheimer's disease: design, synthesis, and characterization of pyrazines. *J Med Chem* **55:** 9107-9119

Bhanot P, Brink M, Samos CH, Hsieh JC, Wang Y, Macke JP, Andrew D, Nathans J, Nusse R (1996) A new member of the frizzled family from Drosophila functions as a Wingless receptor. *Nature* **382:** 225-230

Bilic J, Huang YL, Davidson G, Zimmermann T, Cruciat CM, Bienz M, Niehrs C (2007) Wnt induces LRP6 signalosomes and promotes dishevelled-dependent LRP6 phosphorylation. *Science* **316:** 1619-1622

Biliran H, Wang Y, Banerjee S, Xu H, Heng H, Thakur A, Bollig A, Sarkar FH, Liao JD (2005) Overexpression of cyclin D1 promotes tumor cell growth and confers resistance to cisplatin-mediated apoptosis in an elastase-myc transgene-expressing pancreatic tumor cell line. *Clin Cancer Res* **11:** 6075-6086

Bitgood MJ, McMahon AP (1995) Hedgehog and Bmp genes are coexpressed at many diverse sites of cell-cell interaction in the mouse embryo. *Dev Biol* **172:** 126-138

Blanpain C, Lowry WE, Geoghegan A, Polak L, Fuchs E (2004) Self-renewal, multipotency, and the existence of two cell populations within an epithelial stem cell niche. *Cell* **118:** 635-648

Bodine PV, Zhao W, Kharode YP, Bex FJ, Lambert AJ, Goad MB, Gaur T, Stein GS, Lian JB, Komm BS (2004) The Wnt antagonist secreted frizzled-related protein-1 is a negative regulator of trabecular bone formation in adult mice. *Mol Endocrinol* **18:** 1222-1237

Boland GM, Perkins G, Hall DJ, Tuan RS (2004) Wnt 3a promotes proliferation and suppresses osteogenic differentiation of adult human mesenchymal stem cells. *J Cell Biochem* **93:** 1210-1230

Bovolenta P, Esteve P, Ruiz JM, Cisneros E, Lopez-Rios J (2008) Beyond Wnt inhibition: new functions of secreted Frizzled-related proteins in development and disease. *J Cell Sci* **121:** 737-746

Boyden LM, Mao J, Belsky J, Mitzner L, Farhi A, Mitnick MA, Wu D, Insogna K, Lifton RP (2002) High bone density due to a mutation in LDL-receptor-related protein 5. *N Engl J Med* **346:** 1513-1521

Bridgewater LC, Lefebvre V, de Crombrugghe B (1998) Chondrocyte-specific enhancer elements in the Col11a2 gene resemble the Col2a1 tissue-specific enhancer. *J Biol Chem* **273:** 14998-15006

Caplan AI, Bruder SP (2001) Mesenchymal stem cells: building blocks for molecular medicine in the 21st century. *Trends Mol Med* **7:** 259-264

Cattaneo E, McKay R (1990) Proliferation and differentiation of neuronal stem cells regulated by nerve growth factor. *Nature* **347:** 762-765

Cavallo RA, Cox RT, Moline MM, Roose J, Polevoy GA, Clevers H, Peifer M, Bejsovec A (1998) Drosophila Tcf and Groucho interact to repress Wingless signalling activity. *Nature* **395:** 604-608

Cawthorn WP, Bree AJ, Yao Y, Du BW, Hemati N, Martinez-Santibanez G, MacDougald OA (2012) Wnt6, Wnt10a and Wnt10b inhibit adipogenesis and stimulate osteoblastogenesis through a beta-catenin-dependent mechanism. *Bone* **50:** 477-489

Chen L, Daley GQ (2008) Molecular basis of pluripotency. *Hum Mol Genet* **17:** R23-27

Chen X, Li X, Wang W, Lufkin T (1996) Dlx5 and Dlx6: an evolutionary conserved pair of murine homeobox genes expressed in the embryonic skeleton. *Ann N Y Acad Sci* **785:** 38-47

Chen Y, Whetstone HC, Lin AC, Nadesan P, Wei Q, Poon R, Alman BA (2007a) Beta-catenin signaling plays a disparate role in different phases of fracture repair: implications for therapy to improve bone healing. *PLoS Med* **4:** e249

Chen Y, Whetstone HC, Youn A, Nadesan P, Chow EC, Lin AC, Alman BA (2007b) Beta-catenin signaling pathway is crucial for bone morphogenetic protein 2 to induce new bone formation. *J Biol Chem* **282:** 526-533

Cheng A, Genever PG (2010) SOX9 determines RUNX2 transactivity by directing intracellular degradation. *J Bone Miner Res* **25:** 2680-2689

Cheng H, Jiang W, Phillips FM, Haydon RC, Peng Y, Zhou L, Luu HH, An N, Breyer B, Vanichakarn P, Szatkowski JP, Park JY, He TC (2003) Osteogenic activity of the fourteen types of human bone morphogenetic proteins (BMPs). *J Bone Joint Surg Am* **85-A:** 1544-1552

Cheng SL, Lou J, Wright NM, Lai CF, Avioli LV, Riew KD (2001) In vitro and in vivo induction of bone formation using a recombinant adenoviral vector carrying the human BMP-2 gene. *Calcif Tissue Int* **68:** 87-94

Cho J, Rameshwar P, Sadoshima J (2009) Distinct roles of glycogen synthase kinase (GSK)-3alpha and GSK-3beta in mediating cardiomyocyte differentiation in murine bone marrow-derived mesenchymal stem cells. *J Biol Chem* **284:** 36647-36658

Clement-Lacroix P, Ai M, Morvan F, Roman-Roman S, Vayssiere B, Belleville C, Estrera K, Warman ML, Baron R, Rawadi G (2005) Lrp5-independent activation of Wnt signaling by lithium chloride increases bone formation and bone mass in mice. *Proc Natl Acad Sci U S A* **102:** 17406-17411

Clevers H, Nusse R (2012) Wnt/beta-Catenin Signaling and Disease. *Cell* **149:** 1192-1205

Cox WG, Singer VL (1999) A high-resolution, fluorescence-based method for localization of endogenous alkaline phosphatase activity. *J Histochem Cytochem* **47:** 1443-1456

da Silva Meirelles L, Chagastelles PC, Nardi NB (2006) Mesenchymal stem cells reside in virtually all post-natal organs and tissues. *J Cell Sci* **119:** 2204-2213

Da Violante G, Zerrouk N, Richard I, Provot G, Chaumeil JC, Arnaud P (2002) Evaluation of the cytotoxicity effect of dimethyl sulfoxide (DMSO) on Caco2/TC7 colon tumor cell cultures. *Biol Pharm Bull* **25:** 1600-1603

Dahéron L, Opitz SL, Zaehres H, Lensch MW, Lensch WM, Andrews PW, Itskovitz-Eldor J, Daley GQ (2004) LIF/STAT3 signaling fails to maintain self-renewal of human embryonic stem cells. *Stem Cells* **22:** 770-778

Date T, Doiguchi Y, Nobuta M, Shindo H (2004) Bone morphogenetic protein-2 induces differentiation of multipotent C3H10T1/2 cells into osteoblasts, chondrocytes, and adipocytes in vivo and in vitro. *J Orthop Sci* **9:** 503-508

Davies SP, Reddy H, Caivano M, Cohen P (2000) Specificity and mechanism of action of some commonly used protein kinase inhibitors. *Biochem J* **351:** 95-105

Day TF, Guo X, Garrett-Beal L, Yang Y (2005) Wnt/beta-catenin signaling in mesenchymal progenitors controls osteoblast and chondrocyte differentiation during vertebrate skeletogenesis. *Dev Cell* **8:** 739-750

De Bari C, Dell'Accio F, Vandenabeele F, Vermeesch JR, Raymackers JM, Luyten FP (2003) Skeletal muscle repair by adult human mesenchymal stem cells from synovial membrane. *J Cell Biol* **160:** 909-918

de Boer J, Siddappa R, Gaspar C, van Apeldoorn A, Fodde R, van Blitterswijk C (2004) Wnt signaling inhibits osteogenic differentiation of human mesenchymal stem cells. *Bone* **34:** 818-826

De Luca F, Barnes KM, Uyeda JA, De-Levi S, Abad V, Palese T, Mericq V, Baron J (2001) Regulation of growth plate chondrogenesis by bone morphogenetic protein-2. *Endocrinology* **142:** 430-436

De Robertis EM, Kuroda H (2004) Dorsal-ventral patterning and neural induction in Xenopus embryos. *Annu Rev Cell Dev Biol* **20:** 285-308

de Vries F, Bracke M, Leufkens HGA, Lammers JWJ, Cooper C, van Staa TP (2007) Fracture risk with intermittent high-dose oral glucocorticoid therapy. *Arthritis and Rheumatism* **56:** 208-214

de Wert G, Mummery C (2003) Human embryonic stem cells: research, ethics and policy. *Human Reproduction* **18:** 672-682

Depew MJ, Liu JK, Long JE, Presley R, Meneses JJ, Pedersen RA, Rubenstein JL (1999) Dlx5 regulates regional development of the branchial arches and sensory capsules. *Development* **126:** 3831-3846

Diefenderfer DL, Osyczka AM, Reilly GC, Leboy PS (2003) BMP responsiveness in human mesenchymal stem cells. *Connect Tissue Res* **44 Suppl 1:** 305-311

Dodig M, Tadic T, Kronenberg MS, Dacic S, Liu YH, Maxson R, Rowe DW, Lichtler AC (1999) Ectopic Msx2 overexpression inhibits and Msx2 antisense stimulates calvarial osteoblast differentiation. *Dev Biol* **209:** 298-307

Dominici M, Le Blanc K, Mueller I, Slaper-Cortenbach I, Marini F, Krause D, Deans R, Keating A, Prockop D, Horwitz E (2006) Minimal criteria for defining multipotent mesenchymal stromal cells. The International Society for Cellular Therapy position statement. *Cytotherapy* **8:** 315-317

Dong YF, Soung do Y, Schwarz EM, O'Keefe RJ, Drissi H (2006) Wnt induction of chondrocyte hypertrophy through the Runx2 transcription factor. *J Cell Physiol* **208:** 77-86

Ducy P, Karsenty G (1995) Two distinct osteoblast-specific cis-acting elements control expression of a mouse osteocalcin gene. *Mol Cell Biol* **15:** 1858-1869

Ducy P, Zhang R, Geoffroy V, Ridall AL, Karsenty G (1997) Osf2/Cbfa1: a transcriptional activator of osteoblast differentiation. *Cell* **89:** 747-754

Eijken M, Meijer IM, Westbroek I, Koedam M, Chiba H, Uitterlinden AG, Pols HA, van Leeuwen JP (2008) Wnt signaling acts and is regulated in a human osteoblast differentiation dependent manner. *J Cell Biochem* **104:** 568-579

Eiselleova L, Peterkova I, Neradil J, Slaninova I, Hampl A, Dvorak P (2008) Comparative study of mouse and human feeder cells for human embryonic stem cells. *Int J Dev Biol* **52:** 353-363

Engler TA, Henry JR, Malhotra S, Cunningham B, Furness K, Brozinick J, Burkholder TP, Clay MP, Clayton J, Diefenbacher C, Hawkins E, Iversen PW, Li Y, Lindstrom TD, Marquart AL, McLean J, Mendel D, Misener E, Briere D, O'Toole JC, Porter WJ, Queener S, Reel JK, Owens RA, Brier RA, Eessalu TE, Wagner JR, Campbell RM, Vaughn R (2004) Substituted 3-imidazo[1,2-a]pyridin-3-yl- 4-(1,2,3,4-tetrahydro-[1,4]diazepino-[6,7,1-hi]indol-7-yl)pyrrole-2,5-diones as highly selective and potent inhibitors of glycogen synthase kinase-3. *J Med Chem* **47:** 3934-3937

Enomoto-Iwamoto M, Enomoto H, Komori T, Iwamoto M (2001) Participation of Cbfa1 in regulation of chondrocyte maturation. *Osteoarthritis Cartilage* **9 Suppl A:** S76-84

Etheridge SL, Spencer GJ, Heath DJ, Genever PG (2004) Expression profiling and functional analysis of wnt signaling mechanisms in mesenchymal stem cells. *Stem Cells* **22:** 849-860

Evans MJ, Kaufman MH (1981) Establishment in culture of pluripotential cells from mouse embryos. *Nature* **292:** 154-156

Fajas L, Schoonjans K, Gelman L, Kim JB, Najib J, Martin G, Fruchart JC, Briggs M, Spiegelman BM, Auwerx J (1999) Regulation of peroxisome proliferator-activated receptor gamma expression by adipocyte differentiation and determination factor 1/sterol regulatory element binding protein 1: implications for adipocyte differentiation and metabolism. *Mol Cell Biol* **19:** 5495-5503

Fei Y, Xiao L, Doetschman T, Coffin DJ, Hurley MM (2011) Fibroblast growth factor 2 stimulation of osteoblast differentiation and bone formation is mediated by modulation of the Wnt signaling pathway. *J Biol Chem* **286:** 40575-40583

Fischer L, Boland G, Tuan RS (2002) Wnt signaling during BMP-2 stimulation of mesenchymal chondrogenesis. *J Cell Biochem* **84:** 816-831

Fleming HE, Janzen V, Lo Celso C, Guo J, Leahy KM, Kronenberg HM, Scadden DT (2008) Wnt signaling in the niche enforces hematopoietic stem cell quiescence and is necessary to preserve self-renewal in vivo. *Cell Stem Cell* **2:** 274-283

Frank O, Heim M, Jakob M, Barbero A, Schäfer D, Bendik I, Dick W, Heberer M, Martin I (2002) Real-time quantitative RT-PCR analysis of human bone marrow stromal cells during osteogenic differentiation in vitro. *J Cell Biochem* **85:** 737-746

Freeman SD, Moore WM, Guiral EC, Holme AD, Turnbull JE, Pownall ME (2008) Extracellular regulation of developmental cell signaling by XtSulf1. *Dev Biol* **320:** 436-445

Freytag SO, Paielli DL, Gilbert JD (1994) Ectopic expression of the CCAAT/enhancer-binding protein alpha promotes the adipogenic program in a variety of mouse fibroblastic cells. *Genes Dev* **8:** 1654-1663

Friedenstein AJ, Chailakhjan RK, Lalykina KS (1970) The development of fibroblast colonies in monolayer cultures of guinea-pig bone marrow and spleen cells. *Cell Tissue Kinet* **3:** 393-403

Friedenstein AJ, Piatetzky S, II, Petrakova KV (1966) Osteogenesis in transplants of bone marrow cells. *J Embryol Exp Morphol* **16:** 381-390

Frith J, Genever P (2008) Transcriptional Control of Mesenchymal Stem Cell Differentiation. *Transfus Med Hemother* **35:** 216-227

Fu Y, Luo N, Klein RL, Garvey WT (2005) Adiponectin promotes adipocyte differentiation, insulin sensitivity, and lipid accumulation. *J Lipid Res* **46:** 1369-1379

Fukui Y, Masui S, Osada S, Umesono K, Motojima K (2000) A new thiazolidinedione, NC-2100, which is a weak PPAR-gamma activator, exhibits potent antidiabetic effects and induces uncoupling protein 1 in white adipose tissue of KKAy obese mice. *Diabetes* **49:** 759-767

Gambardella A, Nagaraju CK, O'Shea PJ, Mohanty ST, Kottam L, Pilling J, Sullivan M, Djerbi M, Koopmann W, Croucher PI, Bellantuono I (2011) Glycogen synthase kinase-3alpha/beta inhibition promotes in vivo amplification of endogenous mesenchymal progenitors with osteogenic and adipogenic potential and their differentiation to the osteogenic lineage. *J Bone Miner Res* **26:** 811-821

Gaur T, Lengner CJ, Hovhannisyan H, Bhat RA, Bodine PV, Komm BS, Javed A, van Wijnen AJ, Stein JL, Stein GS, Lian JB (2005) Canonical WNT signaling promotes osteogenesis by directly stimulating Runx2 gene expression. *J Biol Chem* **280:** 33132-33140

Gerdes J, Lemke H, Baisch H, Wacker HH, Schwab U, Stein H (1984) Cell cycle analysis of a cell proliferation-associated human nuclear antigen defined by the monoclonal antibody Ki-67. *J Immunol* **133:** 1710-1715

Ghannam S, Bouffi C, Djouad F, Jorgensen C, Noël D (2010) Immunosuppression by mesenchymal stem cells: mechanisms and clinical applications. *Stem Cell Res Ther* **1:** 2

Gijsbers L, Man HY, Kloet SK, de Haan LH, Keijer J, Rietjens IM, van der Burg B, Aarts JM (2011) Stable reporter cell lines for peroxisome proliferator-activated receptor γ (PPARγ)-mediated modulation of gene expression. *Anal Biochem* **414:** 77-83

Gitelman SE, Kirk M, Ye JQ, Filvaroff EH, Kahn AJ, Derynck R (1995) Vgr-1/BMP-6 induces osteoblastic differentiation of pluripotential mesenchymal cells. *Cell Growth Differ* **6:** 827-836

Gong Y, Slee RB, Fukai N, Rawadi G, Roman-Roman S, Reginato AM, Wang H, Cundy T, Glorieux FH, Lev D, Zacharin M, Oexle K, Marcelino J, Suwairi W, Heeger S, Sabatakos G, Apte S, Adkins WN, Allgrove J, Arslan-Kirchner M, Batch JA, Beighton P, Black GC, Boles RG, Boon LM, Borrone C, Brunner HG, Carle GF, Dallapiccola B, De Paepe A, Floege B, Halfhide ML, Hall B, Hennekam RC, Hirose T, Jans A, Juppner H, Kim CA, Keppler-Noreuil K, Kohlschuetter A, LaCombe D, Lambert M, Lemyre E, Letteboer T, Peltonen L, Ramesar RS, Romanengo M, Somer H, Steichen-Gersdorf E, Steinmann B, Sullivan B, Superti-Furga A, Swoboda W, van den Boogaard MJ, Van Hul W, Vikkula M, Votruba M, Zabel B, Garcia T, Baron R, Olsen BR, Warman ML (2001) LDL receptor-related protein 5 (LRP5) affects bone accrual and eye development. *Cell* **107:** 513-523

Gould TD, Einat H, O'Donnell KC, Picchini AM, Schloesser RJ, Manji HK (2007) Beta-catenin overexpression in the mouse brain phenocopies lithium-sensitive behaviors. *Neuropsychopharmacology* **32:** 2173-2183

Gregory CA, Perry AS, Reyes E, Conley A, Gunn WG, Prockop DJ (2005) Dkk-1-derived synthetic peptides and lithium chloride for the control and recovery of adult stem cells from bone marrow. *Journal of Biological Chemistry* **280:** 2309-2323

Gupta S, Takebe N, Lorusso P (2010) Targeting the Hedgehog pathway in cancer. *Ther Adv Med Oncol* **2:** 237-250

Hakki SS, Bozkurt SB, Hakki EE, Korkusuz P, Purali N, Koç N, Timucin M, Ozturk A, Korkusuz F (2012) Osteogenic differentiation of MC3T3-E1 cells on different titanium surfaces. *Biomed Mater* **7:** 045006

Harrison CA, Al-Musawi SL, Walton KL (2011) Prodomains regulate the synthesis, extracellular localisation and activity of TGF-β superfamily ligands. *Growth Factors* **29:** 174-186

Hassan MQ, Javed A, Morasso MI, Karlin J, Montecino M, van Wijnen AJ, Stein GS, Stein JL, Lian JB (2004) Dlx3 transcriptional regulation of osteoblast differentiation: temporal recruitment of Msx2, Dlx3, and Dlx5 homeodomain proteins to chromatin of the osteocalcin gene. *Mol Cell Biol* **24:** 9248-9261

He TC, Sparks AB, Rago C, Hermeking H, Zawel L, da Costa LT, Morin PJ, Vogelstein B, Kinzler KW (1998) Identification of c-MYC as a target of the APC pathway. *Science* **281**

Heath DJ, Chantry AD, Buckle CH, Coulton L, Shaughnessy JD, Evans HR, Snowden JA, Stover DR, Vanderkerken K, Croucher PI (2009) Inhibiting Dickkopf-1 (Dkk1) removes suppression of bone formation and prevents the development of osteolytic bone disease in multiple myeloma. *J Bone Miner Res* **24:** 425-436

Heo JS, Lee SY, Lee JC (2010) Wnt/beta-catenin signaling enhances osteoblastogenic differentiation from human periodontal ligament fibroblasts. *Molecules and Cells* **30:** 449-454

Hessle L, Johnson KA, Anderson HC, Narisawa S, Sali A, Goding JW, Terkeltaub R, Millan JL (2002) Tissue-nonspecific alkaline phosphatase and plasma cell membrane glycoprotein-1 are central antagonistic regulators of bone mineralization. *Proc Natl Acad Sci U S A* **99:** 9445-9449

Hijiya N, Setoguchi M, Matsuura K, Higuchi Y, Akizuki S, Yamamoto S (1994) Cloning and characterization of the human osteopontin gene and its promoter. *Biochem J* **303 (Pt 1):** 255-262

Hill CS (2009) Nucleocytoplasmic shuttling of Smad proteins. *Cell Res* **19:** 36-46

Hill TP, Spater D, Taketo MM, Birchmeier W, Hartmann C (2005) Canonical Wnt/beta-catenin signaling prevents osteoblasts from differentiating into chondrocytes. *Dev Cell* **8:** 727-738

Horwitz EM, Gordon PL, Koo WK, Marx JC, Neel MD, McNall RY, Muul L, Hofmann T (2002) Isolated allogeneic bone marrow-derived mesenchymal cells engraft and stimulate growth in children with osteogenesis imperfecta: Implications for cell therapy of bone. *Proc Natl Acad Sci U S A* **99:** 8932-8937

Horwitz EM, Le Blanc K, Dominici M, Mueller I, Slaper-Cortenbach I, Marini FC, Deans RJ, Krause DS, Keating A (2005) Clarification of the nomenclature for MSC: The International Society for Cellular Therapy position statement. *Cytotherapy* **7:** 393-395

Hu E, Tontonoz P, Spiegelman BM (1995) Transdifferentiation of myoblasts by the adipogenic transcription factors PPAR gamma and C/EBP alpha. *Proc Natl Acad Sci U S A* **92:** 9856-9860

Hu H, Hilton MJ, Tu X, Yu K, Ornitz DM, Long F (2005) Sequential roles of Hedgehog and Wnt signaling in osteoblast development. *Development* **132:** 49-60

Hu W, Ye Y, Zhang W, Wang J, Chen A, Guo F (2013) miR‐142‐3p promotes osteoblast differentiation by modulating Wnt signaling. *Mol Med Report* **7:** 689-693

Ikeda T, Kamekura S, Mabuchi A, Kou I, Seki S, Takato T, Nakamura K, Kawaguchi H, Ikegawa S, Chung UI (2004) The combination of SOX5, SOX6, and SOX9 (the SOX trio) provides signals sufficient for induction of permanent cartilage. *Arthritis Rheum* **50:** 3561-3573

Im GI, Lee JM, Kim HJ Wnt inhibitors enhance chondrogenesis of human mesenchymal stem cells in a long-term pellet culture. *Biotechnol Lett* **33:** 1061-1068

Jackson A, Vayssiere B, Garcia T, Newell W, Baron R, Roman-Roman S, Rawadi G (2005) Gene array analysis of Wnt-regulated genes in C3H10T1/2 cells. *Bone* **36:** 585-598

Jaiswal N, Haynesworth SE, Caplan AI, Bruder SP (1997) Osteogenic differentiation of purified, culture-expanded human mesenchymal stem cells in vitro. *J Cell Biochem* **64:** 295-312

Janda CY, Waghray D, Levin AM, Thomas C, Garcia KC (2012) Structural basis of Wnt recognition by Frizzled. *Science* **337:** 59-64

Jawad MU, Fritton KE, Ma T, Ren PG, Goodman SB, Ke HZ, Babij P, Genovese MC (2013) Effects of sclerostin antibody on healing of a non-critical size femoral bone defect. *J Orthop Res* **31:** 155-163

Jia J, Amanai K, Wang G, Tang J, Wang B, Jiang J (2002) Shaggy/GSK3 antagonizes Hedgehog signalling by regulating Cubitus interruptus. *Nature* **416:** 548-552

Jiang Y, Jahagirdar BN, Reinhardt RL, Schwartz RE, Keene CD, Ortiz-Gonzalez XR, Reyes M, Lenvik T, Lund T, Blackstad M, Du J, Aldrich S, Lisberg A, Low WC, Largaespada DA, Verfaillie CM (2002) Pluripotency of mesenchymal stem cells derived from adult marrow. *Nature* **418:** 41-49

Jin EJ, Lee SY, Choi YA, Jung JC, Bang OS, Kang SS (2006) BMP-2-enhanced chondrogenesis involves p38 MAPK-mediated down-regulation of Wnt-7a pathway. *Mol Cells* **22:** 353-359

Kahler RA, Galindo M, Lian J, Stein GS, van Wijnen AJ, Westendorf JJ (2006) Lymphocyte enhancer-binding factor 1 (Lef1) inhibits terminal differentiation of osteoblasts. *J Cell Biochem* **97:** 969-983

Kahler RA, Westendorf JJ (2003) Lymphoid enhancer factor-1 and beta-catenin inhibit Runx2-dependent transcriptional activation of the osteocalcin promoter. *J Biol Chem* **278:** 11937-11944

Kang S, Bennett CN, Gerin I, Rapp LA, Hankenson KD, MacDougald OA (2007) Wnt signaling stimulates osteoblastogenesis of mesenchymal precursors by suppressing CCAAT/enhancer-binding protein alpha and peroxisome proliferator-activated receptor gamma. *Journal of Biological Chemistry* **282:** 14515-14524

Kavsak P, Rasmussen RK, Causing CG, Bonni S, Zhu H, Thomsen GH, Wrana JL (2000) Smad7 binds to Smurf2 to form an E3 ubiquitin ligase that targets the TGF beta receptor for degradation. *Mol Cell* **6:** 1365-1375

Kaytor MD, Orr HT (2002) The GSK3 beta signaling cascade and neurodegenerative disease. *Curr Opin Neurobiol* **12:** 275-278

Keller G, Snodgrass HR (1999) Human embryonic stem cells: The future is now. *Nature Medicine* **5:** 151-152

Kern S, Eichler H, Stoeve J, Klüter H, Bieback K (2006) Comparative analysis of mesenchymal stem cells from bone marrow, umbilical cord blood, or adipose tissue. *Stem Cells* **24:** 1294-1301

Kim IS, Otto F, Zabel B, Mundlos S (1999) Regulation of chondrocyte differentiation by Cbfa1. *Mech Dev* **80:** 159-170

Kim JB, Spiegelman BM (1996) ADD1/SREBP1 promotes adipocyte differentiation and gene expression linked to fatty acid metabolism. *Genes Dev* **10:** 1096-1107

Kim K, Doi A, Wen B, Ng K, Zhao R, Cahan P, Kim J, Aryee MJ, Ji H, Ehrlich LI, Yabuuchi A, Takeuchi A, Cunniff KC, Hongguang H, McKinney-Freeman S, Naveiras O, Yoon TJ, Irizarry RA, Jung N, Seita J, Hanna J, Murakami P, Jaenisch R, Weissleder R, Orkin SH, Weissman IL, Feinberg AP, Daley GQ (2010) Epigenetic memory in induced pluripotent stem cells. *Nature* **467:** 285-290

Kim KI, Cho HJ, Hahn JY, Kim TY, Park KW, Koo BK, Shin CS, Kim CH, Oh BH, Lee MM, Park YB, Kim HS (2006) Beta-catenin overexpression augments angiogenesis and skeletal muscle regeneration through dual mechanism of vascular endothelial growth factor-mediated endothelial cell proliferation and progenitor cell mobilization. *Arterioscler Thromb Vasc Biol* **26:** 91-98

Kitagawa M, Hatakeyama S, Shirane M, Matsumoto M, Ishida N, Hattori K, Nakamichi I, Kikuchi A, Nakayama K (1999) An F-box protein, FWD1, mediates ubiquitin-dependent proteolysis of beta-catenin. *EMBO J* **18:** 2401-2410

Koga T, Matsui Y, Asagiri M, Kodama T, de Crombrugghe B, Nakashima K, Takayanagi H (2005) NFAT and Osterix cooperatively regulate bone formation. *Nat Med* **11:** 880-885

Komori T, Yagi H, Nomura S, Yamaguchi A, Sasaki K, Deguchi K, Shimizu Y, Bronson RT, Gao YH, Inada M, Sato M, Okamoto R, Kitamura Y, Yoshiki S, Kishimoto T (1997) Targeted disruption of Cbfa1 results in a complete lack of bone formation owing to maturational arrest of osteoblasts. *Cell* **89:** 755-764

Krause U, Harris S, Green A, Ylostalo J, Zeitouni S, Lee N, Gregory CA (2010) Pharmaceutical modulation of canonical Wnt signaling in multipotent stromal cells for improved osteoinductive therapy. *Proc Natl Acad Sci U S A* **107:** 4147-4152

Krishnan V, Bryant HU, Macdougald OA (2006) Regulation of bone mass by Wnt signaling. *J Clin Invest* **116:** 1202-1209

Kuhl M, Pandur P (2008) Dorsal axis duplication as a functional readout for Wnt activity. *Methods Mol Biol* **469:** 467-476

Kulkarni NH, Onyia JE, Zeng Q, Tian X, Liu M, Halladay DL, Frolik CA, Engler T, Wei T, Kriauciunas A, Martin TJ, Sato M, Bryant HU, Ma YL (2006) Orally bioavailable GSK-3alpha/beta dual inhibitor increases markers of cellular differentiation in vitro and bone mass in vivo. *J Bone Miner Res* **21:** 910-920

Kulkarni NH, Wei T, Kumar A, Dow ER, Stewart TR, Shou J, N'cho M, Sterchi DL, Gitter BD, Higgs RE, Halladay DL, Engler TA, Martin TJ, Bryant HU, Ma YL, Onyia JE (2007) Changes in osteoblast, chondrocyte, and adipocyte lineages mediate the bone anabolic actions of PTH and small molecule GSK-3 inhibitor. *J Cell Biochem* **102:** 1504-1518

Kurata H, Guillot PV, Chan J, Fisk NM (2007) Osterix induces osteogenic gene expression but not differentiation in primary human fetal mesenchymal stem cells. *Tissue Eng* **13:** 1513-1523

Lanzendorf SE, Boyd CA, Wright DL, Muasher S, Oehninger S, Hodgen GD (2001) Use of human gametes obtained from anonymous donors for the production of human embryonic stem cell lines. *Fertility and Sterility* **76:** 132-137

Lee KS, Kim HJ, Li QL, Chi XZ, Ueta C, Komori T, Wozney JM, Kim EG, Choi JY, Ryoo HM, Bae SC (2000) Runx2 is a common target of transforming growth factor beta1 and bone morphogenetic protein 2, and cooperation between Runx2 and Smad5 induces osteoblast-specific gene expression in the pluripotent mesenchymal precursor cell line C2C12. *Mol Cell Biol* **20:** 8783-8792

Lee MH, Kim YJ, Kim HJ, Park HD, Kang AR, Kyung HM, Sung JH, Wozney JM, Ryoo HM (2003a) BMP-2-induced Runx2 expression is mediated by Dlx5, and TGF-beta 1 opposes the BMP-2-induced osteoblast differentiation by suppression of Dlx5 expression. *J Biol Chem* **278:** 34387-34394

Lee MH, Kwon TG, Park HS, Wozney JM, Ryoo HM (2003b) BMP-2-induced Osterix expression is mediated by Dlx5 but is independent of Runx2. *Biochem Biophys Res Commun* **309:** 689-694

Lefebvre V, Behringer RR, de Crombrugghe B (2001) L-Sox5, Sox6 and Sox9 control essential steps of the chondrocyte differentiation pathway. *Osteoarthritis Cartilage* **9 Suppl A:** S69-75

Lengner CJ, Hassan MQ, Serra RW, Lepper C, van Wijnen AJ, Stein JL, Lian JB, Stein GS (2005) Nkx3.2-mediated repression of Runx2 promotes chondrogenic differentiation. *J Biol Chem* **280:** 15872-15879

Levy L, Howell M, Das D, Harkin S, Episkopou V, Hill CS (2007) Arkadia activates Smad3/Smad4-dependent transcription by triggering signal-induced SnoN degradation. *Mol Cell Biol* **27:** 6068-6083

Li FQ, Singh AM, Mofunanya A, Love D, Terada N, Moon RT, Takemaru K (2007) Chibby promotes adipocyte differentiation through inhibition of beta-catenin signaling. *Mol Cell Biol* **27:** 4347-4354

Li H, Yu B, Zhang Y, Pan Z, Xu W (2006) Jagged1 protein enhances the differentiation of mesenchymal stem cells into cardiomyocytes. *Biochem Biophys Res Commun* **341:** 320-325

Li VS, Ng SS, Boersema PJ, Low TY, Karthaus WR, Gerlach JP, Mohammed S, Heck AJ, Maurice MM, Mahmoudi T, Clevers H (2012) Wnt signaling through inhibition of β-catenin degradation in an intact Axin1 complex. *Cell* **149:** 1245-1256

Li XF, Liu P, Liu WZ, Maye P, Zhang JH, Zhang YH, Hurley M, Guo CY, Boskey A, Sun L, Harris SE, Rowe DW, Ke HZ, Wu DQ (2005) Dkk2 has a role in terminal osteoblast differentiation and mineralized matrix formation. *Nature Genetics* **37:** 945-952

Lin FT, Lane MD (1992) Antisense CCAAT/enhancer-binding protein RNA suppresses coordinate gene expression and triglyceride accumulation during differentiation of 3T3-L1 preadipocytes. *Genes Dev* **6:** 533-544

Linhart HG, Ishimura-Oka K, DeMayo F, Kibe T, Repka D, Poindexter B, Bick RJ, Darlington GJ (2001) C/EBPalpha is required for differentiation of white, but not brown, adipose tissue. *Proc Natl Acad Sci U S A* **98:** 12532-12537

Lissenberg-Thunnissen SN, de Gorter DJ, Sier CF, Schipper IB (2011) Use and efficacy of bone morphogenetic proteins in fracture healing. *Int Orthop* **35:** 1271-1280

Liu C, Li Y, Semenov M, Han C, Baeg GH, Tan Y, Zhang Z, Lin X, He X (2002) Control of beta-catenin phosphorylation/degradation by a dual-kinase mechanism. *Cell* **108:** 837-847

Liu G, Vijayakumar S, Grumolato L, Arroyave R, Qiao H, Akiri G, Aaronson SA (2009) Canonical Wnts function as potent regulators of osteogenesis by human mesenchymal stem cells. *J Cell Biol* **185:** 67-75

Liu L, Nam S, Tian Y, Yang F, Wu J, Wang Y, Scuto A, Polychronopoulos P, Magiatis P, Skaltsounis L, Jove R (2011) 6-Bromoindirubin-3'-oxime inhibits JAK/STAT3 signaling and induces apoptosis of human melanoma cells. *Cancer Res* **71:** 3972-3979

Livak KJ, Schmittgen TD (2001) Analysis of relative gene expression data using real-time quantitative PCR and the 2(-Delta Delta C(T)) Method. *Methods* **25:** 402-408

Locatelli F, Corti S, Donadoni C, Guglieri M, Capra F, Strazzer S, Salani S, Del Bo R, Fortunato F, Bordoni A, Comi GP (2003) Neuronal differentiation of murine bone marrow Thy-1-and Sca-1-positive cells. *Journal of Hematotherapy & Stem Cell Research* **12:** 727-734

Long F, Chung UI, Ohba S, McMahon J, Kronenberg HM, McMahon AP (2004) Ihh signaling is directly required for the osteoblast lineage in the endochondral skeleton. *Development* **131:** 1309-1318

Luciani A, Villella VR, Esposito S, Brunetti-Pierri N, Medina D, Settembre C, Gavina M, Pulze L, Giardino I, Pettoello-Mantovani M, D'Apolito M, Guido S, Masliah E, Spencer B, Quaratino S, Raia V, Ballabio A, Maiuri L (2010) Defective CFTR induces aggresome formation and lung inflammation in cystic fibrosis through ROS-mediated autophagy inhibition. *Nat Cell Biol* **12:** 863-875

Lutz M, Knaus P (2002) Integration of the TGF-beta pathway into the cellular signalling network. *Cell Signal* **14:** 977-988

Majumdar MK, Wang E, Morris EA (2001) BMP-2 and BMP-9 promotes chondrogenic differentiation of human multipotential mesenchymal cells and overcomes the inhibitory effect of IL-1. *J Cell Physiol* **189:** 275-284

Mao J, Wang J, Liu B, Pan W, Farr GH, Flynn C, Yuan H, Takada S, Kimelman D, Li L, Wu D (2001) Low-density lipoprotein receptor-related protein-5 binds to Axin and regulates the canonical Wnt signaling pathway. *Mol Cell* **7:** 801-809

Marie PJ (2008) Transcription factors controlling osteoblastogenesis. *Arch Biochem Biophys* **473:** 98-105

Marsell R, Sisask G, Nilsson Y, Sundgren-Andersson AK, Andersson U, Larsson S, Nilsson O, Ljunggren O, Jonsson KB (2012) GSK-3 inhibition by an orally active small molecule increases bone mass in rats. *Bone* **50:** 619-627

Martin GR (1981) Isolation of a pluripotent cell line from early mouse embryos cultured in medium conditioned by teratocarcinoma stem cells. *Proc Natl Acad Sci U S A* **78:** 7634-7638

Meijer L, Skaltsounis AL, Magiatis P, Polychronopoulos P, Knockaert M, Leost M, Ryan XP, Vonica CA, Brivanlou A, Dajani R, Crovace C, Tarricone C, Musacchio A, Roe SM, Pearl L, Greengard P (2003) GSK-3-selective inhibitors derived from Tyrian purple indirubins. *Chem Biol* **10:** 1255-1266

Mikels AJ, Nusse R (2006) Wnts as ligands: processing, secretion and reception. *Oncogene* **25:** 7461-7468

Minguell JJ, Erices A, Conget P (2001) Mesenchymal stem cells. *Exp Biol Med (Maywood)* **226:** 507-520

Moldes M, Boizard M, Liepvre XL, Feve B, Dugail I, Pairault J (1999) Functional antagonism between inhibitor of DNA binding (Id) and adipocyte determination and differentiation factor 1/sterol regulatory element-binding protein-1c (ADD1/SREBP-1c) trans-factors for the regulation of fatty acid synthase promoter in adipocytes. *Biochem J* **344 Pt 3:** 873-880

Molenaar M, van de Wetering M, Oosterwegel M, Peterson-Maduro J, Godsave S, Korinek V, Roose J, Destrée O, Clevers H (1996) XTcf-3 transcription factor mediates beta-catenin-induced axis formation in Xenopus embryos. *Cell* **86:** 391-399

Moustakas A, Heldin CH (2009) The regulation of TGFbeta signal transduction. *Development* **136:** 3699-3714

Mueller E, Drori S, Aiyer A, Yie J, Sarraf P, Chen H, Hauser S, Rosen ED, Ge K, Roeder RG, Spiegelman BM (2002) Genetic analysis of adipogenesis through peroxisome proliferator-activated receptor gamma isoforms. *J Biol Chem* **277:** 41925-41930

Muraglia A, Cancedda R, Quarto R (2000) Clonal mesenchymal progenitors from human bone marrow differentiate in vitro according to a hierarchical model. *J Cell Sci* **113 (Pt 7):** 1161-1166

Muramatsu S, Wakabayashi M, Ohno T, Amano K, Ooishi R, Sugahara T, Shiojiri S, Tashiro K, Suzuki Y, Nishimura R, Kuhara S, Sugano S, Yoneda T, Matsuda A (2007) Functional gene screening system identified TRPV4 as a regulator of chondrogenic differentiation. *J Biol Chem* **282:** 32158-32167

Murtaugh LC, Zeng L, Chyung JH, Lassar AB (2001) The chick transcriptional repressor Nkx3.2 acts downstream of Shh to promote BMP-dependent axial chondrogenesis. *Dev Cell* **1:** 411-422

Myster DL, Duronio RJ (2000) To differentiate or not to differentiate? *Curr Biol* **10:** R302-304

Nakahara T, Sato H, Shimizu T, Tanaka T, Matsui H, Kawai-Kowase K, Sato M, Iso T, Arai M, Kurabayashi M (2010) Fibroblast growth factor-2 induces osteogenic differentiation through a Runx2 activation in vascular smooth muscle cells. *Biochem Biophys Res Commun* **394:** 243-248

Nakashima K, Zhou X, Kunkel G, Zhang Z, Deng JM, Behringer RR, de Crombrugghe B (2002) The novel zinc finger-containing transcription factor osterix is required for osteoblast differentiation and bone formation. *Cell* **108:** 17-29

Nieuwkoop PD, Faber J (1994) Normal table of *Xenopus laevis*. *Garland Publishing, New York*

Niwa H, Ogawa K, Shimosato D, Adachi K (2009) A parallel circuit of LIF signalling pathways maintains pluripotency of mouse ES cells. *Nature* **460:** 118-122

O'Shea PJ, Kim DW, Logan JG, Davis S, Walker RL, Meltzer PS, Cheng SY, Williams GR (2012) Advanced bone formation in mice with a dominant-negative mutation in the thyroid hormone receptor β gene due to activation of Wnt/β-catenin protein signaling. *J Biol Chem* **287:** 17812-17822

Okamura M, Kudo H, Wakabayashi K, Tanaka T, Nonaka A, Uchida A, Tsutsumi S, Sakakibara I, Naito M, Osborne TF, Hamakubo T, Ito S, Aburatani H, Yanagisawa M, Kodama T, Sakai J (2009) COUP-TFII acts downstream of Wnt/beta-catenin signal to silence PPARgamma gene expression and repress adipogenesis. *Proc Natl Acad Sci U S A* **106:** 5819-5824

Pecina M, Giltaij LR, Vukicevic S (2001) Orthopaedic applications of osteogenic protein-1 (BMP-7). *Int Orthop* **25:** 203-208

Pelttari K, Steck E, Richter W (2008) The use of mesenchymal stem cells for chondrogenesis. *Injury* **39 Suppl 1:** S58-65

Phillips JE, Gersbach CA, Wojtowicz AM, Garcia AJ (2006) Glucocorticoid-induced osteogenesis is negatively regulated by Runx2/Cbfa1 serine phosphorylation. *J Cell Sci* **119:** 581-591

Phinney DG, Kopen G, Righter W, Webster S, Tremain N, Prockop DJ (1999) Donor variation in the growth properties and osteogenic potential of human marrow stromal cells. *J Cell Biochem* **75:** 424-436

Pittenger MF, Mackay AM, Beck SC, Jaiswal RK, Douglas R, Mosca JD, Moorman MA, Simonetti DW, Craig S, Marshak DR (1999) Multilineage potential of adult human mesenchymal stem cells. *Science* **284:** 143-147

Plutzky J (1999) Atherosclerotic plaque rupture: emerging insights and opportunities. *Am J Cardiol* **84:** 15J-20J

Polakis P (2012) Wnt signaling in cancer. *Cold Spring Harb Perspect Biol* **4**

Prestwich TC, Macdougald OA (2007) Wnt/beta-catenin signaling in adipogenesis and metabolism. *Curr Opin Cell Biol* **19:** 612-617

Quarto N, Behr B, Longaker MT (2010) Opposite spectrum of activity of canonical Wnt signaling in the osteogenic context of undifferentiated and differentiated mesenchymal cells: implications for tissue engineering. *Tissue Eng Part A* **16:** 3185-3197

Quirici N, Soligo D, Bossolasco P, Servida F, Lumini C, Deliliers GL (2002) Isolation of bone marrow mesenchymal stem cells by anti-nerve growth factor receptor antibodies. *Experimental Hematology* **30:** 783-791

Raff M (2003) Adult stem cell plasticity: fact or artifact? *Annu Rev Cell Dev Biol* **19:** 1-22

Rangappa S, Entwistle JW, Wechsler AS, Kresh JY (2003) Cardiomyocyte-mediated contact programs human mesenchymal stem cells to express cardiogenic phenotype. *J Thorac Cardiovasc Surg* **126:** 124-132

Ring DB, Johnson KW, Henriksen EJ, Nuss JM, Goff D, Kinnick TR, Ma ST, Reeder JW, Samuels I, Slabiak T, Wagman AS, Hammond ME, Harrison SD (2003) Selective glycogen synthase kinase 3 inhibitors potentiate insulin activation of glucose transport and utilization in vitro and in vivo. *Diabetes* **52:** 588-595

Robledo RF, Rajan L, Li X, Lufkin T (2002) The Dlx5 and Dlx6 homeobox genes are essential for craniofacial, axial, and appendicular skeletal development. *Genes Dev* **16:** 1089-1101

Rosen ED, Hsu CH, Wang X, Sakai S, Freeman MW, Gonzalez FJ, Spiegelman BM (2002) C/EBPalpha induces adipogenesis through PPARgamma: a unified pathway. *Genes Dev* **16:** 22-26

Rosen ED, Sarraf P, Troy AE, Bradwin G, Moore K, Milstone DS, Spiegelman BM, Mortensen RM (1999) PPAR gamma is required for the differentiation of adipose tissue in vivo and in vitro. *Mol Cell* **4:** 611-617

Rossert JA, Chen SS, Eberspaecher H, Smith CN, de Crombrugghe B (1996) Identification of a minimal sequence of the mouse pro-alpha 1(I) collagen promoter that confers high-level osteoblast expression in transgenic mice and that binds a protein selectively present in osteoblasts. *Proc Natl Acad Sci U S A* **93:** 1027-1031

Saito T, Ikeda T, Nakamura K, Chung UI, Kawaguchi H (2007) S100A1 and S100B, transcriptional targets of SOX trio, inhibit terminal differentiation of chondrocytes. *EMBO Rep* **8:** 504-509

Sakaguchi Y, Sekiya I, Yagishita K, Muneta T (2005) Comparison of human stem cells derived from various mesenchymal tissues: superiority of synovium as a cell source. *Arthritis Rheum* **52:** 2521-2529

Salem HK, Thiemermann C (2010) Mesenchymal stromal cells: current understanding and clinical status. *Stem Cells* **28:** 585-596

Sampath TK, Maliakal JC, Hauschka PV, Jones WK, Sasak H, Tucker RF, White KH, Coughlin JE, Tucker MM, Pang RH, et al. (1992) Recombinant human osteogenic protein-1 (hOP-1) induces new bone formation in vivo with a specific activity comparable with natural bovine osteogenic protein and stimulates osteoblast proliferation and differentiation in vitro. *J Biol Chem* **267:** 20352-20362

Samulin J, Berget I, Lien S, Sundvold H (2008) Differential gene expression of fatty acid binding proteins during porcine adipogenesis. *Comp Biochem Physiol B Biochem Mol Biol* **151:** 147-152

Sarugaser R, Hanoun L, Keating A, Stanford WL, Davies JE (2009) Human mesenchymal stem cells self-renew and differentiate according to a deterministic hierarchy. *PLoS One* **4:** e6498

Sasai Y, Lu B, Steinbeisser H, Geissert D, Gont LK, De Robertis EM (1994) Xenopus chordin: a novel dorsalizing factor activated by organizer-specific homeobox genes. *Cell* **79:** 779-790

Sasaki H, Hui C, Nakafuku M, Kondoh H (1997) A binding site for Gli proteins is essential for HNF-3beta floor plate enhancer activity in transgenics and can respond to Shh in vitro. *Development* **124:** 1313-1322

Semba I, Nonaka K, Takahashi I, Takahashi K, Dashner R, Shum L, Nuckolls GH, Slavkin HC (2000) Positionally-dependent chondrogenesis induced by BMP4 is co-regulated by Sox9 and Msx2. *Dev Dyn* **217:** 401-414

Semenov MV, He X (2006) LRP5 mutations linked to high bone mass diseases cause reduced LRP5 binding and inhibition by SOST. *J Biol Chem* **281:** 38276-38284

Semënov M, Tamai K, He X (2005) SOST is a ligand for LRP5/LRP6 and a Wnt signaling inhibitor. *J Biol Chem* **280:** 26770-26775

Shand J, Berg J, Bogue C (2012) Human Embryonic Stem Cell (hESC) and Human Embryo Research. *Pediatrics* **130:** 972-977

Shi CM, Zhu Y, Su YP, Cheng TM (2006) Stem cells and their applications in skin-cell therapy. *Trends in Biotechnology* **24:** 48-52

Shi Y, Wang YF, Jayaraman L, Yang H, Massagué J, Pavletich NP (1998) Crystal structure of a Smad MH1 domain bound to DNA: insights on DNA binding in TGF-beta signaling. *Cell* **94:** 585-594

Shtutman M, Zhurinsky J, Simcha I, Albanese C, D'Amico M, Pestell R, Ben-Ze'ev A (1999) The cyclin D1 gene is a target of the beta-catenin/LEF-1 pathway. *Proceedings of the National Academy of Sciences of the United States of America* **96:** 5522-5527

Shui C, Spelsberg TC, Riggs BL, Khosla S (2003) Changes in Runx2/Cbfa1 expression and activity during osteoblastic differentiation of human bone marrow stromal cells. *J Bone Miner Res* **18:** 213-221

Siddappa R, Licht R, van Blitterswijk C, de Boer J (2007) Donor variation and loss of multipotency during in vitro expansion of human mesenchymal stem cells for bone tissue engineering. *J Orthop Res* **25:** 1029-1041

Sinha KM, Yasuda H, Coombes MM, Dent SY, de Crombrugghe B (2010) Regulation of the osteoblast-specific transcription factor Osterix by NO66, a Jumonji family histone demethylase. *EMBO J* **29:** 68-79

Sisask G, Marsell R, Sundgren-Andersson A, Larsson S, Nilsson O, Ljunggren O, Jonsson KB (2013) Rats treated with AZD2858, a GSK3 inhibitor, heal fractures rapidly without endochondral bone formation. *Bone* **54:** 126-132

Smits P, Li P, Mandel J, Zhang Z, Deng JM, Behringer RR, de Crombrugghe B, Lefebvre V (2001) The transcription factors L-Sox5 and Sox6 are essential for cartilage formation. *Dev Cell* **1:** 277-290

Sokol S, Christian JL, Moon RT, Melton DA (1991) Injected Wnt RNA induces a complete body axis in Xenopus embryos. *Cell* **67:** 741-752

Sordi V, Malosio ML, Marchesi F, Mercalli A, Melzi R, Giordano T, Belmonte N, Ferrari G, Leone BE, Bertuzzi F, Zerbini G, Allavena P, Bonifacio E, Piemonti L (2005) Bone marrow mesenchymal stem cells express a restricted set of functionally

active chemokine receptors capable of promoting migration to pancreatic islets. *Blood* **106:** 419-427

Southwood LL, Frisbie DD, Kawcak CE, Ghivizzani SC, Evans CH, McIlwraith CW (2004) Evaluation of Ad-BMP-2 for enhancing fracture healing in an infected defect fracture rabbit model. *J Orthop Res* **22:** 66-72

Spangrude GJ, Heimfeld S, Weissman IL (1988) Purification and characterization of mouse hematopoietic stem cells. *Science* **241:** 58-62

Spemann H. MH (1924) Induction of embryonic primordia by implantation of organizers from a different species. *Roux's Arch Entw Mech* **100:** 599–638

Spencer GJ, Utting JC, Etheridge SL, Arnett TR, Genever PG (2006) Wnt signalling in osteoblasts regulates expression of the receptor activator of NFkappaB ligand and inhibits osteoclastogenesis in vitro. *J Cell Sci* **119:** 1283-1296

St-Jacques B, Hammerschmidt M, McMahon AP (1999) Indian hedgehog signaling regulates proliferation and differentiation of chondrocytes and is essential for bone formation. *Genes Dev* **13:** 2072-2086

Strecker S, Fu Y, Liu Y, Maye P (2012) Generation and characterization of osterix-cherry reporter mice. *Genesis*

Suda Y, Suzuki M, Ikawa Y, Aizawa S (1987) Mouse embryonic stem cells exhibit indefinite proliferative potential. *J Cell Physiol* **133:** 197-201

Sugioka K, Mizumoto K, Sawa H (2011) Wnt regulates spindle asymmetry to generate asymmetric nuclear β-catenin in C. elegans. *Cell* **146:** 942-954

Suzuki A, Thies RS, Yamaji N, Song JJ, Wozney JM, Murakami K, Ueno N (1994) A truncated bone morphogenetic protein receptor affects dorsal-ventral patterning in the early Xenopus embryo. *Proc Natl Acad Sci U S A* **91:** 10255-10259

Tadic T, Dodig M, Erceg I, Marijanovic I, Mina M, Kalajzic Z, Velonis D, Kronenberg MS, Kosher RA, Ferrari D, Lichtler AC (2002) Overexpression of Dlx5 in chicken calvarial cells accelerates osteoblastic differentiation. *J Bone Miner Res* **17:** 1008-1014

Taipale J, Cooper MK, Maiti T, Beachy PA (2002) Patched acts catalytically to suppress the activity of Smoothened. *Nature* **418:** 892-897

Takahashi K, Tanabe K, Ohnuki M, Narita M, Ichisaka T, Tomoda K, Yamanaka S (2007) Induction of pluripotent stem cells from adult human fibroblasts by defined factors. *Cell* **131:** 861-872

Takahashi K, Yamanaka S (2006) Induction of pluripotent stem cells from mouse embryonic and adult fibroblast cultures by defined factors. *Cell* **126:** 663-676

Takahashi S, Yokota C, Takano K, Tanegashima K, Onuma Y, Goto J, Asashima M (2000) Two novel nodal-related genes initiate early inductive events in Xenopus Nieuwkoop center. *Development* **127:** 5319-5329

Takahashi T (2011) Overexpression of Runx2 and MKP-1 stimulates transdifferentiation of 3T3-L1 preadipocytes into bone-forming osteoblasts in vitro. *Calcif Tissue Int* **88:** 336-347

Tang N, Song WX, Luo J, Luo X, Chen J, Sharff KA, Bi Y, He BC, Huang JY, Zhu GH, Su YX, Jiang W, Tang M, He Y, Wang Y, Chen L, Zuo GW, Shen J, Pan X, Reid RR, Luu HH, Haydon RC, He TC (2009) BMP-9-induced osteogenic differentiation of mesenchymal progenitors requires functional canonical Wnt/beta-catenin signalling. *J Cell Mol Med* **13:** 2448-2464

Tang QQ, Lane MD (2000) Role of C/EBP homologous protein (CHOP-10) in the programmed activation of CCAAT/enhancer-binding protein-beta during adipogenesis. *Proc Natl Acad Sci U S A* **97:** 12446-12450

Tang QQ, Otto TC, Lane MD (2003a) CCAAT/enhancer-binding protein beta is required for mitotic clonal expansion during adipogenesis. *Proc Natl Acad Sci U S A* **100:** 850-855

Tang QQ, Otto TC, Lane MD (2003b) Mitotic clonal expansion: a synchronous process required for adipogenesis. *Proc Natl Acad Sci U S A* **100:** 44-49

Thiagarajah JR, Zhao D, Verkman AS (2007) Impaired enterocyte proliferation in aquaporin-3 deficiency in mouse models of colitis. *Gut* **56**

Thomson JA, Itskovitz-Eldor J, Shapiro SS, Waknitz MA, Swiergiel JJ, Marshall VS, Jones JM (1998) Embryonic stem cell lines derived from human blastocysts. *Science* **282:** 1145-1147

Till JE, McCulloch EA (1961) A direct measurement of the radiation sensitivity of normal mouse bone marrow cells. *Radiat Res* **14:** 213-222

Tindall AJ, Pownall ME, Morris ID, Isaacs HV (2005) Xenopus tropicalis peroxidasin gene is expressed within the developing neural tube and pronephric kidney. *Dev Dyn* **232:** 377-384

Tominaga H, Maeda S, Miyoshi H, Miyazono K, Komiya S, Imamura T (2009) Expression of osterix inhibits bone morphogenetic protein-induced chondrogenic differentiation of mesenchymal progenitor cells. *J Bone Miner Metab* **27:** 36-45

Tong Q, Dalgin G, Xu H, Ting CN, Leiden JM, Hotamisligil GS (2000) Function of GATA transcription factors in preadipocyte-adipocyte transition. *Science* **290:** 134-138

Tong Q, Tsai J, Tan G, Dalgin G, Hotamisligil GS (2005) Interaction between GATA and the C/EBP family of transcription factors is critical in GATA-mediated suppression of adipocyte differentiation. *Mol Cell Biol* **25:** 706-715

Tontonoz P, Hu E, Graves RA, Budavari AI, Spiegelman BM (1994) mPPAR gamma 2: tissue-specific regulator of an adipocyte enhancer. *Genes Dev* **8:** 1224-1234

Tropel P, Platet N, Platel JC, Noël D, Albrieux M, Benabid AL, Berger F (2006) Functional neuronal differentiation of bone marrow-derived mesenchymal stem cells. *Stem Cells* **24:** 2868-2876

Tu Q, Valverde P, Chen J (2006) Osterix enhances proliferation and osteogenic potential of bone marrow stromal cells. *Biochem Biophys Res Commun* **341:** 1257-1265

Valcourt U, Moustakas A (2005) BMP Signaling in Osteogenesis, Bone Remodeling and Repair. *European Journal of Trauma* **31:** 464-479

van de Wetering M, Cavallo R, Dooijes D, van Beest M, van Es J, Loureiro J, Ypma A, Hursh D, Jones T, Bejsovec A, Peifer M, Mortin M, Clevers H (1997) Armadillo coactivates transcription driven by the product of the Drosophila segment polarity gene dTCF. *Cell* **88:** 789-799

Varjosalo M, Taipale J (2007) Hedgehog signaling. *J Cell Sci* **120:** 3-6

Vestergaard P, Rejnmark L, Mosekilde L (2005) Reduced relative risk of fractures among users of lithium. *Calcif Tissue Int* **77:** 1-8

Vortkamp A, Lee K, Lanske B, Segre GV, Kronenberg HM, Tabin CJ (1996) Regulation of rate of cartilage differentiation by Indian hedgehog and PTH-related protein. *Science* **273:** 613-622

Wagers AJ, Weissman IL (2004) Plasticity of adult stem cells. *Cell* **116:** 639-648

Wakitani S, Imoto K, Yamamoto T, Saito M, Murata N, Yoneda M (2002) Human autologous culture expanded bone marrow mesenchymal cell transplantation for repair of cartilage defects in osteoarthritic knees. *Osteoarthritis Cartilage* **10:** 199-206

Walsh S, Jordan GR, Jefferiss C, Stewart K, Beresford JN (2001) High concentrations of dexamethasone suppress the proliferation but not the differentiation or further maturation of human osteoblast precursors in vitro: relevance to glucocorticoid-induced osteoporosis. *Rheumatology* **40:** 74-83

Wang FS, Ko JY, Weng LH, Yeh DW, Ke HJ, Wu SL (2009) Inhibition of glycogen synthase kinase-3beta attenuates glucocorticoid-induced bone loss. *Life Sci* **85:** 685-692

Wang FS, Ko JY, Yeh DW, Ke HC, Wu HL (2008) Modulation of Dickkopf-1 attenuates glucocorticoid induction of osteoblast apoptosis, adipocytic differentiation, and bone mass loss. *Endocrinology* **149:** 1793-1801

Wehrli M, Dougan ST, Caldwell K, O'Keefe L, Schwartz S, Vaizel-Ohayon D, Schejter E, Tomlinson A, DiNardo S (2000) arrow encodes an LDL-receptor-related protein essential for Wingless signalling. *Nature* **407:** 527-530

Weinstein RS, Jilka RL, Parfitt AM, Manolagas SC (1998) Inhibition of osteoblastogenesis and promotion of apoptosis of osteoblasts and osteocytes by glucocorticoids - Potential mechanisms of their deleterious effects on bone. *Journal of Clinical Investigation* **102:** 274-282

Weissman IL, Anderson DJ, Gage F (2001) Stem and progenitor cells: Origins, phenotypes, lineage commitments, and transdifferentiations. *Annual Review of Cell and Developmental Biology* **17:** 387-403

Wessely O, Agius E, Oelgeschläger M, Pera EM, De Robertis EM (2001) Neural induction in the absence of mesoderm: beta-catenin-dependent expression of secreted BMP antagonists at the blastula stage in Xenopus. *Dev Biol* **234:** 161-173

Willert K, Brown JD, Danenberg E, Duncan AW, Weissman IL, Reya T, Yates JR, Nusse R (2003) Wnt proteins are lipid-modified and can act as stem cell growth factors. *Nature* **423:** 448-452

Winkler DG, Sutherland MSK, Ojala E, Turcott E, Geoghegan JC, Shpektor D, Skonier JE, Yu C, Latham JA (2005) Sclerostin Inhibition of Wnt-3a-induced C3H10T1/2 Cell Differentiation Is Indirect and Mediated by Bone Morphogenetic Proteins.

Winslow MM, Pan M, Starbuck M, Gallo EM, Deng L, Karsenty G, Crabtree GR (2006) Calcineurin/NFAT signaling in osteoblasts regulates bone mass. *Dev Cell* **10:** 771-782

Wodarz A, Nusse R (1998) Mechanisms of Wnt signaling in development. *Annu Rev Cell Dev Biol* **14:** 59-88

Wrana JL, Attisano L, Wieser R, Ventura F, Massagué J (1994) Mechanism of activation of the TGF-beta receptor. *Nature* **370:** 341-347

Wright M, Aikawa M, Szeto W, Papkoff J (1999) Identification of a Wnt-responsive signal transduction pathway in primary endothelial cells. *Biochem Biophys Res Commun* **263:** 384-388

Wu AM, Till JE, Siminovitch L, McCulloch EA (1968) Cytological evidence for a relationship between normal hemotopoietic colony-forming cells and cells of the lymphoid system. *J Exp Med* **127:** 455-464

Wu L, Wu Y, Lin Y, Jing W, Nie X, Qiao J, Liu L, Tang W, Tian W (2007) Osteogenic differentiation of adipose derived stem cells promoted by overexpression of osterix. *Mol Cell Biochem* **301:** 83-92

Wu Z, Rosen ED, Brun R, Hauser S, Adelmant G, Troy AE, McKeon C, Darlington GJ, Spiegelman BM (1999) Cross-regulation of C/EBP alpha and PPAR gamma

controls the transcriptional pathway of adipogenesis and insulin sensitivity. *Mol Cell* **3:** 151-158

Xiao ZS, Thomas R, Hinson TK, Quarles LD (1998) Genomic structure and isoform expression of the mouse, rat and human Cbfa1/Osf2 transcription factor. *Gene* **214:** 187-197

Xu C, Inokuma MS, Denham J, Golds K, Kundu P, Gold JD, Carpenter MK (2001) Feeder-free growth of undifferentiated human embryonic stem cells. *Nat Biotechnol* **19:** 971-974

Yamamoto A, Nagano T, Takehara S, Hibi M, Aizawa S (2005) Shisa promotes head formation through the inhibition of receptor protein maturation for the caudalizing factors, Wnt and FGF. *Cell* **120:** 223-235

Yang F, Yang D, Tu J, Zheng Q, Cai L, Wang L (2011) Strontium enhances osteogenic differentiation of mesenchymal stem cells and in vivo bone formation by activating Wnt/catenin signaling. *Stem Cells* **29:** 981-991

Yeh WC, Cao Z, Classon M, McKnight SL (1995) Cascade regulation of terminal adipocyte differentiation by three members of the C/EBP family of leucine zipper proteins. *Genes Dev* **9:** 168-181

Zaidi SK, Sullivan AJ, van Wijnen AJ, Stein JL, Stein GS, Lian JB (2002) Integration of Runx and Smad regulatory signals at transcriptionally active subnuclear sites. *Proc Natl Acad Sci U S A* **99:** 8048-8053

Zamani A, Omrani GR, Nasab MM (2009) Lithium's effect on bone mineral density. *Bone* **44:** 331-334

Zeng L, Kempf H, Murtaugh LC, Sato ME, Lassar AB (2002) Shh establishes an Nkx3.2/Sox9 autoregulatory loop that is maintained by BMP signals to induce somitic chondrogenesis. *Genes Dev* **16:** 1990-2005

Zeng X, Huang H, Tamai K, Zhang X, Harada Y, Yokota C, Almeida K, Wang J, Doble B, Woodgett J, Wynshaw-Boris A, Hsieh JC, He X (2008) Initiation of Wnt signaling: control of Wnt coreceptor Lrp6 phosphorylation/activation via frizzled, dishevelled and axin functions. *Development* **135:** 367-375

Zeng X, Tamai K, Doble B, Li S, Huang H, Habas R, Okamura H, Woodgett J, He X (2005) A dual-kinase mechanism for Wnt co-receptor phosphorylation and activation. *Nature* **438:** 873-877

Zhao Q, Eberspaecher H, Lefebvre V, De Crombrugghe B (1997) Parallel expression of Sox9 and Col2a1 in cells undergoing chondrogenesis. *Dev Dyn* **209:** 377-386

Zheng H, Guo Z, Ma Q, Jia H, Dang G (2004) Cbfa1/osf2 transduced bone marrow stromal cells facilitate bone formation in vitro and in vivo. *Calcif Tissue Int* **74:** 194-203

Zhou F, Huang H, Zhang L (2012) Bisindoylmaleimide I enhances osteogenic differentiation. *Protein Cell* **3:** 311-320

Zhu F, Friedman MS, Luo W, Woolf P, Hankenson KD (2012) The transcription factor osterix (SP7) regulates BMP6-induced human osteoblast differentiation. *J Cell Physiol* **227:** 2677-2685